THE UNIVERSITY OF CALGARY

TRANSMISSION LINE DIRECTIONAL PROTECTION USING NEURAL NETWORKS AND FILTERING ALGORITHMS

by

Majid Sanaye-Pasand

A DISSERTATION
SUBMITTED TO THE FACULTY OF GRADUATE STUDIES
IN PARTIAL FULFILLMENT OF THE REQUIREMENTS FOR THE
DEGREE OF DOCTOR OF PHILOSOPHY

DEPARTMENT OF ELECTRICAL AND COMPUTER
ENGINEERING

CALGARY, ALBERTA

June, 1998

Abstract

Power transmission lines are the vital links in power systems providing the essential continuity of service from generating plants to the end users. To maintain stability in a power system it is imperative that any fault in the transmission system be identified by protective relays and the faulted line be isolated from the network with minimal delay.

Faults on transmission lines need to be detected, classified and cleared as fast as possible. Moreover, the fault direction should be identified. Development of different modules of a transmission line protective relaying system is outlined in this dissertation. Different modules such as fault direction identification, fault detection and phase selection modules are designed, implemented and tested.

Neural network technique is employed to design the transmission line fault direction identification module. Different neural network structures are used and four different directional modules are proposed.

A new high speed algorithm, based on impedance measurement is proposed for fault detection and phase selection. Adaptive features are also added to the proposed relaying modules to enable them to track the changing operation conditions of the system.

Off-line studies are performed with the proposed relaying modules on a simulated power system model. The system is subjected to different types of disturbances while it is operating at different operating conditions, and the performance of the proposed modules is evaluated. The results obtained indicate that the proposed

relaying modules perform rapidly and correctly for different system conditions.

The relaying algorithm has been implemented on a digital signal processor board. Using a power system model consisting of a micro-alternator connected to a constant voltage system extensive experimental studies are conducted and the performance of the relaying algorithm is investigated.

The performance of the proposed modules is investigated further using recorded fault data from a high voltage power system. In this way, the performance of the newly designed relaying modules can be further verified in a more realistic environment. Results using various recorded field data are presented.

The results presented in this dissertation confirm the feasibility of the proposed relaying modules.

Acknowledgments

I would like to express my sincere gratitude to my supervisor, Dr. O. P. Malik, for his constant guidance, support and valuable suggestions throughout the whole program. His fruitful supervision enabled me to present this dissertation in this form.

I would also like to thank all the professors and the support staff in the Department of Electrical and Computer Engineering, The University of Calgary, for their help during my study here. I am also indebted to the professors in the Electrical Engineering Department, Tehran University. I have learned a lot from them.

Special thanks go to Mr. G. Hancock and Mr. P. Walsh for their assistance during the laboratory work. Special appreciation also goes to the fellow students in our research group, specially Mr. M. Calvo for their consultation from time to time.

I am greatly indebted to my wife, who has always been patient and encouraging. Without her constant support, I could not have finished this dissertation. My special thanks go to my children, my parents and my parents-in-law for their patience and encouragement through the course of this work.

I also wish to acknowledge the financial support of the Ministry of Culture and Higher Education of I. R. Iran which enabled me to pursue my graduate studies. Partial support of NSERC Canada is also acknowledged.

I am also grateful for the recorded field data provided by the Alberta Power Ltd..

Dedication

To

My Family

Table of Contents

List of Tables

List of Figures

List of Symbols

Computer

A/D	Analog to Digital conversion
AIC	Analog Input Card
CHA, CHB	I/O channels of the DSP board
DAS	Data Acquisition System
DMA	Direct Memory Access
DSP	Digital Signal Processor
I/O	Input/Output
ISA	Industry Standard Architecture PC bus
MUX	Multiplexer
PC	Personal Computer
RAM	Random Access Memory
ROM	Read Only Memory
S/H	Sample and Hold
TMS320C30	Texas Instruments DSP chip

Neural Networks & Signal Processing

ANN	Artificial Neural Network
Avg	Average

BP	Back-Propagation
d_j	desired response of neuron j
exp	exponential function
e_j	error signal at the output of neuron j
$e(w)$	error vector
$E(n)$	instantaneous value of the sum of squared errors
$f(.)$	mapping function
FIR	Finite-duration Impulse Response
I	Identity matrix
$J(w)$	Jacobian matrix of derivatives of each error to each weight
J^{-1}	inverse of matrix J
J^T	transpose of matrix J
M	down-sampling factor
Max	Maximum
Min	Minimum
ML	Marquardt-Levenberg training algorithm
n	sampling number
OR	OR logical function
PCA	Principal Component Analysis
T	sampling period
tanh, *tansig*	hyperbolic tangent sigmoid function
TDNN	Time Delay Neural Network
v_j	net internal activity level of neuron j

w_{kj}	synaptic weight of synapse j belonging to neuron k
x_j	input signal of neuron k
y_k	output signal of neuron k
z^{-1}	unit-delay operator
α	momentum factor
η	learning-rate parameter
$\delta_j(n)$	local gradient of neuron j at iteration n
Δw	small change applied to weight w
$\nabla V(x)$	gradient vector
$\nabla^2 V(x)$	Hessian matrix
$\phi(.)$	activation function
μ	learning parameter
θ_k	threshold applied to neuron k

Power System

1-Φ-g	1-phase to ground faults
2-Φ	2-phase faults
2-Φ-g	2-phase to ground faults
3-Φ-g	3-phase to ground fault
ab, *A-B*	phase *A* to phase *B* fault
abcg, *A-B-C-G*	three phase to ground fault
abg, *A-B-G*	phase *A* to phase *B* to ground fault
ac	alternating current

ac, *A-C*	phase *A* to phase *C* fault
acg, *A-C-G*	phase *A* to phase *C* to ground fault
ag, *A-G*	phase *A* to ground fault
bc, *B-C*	phase *B* to phase *C* fault
bcg, *B-C-G*	phase *B* to phase *C* to ground fault
bg, *B-G*	phase *B* to ground fault
BPA	Bonneville Power Administration
C	Capacitance
CB	Circuit Breaker
cg, *C-G*	phase *C* to ground fault
CT	Current Transformer
dc	direct current
DFR	Digital Fault Recorder
EHV	Extra High Voltage
EMTDC	Electro-magnetic transients simulation program
EMTP	Electro-Magnetic Transients Program
FACTS	Flexible AC Transmission Systems
GVA	Giga-Volt-Amperes
hp	horse power
HVDC	High Voltage Direct Current
iA, iB, iC	phase *A*, *B* and *C* currents
I_{adp}	adaptive setting of current
I_A, I_B	fault currents measured at points A and B

I_f	fault current
I >	phase overcurrent unit
I_n >	neutral overcurrent unit
k_0	residual current factor
kVA	kilo-Volt-Amperes
L	Inductance
MVA	Mega-Volt-Amperes
PSCAD	Power System Computer Aided Design
PT	Potential Transformer
pu	per-unit
R	Resistance
R1, $\cdots$, R5	analog filter resistances
R_f	fault resistance
SCC	Short Circuit Capacity
TCR	Time Constant Regulator
vA, vB, vC	phase A, B and C voltages
V_A	voltage measured at point A
VT	Voltage Transformer
X	Reactance
Z_0	zero sequence impedance
Z_1	positive sequence impedance
ZA, ZB, ZC	phase A, B and C impedances
Z_{adp}	adaptive setting of impedance

Z_l	load impedance
Z_{LA}, Z_{LB}	line impedance, sections A and B
Z_{line}	line impedance
Z_{load}	impedance under load condition
Z_{min}	minimum impedance under load condition
Z_p	replica impedance
Z_r, Z_s	source impedance
Z_R	impedance seen by the relay
$Z <$	underimpedance unit
Δi	deviation of current
Δv	deviation of voltage
ω_0	power system frequency, rad/s

Chapter 1

Introduction

1.1 Power System Protection

1.1.1 Role of Protection

The extensive use of electric energy has made reliable operation of electric power systems a problem of special importance. The function of a power system is to supply electrical energy to customers as reliably and economically as possible. One of the best ways to do this is to have large-scale interconnected power systems. Thus, there has been a trend towards an interconnected network of transmission lines linking generators and loads into large integrated systems, some of which span entire continents [1].

In a large electric power system comprising of hundreds of complex interacting elements, there always exists a possibility of disturbance and fault. The advent of large generating stations and highly interconnected power systems makes early fault identification and rapid equipment isolation imperative to maintain system integrity and stability.

Faults are generally caused by failure of insulation. Some other causes of faults include breaking of conductors and accidents. Such faults may cause:

- interruption in the power supply to the customers
- instability in system operation
- extensive damage to the equipment
- serious hazard to the personnel

To minimize these effects, power system equipment must be protected adequately. Protective relays are used in power systems to protect equipment from excessive damage and to maintain system integrity and stability [2, 3, 4]. A good protective relay should have the following features:

- speed
- accuracy
- reliability
- sensitivity
- selectivity
- ease of maintenance
- minimum cost

1.1.2 Historical Background

Protective relaying is a task of fundamental importance in a modern power system. Early relays for protection of power systems used electro-mechanical technology.

Consequently, they suffered from several associated disadvantages like long operating times due to inertia of moving parts, high burden on Current and Voltage Transformers (CTs and VTs), contact pitting and high maintenance cost. This necessitated the use of more sophisticated relaying techniques.

The next generation used static relays. Static relays fabricated using solid state components were an improvement over the electro-magnetic relays. The use of static relays eliminated some of the drawbacks of the electro-mechanical relays; but there were other limitations such as temperature sensitivity, aging of components, sensitivity to voltage spikes and damage due to overloading.

In their early version they were built assuming pure sinusoidal waveforms as inputs. That is why many utilities did not accept these relays. Later, some modifications were done and their use increased gradually during sixties and early seventies [5].

Recently, computer relaying techniques have been introduced in relaying design. Many individual investigators and manufacturers are developing microprocessor-based devices for the protection of power systems and some devices have become commercially available [5].

1.1.3 Digital Relaying

In a pioneering paper [6], Rockefeller undertook the study of protection of all the power equipment in a substation with a digital computer. Since then, there has been a considerable amount of research work in the area of digital computer relaying. It is evident that a single computer for the protection of all the equipment in a substation

is not a viable concept in view of the presently available computer hardware. The solution to this problem is to use a number of microprocessors dedicated to individual equipment relaying tasks with an inter-computer data exchange facility.

The concept of digital computer relaying has grown rapidly as digital computers have become more powerful, cheaper and reliable. Advances in computer hardware have been accompanied by analytical developments in the field of relaying [7]. Research, design and economics of microprocessor-based relays reached a level where commercial production began several years ago. Successful attempts have been made in designing and developing various microprocessor-based relays [7, 8, 9, 10, 11, 12].

Besides the benefits of digital technology, properly designed microprocessor relays are superior to conventional electro-mechanical and static relays in several ways. Some of the expected benefits of a digital protection scheme include [5]:

- Economy: The cost of digital hardware has been steadily decreasing. The cost of a digital relay is now less than the cost of a comparable analog relay [13]. Although the software development costs for a digital relay are high, as with the development cost of any new device, these would be distributed over many similar devices.

- Performance: The performance of the commercial digital relay is considered to be as good as the corresponding perfect analog relay. A digital relay has some inherent features such as memory action and complex shaping of operational characteristics which lead to better performance.

- Reliability: A high level of diagnostic functions can be realized in a digital relay which makes the relay much more reliable. The digital relay, for example, can

perform self-checking at regular intervals.

- Flexibility: The same hardware with minimal change can be used for different functions by changing only the software program.

- Background tasks: The relaying computer can take over some other tasks such as measuring voltages and currents and monitoring power flows, controlling the opening and closing of circuit breakers and switches and providing backup for other devices [7].

A typical digital relay has a measurement unit and a computation unit. The measurement unit is comprised of data acquisition, conversion and storage. The computation unit uses the data provided by the measuring unit to execute the relaying algorithm. The measurements, fault computations and decision making must be completed within the time available between consecutive data sampling instants.

The analog input power system signals are sampled continuously, the sampling rate is dependent on the application and algorithm used. The raw data samples are stored in the memory of the digital relay. Power system signals include high frequency components during system faults. Depending on the rate at which a signal is sampled, some high frequencies can appear to be a component of the power frequency. This is called alias problem. Anti-aliasing filtering is required in a digital relaying algorithm to minimize the effect this problem [14].

1.2 Transmission Line Protection

Power transmission lines are the vital links providing the essential continuity of service from generating plants to the end users. About two-thirds of the faults in power systems occur in the transmission line network [15]. To maintain stability in a power system it is imperative that any fault in the transmission system be identified and the faulted line be isolated from the network with minimal delay.

Transmission line protection is the most elaborate and challenging function in power system protection. Consequently, it has received extensive attention from the researchers and designers in the area of power system protection. Also, the high cost of conventional transmission line relays naturally makes them a worthwhile research problem to tackle. Moreover, the cost of digital hardware has been steadily decreasing. This is why digital relaying of transmission lines has attracted the attention of many researchers [5]. Computer relaying techniques have been introduced in relaying design and microprocessor-based transmission line relays have been proposed [5, 14].

The most common methods used for transmission line protection include overcurrent, distance, current differential, phase comparison and directional comparison protection schemes.

1.2.1 Overcurrent Protection

One of the earliest and simplest types of protective relays is overcurrent relay. This relay assumes a fault has occurred if the input measured current exceeds its threshold value. The relay tripping time can be made inversely proportional to the amount of

overcurrent [15, 16]. Overcurrent relays get confused when load current is significant compared to fault current.

Fault resistance is one common problem in transmission line protection. Most of the faults on transmission lines are accompanied by fault resistance. For faults between different phases of the line which do not involve the ground, the fault resistance is mainly due to the resistance of arc. For faults involving the ground, however, the fault resistance includes arc resistance as well as the ground resistance. For some ground faults such as contact with trees fault resistance could be very large. Overcurrent relays may not be able to detect faults including high amount of fault resistance.

Directional relay modules are used to limit relay operation to a specified direction. When there is a source at both ends of a transmission line, the relays protecting the line are subjected to fault current flowing in either direction. If nondirectional relays are used, they have to be co-ordinated not only with the relays at the remote end but also with the relays behind them.

Directional-overcurrent relays are combination of directional and overcurrent relay modules. Being simple and less expensive than other transmission line relays, these relays could be used as backup protection for transmission lines.

1.2.2 Distance Protection

Distance relays measure the apparent impedance between the relay and the fault location using the fundamental frequency components of the voltage and current signals. The apparent impedance is compared with the relay setting to determine

whether the fault is in the protected zone area. Fourier transform approach [17, 18], the least square approach [19, 20] and numerical solution of differential equation [21, 22] are some of the numerous digital impedance protection techniques available in the literature.

Impedance protection techniques have operating times of the order of one cycle [23]. Also, distance relays have to be co-ordinated with relays at other substations which might result in complex relay co-ordination programs. Under earth fault conditions on a transmission line, the presence of another nearby circuit in parallel with the transmission line might cause distance protection relays to measure incorrectly. The error is due to the inductive coupling between the two circuits.

For transmission lines supplied from both ends, the voltage drop in the fault from the remote end magnifies the fault resistance as seen at the local bus. It could shift the apparent impedance measured by a distance relay from inside to its outside characteristic and therefore, cause maloperation.

The various limitations of impedance relaying have been highlighted in Ref. [23]. According to this reference, there is an uncertainty associated with the impedance estimated by the relay and this uncertainty depends upon the speed with which these estimates are made.

1.2.3 Unit Protection

Unit protection with its advantage of fast selective fault clearance has been used in power systems from the early stages. The problems of adequately protecting modern power systems with their high degree of interconnection and with the need

of fast clearance times have led some countries to consider adopting unit protection compared with distance protection [15].

Distance relays could be used to trip faults within their first protective zone without any intentional delay. Due to the measurement errors, the first protective zone of a distance relay is usually set to about 80% of the length of the protected transmission line. Faults on the remaining end section of the line are cleared after some time delay. To provide high speed clearing for the remaining end section of the transmission line a pilot communication channel between the line terminals should be used. Unit protection schemes using pilot relays could clear faults on the whole length of the line without any intentional delay.

An essential feature of transmission line unit protection is the provision of a pilot channel over which information can be transmitted between two ends of the line. The communication channels commonly used are power line carrier, leased lines, microwave and fiber optics. There is a tradeoff regarding the bandwidth of the communication channel used. Wideband channels are faster so they enhance the performance but they are also more expensive. Narrowband channels are less expensive but are also slower. The advent of digital communication has enhanced the prospects of wholly digital relays.

Different unit protection schemes have been proposed which transmit different types of information over the communication channel.

1.2.3.1 Current Differential Protection

A current differential protection scheme compares currents at transmission line terminals to discriminate between internal and through fault conditions on the line.

Current differential relays use a single signal, exchanged between terminals to embody the current information for the three phase system. At each line end, summation CTs are used to derive a single phase quantity which is a function of the three phase currents. The sensitivity of the relay can vary with different types of faults and some schemes are known not to perform adequately for certain types of faults such that failure to operate for some internal faults and maloperation for some external faults may occur. The solution appears to be to transmit the instantaneous current information on a per phase basis and make differential measurement for each individual phase [24]. This would involve dependable communication channels linking the various circuit ends.

1.2.3.2 Phase Comparison Protection

In a phase comparison protection scheme, the relative phases of the currents at the ends of the transmission line are compared over a communication channel. When the currents at the terminals are relatively in phase, an internal fault is indicated and the line is tripped. When the currents at the terminals are relatively 180 degrees out of phase, an external fault is indicated and the line is not tripped. Phase comparison protection techniques have been proposed [25], but protection principles of this kind make use of a very reliable communication channel as they involve the exchange of quantitative information across the ends of the protected line.

1.2.3.3 Directional Comparison Protection

A directional comparison protection scheme is based on exchanging directional or command information over the communication channel and therefore pose small

demand on the channel; the channel could act in a simple switching sense. The directional decisions, forward or reverse, are made independently by directional relays at each terminal of the transmission line and then compared over the channel to provide a tripping signal for internal faults or blocking for external faults and loads. Power flow into the line at both terminals indicates an internal fault and the line is tripped. If the power flow is into the line in one end and out of the line at the other end the fault is considered to be external and the line is not tripped. Since directional relays operate only when the fault current flows in the specified tripping direction, they avoid complex co-ordination and the possibility of compromising line protection [26].

Directional comparison relays are set to respond to faults in the protection zone without intentional time delay and therefore, are used where high-speed fault clearing is necessary. Such a scheme detects faults along the whole length of a transmission line quickly and selectively [8]. This type of protection has been widely applied and is becoming popular in modern schemes of system protection particularly where difficult earth-fault conditions prevail [15].

There are several advantages to high speed clearing of faults at both line terminals. The principle advantage of high speed relaying is improvement of stability of the system. Other benefits of high speed relaying are reduced fault damage to insulators, conductors and hardware, reduced safety hazards to substation personnel and line crew from step and touch potentials, reduced stresses on major substation equipment, generators and turbines and the possibility of faster reclosure due to less arc ionization as a result of faster fault clearance.

1.3 Dissertation Objectives

A power system is a very complicated and highly nonlinear system. Advent of new methods and equipment introduced in power systems such as HVDC, FACTS, power electronics equipment and control methods and capacitor-compensated transmission lines has made the power system even more complex. New trends in power system such as deregulation of electric utilities are under way. Deregulation gives consumers the possibility to buy power from any producer in the market. New methods and skills are required in design and analysis of power systems to achieve new solutions for possible new emerging problems as well as some of the old-standing ones.

The main objective of this dissertation is to develop different modules of a transmission line protective relaying system. Different modules such as fault direction identification, fault detection and phase selection modules are designed, implemented and tested. With the increasing magnitude of short-circuit MVA in modern power systems, shorter fault clearing times are becoming necessary. The proposed modules should be fast and robust. Their performance should not be affected by changes in power system conditions and parameters such as source impedance, fault location, fault type, fault inception time and pre-fault power flow direction. The proposed schemes should perform reliably for fault with high amount of fault resistance.

Since the advent of digital protection and its use in industry, many different methods and algorithms have been investigated and developed. Most of the digital relaying algorithms use digital signal processing techniques to process input signals. Rapid development in microcomputer technology, coupled with an equally dramatic cost reduction has provided the opportunity to study and develop new microprocessor

based-relays.

Artificial Neural Networks (ANN), as an alternative approach, have been applied recently to many engineering applications. Successful applications of ANNs in the power engineering area have demonstrated that they could be utilized as an alternative method to solve certain long-standing problems where conventional techniques have experienced difficulties. In this research work, neural network technique is employed to design the transmission line fault direction discrimination module. Different neural network structures are used and four different directional modules are proposed.

A new algorithm, based on impedance measurement and covering a wide range of impedance plane, is proposed for fault detection and phase selection. A fast method to estimate the fundamental frequency power system voltage and current phasors is used. The proposed approach is able to detect faults with high amount of fault resistance.

A protective relaying system responds to faults in a fixed predetermined manner. The predetermined manner, embodied in the characteristics and settings of the relay, is based upon certain assumptions made about power system operating conditions. In time, if the system conditions change the settings of the relay may be inappropriate and the relay might maloperate. Adaptive protection systems permit the protection functions to be adapted automatically in real-time to changing power system conditions. Such procedures maintain optimum protection quality and performance. Adaptive features are also added to the proposed relaying modules to enable them to track the changing operation conditions of the system.

The proposed modules can be employed individually as transmission line protec-

tive modules or together in a directional comparison protection scheme by employing a relay at each end of the line.

1.4 Organization of the Dissertation

There are 10 chapters in this dissertation which are divided into 3 parts:

- **Part I - Theoretical Developments & Simulation Results**

  This part consists of five chapters. Proposed transmission line protective relaying modules are presented and the function of each module is described. Detailed simulation studies of the proposed modules are also presented.

  Transmission line fault direction discrimination problem is discussed in Chapter 2. Neural network approach is proposed as a solution for fault direction identification. A brief review of artificial neural networks is also given in this chapter.

  Neural network technique is employed and two different feedforward networks are proposed to act as the directional module of a transmission line relaying system. Design procedure of the proposed neural network-based directional modules is described in Chapter 3. A typical power system model is used to examine the proposed directional modules under different system conditions. Results of performance studies with the proposed neural network-based approaches are also presented in Chapter 3.

  An important class of neural networks has a recurrent structure. Processing of temporal sequences and signals by recurrent neural networks is discussed

in Chapter 4. A novel recurrent neural network is proposed to determine the direction of faults on transmission lines. Details of the design procedure and the results of off-line performance studies with the proposed recurrent network are given and analysed in Chapter 4.

A different recurrent neural network based on the structure proposed by Elman is presented in Chapter 5. A recurrent network with temporal processing abilities is designed and trained to determine the fault direction on transmission lines rapidly. Test results obtained from the simulation studies under different power system conditions are presented and discussed in this chapter.

It is desirable to develop a fast and reliable method to detect faults on a transmission line and to select faulty phases. A new high speed adaptive module is proposed in Chapter 6 for fault detection and phase selection. Different types of fault starter units are also described in this chapter. The proposed algorithm is tested to evaluate its performance under different operating conditions including faults with high resistance. The design procedure and the results of the simulation studies with the proposed approach are presented in Chapter 6.

- **Part II - Real-Time Implementation**

Another phase of the project involves implementation of the proposed relay modules in real-time. The performance of the proposed relaying modules is investigated further on a physical model of a power system.

The laboratory experimental system set-up is described in Chapter 7. The hardware and software required for implementation are also discussed. Details of implementation of the proposed modules are presented in this chapter.

Results of experimental studies performed on the power system model with the different proposed modules are given in Chapter 8. A wide range of various types of forward and backward faults were applied at different locations on the modelled transmission line and the performance of different proposed modules was extensively investigated. The effect of fault resistance was also studied.

- **Part III - Field Data Tests**

  The performance of the proposed modules is investigated further using recorded fault data from a high voltage power system. The real world complex effects of the power system elements are already included in the recorded real fault data. In this way, the performance of the newly designed relaying modules can be further verified in a more realistic environment than pure simulation. Results using various recorded field data are presented in Chapter 9.

  Finally, conclusions and recommendations for further research are presented in Chapter 10.

Part I

Theoretical Developments & Simulation Results

Chapter 2

Transmission Line Directional Protection - Neural Networks Solution

2.1 Introduction

Artificial neural networks have been studied for many years and have been used in various applications. It has been shown that they are powerful in pattern recognition and classification, and possess generalization capabilities.

The ability of neural networks to learn complex nonlinear input/output relationships reveals them as viable candidates for solving significant power system problems. ANN techniques have been used in power system area in general and in protection area in particular and encouraging results were obtained [27, 28].

The forward or backward fault location with respect to the measurement point on a transmission line should be identified rapidly and reliably. A fault direction identification problem on a transmission line can be treated as a pattern classification problem, and ANNs can be used for determining the direction of a fault on the given transmission line.

The problem of fault direction identification and the need for directional relays in a power system is described in this chapter. Previously proposed directional

algorithms are briefly described and their limitations are discussed. Neural network approach is proposed as a solution for fault direction identification. A brief overview of neural networks is also given in this chapter.

2.2 Transmission Line Fault Direction Discrimination

2.2.1 Directional Protection

Directional units are fundamental to power system protection performing such critical tasks as supervising distance elements and controlling overcurrent elements. Directional relays are used for protection of ring or loop systems as well as radial circuits with sources at both ends [8, 12].

Relays protecting a transmission line, with sources at both ends, are subjected to fault current flowing in either direction (Fig. 2.1). If nondirectional relays are used, they have to be co-ordinated not only with the relays at the remote end but also with the relays behind them. Since directional relays operate only when the fault current causes a power flow in the specified tripping direction, they avoid complex relaying co-ordination and the possibility of compromising line protection. It is, therefore,

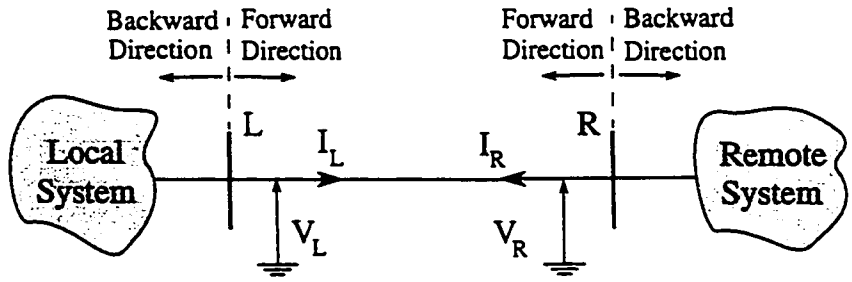

Figure 2.1: A transmission line interconnecting a local and a remote system

desirable to develop directional relays which are able to determine the direction of the fault rapidly and correctly for different operating conditions of the power system.

2.2.2 Directional Comparison Scheme

A directional comparison protection scheme greatly simplifies co-ordination problems and permits high speed tripping. The need for precise relay settings and corresponding calculated system fault currents and voltages is eliminated.

A directional comparison scheme consists of directional relays at each terminal of the transmission line. Using the locally measured quantities, the direction to a fault is independently determined by the relay at each end of the transmission line. These directional decisions are then compared over a communication channel to arrive at a combined trip/block decision. Thus the overall decision time is determined by both the directional relay and the communication link.

In the directional comparison scheme the need for data transmission is low. Unlike some other pilot protection schemes which may call for a great deal of data to be obtained from the remote location, directional comparison requires just to transmit an on/off signal through the channel. Fiber optic channels could be used for high speed communication between the two ends of the transmission line.

In a directional comparison system, a further characteristic could be used to detect high fault levels close to the relay location. For such a case, tripping could be made independent of the directional unit in the station at the opposite end of the transmission line. According to the configuration of power system, this technique enables faults at locations up to 40% of the line length to be tripped without signals being exchanged between the relays at the ends of the line [8].

To ensure that the protection system can trip the line in the case of any possible communication channel failure, provision is made for the relay to trip its local circuit breaker without any directional comparison after a delay determined by a timer [8].

2.2.3 Fault Direction Identification

Direction of a fault on a transmission line can be determined from the relative phase angles of the voltage and current phasors. To determine the direction of the fault, a directional relay uses a reference against which line current can be compared. This reference is known as the polarizing quantity.

With zero sequence component of line current, either a zero sequence current or voltage or both must be used. In power systems with mutual induction problems, the trend is toward the use of negative sequence quantities for the ground directional unit [12].

Conventional negative sequence directional elements base their decision on the phase angle between the negative sequence voltage and current. The directional element measures the negative of the negative sequence source impedance for forward faults. It is an incremental measurement since it is not available unless an unbalanced disturbance hits the system. It will however not be available for a balanced disturbance, i.e. it does not cover three phase faults. Positive sequence is present for all possible faults. Therefore, a conventional directional unit which can be used in all circumstances must be based on positive sequence quantities.

2.2.4 Neural Network Solution

With the present techniques of designing power systems protective relays, one can obtain reasonable performance for more common faults than with the older protection systems. On the other hand, the relaying system performance deteriorates for some extreme cases. Relaying decisions are made based on some pre-assumptions about power system conditions. If the system conditions change, the relaying performance is not guaranteed. Digital-based protective relays might need to perform extensive computations to obtain accurate estimate of the system states and therefore, would not be able to make a quick trip decision. They maloperate in some fault cases as well.

At the same time, the power systems continue to grow in size and complexity and also new components are being introduced. Also the present day tendency of operating generators with small stability margins has made the stability problem even more serious, thus requiring very fast fault clearing time. In this way, one encounters more complicated systems with new dynamic power system problems. Thus one should be ready to meet a new problem with new ideas and techniques.

The majority of power system protection techniques are involved in defining the system state through identifying the pattern of the associated voltage and current waveforms. This means that the development of a protection algorithm can be essentially treated as a problem of pattern recognition/classification. However, due to the many possible causes of faults and the nonlinear operation of some power system devices, conventional pattern recognition methods may not be satisfactory in applications involving complex power systems [29].

Artificial neural networks have been studied for many years and have been used in various applications. It has been shown that they are powerful in pattern recognition and classification, and possess generalization capabilities.

The direction of a fault on a transmission line can be determined from the relative phase angles of the voltage and current phasors. Voltage is usually used as the reference polarizing quantity. The fault current phasor lies within two distinct forward and backward regions with respect to the reference phasor, depending on the power system and fault conditions. The fault direction identification problem can be treated as pattern classification problem, and ANNs can be used for determining the direction of a fault on the given transmission line. The neural network-based directional identifier does not explicitly use the phase information to make its decision. It uses samples of the instantaneous values of the voltage and current waveforms and tries to recognize and classify the input patterns of the network as the forward or backward faults.

2.3 Artificial Neural Networks

Artificial neural networks have a quite long and extensive history. The history of neural network computing is not that long and can be traced to some recent origins [30]. According to some survey articles some major fundamental concepts for neural network computing were introduced in the early 1960s [31]. Since then, much research has been done and today several well defined network architectures are available to apply to a variety of problems. A variety of new implementation ideas were introduced and neural network computing became a well established field by the late

1980s [32, 33].

As detailed introduction about neural networks is already available [31, 33, 34, 35, 36, 37], only a brief summary of some of the concepts of neural networks is given in this section.

2.3.1 Neural Networks - An Overview

Interest in artificial neural networks has been motivated by the recognition that the brain computes in an entirely different manner than the conventional digital computer. In recent years, interest in studying the mechanism and structure of the brain has increased.

The human brain outperforms modern digital computers in pattern recognition and classification of real world data. It can discriminate objects into various pattern classes. Artificial neural networks are systems simulating parts of the human brain [34]. They have been studied for many years in the hope of achieving human-like performance. Neural computing is now one of the most promising technologies in all fields of engineering, resulting in the development of a number of different networks by different researchers.

To achieve good performance, neural networks employ a massive interconnection of simple computing cells referred to as *neurons* or *processing units*. Therefore the following definition of a neural network viewed as an adaptive machine may be offered [35]:

"A neural network is a massively parallel distributed processor that has a natural propensity for storing experimental knowledge and making it available for use".

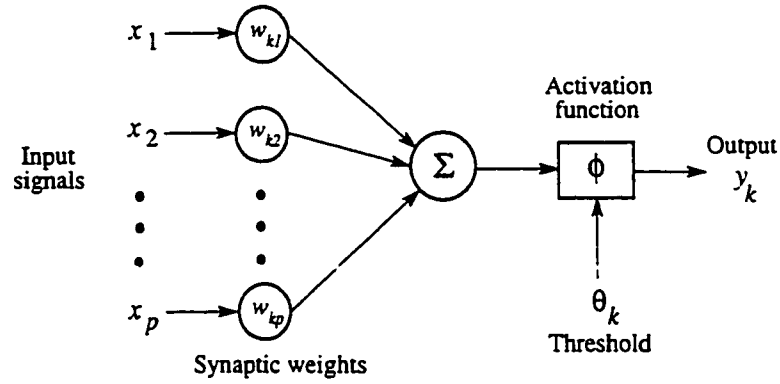

Figure 2.2: Nonlinear model of a neuron

Neurons are the basis of neural networks. The model of a neuron is shown in Fig. 2.2. Each neuron model consists of three basic elements described as [35]:

1. *Synaptic Weights*: The neuron input signals are multiplied by a set of synaptic weights connected to the neuron. These weights are used to store the presented information to the network.

2. *Adder*: This linear combiner is used for summing the input signals each weighted by the respective synapse of the neuron.

3. *Activation Function*: This nonlinear function simulates the chemical process in biological neurons. It limits the permissible amplitude range of the output signal to some finite value.

The model of a neuron also includes an externally applied *threshold* that has the effect of lowering the net input of the activation function.

The manner in which the neurons of a neural network are connected results in different network architectures. A *feedforward* neural network is a simple layered

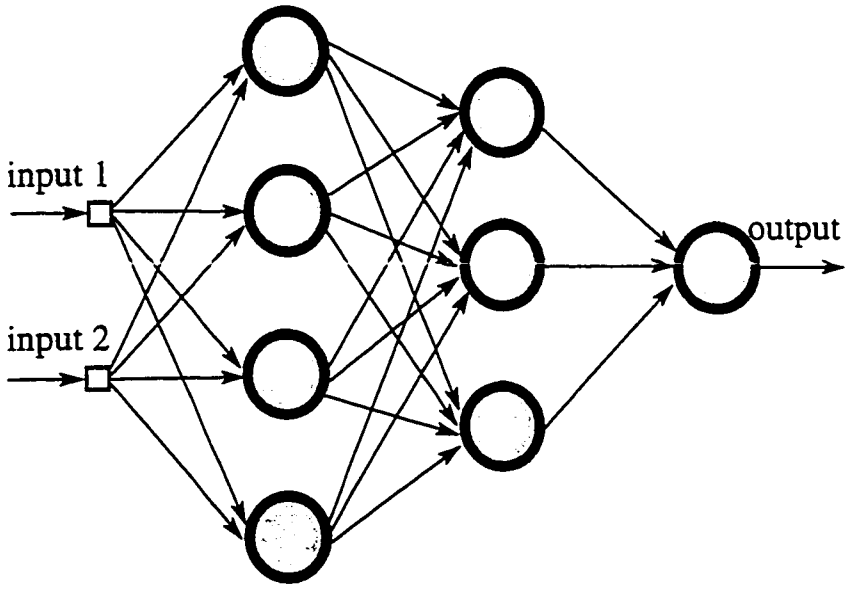

Figure 2.3: A sample two hidden layers feedforward network

collection of processing units connected only in forward direction by links of variable weights. A schematic illustration of a sample feedforward network with two hidden layers is shown in Fig. 2.3. A *recurrent* network distinguishes itself from a feedforward network in that it has at least one feedback loop.

One of the most important properties of ANNs lies in the fact that they learn from examples, rather than being programmed. Knowledge is acquired by the network through a learning process in which a number of input/output pairs are presented to the network. The procedure used to perform the learning process is called *learning algorithm*. The function of learning algorithm is to modify the network parameters in a way that the network would be adapted to the presented information.

2.3.2 Benefits of Neural Networks

A neural network derives its computing power through its massively parallel distributed structure and its ability to learn and generalize. The use of neural networks offers a variety of useful properties and capabilities. Some of the potential benefits of ANNs include [35]:

- Nonlinearity: A neuron is basically a nonlinear device. Consequently, a network made up of interconnection of neurons, is itself nonlinear. A properly trained neural network can perform highly nonlinear mappings.
- Learning: Neural network can learn from the interaction with the environment; it learns from the examples by constructing an input/output mapping for the problem at hand.
- Generalization capability: If a network is trained properly, it would be able to generalize the training information to similar situations which it has never experienced before.
- Complex mappings: Neural networks can synthesize complex mappings which may be very difficult or even impossible to be expressed in mathematical form.
- Robustness and fault tolerance: Neural networks are robust. Even if the input data is incomplete or noisy, the network can still provide satisfactory results. Due to distribution of computational load across many processing units, the network possess some degree of fault tolerance with respect to processor failures.

- High speed: Due to the parallel mechanism, once a neural network is trained, it can provide the ability to solve the mapping problem much faster than conventional methods and other intelligence methods such as expert systems.

2.3.3 Neural Networks Applications in Power Systems

Artificial neural networks have made a significant impact on the industry with the applications in various areas such as process control, optimization nonlinear process and human operator modeling, automatic plant knowledge elicitation and fault detection and monitoring [38].

The application of neural network approach in the power engineering area has a relatively short time span of about 10 years [27, 39]. Various applications have been tried and some field implementations have been realized [40]. However, the initial implementation activity was not equally strong in different countries. Some countries, in particular Japan, were leading in terms of number and variety of implementations [41].

Some applications of artificial neural networks in the power engineering area include [27, 39, 42, 43]:

- Load forecasting
- Power system monitoring and control
- Economic load dispatching
- Unit commitment
- Security assessment

- Power system protection
- Fault detection and classification

2.3.4 Use of Neural Networks in Power System Protection

The number of neural networks applications in power engineering is quite impressive. However, the implementations are not equally spread over the power system applications [40]. While in some areas such as load forecasting a number of practical solutions may have already been implemented, some other areas such as protective relaying and fault analysis are still at an exploratory stage [27].

Neural networks techniques have been proposed by different researchers for solving different power system protection problems. Most of the proposed ANN-based protection algorithms use voltage and current signals in one form or another as the inputs to the network. Using the provided information to the network, the network is trained to learn different patterns presented to it. The trained network is then used to distinguish between different power system conditions. Based on its application, the trained network could be used by the protection system to perform different tasks such as fault detection and classification, fault location and fault direction identification.

The structure of a neural network is application specific. Structural differences might come on account of the number and type of inputs, number and type of outputs and the complexity of the application which would then govern the number of layers and the number of neurons in different layers. These parameters of the network are decided by experimentation which involves training and testing a number of network

configurations. The process is terminated when a suitable network with satisfactory performance is established.

With the recent advances in the area of ANNs, many different ANN architectures and learning methods have been proposed. ANN techniques have been used in power system protection and encouraging results were obtained in various areas such as [9, 28]:

- Transmission line Protection
- Transformer protection
- Generator and Motor protection
- Fault detection and classification
- Fault direction identification
- Fault locating
- High impedance fault detection
- Adaptive autoreclosure

A Neural network is an interconnection of simple computing elements. As these computing elements involve additions and multiplications the network can be implemented on some commonly used processors in digital protection area, e.g. digital signal processors.

2.4 Directional Relay Algorithms

2.4.1 Digital Techniques and Their Limitations

Various digital techniques have been proposed in the literature by different researchers to accomplish the task of transmission line directional relaying. Some of these algorithms are summarized in Refs. [14, 26, 44]. Some of the proposed algorithms use postfault voltage and current phasors following a fault on the system, while others use incremental voltage and current signals.

One of the algorithms using postfault voltage and current signals is presented in Ref. [45]. The proposed algorithm makes use of fundamental frequency components of compensated voltages to make a decision. The direction of a fault is determined by phase angle comparison between two phasors of the compensated voltages. Fundamental frequency components are extracted using one cycle Fourier algorithm. In this algorithm extensive signal processing is used to process the input signals and make a decision. It takes up to 24 *ms* to determine the fault direction. For faults with fault resistance more than 33% of the line impedance, this algorithm may not operate correctly [45].

In recent years, protection principles have been developed which are capable of determining the fault direction from the evaluation of nonsteady-state variables [8]. The inception of a fault on a transmission line causes the voltage and current signals to deviate from their pre-fault values to their post-fault values. Some directional algorithms use the deviation signals of the voltage and current, i.e. Δv and Δi. These deviation signals are the signals which would result at the measuring location

if a voltage equal and opposite to the pre-fault voltage is imposed at the fault location. The deviation signals consist of three major components including system frequency, decaying dc and traveling wave components.

Some high speed algorithms use traveling wave components present in the deviation signals [14]. A constraint associated with protection principles utilizing traveling waves is inadequacy of standard current and voltage transformers in terms of high frequency response. It has been shown that the relaying decisions made on the basis of traveling wave components are valid just for a very short duration and are also quite sensitive to noise in relaying signals and transducers [46]. Another basic problem is that traveling waves of sufficient magnitude are not generated for a fault at zero voltage. Also, extremely high sampling rates, of the order of 13 *kHz* are required [14].

The Vitins algorithm considers the fault trajectory in the Δv-$K\Delta i$ plane, where K is a constant [47]. For a forward fault the trajectory moves from the origin into the second or fourth quadrant depending on the fault incidence angle. A reverse fault moves from the origin into the first or third quadrant. A decision about the direction of a fault is based upon whether the trajectory crosses appropriate thresholds in the Δv-$K\Delta i$ plane. This algorithm apart from its starting point is more based on the non-traveling wave components. The current deviation signal includes a dc component. The magnitude of the decaying dc component is a function of fault incidence angle which is not known in advance. Due to the dc component it is not possible to define an operating characteristic with a constant reach in the Δv-$K\Delta i$ plane.

A different approach using the power system frequency of the deviation signals is proposed in [48]. This approach proposes an improvement to the algorithm described

in [47]. The constant K is set equal to a replica source impedance Z_p. The power frequency components of Δv and Δi are related by the source impedance for a forward fault. If the current deviation signal is made to flow through the replica impedance, a voltage difference is obtained which can be used in conjunction with the Δv to determine the fault direction. These two signals are in phase or in anti-phase with each other depending upon whether the fault is in front or behind of the relay location.

Both of the algorithms presented in Refs. [47, 48] as well as some other similar methods reported in the literature [14, 44], do not have the ability to adapt dynamically to the system operating conditions. These algorithms have operating characteristics in the form of trajectories which depend upon some parameters such as source impedance and fault resistance. Certain assumptions about the system conditions have to be considered for setting the operating characteristics of the relay. If the system conditions become different the performance of the algorithm will be affected and the relay may not respond correctly.

2.4.2 ANN-Based Directional Algorithm

For the problem of transmission line directional relaying, the direction of various kinds of faults at different locations of the line and under different system conditions should be identified. Complex interactions exist amongst voltage and current signals of different phases of the transmission line. Neural networks are able to model complex nonlinear functions and have generalization capability. These capabilities makes them a suitable candidate for solving directional relaying problem using current and

voltage signals as the inputs. Neural networks techniques have been used and ANN-based directional modules are proposed. The proposed modules are discussed in detail in the following chapters.

2.5 Summary

The current and voltage waveforms during a short circuit in a power system are distorted. To determine whether the system is faulty or healthy, an extensive amount of filtering is performed by some digital algorithms to obtain accurate estimates of phasors. This prevents the relay from making a quick trip decision. These algorithms are not able to adapt to the system operating conditions. Neural networks could be considered as a new approach for solving power system protection problems. Inclusion of a neural network in a protection scheme allows the direct use of instantaneous data to determine the state of the power system. In addition, the data window can be quite short and does not need to satisfy particular rules as in the case of digital techniques [9, 27]. This approach maintains the advantages which are inherent in ANNs, such as robustness, speed and generalization capability.

Chapter 3

Directional Protection using Feedforward Neural Networks

3.1 Introduction

Faults on transmission lines need to be detected, classified and cleared as fast as possible. Moreover, the fault direction should be identified. In this chapter a new approach to the transmission line fault direction identification problem is presented and its effectiveness is demonstrated.

Artificial neural networks, composed of many simple neuron-like processing units, have been studied for many years. It has been shown that they are powerful in pattern recognition and classification and can draw complex decision boundaries. To classify forward and backward faults on a given transmission line, neural network's abilities in pattern recognition and classification could be considered as a solution. To demonstrate the applicability of this solution, neural network technique is employed and two feedforward networks are designed and trained.

Details of the design procedure of the two neural network-based directional modules are given in this chapter. Results of performance studies with the proposed modules are also presented in the chapter.

3.2 A Feedforward ANN-Based Directional Module

A feedforward network has been designed to act as the fault direction identification module of a transmission line relaying system. Details of the design procedure are given below.

3.2.1 Power System Model

The training data set of an ANN should contain the necessary information to generalize the problem. Using an electro-magnetic transient program, EMTDC [49] a three phase 240 kV sample power system was simulated and the input/output pair patterns for training and testing the network were generated. A brief introduction about EMTDC program is given in Appendix A.

The one-line diagram of the modeled power system is shown in Fig. 3.1. The simulated power system consists of two equivalent sources labeled as sending-end and receiving-end sources and two 100 km transmission lines connected in series in between the sources. The transmission lines are modeled by frequency dependent parameters and have two conductors per bundle. Details of the transmission lines parameters are given in Appendix B.

The measurement devices are located at the point of connection of transmission lines and look forward towards the receiving-end source. Thus, the line section between the relaying point and the receiving-end source is the forward protection zone and the line section between the relaying point and the sending-end source is the backward line section. Faults in the forward protection section are called forward faults whereas faults occurring on the opposite side of the relay are labeled

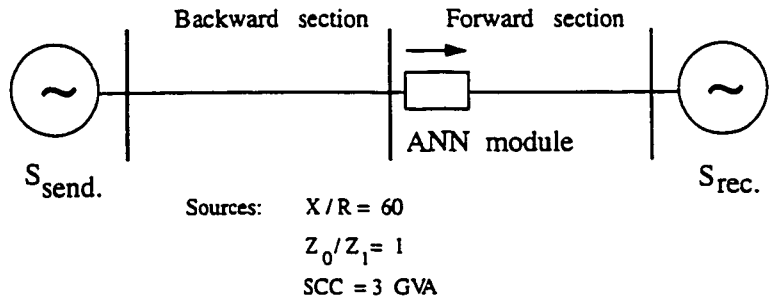

Figure 3.1: One-line diagram of the power system model

as backward faults.

Training patterns were generated by simulating different types of faults on forward and backward regions of the power system. Different parameters and conditions such as fault location, fault resistance, fault inception time and pre-fault power flow direction were changed to obtain training patterns belonging to a wide range of different conditions of the power system. Faults including high amount of resistance, up to 100 Ω, were also considered. In total, 7200 patterns were generated for training the directional neural network.

3.2.2 Input Selection of the Network

Most of the necessary information for determining the disturbances and transients in power systems is usually contained in the voltage and current waveforms. Moreover, being measured by VTs and CTs, the voltage and current waveforms are the most available information in power systems. Therefore, the sampled normalized voltage and current signals measured at the relay location were considered as the input information to the neural network. However, the raw data is often noisy and might provide redundant information. In addition, when a fault occurs on a transmis-

sion line, voltage and current signals develop a decaying dc offset component whose magnitude depends on many factors that are random in nature.

In a pattern recognition/classification problem it is important to represent the raw input data set by a reduced number of effective features while retaining most of the intrinsic information content of the data. In other words, the data set should undergo a dimensionality reduction.

Pre-processing is an useful method to reduce the dimensionality of the input data set. A simple wide 2nd-order Butterworth bandpass filter was used to attenuate the dc component and high frequency noise. The amplitude response of the filter is shown in Fig. 3.2. The passband of the filter is chosen to be 80 Hz. This value allows a considerable reduction of the high frequency and dc components with a small time delay. This pre-processing enhances the training capabilities of the network and decreases the number of required patterns for training the network.

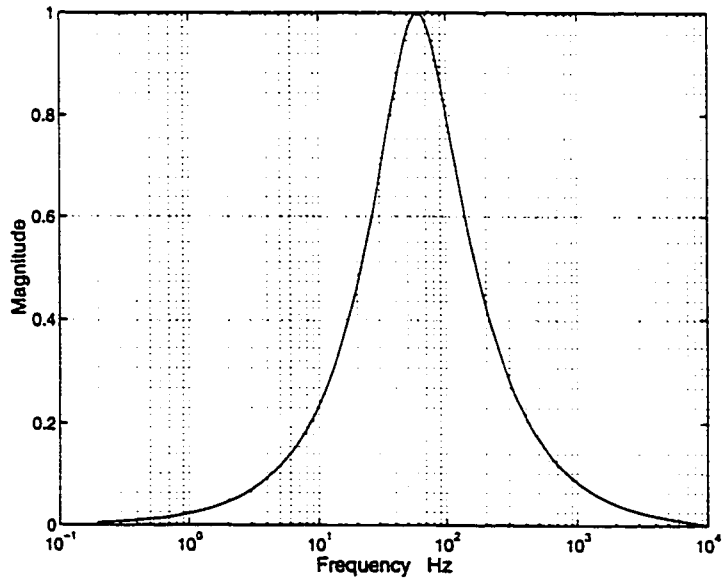

Figure 3.2: Amplitude response of the bandpass filter

It is common to use consecutive samples of all three phase voltages and currents as the inputs to the neural network [50, 51, 52]. To ensure that the network is able to estimate the fault direction in a timely fashion, three phase voltage and current waveforms were sampled at a rate of 20 samples/cycle in this application. This sampling rate is compatible with the sampling rates commonly used in digital relays.

The appropriate data window length is also a major factor which should be considered. It was decided to cover the information of 1/4 of the cycle of the voltage and current inputs. Thus, each phase voltage and current was represented by its 5 consecutive samples. This data window length meets both requirements of speed and reliable operation. Hence, the network's input consists of:

$$i_a(n)T, i_a(n-1)T, ..., i_a(n-4)T, \quad v_a(n)T, v_a(n-1)T, ..., v_a(n-4)T$$
$$i_b(n)T, i_b(n-1)T, ..., i_b(n-4)T, \quad v_b(n)T, v_b(n-1)T, ..., v_b(n-4)T$$
$$i_c(n)T, i_c(n-1)T, ..., i_c(n-4)T, \quad v_c(n)T, v_c(n-1)T, ..., v_c(n-4)T$$

A 30-input network with a single neuron output layer was chosen as the fault direction identification network. The network needs just one output to classify between forward and backward faults. The network's output should be $+1$ for the case of forward faults and -1 for the case of backward faults.

With the 30-input neural network, each input pattern of the sampled current and voltage signals could be represented by a point in a 30-dimensional Euclidean space. The decision surface would be a hyper-surface in the 30-dimensional space. The neural network classifies different input patterns to identify the direction of a fault on a given transmission line.

3.2.3 Training Algorithm

Back-propagation (BP) is one of the most popular learning algorithms. The convergence of BP learning algorithm progresses slowly in general. To speed up the convergence of the algorithm, many techniques have been proposed . These techniques roughly fall into two categories. The first category includes such ideas as varying the learning rate, using momentum and rescaling variables. The second category of research has focused on numerical optimization techniques. The most famous approaches from this category have used conjugate gradient or quasi-Newton methods.

While back-propagation is a steepest descent algorithm, the Marquardt-Levenberg (ML) algorithm is an approximation to the Newton's method. Gradient descent is simply the technique where parameters such as weights and biases are moved in the opposite direction to the error gradient. Each step down the gradient results in smaller errors until an error minima is reached. The rate of convergence could be slightly increased by using momentum or varying the learning rate. ML algorithm, on the other hand, is a nonlinear least squares algorithm applied to the batch learning of multilayer perceptrons. The key step in the ML algorithm is the computation of Jacobian matrix [53]. The ML algorithm update rule for the weight change , Δw is:

$$\Delta w = [J^T(w)J(w) + \mu I]^{-1} J^T(w)e(w) \tag{3.1}$$

where $J(w)$ is the Jacobian matrix of derivatives of each error to each weight, μ is a scalar and $e(w)$ is the error vector. When μ is large, the algorithm becomes steepest descent, while for small μ the algorithm becomes Gauss-Newton.

If enough memory is available, the ML algorithm can result in dramatically reduced training times in comparison with the required training times for either of the variable learning rate and conjugate gradient algorithms. It has also been found that in many cases the ML algorithm converged, while the variable learning rate and conjugate gradient algorithms failed to converge [53]. The major drawback of the ML algorithm is that it requires more memory. For very large networks, the memory requirements of the algorithm make it impractical for some of the current available computers. However, for networks with a few hundred weights the algorithm is very efficient [53]. A brief description of BP and ML training algorithms is given in Appendix C.

3.2.4 Suitable Network Structure

A few different network structures, all having 30 inputs and one output but with different number of neurons in their hidden layers were considered and trained. Training and test patterns were generated by simulating different types of faults on forward and backward regions of the simulated power system.

In basic terms, for multilayer perceptrons differentiability is the only requirement that an activation function would have to satisfy. On the other hand, a multilayer perceptron trained with the back-propagation algorithm in general learns faster when the sigmoidal activation function is asymmetric than when it is nonsymmetric [35]. The activation function $\phi(v)$ is asymmetric if:

$$\phi(-v) = -\phi(v) \tag{3.2}$$

A popular example of an asymmetric function is a sigmoidal nonlinearity in the

form of a *hyperbolic tangent*, defined by:

$$\phi(v) = atanh(bv) \tag{3.3}$$

where a and b are constants. The following function is used as the activation function of the neurons of the network used in this study:

$$tanh(2v) = \frac{2}{1 + exp(-2v)} - 1 \tag{3.4}$$

Various networks considered were trained both with the BP and the ML algorithms. It was found that the networks trained with the ML algorithm provide better results compared with the results of the networks trained with the BP algorithm. Although the computational requirements are much higher for each iteration of the ML algorithm, this is more than compensated by the increased efficiency of the algorithm. The ML algorithm is capable of reducing the network error to a pre-specified value in just about 60 epochs, while the BP algorithm needs a few thousands epochs to decrease the error to the same level. In some cases, even after many thousands of epochs, the BP algorithm is not able to decrease the error to the same level as obtained by the ML algorithm. Therefore, it was decided to use the ML training algorithm for this application.

Different networks with one and two hidden layers were considered and their performance was evaluated in terms of computational requirements, generalization capabilities and response time. It was found that the networks with reasonable number of neurons in one hidden layer can not cover some of the extreme cases such as faults with very high amount of resistance and faults near the relay location. On the other hand, networks with two hidden layers provide better results without

having to have high number of neurons in their hidden layers. The network which showed satisfactory results, while not having a big size, had 30 inputs, 10 neurons in the first hidden layer, 5 neurons in the second hidden layer and one output, fully connected in feedforward structure. Simulation tests were carried out to evaluate the performance of the ANN-based algorithm under different fault conditions and some of the simulation results are presented in the next section.

3.3 Test Results

The proposed neural network was tested with different independent test patterns and promising results were obtained. The results show that the identification of the fault direction by the network is very fast. In most cases, the network is able to classify the fault direction correctly during first two sampling times after the inception of the fault. Determination of fault direction is not affected by the type and location of the fault, fault inception time, pre-fault power flow condition, and the presence of fault resistance.

As an example, the network's output for four different types of forward faults applied at far end of the protection area is shown in Fig. 3.3. In this case the fault location was 95 km from the relay location, with fault resistance of 50 Ω, pre-fault power direction from sending-end to receiving-end and fault inception time 9 ms after phase A voltage zero crossing. For each fault, the output of the network is shown during the first cycle (20 samples) after fault inception at sample number 1. Different faults involve different phases and ground as well. Fault type ag indicates a single phase to ground fault (phase A to G), while fault type ab indicates a phase

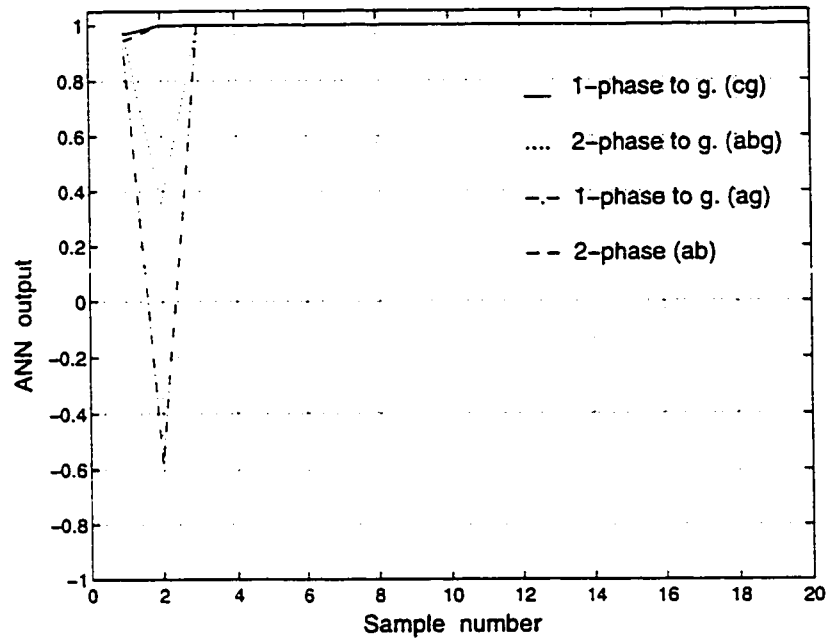

Figure 3.3: 30-input ANN response to forward faults at 95 km, fault resistance 50 Ω, power direction from send. to receiv., inception time 9 ms

to phase fault (phase A to phase B).

In all cases, the directional network correctly identifies the fault direction. After the fault inception, for some cases the network's output might oscillate for a very short time. However, in all cases the network's output becomes equal to 1 two samples after the inception of the fault and then remains stable. Thus, the network identifies the fault direction as forward fault. It shows that the proposed directional module performed correctly and rapidly for far end faults even in the presence of high fault resistance.

The next example tests the network's performance for different types of backward faults on the power system. The network's output for four types of backward faults at 80 km from the relay point is shown in Fig. 3.4. This figure shows that the determination of fault direction is very fast and reliable.

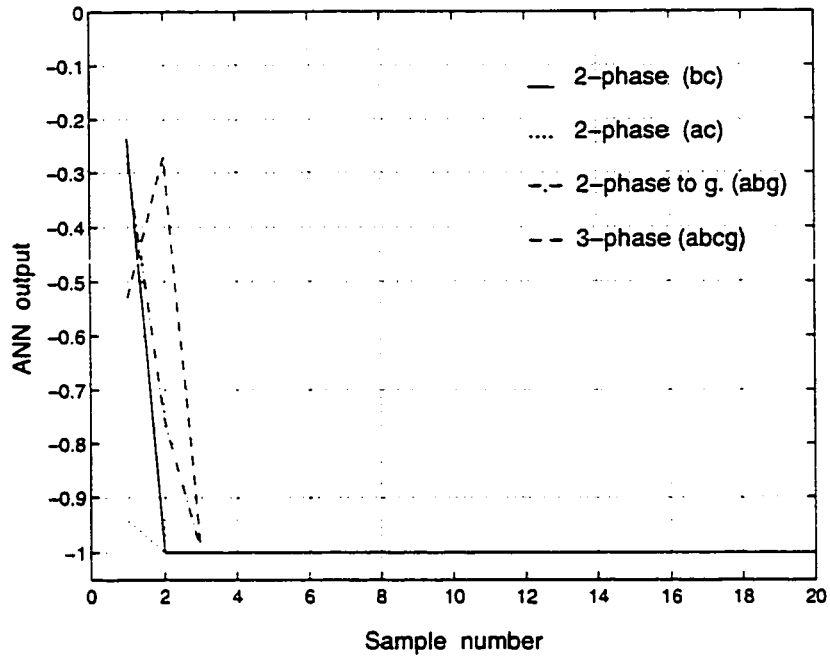

Figure 3.4: 30-input ANN response to backward faults at 80 *km*, fault resistance 50 Ω, power direction from send. to receiv., inception time 14 *ms*

Different types of faults including 1-phase to ground faults *(A-G, B-G, C-G)*, 2-phase to ground faults *(A-B-G, A-C-G, B-C-G)*, 2-phase faults *(A-B, A-C, B-C)* and 3-phase to ground fault *(A-B-C-G)* may occur on a transmission line.

Under the same conditions as those presented in the previous example different backward faults were applied and the output of the feedforward network is shown in three-dimensional space in Fig. 3.5. Using three-dimensional plots makes it possible to show the output of the network for various types of faults at the same fault location.

The network's output for different types of forward faults on transmission line at 50 *km* from the relay location is shown in Fig. 3.6. The directional network identifies the fault direction correctly and rapidly for different types of faults.

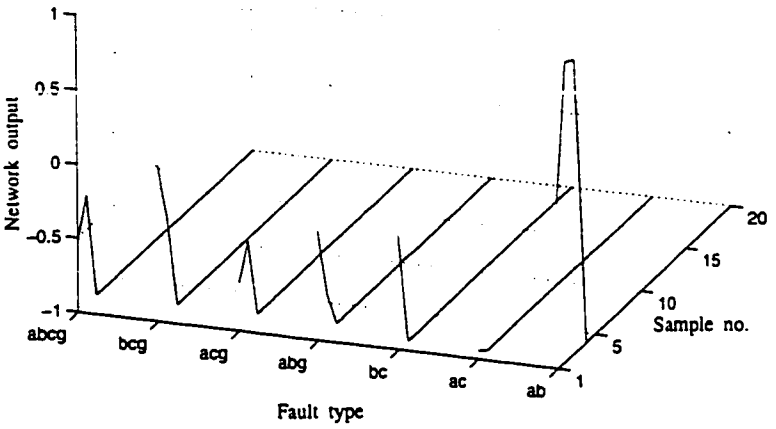

Figure 3.5: 30-input ANN response to backward faults at 80 km, fault resistance 50 Ω, power direction from send. to receiv., inception time 14 ms

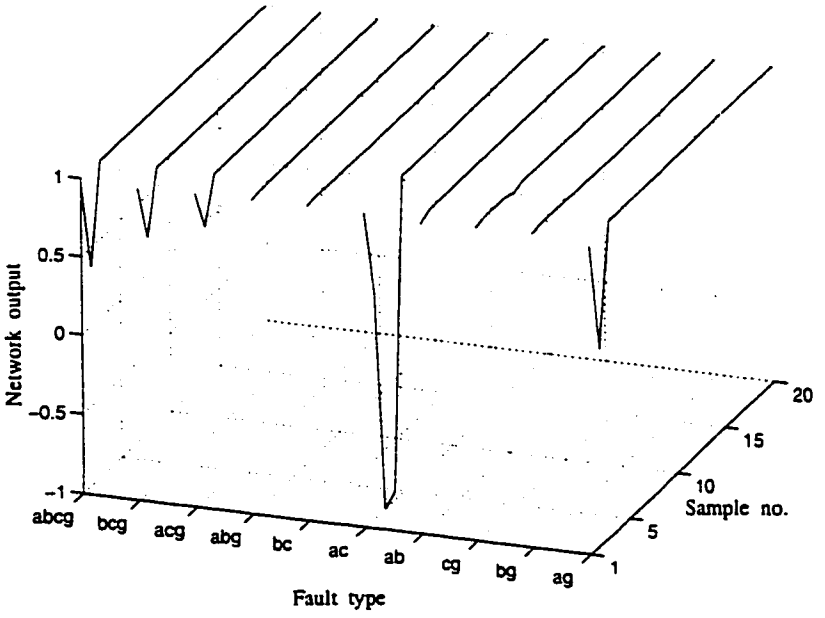

Figure 3.6: 30-input ANN response to forward faults at 50 km, fault resistance 50 Ω, power direction from send. to receiv., inception time 9 ms

In order to further increase the reliability of the fault direction decision, four consecutive outputs of the network may be averaged. Averaged outputs of this post-processing unit which fall above 0.5 and below -0.5 are interpreted as forward and backward faults, respectively.

To demonstrate the direction identification network's capabilities including a post-processing moving average filter, different types of backward faults were applied using the same condition as the case presented in Fig. 3.5. Fig. 3.7 shows the network output with output averaging, while the network output without averaging is shown in Fig. 3.5.

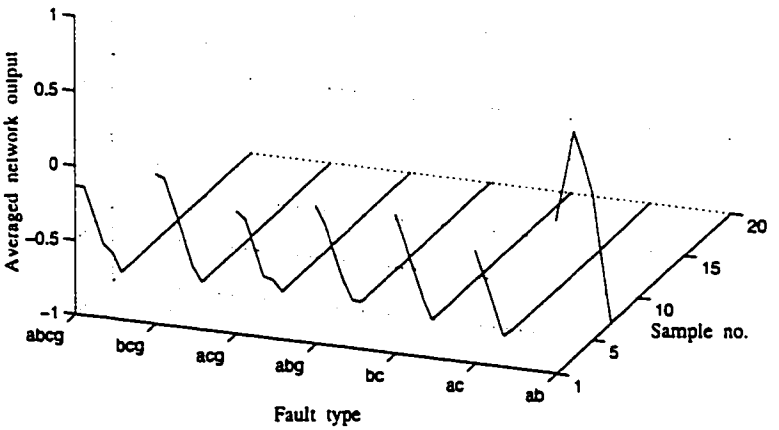

Figure 3.7: 30-input ANN averaged response to backward faults at 80 km, fault resistance 50 Ω, power direction from send. to receiv., inception time 14 ms

The directional module output is set equal to zero prior to the fault inception time. For the first samples after the fault inception, the post-processing unit averages network's output with zeros. Therefore, the speed of the direction decision initially

decreases. For the faults shown in Fig. 3.7, it takes at most six and at least two samples after the fault inception for the output of the moving average filter to fall inside the backward fault area. On average the directional module including an output averager needs just about 2.5 *ms* to classify the fault direction correctly, even for the case of the fault at the end of transmission line with high resistance which is slow in nature.

3.4 A New Network using Less Inputs

3.4.1 Feature Selection

Neural networks have the ability to classify different input patterns into desired output classes. The application of a pattern classification technique requires a selection of features that contain the information needed to discriminate between classes, and which permit efficient computation to limit the amount of the required training data and size of the network. In general, whether or not a feature can be selected is problem dependent.

A key problem in pattern recognition/classification is to represent the raw input data set by a reduced number of effective features and yet retain most of the intrinsic information content of the data. In other words, the data set should undergo a dimensionality reduction in the feature selection stage.

Pre-processing is an useful method to reduce the dimensionality of the input data set. Principal Component Analysis (PCA) provides another technique for dimensionality reduction [35]. The main idea in PCA technique is to project each

waveform along its eigenvectors and only retain the projections corresponding to the principal eigenvalues of the covariance matrix of the input waveforms. If a few of the eigenvectors contain a majority of the overall energy, then the dimensionality of the data can be greatly reduced, without losing much information.

Ref. [54] describes a novel method for input variable selection for artificial neural network-based short-term load forecasting. To test the viability of the method, real load data for two US-based electric utilities are used. Results obtained compare favorably to the ones reported in the literature, indicating that more parsimonious set of input variables can be used in load forecasting without sacrificing the accuracy of the forecast. This allows more compact ANNs, smaller training sets and easier training [54].

3.4.2 Input Selection for a New Network

The direction of a fault on a transmission line can be determined from the relative phase angles of the voltage and current phasors. Voltage is usually used as the reference polarizing quantity. The fault current phasor lies within two distinct forward and backward regions with respect to the reference phasor, depending on the power system and fault conditions. The neural network-based directional identifier does not explicitly use the phase information to make its decision. It uses samples of the voltage and current waveforms and tries to learn and recognize the hidden relationships that may exist in the input patterns.

It is common to present samples of all three phase voltage and current information to the classification network as its inputs. However, there may be some redundant

information in this whole set of inputs. The network may be able to use a subset of the voltage and current data to identify the direction of the fault. In such a case, the network's size would be reduced and a smaller size network with less number of connection weights could perform the direction estimation job.

Different types of forward and backward faults were applied to the power system and the voltages and currents at the relay location were studied. Fig. 3.8 shows the filtered voltage and current of phase A for two different forward and backward faults. All other conditions, like fault location, fault resistance, phases involved in the fault and pre-fault power direction are similar for these forward and backward faults. Both faults were applied at time 212 ms. As is shown in the figure, both pre-fault voltages and pre-fault currents are the same for both cases. Post-fault voltages are very similar for forward and backward faults, while post-fault currents are about 180 degrees out of phase. Investigations reveal that the forward and backward fault voltages of the other two phases have very similar pattern as well.

It seems that for this example the input voltages provide the same information to the network for both cases of forward and backward faults. Therefore, it might be concluded that the network should be able to distinguish between different input patterns without using the voltage inputs. However, more studies indicate that just current inputs do not provide enough information to the network to distinguish between forward and backward faults in all possible combinations of different conditions the power system may encounter.

Fig. 3.9 shows the filtered current and voltage of phase A for two different forward and backward faults. In this case, all conditions for the two faults were the same except that for the first fault the pre-fault power flow direction was from sending-end

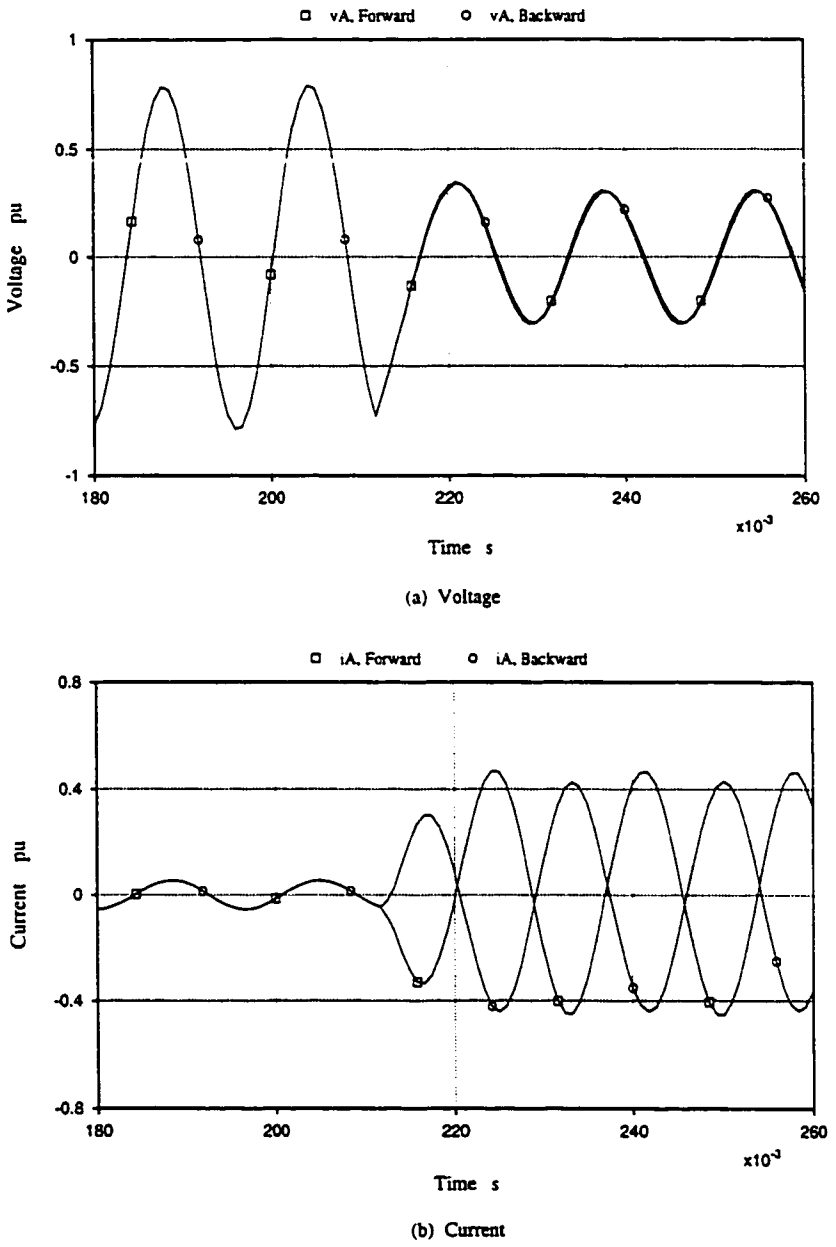

Figure 3.8: Normalized filtered voltage and current of phase A for two different forward and backward faults with identical system conditions

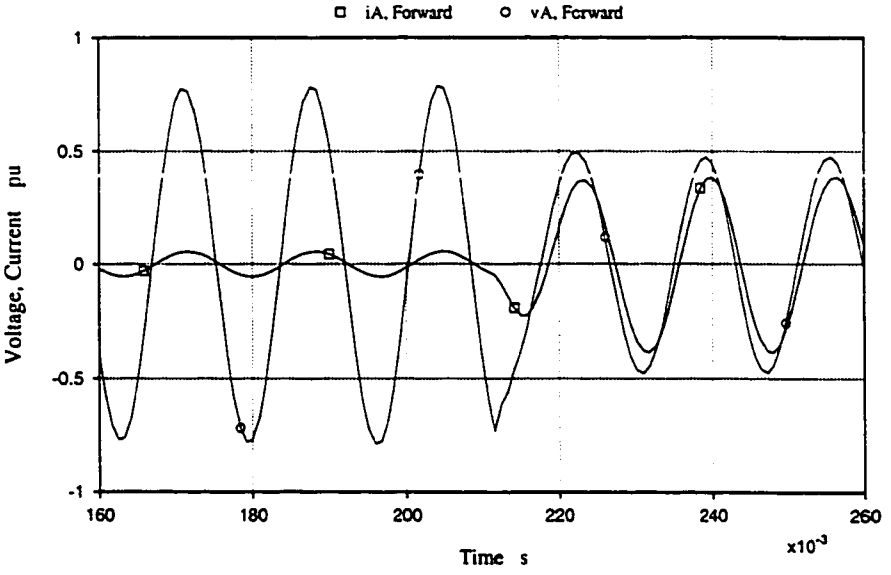

(a) Forward

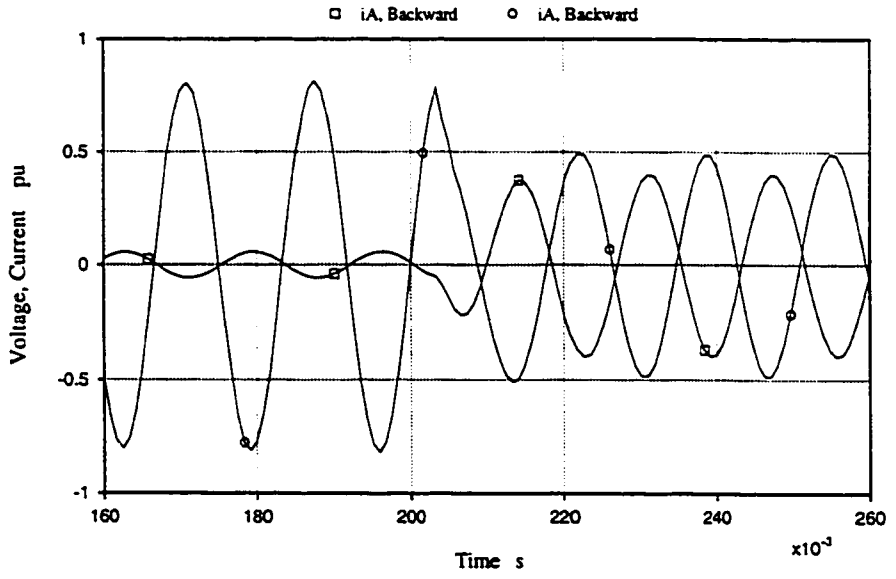

(b) Backward

Figure 3.9: Normalized filtered voltage and current of phase A for two different forward and backward faults with different power flow directions and fault inception times

to receiving-end , while for the other fault the direction was from receiving-end to sending-end. Moreover, for the forward case, the fault was applied to the system at time 214 ms, while for the backward case the fault hit the power system about half a cycle earlier. As shown in Fig. 3.9, forward and backward faults have different inception times. However, considering its own inception time as the origin in each case, both pre-fault and post-fault currents for the two cases have a very similar pattern. Therefore, the network using just current information inputs may become confused in identifying these two cases.

Phase A voltage for the two cases is also shown in Fig. 3.9. It is clear that the two waveforms are different after the fault inception times. So, they could provide some extra information to the network to help it to distinguish between these two different cases. It shows that for a fault directional module a voltage signal is required as a polarizing reference, thus supporting the theory used in classical directional relays.

Extensive studies were performed and it was found that a feedforward network, which uses all three phase currents information but just one phase voltage information is able to classify forward and backward faults correctly. The phase A voltage was used in this case as the reference.

3.5 Reduced Size Network Simulation Studies

3.5.1 Test Results

A few different network structures, all having 20 inputs (5 consecutive samples of all currents and just one of the voltages) and one output but with different number of

neurons in their hidden layers were considered and trained. A new network with 20 inputs, two hidden layers with 10 and 5 neurons, respectively and a single neuron output layer showed satisfactory results and was considered for the studies in this section.

The new network was trained using the ML training algorithm. Compared with the previous 30-input network, the new 20-input network has a smaller size. As a result, the memory and computational requirements are reduced and therefore, the network training time for each iteration decreases considerably. Also the new network's convergence speed is faster. Compared with the number of epochs needed for the previous 30-input network, the new smaller network needs 30% less number of epochs to reduce the error to the same level. For the same number of epochs, the validation set error for the smaller network is 15% less. Therefore, the new network not only has a smaller structure, but also provides better quality compared with the network which uses all three phase currents and voltages data. Due to a smaller size, the new network has less operation time as well.

To examine the capabilities of this new network, different faults were applied on the system and some of the test results are presented. The network output for different backward faults at 70 *km* behind the relay point is shown in Fig. 3.10. The network is able to classify faults with 100 Ω fault resistance very fast.

With the same condition as the case presented in Fig. 3.5, the network response for the same backward faults is shown in Fig. 3.11. This figure shows that the network responds very fast and correctly. Moreover, comparing Fig. 3.11 with Fig. 3.5, it is found that the new network performed faster than the previous 30 inputs network.

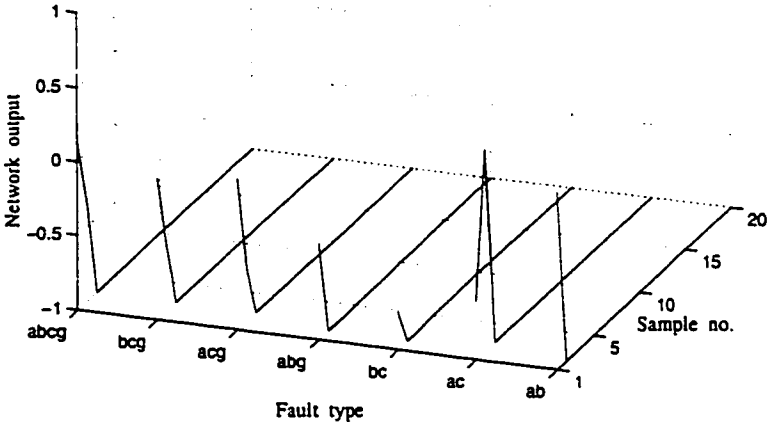

Figure 3.10: 20-input ANN response to backward faults at 70 km, fault resistance 100 Ω, power direction from receiv. to send., inception time 9 ms

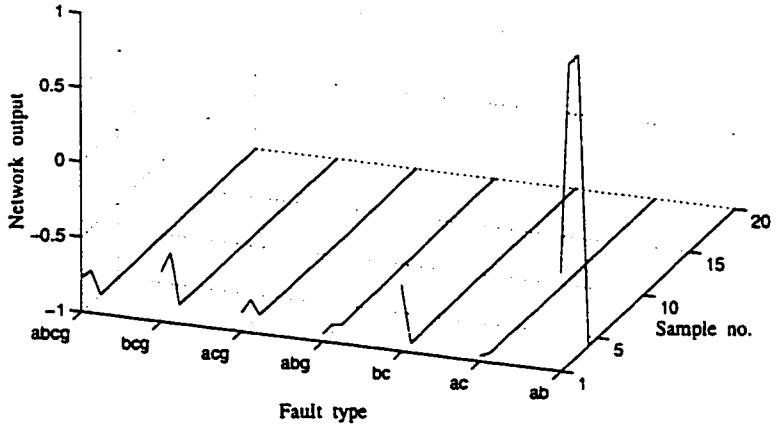

Figure 3.11: 20-input ANN response to backward faults at 80 km, fault resistance 50 Ω, power direction from send. to receiv., inception time 14 ms

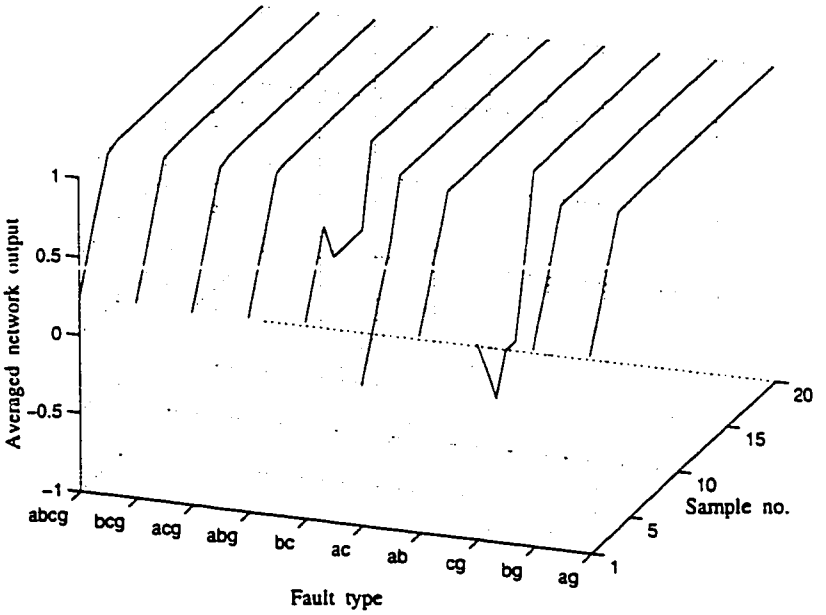

Figure 3.12: 20-input ANN averaged response to forward faults at 95 km, fault resistance 50 Ω, power direction from send. to receiv., inception time 3 ms

The network was tested for faults at 95% of the transmission line's length. The averaged output of the network is shown in Fig. 3.12. It shows that the network performed correctly for the far end faults even in the presence of high amount of fault resistance.

Using conventional methods, it is not easy to identify the direction of faults that occur near the relay location [50]. Different faults with a small amount of resistance were simulated at 5% of the line's length on the backward area of the power system and the network's performance is presented in Fig. 3.13. It shows that the network is able to classify the faults near the relay location correctly in a timely fashion. The average time needed to classify the fault direction is less than 2.5 ms.

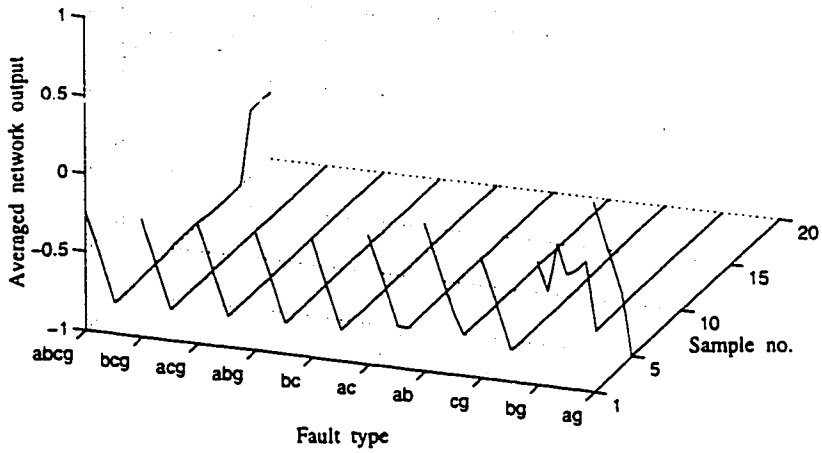

Figure 3.13: 20-input ANN averaged response to backward faults at 5 km, fault resistance 5 Ω, power direction from receiv. to send., inception time 12 ms

3.5.2 Faults at the Relay Location

Identification of the direction of faults which occur at the relay location is a difficult task. For the faults at the relay location, depending upon the fault type, input voltages to a directional module may become zero which might cause maloperation. For a three phase to ground fault all the voltages go to zero. The directional module input voltages initially remain non-zero due to the front-end anti-aliasing filters. However, the output of the anti-aliasing voltage filters goes to zero after some time from fault inception time. Memory action can be used in the design of a fault directional module in order to properly discriminate the fault direction with zero input voltages.

The capabilities of the directional network were also examined for faults at the

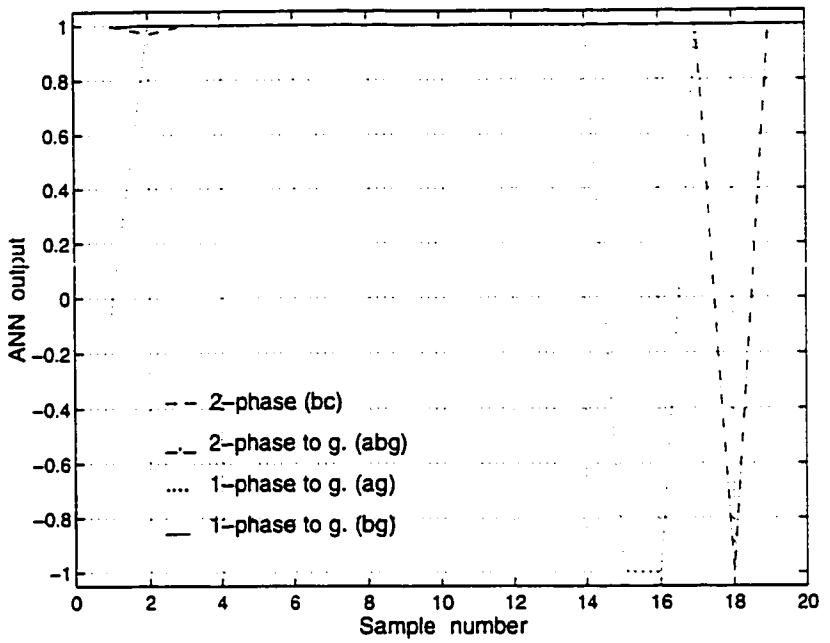

Figure 3.14: 20-input ANN response to forward faults at the relay location, fault resistance 1 Ω, power direction from send. to receiv., inception time 12 ms

relay location. The output of the network for different types of forward faults at the relay location is shown in Fig. 3.14. After fault inception the network initially identifies the fault direction correctly in all cases. However, for some cases after some time the output of the network begins to oscillate.

Through different studies it was found that the network is able to correctly identify the fault direction for faults at the relay location for at least half cycle after the fault inception.

3.5.3 Directional Relay

The directional relay has two components. The first component is the proposed neural network-based fault direction discrimination module. The second component

is a fast fault detector module which works in parallel with the ANN-based directional module. When the system is healthy, the fault detector output is zero and the directional module output is deactivated, i.e. set equal to zero.

When a fault happens in the system, the fault detector module senses the fault quickly and activates the output of the directional module. It was found through different tests that the fault detector module in most cases is able to detect the fault during the first two samples after the occurrance of the fault.

For the examples presented in this chapter, it was assumed that the fault detector instantly detected the fault after its inception and activated the directional module output. Thus, the time needed to identify the fault direction was determined by the directional module alone.

It is assumed now that for a fault case, the fault detector needs two sampling periods (about 1.7 ms) to detect the fault. So, it seems that the operation of the directional relay to detect the fault and discriminate its direction would be delayed by 1.7 ms due to this extra time for detecting the fault.

After the fault inception the output of the ANN-based directional module might oscillate for a short time before the input data window of the network enters the post-fault data region. During this period the currents and voltages of the faulty circuits have not increased/decreased considerably from their pre-fault values. This time period overlaps with the detection time of the detector module. When the detector module detects the fault, the directional module identifies the fault direction very fast without oscillation because the input data to the network are mostly from post-fault data. As a result, the delay in detecting the fault does not have much effect on the total operation time of the directional rely.

Different studies were performed using the fault detector and directional modules working together as a directional relay. It was found that the detection time of the detector module usually has a minor effect on the time needed to identify the fault direction.

3.6 Summary

A transmission line fault direction identification method based on neural network approach is described in this chapter. A feedforward network is designed and trained to act as the directional module of a transmission line relaying system. The designed neural network uses samples of all three phase voltages and currents to identify the fault direction. Simulation studies are performed and the performance of the ANN-based directional module is evaluated. Influence of changing different parameters such as fault type, fault location, fault inception time, pre-fault power flow condition and fault resistance on the network's performance is investigated. Results obtained indicate that the network is able to classify forward and backward faults very rapidly.

Next, a reduced size network using a subset of the voltage and current information is proposed as a fault directional module. Extensive simulation studies have been performed and promising results are obtained. Results obtained show that the proposed network is able to detect the fault direction very fast and reliably.

Chapter 4

A Recurrent Network Directional Module

4.1 Introduction

The direction of a fault on a transmission line needs to be identified rapidly and correctly. A fault direction discrimination problem on a transmission line can be treated as a pattern classification problem, and ANNs can be used for determining the direction of a fault on the given transmission line.

With the recent advances in ANNs, many different ANN structures and learning methods have been proposed. An important class of neural networks has a recurrent structure. This class of neural networks distinguishes itself from a feedforward network in that it has feedback loops in its structure.

In this chapter, a novel recurrent neural network is proposed to determine the direction of fault on transmission lines [55]. The proposed neural network uses instantaneous values of the three phase line currents and one of the phase voltages to make the decision. The ANN-based algorithm is tested and its performance is evaluated. Details of the design procedure and the results of performance studies with the proposed recurrent network are given and analysed in this chapter.

4.2 Temporal Processing

4.2.1 Feedforward Neural Networks

A standard neural network models a synapse by a single weight parameter. This way, the traditional model of the neuron can be considered as a static structure mapping input to output. A limitation of this model is that it only accounts for the spatial behavior of a neuron by incorporating a set of fixed synaptic weights at the input end of the model. A common configuration is to arrange a feedforward structure using the model neurons. While this increases the class of functional mappings, it is still a static mapping from input to output. This form of static input-output mapping is well suited for pattern recognition applications where both the input and output vectors represent spatial patterns that are independent of time. To extend the usefulness of this model for temporal processing, it is necessary to modify it so as to account for the temporal nature of the input data.

4.2.2 Temporal Sequence Processing

Time is clearly an important factor in many of the cognitive tasks encountered in practice. It is inextricably bound up with many behaviors which express themselves as temporal sequences. Thus, the question of how to represent time in connectionist models and, in particular, how to extend the design of a feedforward network so that it assumes a time-varying form and therefore will be able to deal with time-varying signals and sequences is very important. The answer to these questions is to allow time to be represented by the effect it has on signal processing. This

means providing the mapping network dynamic properties that make it responsive to time-varying signals [35].

In short, for a neural network to be dynamic, it must be given memory [56]. One way to accomplish this requirement is to introduce time delays into the synaptic structure of the network in one form or another. One popular technique which uses time delays is the Time Delay Neural Network (TDNN). TDNN is a multilayer feedforward network whose hidden and output neurons are replicated across time [57].

The TDNN topology is in fact embodied in a feedforward network in which each synapse is represented by a Finite-duration Impulse Response (FIR) filter. This latter network is referred to as FIR neural network. The FIR neural network uses temporal model of the neuron to construct a feedforward network [58].

4.2.3 Recurrent Neural Networks

Another way in which a neural network can assume dynamic behavior is to make it recurrent. A recurrent neural network distinguishes itself from a feedforward network in that it uses at least one feedback loop in its structure. Feedback is said to exist in a dynamic system whenever the output of an element in the system influences in part the input applied to that particular element.

Different types of recurrent networks have been proposed by different researchers. The difference between these networks lies in their structures and the way they handle the feedback. For example, a recurrent network may consist of a single layer of neurons with each neuron feeding its output signal back to the inputs of all the other

neurons. In this structure, there are no self-feedback loops in the network. Another class of recurrent networks uses both hidden neurons and self-feedback connections in their structure.

The presence of feedback loops has a profound impact on the learning capability of the network and its performance. The recurrent connections allow the hidden units of the network to see their own previous output, so that the subsequent behavior can be shaped by the previous response. These recurrent connections are what give the network memory. Moreover, the use of feedback loops results in a nonlinear dynamic behavior of the network by virtue of the nonlinear nature of the neurons.

Samples of phase voltage and current waveforms are usually used as the inputs to a neural network-based protective relay. The voltage and current are time-varying signals. Therefore, a network with temporal processing abilities should be considered.

The conventional static neural network architectures and algorithms are not well suited for patterns that vary over time. The prototypical use of neural networks is in structural pattern recognition. In such a task, the network uses a collection of features presented to it to classify the input feature patterns into different classes. In this method, the network is presented with all relevant information simultaneously. In contrast, temporal pattern recognition involves processing of patterns which evolve over time. In the present work, a novel recurrent neural network is proposed as the directional module of a transmission line protection system.

4.3 Proposed Recurrent Network Architecture

A neural network is a massively parallel distributed processor that has a natural propensity for storing experiential knowledge and making it available for use [35]. A key point is how to represent knowledge in the network. In real world applications of intelligent machines, including neural networks, it can be said that a good solution depends on a good representation of knowledge.

4.3.1 Knowledge Representation

A major task for a neural network is to learn a model of the world (environment) in which it is embedded. Knowledge of the world consists of two kinds of information [35], observation examples and the known states of the environment. Each example consists of an input and the desired output of the network. The known world state is represented by facts about what is and what has been known about the environment. This form of knowledge is referred to as prior information.

Learning from a set of training examples deals with an unknown input-output mapping function *f(.)*. In effect, the learning process exploits the information contained in the examples about the function *f(.)* to infer an approximate implementation of it. When feasible, learning from examples is a convenient approach. In many practical situations, some knowledge about the function *f(.)* is available. In these cases it would be inefficient to take blind examples without taking advantage of what is already known about the function.

A hint is any piece of information about the function *f(.)*. It may take the form of a global constraint on *f(.)* or may be partial information about its implementation.

The process of learning from examples may be generalized to include learning from hints, which is achieved by allowing the prior information that is available about the function *f(.)* to be included in the learning process [59, 60]. Such information may include any knowledge about the function *f(.)* that may be used to accelerate the search for its approximate realization [35].

4.3.2 Specialized Structure Network

Interneuron connections of the network are used to store the knowledge. The specialized structure built into the design of a neural network reflects prior information about the characteristics of the activation pattern being classified. Therefore, any information about the function can be used as a hint to structure the network.

An important issue that has to be addressed, of course, is how to develop a specialized structure by building prior information into its design. To do this, unfortunately there are no well defined rules. The manner in which the neurons of a recurrent network are structured and connected is problem dependent. One may use engineering judgment and analysis to find the suitable network structure for the problem at hand.

A specialized structure recurrent network is proposed next to perform as a transmission line fault direction detection module.

4.3.3 Fault Direction Detection Network's Structure

Samples of the voltage and current waveforms are used in a neural network-based direction detection relay to determine the fault direction. The network learns from

experience gained during training and recognizes the hidden relationships that exist in the pattern observed during the learning phase. An equation of the decision boundary describing the classification is embedded in the network.

When a fault occurs, the network should be able to initially recognize the fault direction and as the time passes the output of the network should remain stable for the incoming samples after the fault inception. The output of a feedforward network at each sampling time only depends on the input data set of the network at the same sampling time. To consider the effect of time in the network structure, it would be appropriate to make the network recurrent. The output of the network could be made dependent on the new set of the input data as well as the previous amounts of the output to make it stable after the fault inception time.

Feedforward neural networks have been already proposed as transmission line fault direction discriminators [50, 51, 61]. A feedforward network structure classifies different input patterns independently. The order in which the patterns are presented to the network is not considered. There is a possibility that for some cases two consecutive input patterns would be classified into different classes. The network's output may become oscillatory in some extreme cases [50]. In order to further increase the reliability of the fault direction decision, a post processing unit, e.g. an output averager is usually used to smooth up the output of the feedforward network-based fault directional module.

For the problem at hand, it was decided to use a feedforward neural network structure with the addition of a self-feedback connection from the output of the last layer of the network to itself. This way, the output of the recurrent network depends on both the inputs and the previous outputs. It helps the output of the network

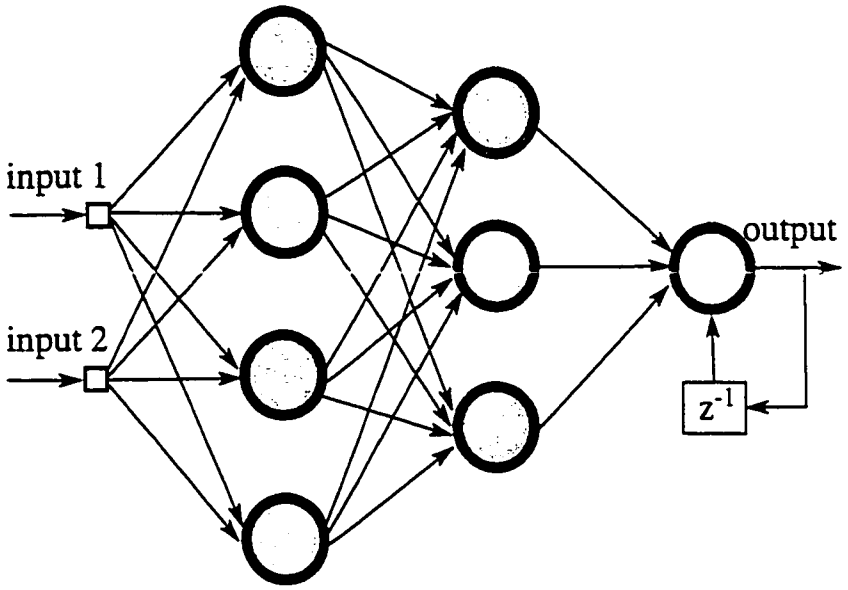

Figure 4.1: A schematic diagram of the proposed recurrent network structure

to remain stable after inception of the fault. Moreover, the network's output track becomes smooth. The network can be used as a stand alone unit, without averaging, to determine the fault direction.

A schematic diagram of the suggested network structure is shown in Fig. 4.1. In the next section this recurrent structure is used to design a transmission line fault direction detection network.

4.4 Direction Detection Network Design

4.4.1 Generation of Training Data

One of the main properties of ANNs is that they learn from examples, rather than being programmed. A set of training data including input/output pairs is usually

presented to the network and the network tries to learn and generalize these examples.

The training data set of an ANN should contain the necessary information to generalize the problem. Using the power system model shown in Fig. 3.1 training patterns were generated by simulating different types of faults on forward and backward regions of the power system. Fault location, fault resistance, fault inception time and pre-fault power flow direction were changed to obtain training patterns belonging to a wide range of different conditions of the power system. Faults including high amount of resistance were also considered. The training data set used for training the recurrent network is the same as the one used for training the feedforward networks.

4.4.2 Network's Inputs and Output

Consecutive samples of phase voltages and currents are usually chosen as the inputs to the neural network. The appropriate input data window length is a major factor which should be considered. Through a series of studies, it was found that a window length of 4 samples sampled at 1.2 kHz provides enough information to the recurrent network in this application. This sampling rate is compatible with the sampling rates commonly used in digital relays.

It is common to present samples of all three phase voltage and current information to the classification network as its inputs [50, 51, 61]. However, there may be some redundant information in this whole set of inputs. The network may be able to use a subset of the voltage and current data to identify the direction of the fault. In

such a case, the network's size would be reduced and a smaller size network with less number of connection weights could perform the direction detection job.

Different types of forward and backward faults were applied to the power system and the voltages and currents at the relay location were studied.

Extensive studies were performed and it was found that a recurrent network with the suggested structure, which uses all three phase current information but just one phase voltage information is able to classify forward and backward faults correctly. The recurrent network therefore, should have 16 inputs. The phase A voltage was used in this case as the reference. Hence, the network's input consists of:

$$i_a(n)T, i_a(n-1)T, i_a(n-2)T, i_a(n-3)T,\ i_b(n)T, i_b(n-1)T, i_b(n-2)T, i_b(n-3)T$$
$$i_c(n)T, i_c(n-1)T, i_c(n-2)T, i_c(n-3)T,\ v_a(n)T, v_a(n-1)T, v_a(n-2)T, v_a(n-3)T$$

The voltage and current input signals are filtered using the filter shown in Fig. 3.2 before being fed to the network.

The network needs just one output to classify between forward and backward faults. The network's output should be $+1$ for the case of forward faults and -1 for the case of backward faults.

4.4.3 Network Structure and Training

A few different networks, all having 16 inputs and one output but with different number of neurons in the hidden layer and different number of tap delays in the self-feedback loop were considered and trained. Training patterns were generated by simulating different types of faults on forward and backward regions of the sim-

ulated power system. Independent test patterns were also generated to validate the network's performance. Faults including very high amount of resistance, up to 100 Ω, were also considered.

The directional module output is set equal to zero prior to detection of the fault. For the recurrent network, the output of the network depends on the present input as well as the previous history of the output. Its track is gradual; it does not jump from zero to $1/-1$. Depending upon the fault type, the output gradually increases/decreases from zero towards $1/-1$.

In the training stage, the output track can be considered suitably. This way, the network learns the transition as it is specified, not as it decides by itself. So, one can decide about appropriate pattern of the transition period.

Different networks with one and two hidden layers were considered. It was found that the networks with reasonable number of neurons in one hidden layer can not cover some of the very extreme cases such as faults with very high resistance. On the other hand, networks with two hidden layers provide better results without having to have high number of neurons in their hidden layers.

Various networks considered were trained to estimate the direction of a fault on power transmission lines. The network which showed satisfactory results, while not having a big size, had just 16 inputs (4 consecutive samples of each of the three currents and any one of the three voltages), 8 neurons in the first hidden layer, 4 neurons in the second hidden layer and one single output neuron. The feedback loop contained 3 tap delays of the output.

The proposed structure results in a small size network. Feedforward neural networks have been proposed in the literature to detect the direction of faults on trans-

Table 4.1: Comparison of Different Neural Networks

Neural Network	Ref. [50]	Ref. [51]	Ref. [61]	Recurrent
Structure	24-20-12-1	30-12-4-1	30-10-5-1	16-8-4(+3)-1
No of inputs	24	30	30	16
No of neurons	33	17	16	13
No of weights & biases	765	429	371	180

mission lines [50, 51, 61]. The size of the proposed recurrent network is compared with the size of these feedforward networks in Table 4.1.

The trained recurrent network was tested with different independent test patterns and promising results were obtained. The results obtained indicate that the proposed network is able to detect the fault direction very fast and reliably. The determination of direction is not affected by the type and location of the fault, power flow condition, and the presence of fault resistance. Some of the simulation results are presented in the next section. For these examples, it is assumed that the fault detector instantly detects the fault after its inception and activates the directional module output.

4.5 Performance Evaluation Studies

The proposed recurrent network has been used to determine the fault direction from the temporal input patterns of voltage and currents. The network outputs which fall above 0.5 and below -0.5 are interpreted as forward and backward faults, respectively. A validation data set consisting of different types of forward and backward faults, 170 faults away from the relay location and 30 faults at the relay location, was generated using the power system model shown in Fig. 3.1. The fault patterns of the validation set were different than the fault patterns used to train the network.

For different faults of the validation set, fault location, fault resistance, fault inception time, source impedance and pre-fault power flow direction were changed to investigate the effects of these factors on the performance of the network. Extreme cases like faults at the far ends of the transmission line with high amount of fault resistance and also faults near the relay location with zero fault resistance were also included in the validation data set.

4.5.1 Faults Away from the Relay Location

To evaluate its capabilities, the proposed network was tested using the validation data set. In all 170 fault cases away from the relay location the network was able to determine the fault direction correctly. Determination of the fault direction is not affected by the various changes in the power system. Table 4.2 summarizes the fault direction detection time for different types of faults. The average overall direction detection time is 4.5 ms. It shows that the trained network only takes about one-fourth of a cycle to correctly determine the fault direction. Most of the faults included in the validation data set had high amount of fault resistance, such as 50 Ω. In general, the time needed to identify the direction of more usual faults with small amount of fault resistance is even less. Some of the test results are presented in the following subsections.

Table 4.2: Fault direction detection time (ms)

Fault type	1-Φ-g	2-Φ	2-Φ-g	3-Φ-g	Avg.
Detection Time	4.9	4.8	4.7	3.9	4.5

4.5.1.1 Forward Faults

Network's output for different types of forward faults applied on the power system is shown in Fig. 4.2. In this case the fault location was 95 *km* from the relay location, with fault resistance of 50 Ω, pre-fault power direction from sending-end to receiving-end and fault inception time 3 *ms* after phase *A* voltage zero crossing. For each fault, the output of the recurrent network is represented during the first cycle after fault inception (20 samples). Different faults involve different phases and ground as well. Fault type ag indicates a single phase to ground fault (phase *A* to ground), while fault type bc indicates a phase to phase fault (phase *B* to phase *C*). This figure shows that the determination of fault direction is fast and reliable.

The output of the 20-input feedforward network for the same faults and under the same system condition is presented in Fig. 3.12. Comparing Fig. 4.2 with Fig. 3.12, it is found that the new network performed better than the feedforward network. The network's output smoothly increases from its pre-fault value of zero towards one.

Fig. 4.3 shows the output of the network for different forward faults at 50 *km* from the relay location. The network output smoothly increases towards 1 and stays stable afterwards. For the faults presented in Fig. 4.3, it takes at most six and at least four samples for the output of the recurrent network to fall inside the forward fault area. For this case, the average time needed to classify the fault direction is 3.8 *ms*.

The network was tested with the faults at far end of the protection zone with 100 Ω fault resistance. Different forward faults were applied at 95% of the forward

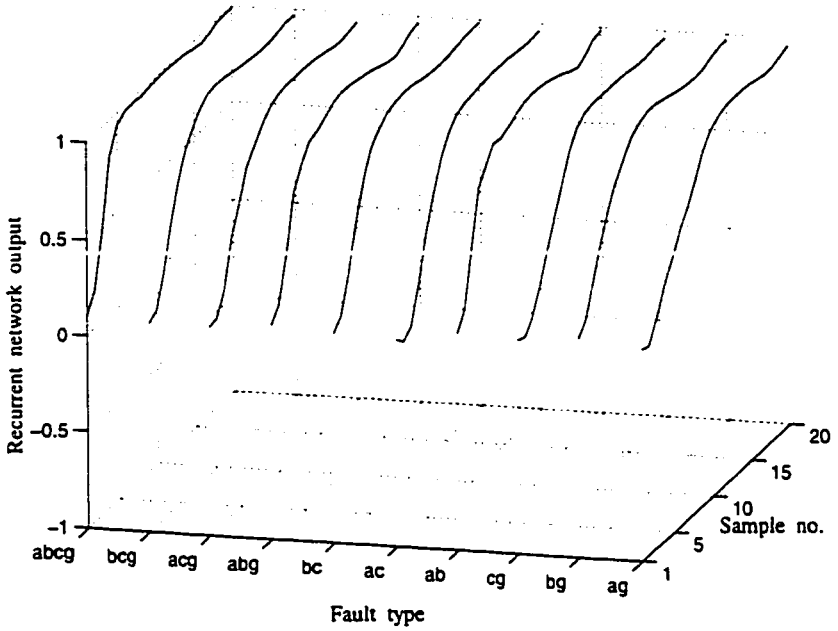

Figure 4.2: Recurrent ANN response to forward faults at 95 km, fault resistance 50 Ω, power direction from send. to receiv., inception time 3 ms

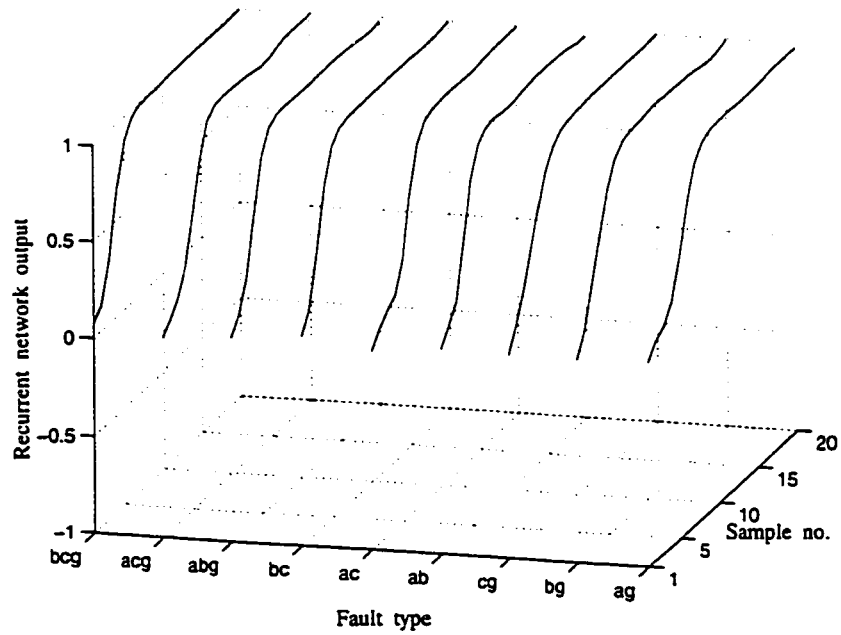

Figure 4.3: Recurrent ANN response to forward faults at 50 km, fault resistance zero, power direction from send. to receiv., inception time zero ms

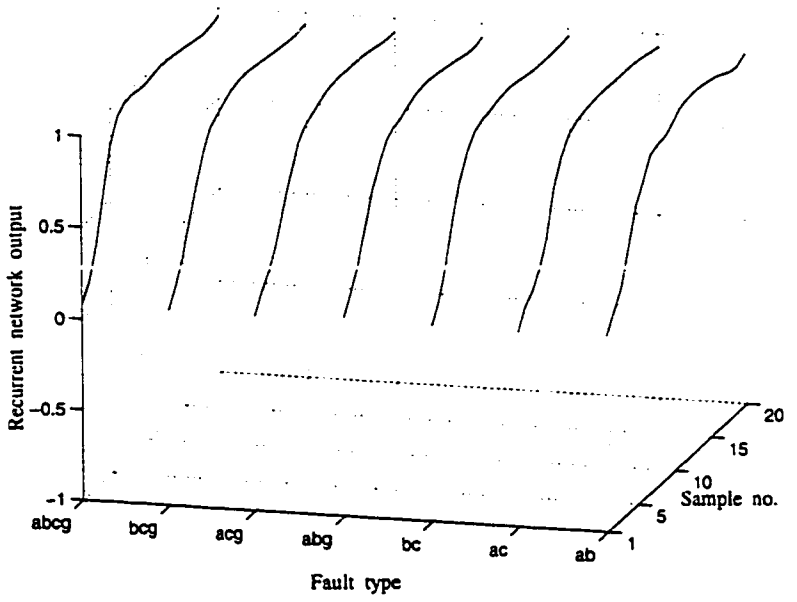

Figure 4.4: Recurrent ANN response to forward faults at 95 km, fault resistance 100 Ω, power direction from send. to receiv., inception time 1 ms

line's length and the results are shown in Fig. 4.4. Outputs of the network in all cases classify the fault direction correctly and rapidly. It shows that the network performed correctly for the far end faults even in the presence of very high amount of fault resistance.

4.5.1.2 Backward Faults

Using conventional methods, it is not easy to estimate the direction of faults that occur near the relay location [50]. Different backward faults with zero fault resistance were simulated at 5% of the backward line's length and the network's performance is presented in Fig. 4.5. This study demonstrates that the network is able to classify the faults near the relay location correctly in a timely fashion. On average, the directional module needs just about 3.9 ms to classify the fault direction correctly.

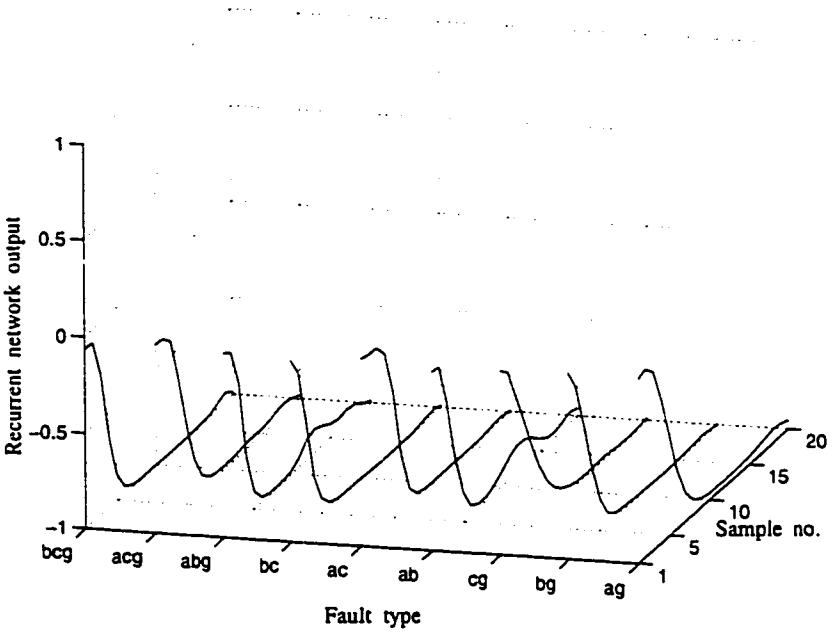

Figure 4.5: Recurrent ANN response to backward faults at 5 km, fault resistance zero, power direction from receiv. to send., inception time 1 ms

With the same condition as the case presented in Fig. 4.5, the recurrent ANN-based directional relay response for the same backward faults is shown in Fig. 4.6. For the faults presented in Fig. 4.5, it was assumed that the fault detector instantly detected the fault after its inception and activated the directional module output. For the faults presented in Fig. 4.6, it is assumed that the fault detector needs two samples to detect the fault. Therefore, the directional relay output would be zero for the first two samples after fault inception.

Comparing Fig. 4.5 with Fig. 4.6, it is found that the overall response in both cases is very similar. As a result, the delay in detecting the fault does not have much effect on the total operation time of the directional rely.

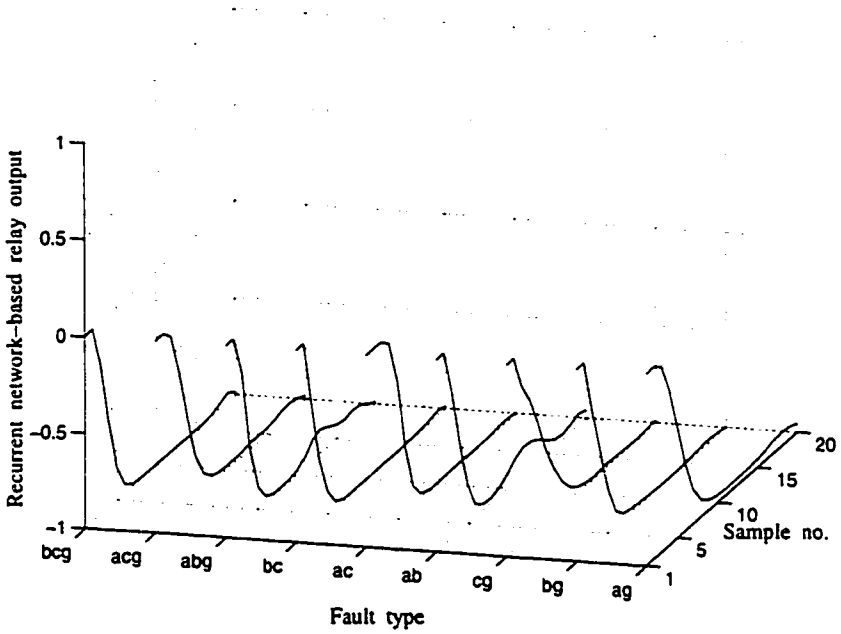

Figure 4.6: Recurrent ANN-based directional relay response to backward faults at 5 km, fault resistance zero, power direction from receiv. to send., inception time 1 ms, fault detection 2 samples after fault inception

4.5.2 Faults at the Relay Location

The capabilities of the new network were also examined for faults at the relay location.

Memory action should be used in the design of a fault direction detection module in order to properly discriminate the fault direction with zero input voltages. The proposed recurrent network uses feedback loops in its structure. The output of the network depends both on the input and the previous outputs of the network. Therefore, using its built-in memory the network should be able to correctly determine the direction of fault at the relay location and remain stable at least for some time after the fault inception.

Thirty different forward and backward faults with different power system conditions were applied at the relay location and the network's performance was investigated. In all cases except one of the three phase to ground faults, the directional module performed correctly. Three phase to ground faults rarely occur on transmission lines. The frequency of occurrance of such faults on a power system is just about 3% [16]. Even for this case, the network initially classified the fault direction correctly and the output indicated the correct class for more than three-fourth of the cycle. The fault direction detection time for different types of faults is shown in Table 4.3. The overall direction detection time average is 4.6 ms.

Table 4.3: Fault direction detection time for faults at the relay location (ms)

Fault type	1-Φ-g	2-Φ	2-Φ-g	3-Φ-g	Avg.
Detection time	5.6	4.4	4.3	3.6	4.6

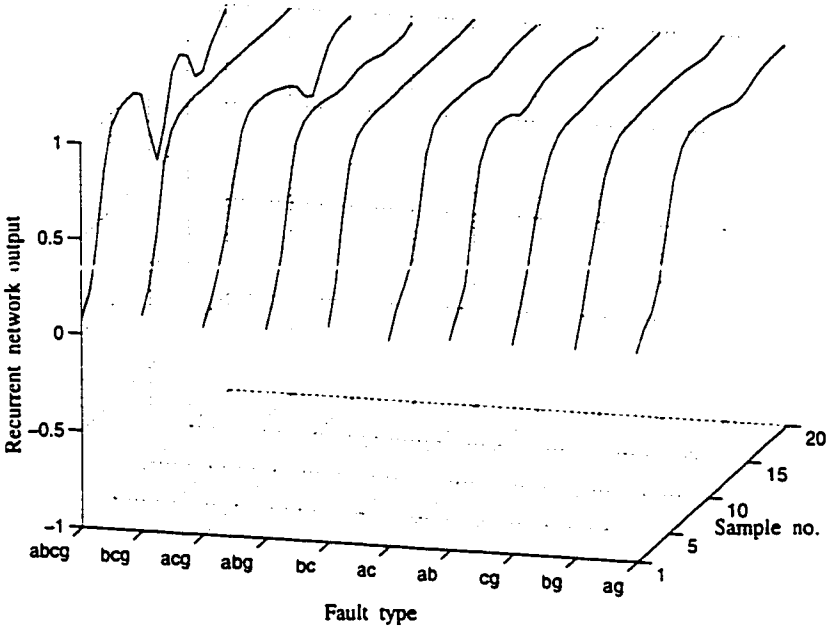

Figure 4.7: Recurrent ANN response to forward faults at the relay location, fault resistance zero, power direction from send. to receiv., inception time zero ms

The output of the recurrent network for different types of forward faults at the relay location with zero fault resistance is shown Fig. 4.7. Although the network uses just one of the phase voltages as the input, Fig. 4.7 shows that the network is able to correctly classify all the fault types at the relay location.

The network output for a few faults with different power system conditions is presented in this section. The main emphasis is on checking the network's performance under extreme fault cases. In general, the network performs better and faster for more usual fault cases.

4.6 Summary

In this chapter a novel transmission line direction detection module is proposed. Neural network's abilities in pattern recognition and classification are used to design a recurrent neural network-based directional module. The internal feedback loop of the recurrent network provides the network with memory. Simulation studies are performed and the network's performance is investigated. Influence of changing system parameters such as fault location, fault resistance, fault inception time, and pre-fault power flow direction is studied. The performance of the proposed network is also checked for faults including high amount of resistance and also faults at the relay location.

The designed neural network uses samples of all three phase current information but just one phase voltage information to identify the fault direction. Through extensive studies it is found that although the proposed network has a small size, it is able to classify forward and backward faults correctly and rapidly. The network can be used as a stand alone unit to determine the fault direction.

Compared with the feedforward neural network-based directional modules, the proposed recurrent module performs better specially for extreme fault cases and faults at the relay location.

Chapter 5

Directional Protection using an Elman Network

5.1 Introduction

Detection of the direction of a fault on a transmission line is essential to the proper performance of a power system. It would be desirable to develop a high speed and accurate approach to determine the fault direction for different power system conditions. The objective of this chapter is to design an ANN-based system capable of providing a fast and reliable estimate of the direction of a fault on power transmission lines.

Samples of phase voltage and current waveforms are usually used as the inputs to the neural network. The voltage and current are time-varying signals. Therefore, a network with temporal processing abilities should be considered. In the present work, use of an Elman recurrent neural network to determine the fault direction on transmission lines is investigated [62].

The ANN-based algorithm is tested to evaluate the performance of the proposed method in terms of accuracy, robustness and speed. Details of the design procedure and the results of performance studies with the proposed network are given and analysed in this chapter. System simulation studies show that the proposed approach is able to detect the direction of a fault on a transmission line rapidly and correctly.

5.2 Temporal Pattern Recognition

5.2.1 Static Neural Networks

The feedforward algorithm has established itself as the most popular method for the design of neural networks. However, a major limitation of standard feedforward algorithm is that it can only learn input-output mapping that is static [35]. Consequently, the traditional feedforward network has a static structure that maps an input vector onto an output vector. This form of static input-output mapping is well suited for pattern recognition applications where both the input and output vectors represent spatial patterns that are independent of time.

Time is an important factor in many of the cognitive tasks encountered in practice as it allows one to deal with time-varying signals and sequences. Time in mapping networks provides dynamic properties that make them responsive to time-varying signals.

The conventional static neural network architectures and algorithms are not well suited for patterns that vary over time. A feedforward neural network structure classifies different input patterns independently. The order in which the patterns are presented to the network is not considered. In contrast, temporal pattern recognition technique involves processing of patterns which evolve over time.

5.2.2 Temporal Processing

In parallel distributed processing models, the processing of sequential inputs has been accomplished in several ways. The most common solution is to attempt to

parallelize time by giving it a spatial representation. Time is explicitly represented by associating the serial order of the pattern with the dimensionality of the pattern vector. The first temporal event is represented by the first element in the pattern vector, the second temporal event is represented by the second position in the pattern vector, and so on. The entire pattern vector is processed in parallel by the model.

However, there are problems with this approach and it is ultimately not the best solution. This approach requires that there be some interface with the world which buffers the input so that it can be represented all at once. Furthermore, it suggests that all the input vectors be of the same length which is particularly troublesome in domains such as language. Most seriously, this approach does not easily distinguish relative temporal position from absolute temporal position [56]. A better approach would be to represent time implicitly rather than explicitly. That is, time is represented by the effect it has on processing and not as an additional dimension of the input.

5.2.3 Elman Network

A neural network can assume dynamic behavior by making it recurrent, that is, to build feedback into its structure. The recurrent connections allow the hidden units of the network to see their own previous output, so that the subsequent behavior can be shaped by previous response. A few different types of recurrent networks have been proposed by different researchers, including Real-Time Recurrent Network [63], Partially Recurrent Network [64] and Elman Network [56]. The difference between these networks lies in their structures and the way they handle the feedback.

Elman network is a two-layer feedforward network with the addition of a recurrent connection from the output of the hidden layer to its input. The delay in this connection stores values from the previous time step, which can be used in the current time step. This feedback path allows the Elman network to learn to recognize and generate temporal patterns.

The architecture of the Elman network is shown in Fig. 5.1. The network is augmented at the input level by additional units, called *context* units. These units are also hidden in the sense that they interact exclusively with other nodes internal to the network, and not the outside world [56].

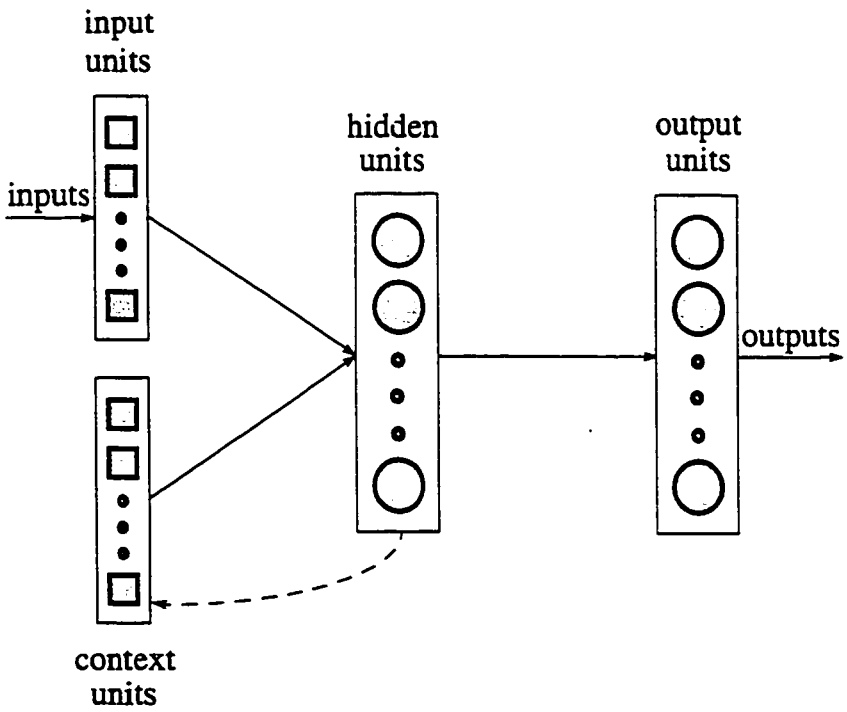

Figure 5.1: Elman network architecture, solid lines represent the trainable connections

The augmented input units, including both the input units and the context units activate the hidden units. The hidden units feed forward to activate the output units as well as they feed back to activate the context units. The number of context units is equal to the number of hidden units. Activations are copied from hidden layer to the context layer on a one-for-one basis with fixed weights of 1.0. The context unit values at time step $n+1$ are exactly the same as the hidden unit values at time step n. Therefore, the context units provide the network with memory.

5.3 The Proposed Elman Network Design

An Elman recurrent network was designed to act as the fault direction detection module of a transmission line relaying system. Details of the design procedure are given below.

5.3.1 Feature Selection

The application of a pattern classification technique requires a selection of features that contain the information needed to discriminate between classes, and which permit efficient computation to limit the amount of the required training data and size of the network. The sampled normalized voltage and current signals measured at the relay location are considered as the appropriate input information to the neural network. Voltage and current waveforms are sampled at a rate of 20 samples/cycle.

Preprocessing is a useful method to reduce the dimensionality of the input data set. The sampled waveforms are filtered before being fed to the network. The filter shown in Fig. 3.2 has been used to attenuate the dc component and high frequency

noise. This preprocessing enhances the training capabilities of the network and decreases the number of required patterns for training the network.

5.3.2 Network's Inputs and Output

It is common to present samples of all three phase voltage and current information to the classification network as its inputs. Various studies were performed and it was found that an Elman network, which uses all three phase currents information but just one phase voltage information is able to classify forward and backward faults correctly. The phase A voltage was used in this case as the reference. Therefore, samples of all three phase currents and just phase A voltage were considered as the inputs to the network.

The network needs just one output to classify between forward and backward faults. The network's output should be $+1$ for the case of forward faults and -1 for the case of backward faults. So, the *tansig* nonlinear function was chosen for both hidden and output layers of the network.

5.3.3 Directional Elman Network

A few different network structures, all having one output but with different number of inputs and different number of neurons in the hidden layer were considered and trained. Training and test patterns were generated by simulating different types of faults on forward and backward regions of the simulated power system.

Consecutive samples of three phase voltages and currents are usually chosen as the inputs to the neural network. The appropriate input data window length is a major factor which should be considered. In Refs. [51, 61] each phase voltage

and current was represented by its 5 consecutive samples and 30-input feedforward networks with two hidden layers were designed.

The Elman network has some kind of memory in its structure. Therefore, compared with the previously proposed 30-input networks, it should be able to use a smaller size of window and less number of inputs to cover the necessary input information to the network.

Different networks with different input data window lengths were considered. As the length of the input data decreases, more hidden neurons should be added in the only hidden layer of the network to capture and save enough information in the network's memory. This in turn results in increasing the size of the network.

Various networks considered were trained to estimate the direction of a fault on power transmission lines. The network which showed satisfactory results, while not having a big size, had just 12 inputs (3 consecutive samples of all currents and just one of the voltages), 12 hidden neurons and one single output neuron.

5.4 Test Results and Discussion

Using the power system model shown in Fig. 3.1 different types of faults were simulated and the performance of the proposed directional network was investigated. The trained network was tested with 340 different independent test patterns and promising results were obtained. It was found that the network's overall performance average was about 99.5%. Some of the simulation results are presented in this section. For the examples presented, it is assumed that the fault detector instantly detects the fault after its inception and activates the directional module output.

5.4.1 Faults Away from the Relay Location

The proposed network was tested with a set of 300 different faults including extreme cases like faults near the relay location with zero fault resistance and also faults at the far ends of the transmission line with high amount of fault resistance. In all cases except one of the extreme cases, which was a rare fault with 100 Ω fault resistance, the network was able to determine the fault direction correctly. The network output for a few faults with different power system conditions is presented in this subsection.

The network's output for different types of forward faults on the transmission line is shown in Fig. 5.2. Fault location was 95 km from the relay location, with fault resistance of 50 Ω, pre-fault power direction from sending-end to receiving-end and fault inception time 5 ms after phase A voltage zero crossing. For each fault, the output of the recurrent network is represented during the first cycle after the fault inception. Different faults involve different phases and ground as well. This figure shows that the identification of fault direction is very fast and reliable.

A feedforward network structure classifies different input patterns independently. The order in which the patterns are presented to the network is not considered. There is a possibility that for some cases two consecutive input patterns would be classified into different classes. The network's output may become oscillatory in some extreme cases [50]. In order to further increase the reliability of the fault direction decision, a post processing unit, e.g. an output averager is usually used to smooth up the output of the feedforward network-based fault directional module. For the recurrent Elman network, the output of the network depends on the present input as well as the previous history of the inputs. Its track is smooth; it does not jump from one region

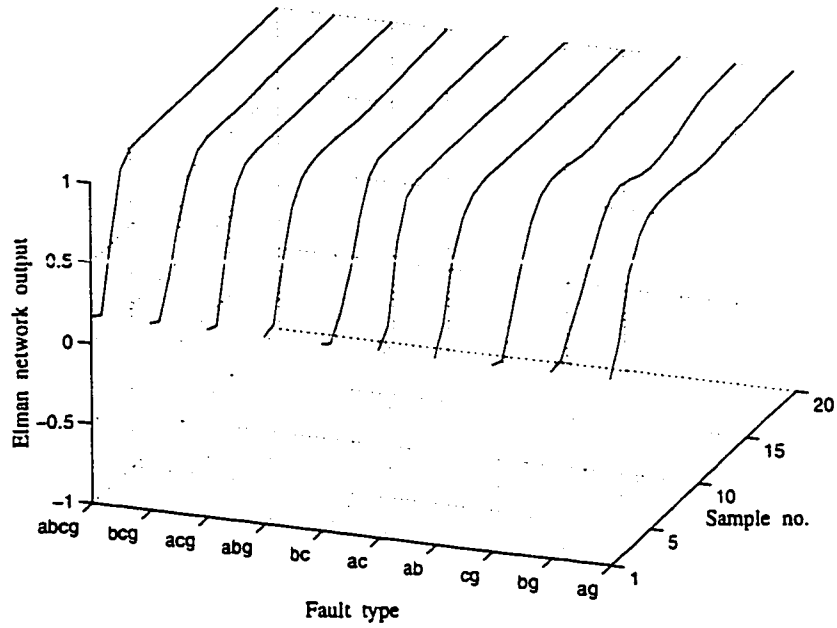

Figure 5.2: Elman network response to forward faults at 95 km, fault resistance 50 Ω, power direction from send. to receiv., inception time 5 ms

to another region. The output smoothly increases/decreases from its pre-fault value of zero towards $1/-1$. For the recurrent network, therefore, averaging would not be necessary. It can be used as a stand alone unit to determine the fault direction.

The network outputs which fall above 0.5 and below -0.5 are interpreted as forward and backward faults, respectively. For the faults presented in Fig. 5.2, it takes at most five and at least three samples for the output of the recurrent network to fall inside the forward fault area. On average the directional module needs just about 3 ms to classify the fault direction correctly.

The next example tests the network for faults that occur near the relay location. Different backward faults with zero fault resistance were simulated at 5% of the backward line's length and the network's performance is presented in Fig. 5.3. It shows that the network is able to classify the faults near the relay location correctly

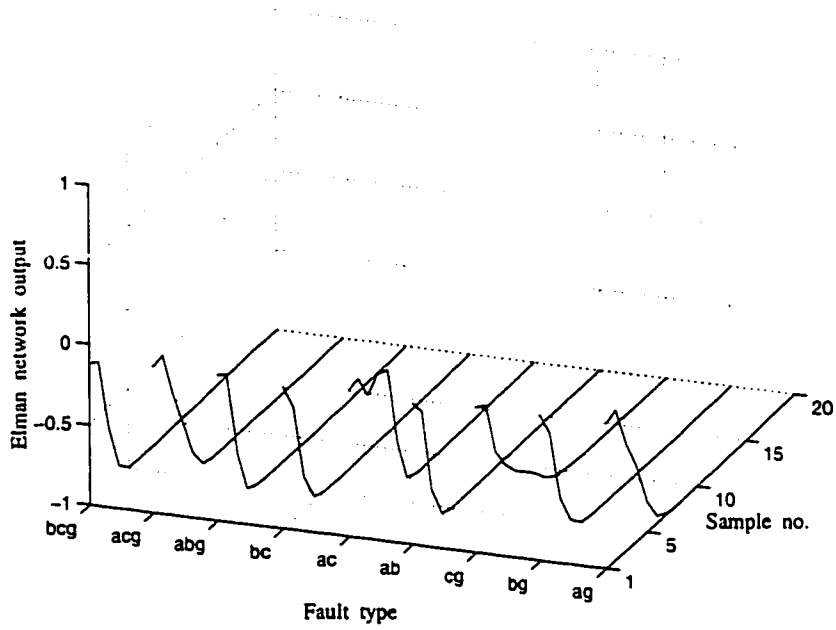

Figure 5.3: Elman network response to backward faults at 5 *km*, fault resistance zero, power direction from receiv. to send., inception time 1 *ms*

in a timely fashion. The average time needed to classify the fault direction is 3.1 *ms*.

The next example tests the network's performance for faults at the far end of the protection area with 100 Ω fault resistance. Different forward faults were applied at 95 *km* from the relay location and the results are shown in Fig. 5.4. It shows that the network performed correctly for the far end faults even in the presence of very high amount of fault resistance.

Fig. 5.5 shows the output of the network for different forward faults during four cycles (80 samples) after the inception of the fault. The sending-end source impedance was reduced by a factor of 20. Outputs of the network in all cases classify the fault direction correctly. The fault direction detection is very fast. The output of the network is stable for four cycles, although the network was trained just with the data samples of the first cycle after the fault inception. This study demonstrates

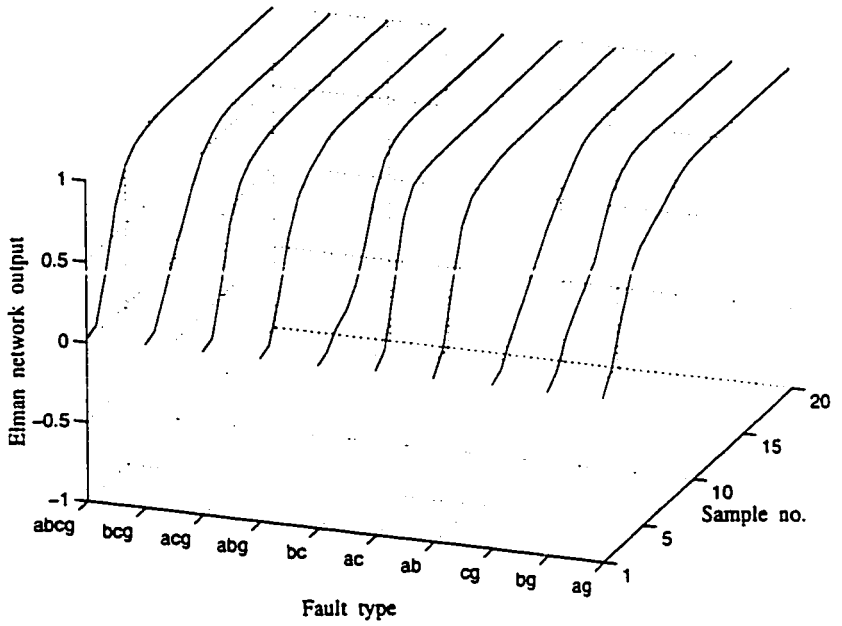

Figure 5.4: Elman network response to forward faults at 95 *km*, fault resistance 100 Ω, power direction from send. to receiv., inception time 12 *ms*

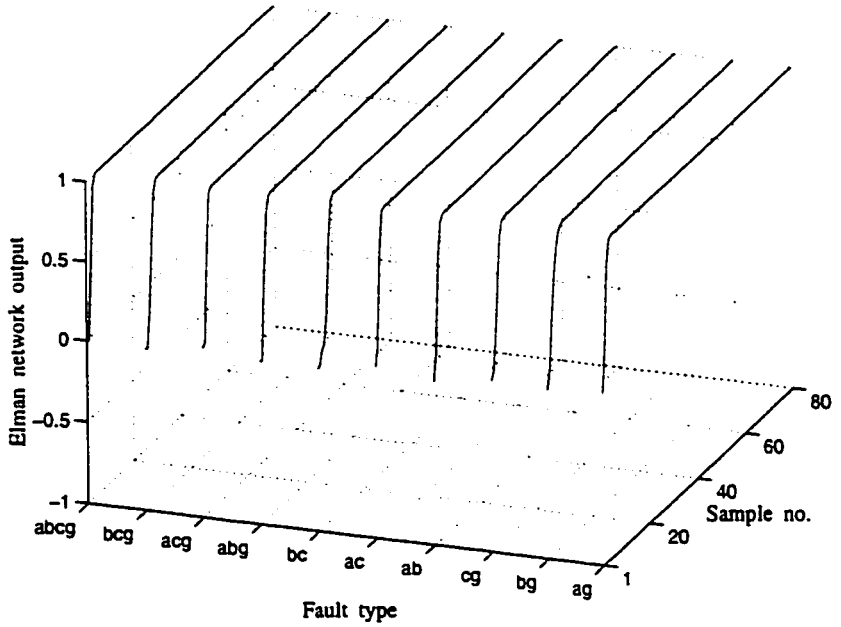

Figure 5.5: Elman network response to forward faults at 90 *km*, fault resistance zero, power direction from send. to receiv., inception time 12 *ms*, send. source imp. reduced by 20

that the proposed method is not affected by the variation of source impedance.

The results presented in this subsection mainly demonstrate the network's performance for some extreme fault cases. In general, the network performs better and faster for more usual cases such as low resistance faults around the middle of the protected areas.

5.4.2 Faults at the Relay Location

Identification of the direction of a fault located at the relay by using conventional methods is difficult. Memory action should be used in the design of a fault direction detection module in order to properly discriminate the fault direction with zero input voltages. The Elman network uses built-in memory in its structure and the output of the network depends on the previous history of the inputs. Therefore, it should have some ability to detect the direction of faults at the relay location correctly.

The capabilities of the new network were examined for faults at the relay location. Forty different forward and backward faults at the relay location were applied to the system and the network's performance was investigated. In all cases except one backward fault, the directional module performed correctly. Even for this case, the network initially classified the fault direction correctly and the output indicated the correct class for about two-thirds of the cycle.

The output of the network for different types of forward faults at the relay location with zero fault resistance is shown Fig. 5.6. Although the network uses just one of the phase voltages as the input, Fig. 5.6 shows that the network is able to correctly classify all the fault cases at the relay location.

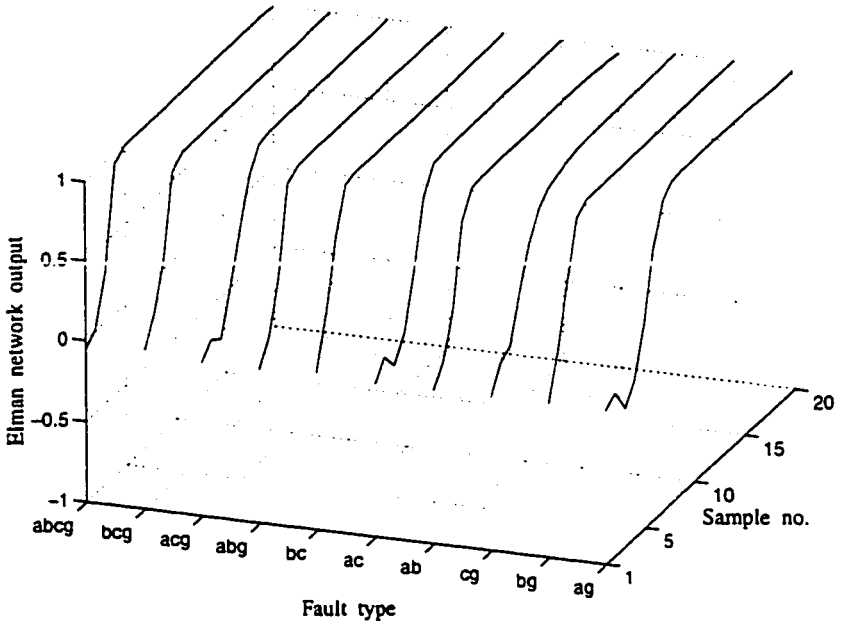

Figure 5.6: Elman network response to forward faults at the relay location, fault resistance zero, power direction from send. to receiv., inception time zero *ms*

5.4.3 Sequential Faults

Evolving faults might occur one after another before a protective relay has made its decision and sent the appropriate trip signal to the circuit breaker. The performance of the proposed network was evaluated for different evolving sequential faults on the power system shown in Fig. 3.1.

Fig. 5.7 illustrates the results obtained for the following conditions: two *C-G* and *B-C-G* sequential faults in front of the relay at 60 *km*, fault resistance 1 Ω, pre-fault power direction from receiving-end source to sending-end source. It is assumed that first an *C-G* fault happens on the transmission line and then, after 4 *ms*, it changes to a *B-C-G* fault.

Network's output is shown in Fig. 5.7 during three cycles after the inception of

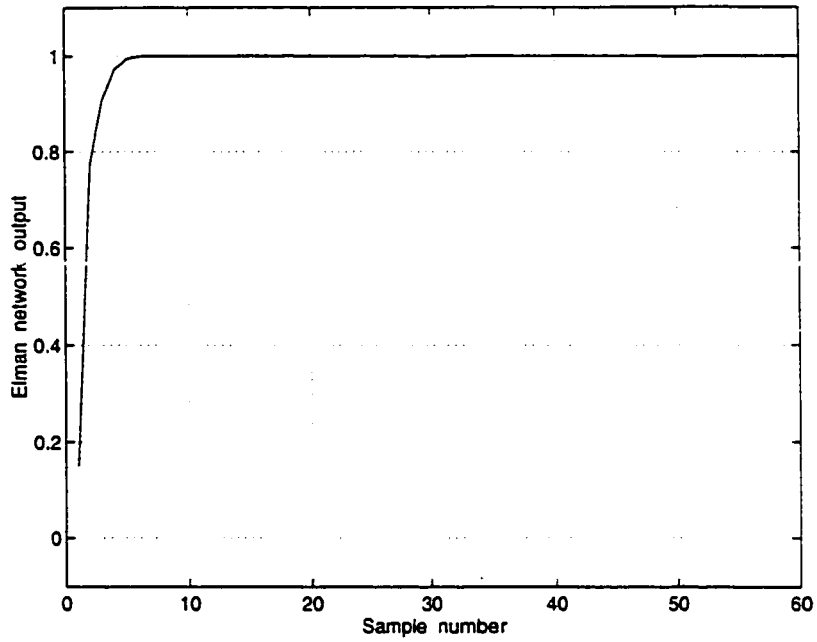

Figure 5.7: Elman network response to the *C-G* and *B-C-G* sequential forward faults

the fault at sample number 1. It shows that the network detects the fault direction correctly and very rapidly for these sequential faults.

For the next example the test conditions were: two *B-G* and *A-B-G* sequential faults in front of the relay at 80 *km*, pre-fault power direction from receiving-end source to sending-end source, the receiving-end source impedance reduced by a factor of 2. First a high resistive *B-G* fault with fault resistance of 50 Ω occurs on the line and then 10 *ms* later it changes to a *A-B-G* fault with 1 Ω fault resistance.

The output of the network is shown in Fig. 5.8. The network initially identifies the fault direction for the high resistive fault correctly. Network's output remains stable after the fault changes from a single phase to ground fault to a double phase to ground fault.

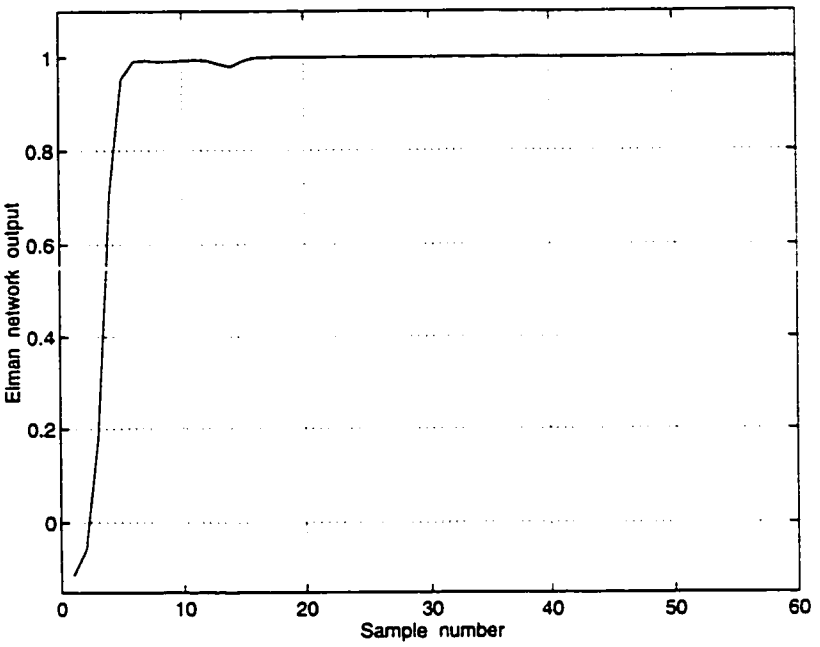

Figure 5.8: Elman network response to the *B-G* and *A-B-G* sequential forward faults

5.4.4 Cross-Country Faults

The proposed algorithm was tested to check its performance during cross-country faults. The term cross-country faults is used to describe simultaneous earth faults which occur on different line sections and on different phases [8].

As an example, two different faults were applied in front of the relay at different locations on the transmission line and the network's output is shown in Fig. 5.9. For this example the test conditions were: phase B to ground fault at 70 km, phase C to ground fault at 100 km, fault resistance 3 Ω for both faults, pre-fault power direction from sending-end to receiving-end. As shown in Fig. 5.9, the network detects the direction correctly in just about 1.6 ms after the inception of faults.

For the next example the test conditions were: phase A to ground fault at 80

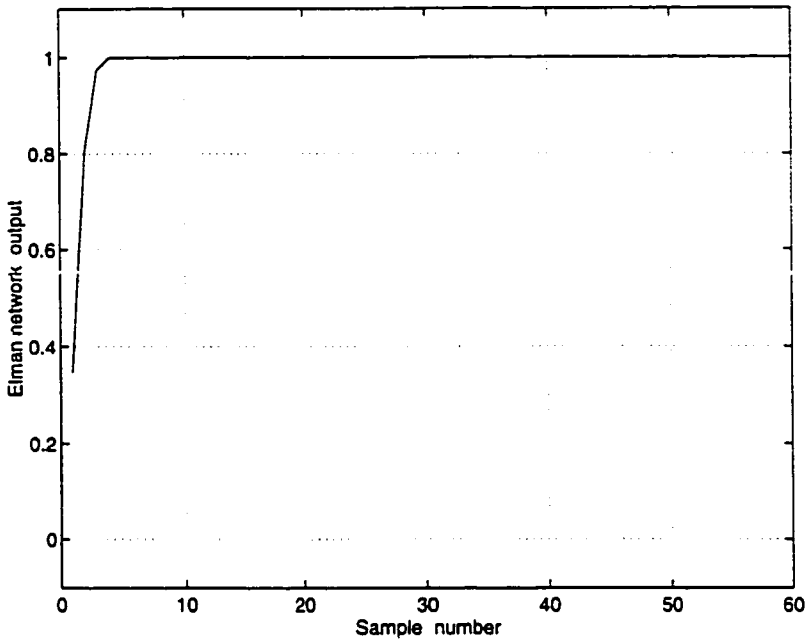

Figure 5.9: Elman network response to the B-G and C-G cross-country forward faults

km, phase C to ground fault at 100 *km*, fault resistance 1 Ω for both faults, pre-fault power direction from sending-end to receiving-end. It is assumed that first the C-G fault occurs on the transmission line and then 4 *ms* later the A-G fault occurs on a different location of the line.

Network's output is shown in Fig. 5.10 for this evolving cross-country fault. The network performs correctly and rapidly when tested with two different faults at different locations and with different inception times.

5.4.5 Measurements at Both Terminals

A directional comparison protection scheme uses directional relays at both ends of the transmission line to identify the fault direction at each terminal of the line. The Elman network module was installed at both ends of the right hand side transmission

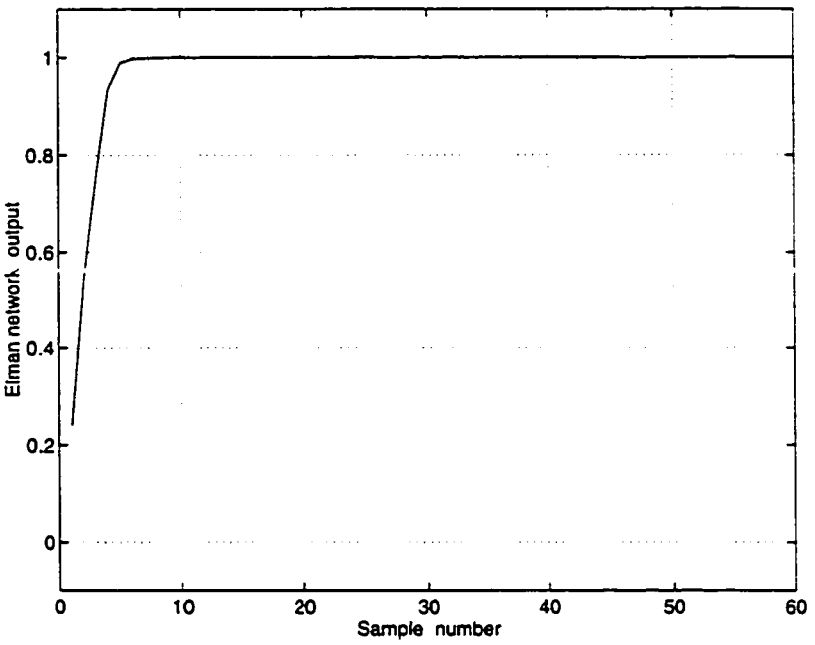

Figure 5.10: Elman network response to the *A-G* and *C-G* evolving cross-country forward faults

line of the power system model shown in Fig. 3.1. Simulation studies were performed and it was found that for an internal fault on the transmission line, networks at both ends of the transmission line rapidly identify the fault direction as a forward fault.

As an example the network's output for a single phase to ground *B-G* fault on the transmission line during three cycles after the inception of the fault is shown Fig. 5.11 . For this example the test conditions were: phase *B* to ground fault at 60 *km* from the left hand side terminal, fault resistance 5 Ω, pre-fault power direction from sending-end to receiving-end.

Fault data from both ends of the transmission line was processed by the Elman network. As shown in Fig. 5.11, the network identifies the forward fault in both cases correctly and rapidly. It shows that the proposed module can be used for high speed directional comparison relaying.

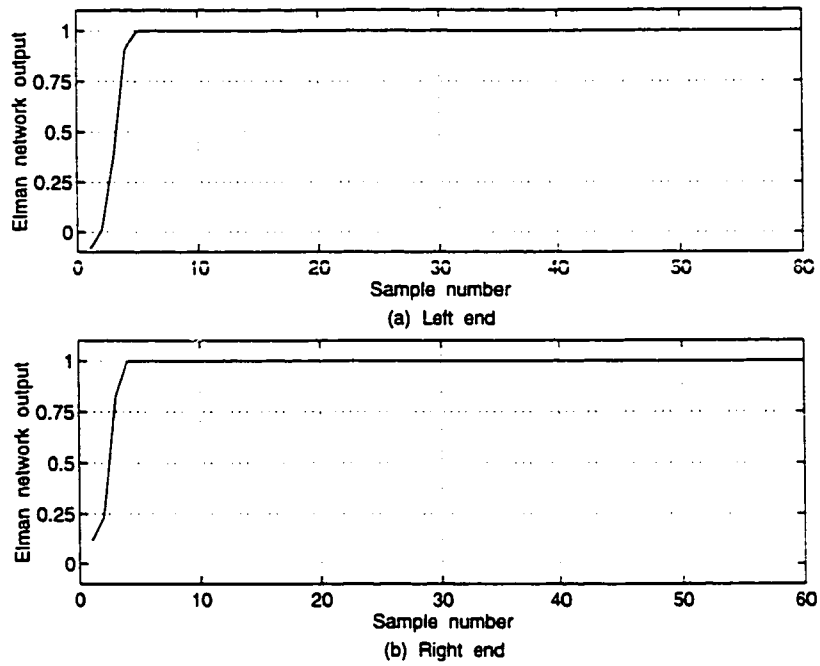

Figure 5.11: Elman network response to the *B-G* fault, measurements at both ends

5.5 Summary

A novel directional detection module for protecting transmission line is described in this chapter. The proposed approach is based on the use of recurrent neural network technique. The recurrent connections provide the neural network with memory. The designed neural network uses samples of all three phase current information but just one phase voltage information to identify the fault direction. The directional module network is extensively tested by independent test fault patterns and promising results are obtained. The performance of the proposed network is also checked for high resistance faults and also for faults at the relay location. Extensive studies indicate that the network is able to classify forward and backward faults very rapidly. The determination of direction is not affected by the type and location of the fault, pre-

fault power flow condition, source impedance variation and the presence of fault resistance. It shows that the proposed network is very powerful in processing the voltage and current temporal input signals.

Compared with the feedforward neural network-based directional modules, the proposed recurrent module performs better specially for extreme fault cases and faults at the relay location. Based on the simulation results, it was found that the performance of two recurrent networks proposed in Chapters 4 and 5 are comparable, though the Elman network is faster.

Neural network based approaches can be used as a part of a new generation of high-speed directional relays for power systems. They are suitable to realize a very fast transmission line directional comparison protection scheme.

Chapter 6

High Speed Fault Detection & Phase Selection

6.1 Introduction

Faults on transmission lines need to be detected rapidly, classified correctly and cleared as fast as possible. A fault detector module is used in several protective relays. This module can be used to start other relaying modules.

Phase selector module is also an important part of a protective relay. Fault classification is essential for single pole auto-reclosure schemes. Autoreclosure schemes as applied to EHV systems have, by offering benefits such as maintenance of system stability and synchronism, been the major cause of a substantial improvement in the continuity of the supply. It is desirable to develop a fast and reliable method to detect faults on a transmission line and to select faulty phases.

Most of the faults on power systems result in a substantial increase in current flow towards the fault point. However, for faults including high amount of fault resistance the current may not increase substantially. Thus, they can not be reliably detected by conventional based starters.

Fault resistance is an operational problem and is dependent on various factors such as voltage level, tower footing resistance, resistivity of soil, etc. Fault resistance produces an error in the impedance measurement and thus could affect the accuracy

of underimpedance starters severely.

A new underimpedance starter which covers a wider area of impedance plane is proposed for fault detection and phase selection. The suggested starting algorithm is not subject to the limitations of conventional underimpedance starters in response to faults with high resistance.

The proposed starter is able to rapidly and correctly detect and classify different fault types on the protected transmission line under different power system conditions. This module in conjunction with a directional module could be used in a directional comparison transmission line protection scheme [55, 62].

The proposed algorithm is tested to evaluate its performance under different operating conditions. The design procedure and the results of the performance studies with the proposed approach are presented in this chapter.

6.2 Starting Systems

An important part of a protective relay is its starter/selector module. A total of ten possible faults including 1-phase to ground faults *(A-G, B-G, C-G)*, 2-phase to ground faults *(A-B-G, A-C-G, B-C-G)*, 2-phase faults *(A-B, A-C, B-C)* and 3-phase fault *(A-B-C)* may occur on a transmission line. The selector module is responsible for classifying the type of fault that has occurred on the system.

The fault type is not known a priori. Therefore, the simplest distance relaying algorithms would have to process six single-phase distance equations corresponding to three phase to ground faults and three phase to phase faults. Early and even some modern microprocessors would be hard pressed to process all six equations between

successive samples [7].

A considerable saving in computation time can be achieved by utilizing a first stage which determines the fault type. In general, only one of the six equations would be processed for any fault, and considerable computational efficiency would be achieved. The main purpose of the starters in distance relays with a single measuring system is to select and apply to the measuring system the correct currents and voltages according to the type of fault. Switched distance relays, with a single measuring element lie in this category of distance relays. Such relays, having fewer components and being cheaper than the full scheme, have been widely applied in some countries particularly in medium voltage levels [15].

Fault detectors or starters are used not only in relays with single measurement system but also in the relays with six measurement systems. Selecting the correct currents and voltages according to the type of the fault is no longer necessary in distance relays with six measurement systems. Nevertheless, they are still included to perform other functions. Starting relays are necessary where the communication channel used for unit protection is not continuously employed. Other tasks performed by the starters are [8]: reversal of measuring direction at a definable time after fault incidence, enabling the fault digital recorders, switching the reach of first zone of distance relays, enabling tripping by other functional units of the relay and redundant back-up protection for the measuring systems.

In addition, starter output information could be used for single pole auto-reclosure schemes. Single pole auto-reclosure has long been recognized as an effective means of improving system security and reliability and is quite extensively used by many utilities. It involves tripping only the faulted phase under single-phase to ground

fault condition. The benefits of single pole auto-reclosure are particularly apparent in applications where economic and/or stability considerations preclude the use of three-phase auto-reclosure.

6.2.1 Current/Voltage Starters

Phase selector schemes based upon currents and/or voltages produce correct fault classification under most reasonable conditions but do misclassify in a significant number of cases.

The simplest form of the phase selector module uses instantaneous overcurrent starting elements. Under the fault condition, the phase current exceeds the current setting of the starter, causing the starter element to operate. Current based classifiers get confused when load current is significant compared to fault current. Conventional overcurrent based starters may not be able to detect the fault including high amount of fault resistance.

Undervoltage starting is sometimes used together with overcurrent starting. The undervoltage setting is constrained by the need for reliable operation for remote faults (undetected by the overcurrent feature) while maintaining stability of the sound-phase elements during close-in earth fault conditions. For remote low current faults, no clear undervoltage condition arises at the relay location. In the case of a close-in fault on a weak system, all voltages deviate significantly from the nominal value [15].

6.2.2 Impedance Starters

Fault detection and classification schemes based upon impedance starters are used in several practical relaying algorithms [8]. Various types of impedance starters have been used, but the most common type has been the plain impedance having a circular characteristic centered on the origin of the impedance plane. The starter compares the magnitude of the apparent impedance with the radius of the circle. The term apparent impedance is defined as the loop impedance when the voltages and currents entering the relay are used to calculate the impedance to the fault.

Using plain impedance starters, difficulties may sometimes be encountered on long lines where load encroachment may be a problem. This may be overcome to some extent by using offset impedance starting relays although the benefits may not be too significant for large lagging loads. Some other starters use a so-called polygon characteristic. Based on the application, the reach of the impedance starters could be selected for each unit individually.

Six-unit distance units with circular or polygon characteristics may get confused for phase selection. Although distance elements have been designed with a definite type of fault detection, they will respond to other types of faults as well [12]. A measuring unit for detecting phase faults must not emit a trigger signal in response to an earth fault. However, depending on the system conditions and parameters it could happen that the covering area of a phase unit largely coincides with the covering area of an earth unit, thus causing spurious classification.

The starter should accommodate as much fault resistance as possible consistent with stability under load condition. This is particularly so where the application is

to a system without an earth wire. In the case of the remote faults, fed from a local weak source the infeed effect of a remote strong source magnifies the fault resistance effect considerably.

6.2.3 Fault Resistance Considerations

Of essential importance in assessing the effectiveness of the polar characteristics of impedance starting schemes is the range of fault resistance they can cover. This is especially important in the case of earth-fault conditions.

Generally, there is always some resistance at the location of a fault on an overhead line. Unless the fault is solid, an arc whose resistance varies with the arc length and magnitude of the fault current is usually drawn through the air. Arc resistance is usually not an important factor in phase faults. For ground faults, arc resistance may be an important factor because of the longer arcs that can occur. Also, relatively high tower footing may appreciably increase the fault resistance and limit the fault current.

If the towers are connected by a ground conductor, the fault resistance is the equivalent resistance of all footing resistances. Taking all the factors into account, the fault resistance will normally be in the range of 1 to 10 Ω [8]. Higher values up to a few hundred ohms are to be expected for ground faults via wooden masts or trees (lines without ground conductor) or broken conductors lying on the ground.

Although the majority of faults with high fault resistance involve ground, a high resistance fault may also exist between two phase conductors as the case of a tree limb lying across two phase conductors.

Neither of the circular or polygon characteristics could cover some faults with high resistance.

6.3 Measurement Errors

6.3.1 Fault Resistance

Impedance starters measure the positive sequence impedance as seen at the point of relay location in the forward direction.

For a simple two-bus system with generation only at one end, the error in the measured positive sequence impedance is due to the magnitude of the fault resistance [65]. Under normal condition, the impedance seen by the relay at point A in Fig. 6.1. is given by:

$$Z_R = Z_{LA} + Z_{LB} + Z_l \tag{6.1}$$

For a fault with fault resistance of R_f, the apparent impedance seen by the relay at point A is:

$$Z_R = Z_{LA} + Z_{lf} \tag{6.2}$$

$$Z_{lf} = \frac{(Z_{LB} + Z_l)\, R_f}{Z_{LB} + Z_l + R_f} \tag{6.3}$$

With $R_f = 0$, $Z_{lf} = 0$ and, therefore, the fault impedance seen by the relay is correct. However, when R_f is not equal to zero, the relay measures Z_R as given by eqn. 6.2 which is obviously not correct.

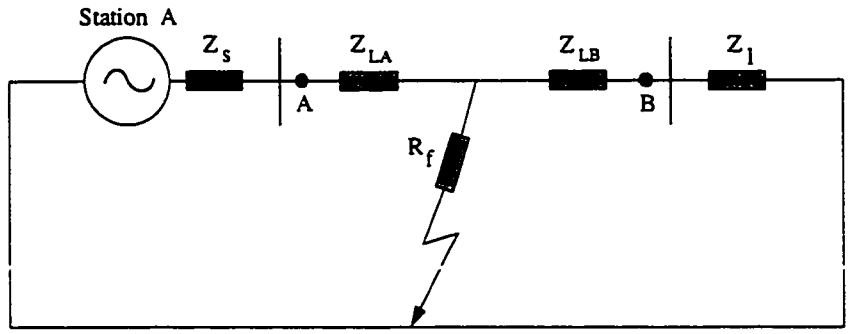

Figure 6.1: A two-bus system with generation only at one end

The situation becomes more complicated for a two-bus system with generation at both ends (Fig. 6.2). The error term Z_{lf} in this case is very complicated and can have uncertain values.

For a fault with fault resistance R_f fed from both A and B points, currents I_A and I_B will have a phase relationship determined by the prefault load transfer conditions. Assuming the measurement is at point A and the current I_A and voltage V_A are measured, the fault resistance causes the relay to measure an impedance other than the effective one to the fault location, Z_{LA}. The impedance measurement thus includes an error which because of phase-shift between the currents I_A and I_B falsifies both the resistance and reactance of the fault loop. In general terms, the

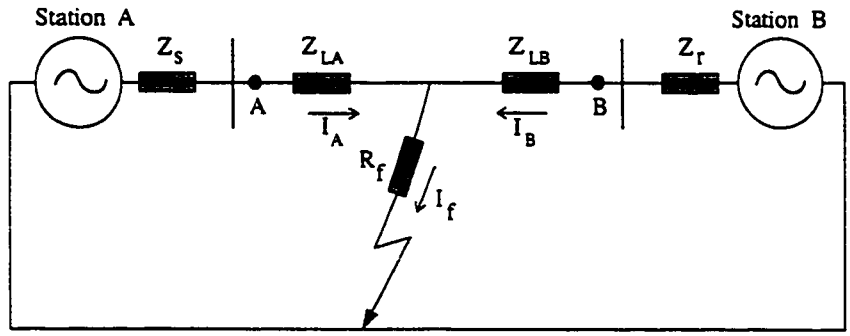

Figure 6.2: A two-bus system with generation at both ends

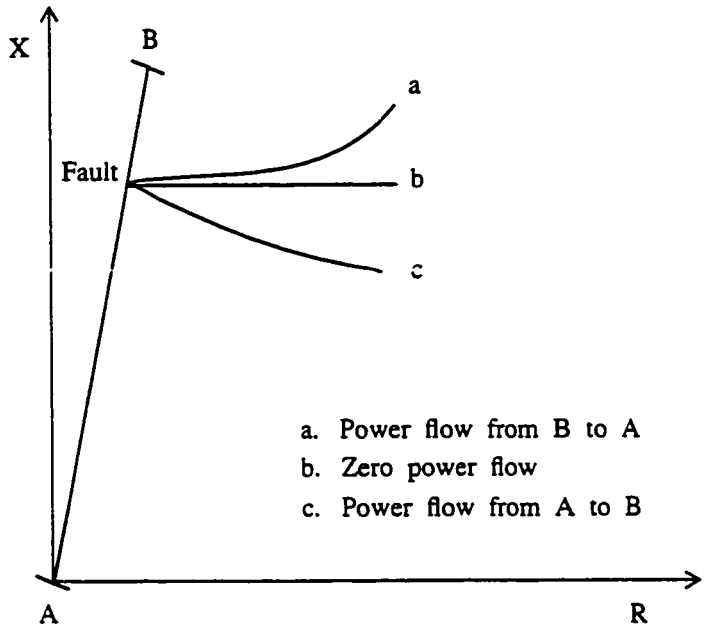

Figure 6.3: Effect of fault resistance on the measured impedance

apparent impedance presented to relay at point A is given by:

$$Z_R = Z_{LA} + k\,R_f \tag{6.4}$$

where k is a complex factor which depends on the through-load transfer at the instant of fault inception [15].

The apparent reactive component may be positive or negative depending on the direction of power transfer as illustrated in Fig. 6.3, which shows the loci of measured impedance for different load conditions at a particular fault location.

There is a basic problem of accommodating fault resistance, the value of which as seen by the relay may be larger than the real value as a result of remote fault infeeds. For a fault at the end of the transmission line (near to the B station) fed from a strong B source and a weak A source, the ratio of I_f/I_A could be very high.

This in turn, can increase the fault resistance effect by an order of magnitude or even more.

6.3.2 Zero Sequence

It is common to compensate the measured impedance for correct earth fault measurements, using for example residual current compensation [12]. For earth faults the measurement system is fed with the phase current plus k_0 times the residual current. The value of the residual current factor, k_0, depends on the ratio of the positive and zero sequence impedances. In this way, the starter measures the phase impedance (positive sequence impedance). In many applications this compensation results in incorrect operation of sound-phase starters for close-in earth fault conditions. For this reason, such compensation sometimes is omitted from impedance starters. This in turn, introduces some error in the impedance measurement of the earth faults.

Another problem which makes the earth fault measurement complicated is the uncertainty of determining accurately the zero-sequence impedance. The system impedance can vary due to changes in earth resistivity or because of mutual coupling between parallel lines. Practical levels of mismatch between relay zero-sequence setting and system zero-sequence impedance for practical values of positive-sequence to zero-sequence current ratio can yield measurement errors of up to 10% [15].

For the phase faults, mutual coupling effects and fault resistance have little influence, and the apparent impedance is the same as the impedance to the fault. However, for the earth faults the influence of mutual coupling and fault resistance is more severe. Fault resistance and zero sequence mutual effects from other lines tend

to make the apparent impedance different from the actual impedance to the fault [66, 67].

Some other errors in the measurement of the positive sequence impedance include [65]:

- proximity to generators, changes in the topology of the network, changes in the number of generating units operating in the system, etc.
- variation in the overhead line parameters due to a variety of factors such as operating temperature, relative permability, conductivity and corona.
- neglecting the mutual coupling between phases and between adjacent lines. On an untransposed line, the errors due to this assumption could have some impact.
- inaccurate measurement due to the transient response of current and voltage transformers [68] and their transformation errors.
- presence of dc offset transients.
- ineffective filtering of the fundamental components of the transient voltage and current signals for different network topologies [69].

6.4 The New Starter Module Design

A new underimpedance starter which accommodates larger fault resistance and its performance is more immune to the measurement errors is proposed in this section.

Under the load condition, the measured impedance seen by the relay lies in a region around the horizontal axis of the impedance plane. The minimum load impedance Z_{min} is reached at the maximum load current. Depending on the power flow direction and the load power factor, the measured impedance lies on one of the four quadrants. The region covering the load impedance loci at different conditions is defined as the load region. A region covering the load region with a margin is considered and defined as the safe region. Fig. 6.4. shows the right hand side of the impedance plane including these regions. Under no load or very small load transfer condition, the relay measures a small reactive current flowing into or out of transmission line. The measured impedance in this case lies around the imaginary axis of the impedance plane. The reach of the impedance starter is limited by a big circle to keep these measurements out of its reach.

Detection of faults on the transmission system is based on the fact that the impedance measured at the relay location under normal condition (i.e. load impedance = quotient of load voltage divided by load current) is inside the safe region. Under abnormal conditions the measured impedance vector moves out of this region. It is assumed that if the apparent impedance seen by the relay lies in the safe region the system is healthy, otherwise unhealthy (faulty). The proposed underimpedance starter is able to detect most of the faults unseen by underimpedance starters of the circular and other suggested characteristics.

Fig. 6.5 shows a simplified block diagram of the proposed algorithm. The selector module comprises of three impedance starters, each responsible for one of the 3 phases of the transmission line. After being filtered and sampled, the phase voltages and currents are processed using a fast and simple method to estimate the impedance.

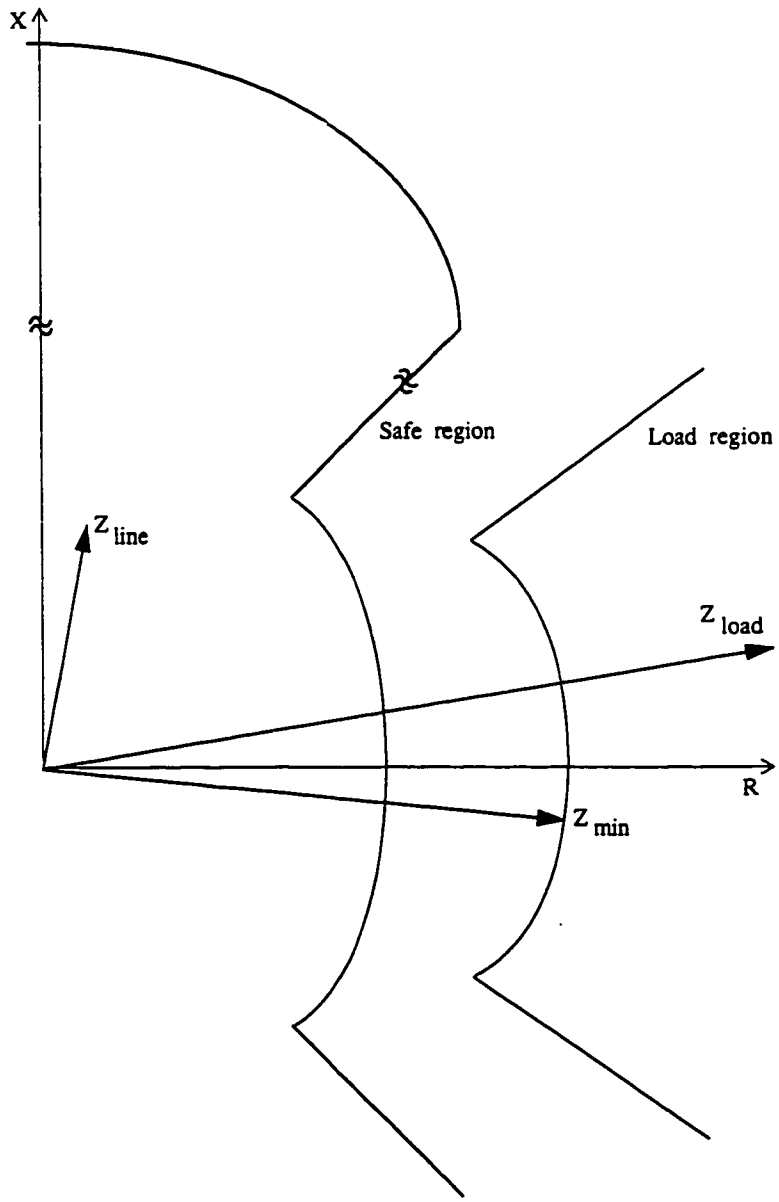

Figure 6.4: Impedance regions of the impedance starting unit

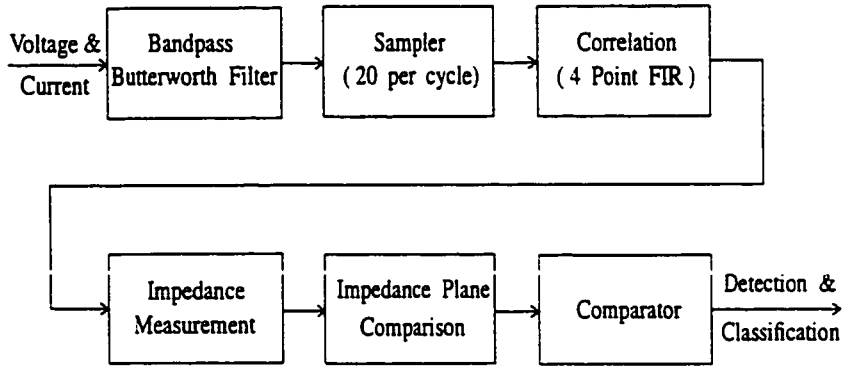

Figure 6.5: Block diagram of the proposed underimpedance starters

Then the measured impedance is compared with the safe region of the impedance plane.

A simple wide bandpass 2nd-order Butterworth filter was used to attenuate the dc component and high frequency noise (Fig. 3.2). The passband of the filter is chosen to be 80 Hz. This value allows a considerable reduction of the high frequency and dc components. This preprocessing helps the impedance measurement algorithm to calculate the fundamental frequency voltage and current phasors more accurately.

6.4.1 Least-square Error Algorithm

A number of algorithms can be regarded as impedance calculations in that the fundamental frequency components of both voltages and currents are obtained from the samples. The ratio of appropriate voltages and currents then provides the impedance to the fault. The performance of all of theses algorithms is dependent on obtaining fast and accurate estimates of the fundamental frequency components of a signal from a few samples.

Least-square error algorithm was used in this work to estimate voltage and current

phasors. This algorithm involves processing a total number of measurements that exceeds the number of parameters to be determined. In its simplest form such a problem can be cast as that of solving an overdefined set of equations of the form of [7]:

$$Ax = b \tag{6.5}$$

where A and b are known and x is to be determined. The equation is overdefined if there are more b's than x's.

A more reasonable approach to the solution of this equation is to recognize that there is an error and write:

$$b = Ax + e \tag{6.6}$$

The solution x which minimizes $e^T e$ can be obtained from:

$$\hat{x} = (A^T A)^{-1} A^T b \tag{6.7}$$

The calculation in the above equation is sometimes referred to as pseudo inverse.

Assume that the voltage and current waveforms can be written in the form of:

$$y(t) = Y_c \cos \omega_0 t + Y_s \sin \omega_0 t \tag{6.8}$$

where $y(t)$ is the instantaneous value of voltage and/or current waveform, ω_0 is the fundamental power system frequency and Y_c and Y_s are real numbers.

To obtain the voltage and current phasors, a moving 4 point sample data window was considered and based on the least-square error algorithm the parameters of 4 point FIR filters were calculated. This method provides a fast and simple method to estimate the impedance.

Voltage and current in power systems are generally not pure sinusoidal under transient conditions. They may contain harmonics, noise and decaying dc components. Therefore, using a short window of 4 points may not provide quite accurate impedance measurement. However, it should be noticed that voltage and current signals are passed through a bandpass filter before being fed to the 4 point FIR filters. This bandpass filter attenuates high frequencies as well as dc components. Moreover, even if the impedance measurement is not completely accurate and is a little oscillatory, it should be considered that this module is just responsible for distinguishing between healthy and non-healthy cases and detecting the faulty cases rapidly and not for accurate impedance measurement. A different distance module, if necessary, by using a more sophisticated impedance measurement scheme would be responsible for precise impedance measurement and preventing from overreaching.

6.4.2 Impedance Comparison

Depending on the magnitude of the power system parameters and the power system condition, for some cases a single-phase to ground fault could result in the impedance measurement of the healthy phases being out of the safe region, thereby activating the starters of the healthy phases.

To overcome this problem, it is suggested that the measured apparent impedances of the phases be compared with each other. In the case that the measured impedance of one of the phases enters the fault region of the impedance plane but its magnitude is much greater than the magnitude of the measured impedances of the other phases, the output of the relevant starter would be deactivated. This modification improves

the performance of the phase selection algorithm.

Three high-setting overcurrent starting elements were also considered. The magnitudes of phase currents are already calculated for impedance phasor estimation and are available. They should just be compared with a setting value in an overcurrent scheme.

In the case this module is used in a directional comparison protection scheme, if a high level fault near the relay is detected by the overcurrent starters tripping would be independent of the directional unit at the other end of the transmission line. This method eliminates the necessary time delay to receive the confirmation signal from the other end of the transmission line. Heavy faults at locations up to one third of the line's length are set to be tripped without any communication time delay. Using different settings, the overcurrent module may also be used to provide backup protection in the case of a failure in the transmission channel.

The output of the three impedance starters were ORed with the output of three overcurrent starting elements. This combination could speed up fault detection and classification for close-in high current faults. The combined output of each individual set of underimpedance and overcurrent starters for each phase is the starter signal for that specific phase. For example, the ORed outputs of phase A underimpedance and overcurrent starters determine the phase A starter output signal.

The outputs of three phase starters are ORed together and the resultant signal is ORed with the output of a neutral current overcurrent unit. The sensitivity of the neutral current unit is limited due to the mutual couplings and untransposed transmission lines effects. The resultant signal is considered as the fault detection signal. A block diagram showing output signals of the phase starters and detector is

depicted in Fig. 6.6.

This combination of underimpedance and overcurrent starters results in a fast and reliable starter scheme which is able to detect and classify faults for different power system conditions with wide system parameters.

This scheme, using just 3 impedance measurement units, is able to correctly detect and classify all types of faults including 1-phase to ground, 2-phase to ground, 2-phase and 3-phase faults.

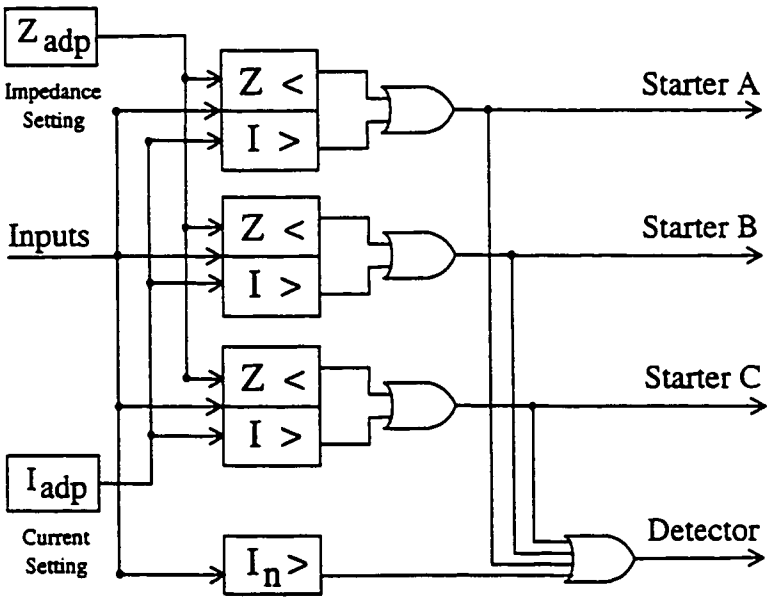

Figure 6.6: Block diagram showing the outputs of phase starters and fault detector

6.4.3 Adaptive Settings

Adaptive protection systems permit the protection functions to be adapted automatically in real time to changing power system conditions. Such procedures maintain optimum protection quality and performance. Adaptive relaying is a subject of rel-

atively recent origin. It has been defined as follows [70]:

"Adaptive protection is a protection philosophy which permits and seeks to make adjustments to various protection functions in order to make them more attuned to prevailing power system conditions".

The key concept in adaptive protection is to vary the settings or configuration of the protection system in response to changes in the power system caused by changing loads, network switching operations or faults [7]. As one begins to modify relay performance based upon changing conditions on the power system, one approaches the classic concept of feed-back control. Indeed, adaptive relaying is a feed-back control system.

Settings of the underimpedance and overcurrent starter units were adaptively changed based on the transmission line power flow amount. For large amounts of power transfer, the measured current at the relay location is big and the measured impedance vector lies in the load region somewhere around the Z_{min} point. For small amounts of load transfer, however, the measured current is small and the impedance measurement algorithm measures an impedance much bigger than the Z_{min} and well inside the load region. For low power transfers the setting of the current starters is reduced and the safe region of the underimpedance stater in impedance plane is moved towards the right.

The three measured phase impedance and current magnitudes were sampled and averaged with a frequency of 10 Hz. The current setting is adjusted at 1.5 times the averaged measured current and the impedance setting is adjusted at 0.7 times the averaged measured impedance.

For the case of small amount of load transfer, the load could increase by more

than 50% in a short period of time. To prevent the current and underimpedance starters to detect these kinds of load jumps as a faulty case, a minimum amount for current setting and a maximum amount for impedance setting are considered. These two limits are determined by the biggest possible jump in the load transfer level. The current and impedance settings are also compared with the maximum possible amount of load transfer settings. The block diagram of the adaptive setting procedure of the underimpedance starters is shown in Fig. 6.7.

This adaptive setting modification results in covering a bigger category of system faulty cases and detecting faults more rapidly as well.

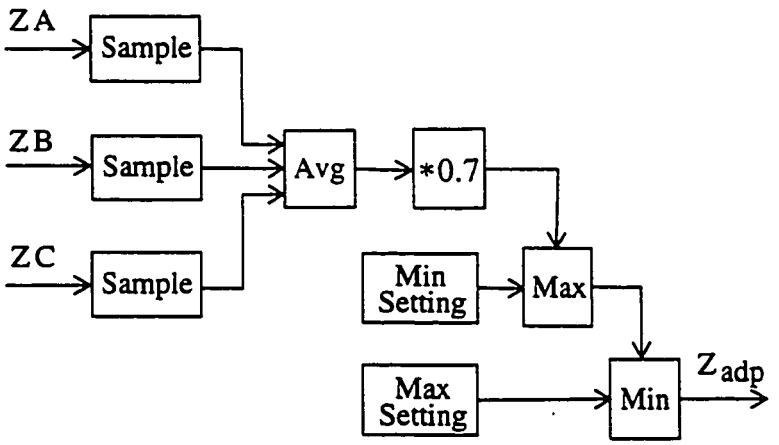

Figure 6.7: Adaptive changing of the settings of the underimpedance starters

In the next section, a two-bus power system fed from both ends is considered and the capabilities of the proposed starter algorithm are examined.

6.5 Simulation Studies

6.5.1 Simulation Model

To investigate the performance of the proposed algorithm, a 240 kV power system with two sending end and receiving end sources was considered. A 200 km transmission line, modeled by frequency dependent parameters, connects two sources and the measurement devices are located at 50 km from the sending end source. Using this power system model, shown in Fig. 6.8, simulation studies were performed and the results are presented.

6.5.2 Fault Studies

A wide range of faults was applied in order to assess the performance of the proposed algorithm. Different faults with different instants in the cycle, different source impedances and fault resistances and at different locations were performed. The magnitude of source impedance in practice may vary significantly as different elements of the network are switched and the system is reconfigured to meet the prevailing demand. The performance of the algorithm has been evaluated for varying source

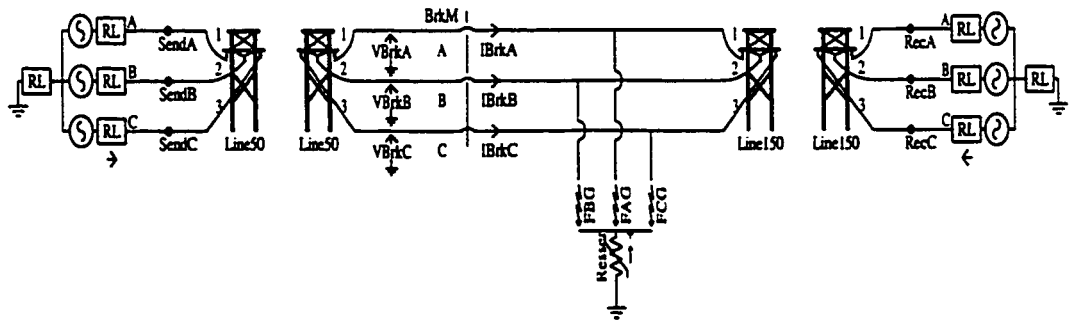

Figure 6.8: Power System Model

impedance values. High amount of fault resistances were also considered. Some of the results are presented in this section.

Fig. 6.9 shows the results of a study for the detector and phase A starter. Ten different ground and phase faults were applied in front of the relay at 50 *km*. For ground faults, the fault resistance was 20 Ω. The Short Circuit Capacity (SCC = $\sqrt{3}$ * nominal voltage * short circuit current) of the sending-end source was 6 GVA, while receiving-end SCC was 3 GVA. The relative phase angle difference for the two sources was zero degrees prior to the fault.

A phase to ground A-G fault was applied to the system at 0.2 s and then cleared at 0.25 s. Next, a B-G fault was applied at 0.3 s and cleared at 0.35 s. In the same manner, at each 0.1 s time interval a different fault was applied and then cleared after 50 ms.

The phase A current is shown in the top of Fig. 6.9. The outputs of the detector and phase A starter for different fault types are also shown in this figure. Normally the two outputs will overlap each other as their magnitude is the same. Therefore, for clarity in display, the starter output is multiplied by a factor of 0.85. It shows that phase A starter was able to classify the faults involving phase A, while being stable for other phase to ground faults. The fault detector detects the fault in all cases rapidly. On average, it takes just about 3 sampling periods to detect a fault after its inception.

The next example evaluates the performance of the algorithm for heavy faults at relay location. To make an extreme case, the SCC of the sending-end source was taken as 10 GVA. This is indicative of a very strong source. Moreover, the length of the line behind the relay was decreased to 20 *km*. The relative angle of the

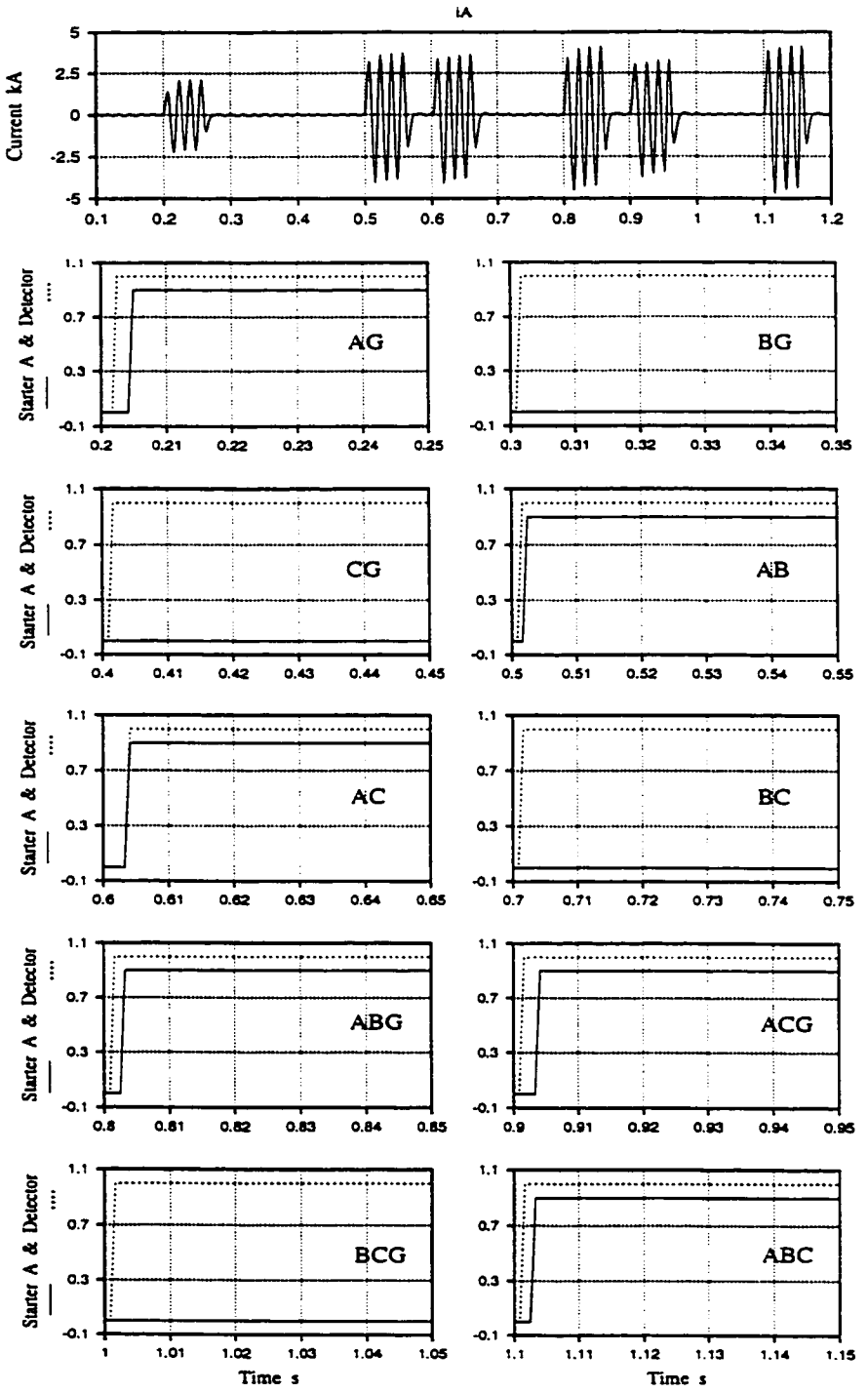

Figure 6.9: Phase *A* starter and detector outputs for faults at 50 *km*, fault resistance 20 Ω for ground faults, SCC ratio 2, angle zero degree

receiving-end source with respect to sending-end source was 30 degrees. The ratio of the SCC of the sending-end source to the SCC of the receiving-end source was taken to be 1. Similar to the previous case, ten different types of faults were applied in front of the relay at the relay location with fault resistance of 1 Ω for the ground faults and the results are shown in Fig. 6.10. In all cases, faults are detected and classified correctly and very rapidly.

The performance of the algorithm was checked for faults with high amount of fault resistance. Fig. 6.11 illustrates the results obtained for the following conditions: ten different faults in front of the relay at 50 *km*, fault resistance 80 Ω for ground faults, SCC ratio 1/5, relative angle 30 degrees. It shows that the algorithm is able to detect faults with very high amount of fault resistance. Moreover, the phase A starter responds to faults involving phase A.

With the conditions similar to that of Fig. 6.11, an A-G fault with zero fault resistance was applied. Phase A measured impedance for two A-G faults with zero and 80 Ω fault resistance are compared with the safe region of the impedance plane in Fig. 6.12.

The next example tests the algorithm for faults at the end of the transmission line. The test conditions were: ten different faults at the receiving-end source, fault resistance 10 Ω for ground faults, SCC ratio 1/10, relative angle 30 degrees. The sending-end source was chosen as a weak source, while the receiving-end source was very strong. These set of parameters result in a very extreme case for the power system. In this case, the fault resistance is magnified considerably. For a phase A to ground fault *(A-G)* , the ratio of the fault currents from two sources is about 100. The phase A current is shown in the top of Fig. 6.13. It shows that for the A-G

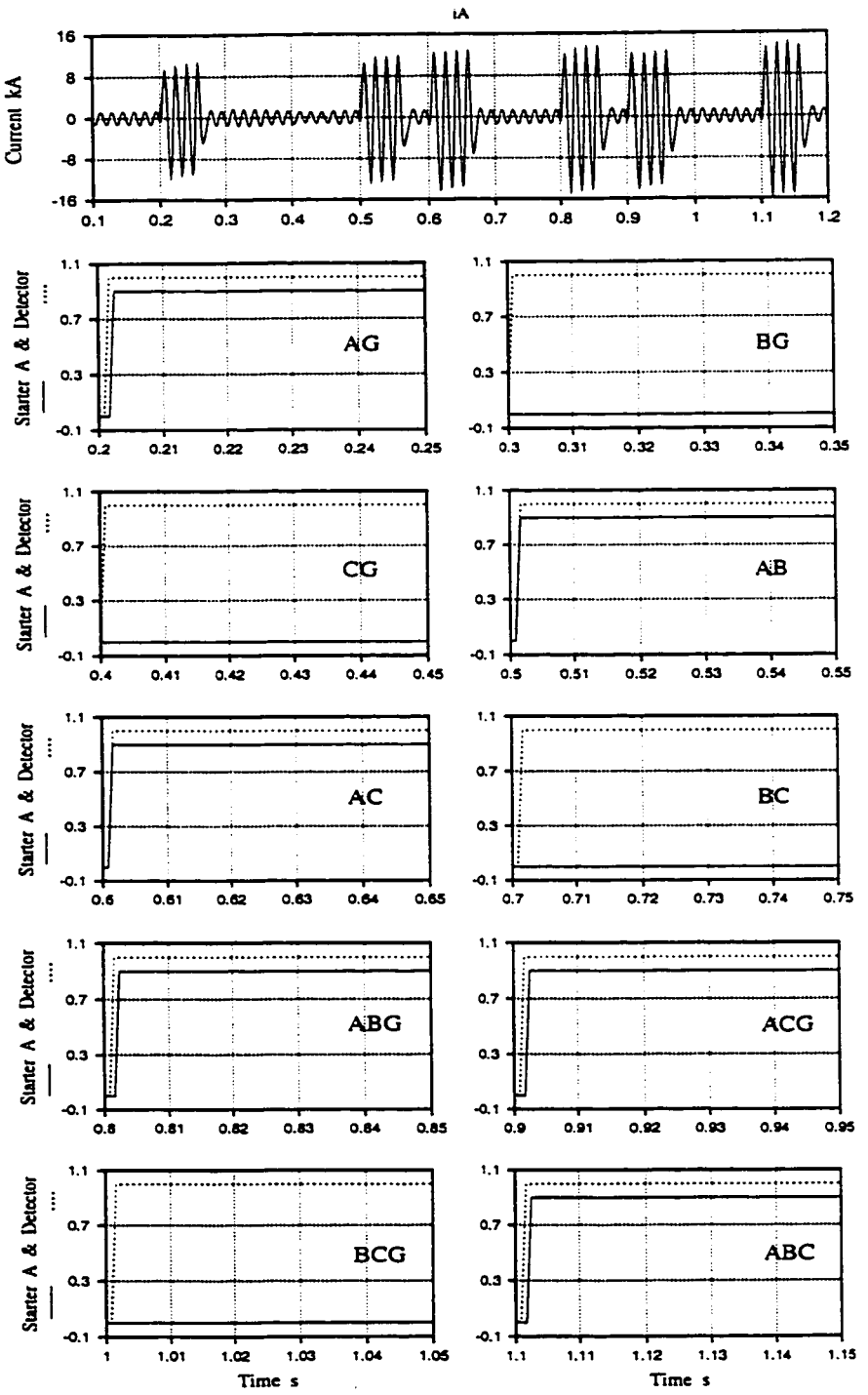

Figure 6.10: Phase *A* starter and detector outputs for faults at relay location, fault resistance 1 Ω for ground faults, SCC ratio 1, angle 30 degrees

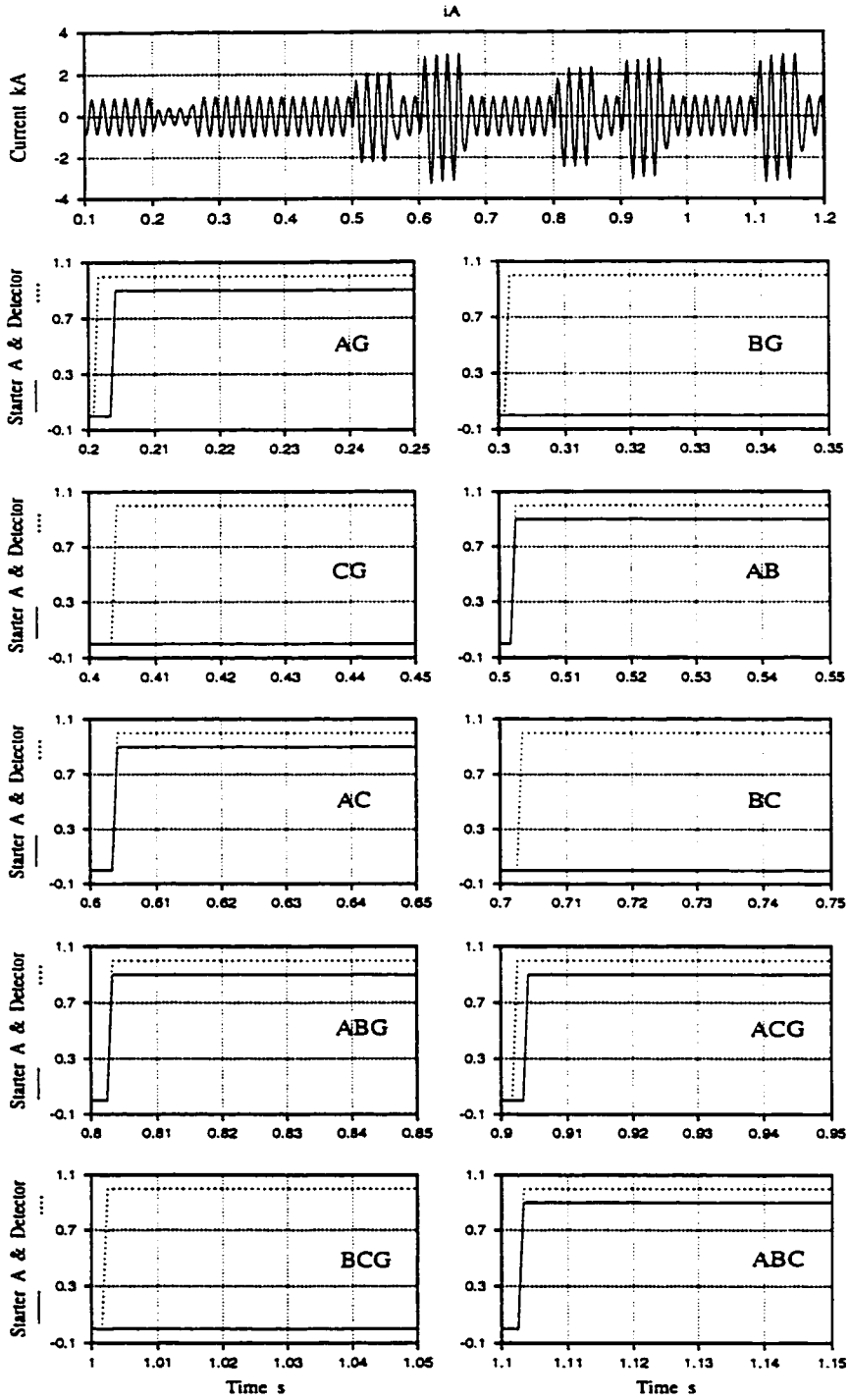

Figure 6.11: Phase A starter and detector outputs for faults at 50 km, fault resistance 80 Ω for ground faults, SCC ratio 1/5, angle 30 degrees

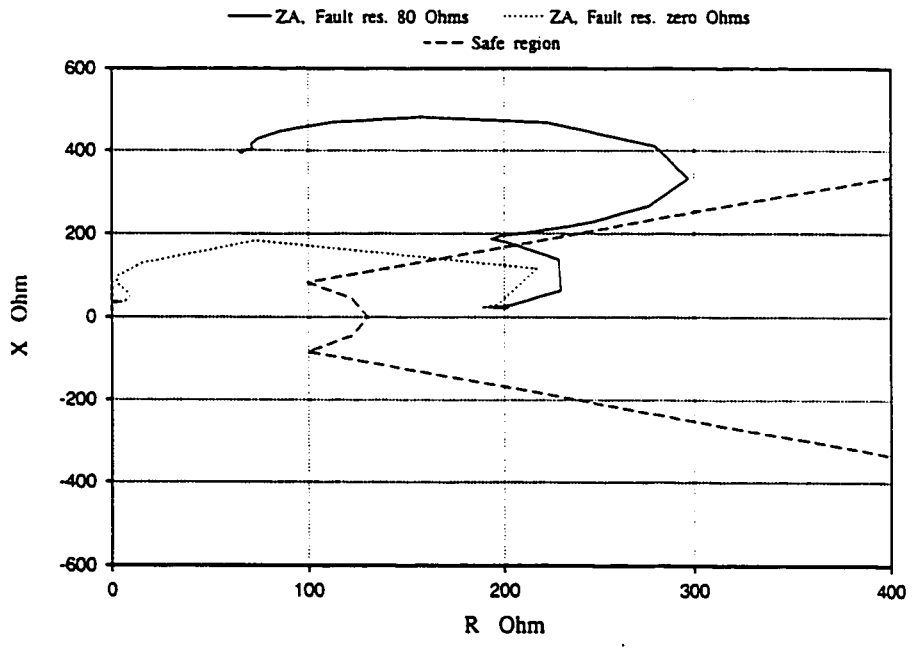

Figure 6.12: Phase A impedance trajectory for two A-G faults with zero and 80 Ω fault resistance

fault, the phase A current is even less than the normal load current.

Phase A starter and detector outputs for different fault types are shown in Fig. 6.13. On average the detection module needs just about 4 ms to detect different faults correctly, even for the case of the fault at the end of transmission line with high resistance which is slow in nature. The phase starters using adaptive routine perform faster and better compared with the starters using fixed setting values.

The adaptive routine adjusts the settings to the proper values. For the next example the test conditions were: phase A to ground fault at the receiving-end source, fault resistance 4 Ω, SCC ratio 1/10, relative angle zero degree. The infeed effect of the receiving-end source magnifies the fault resistance. The phase A measured impedance trajectory for the A-G fault is compared with the two safe regions, one with adaptive setting and the other one with constant setting in Fig. 6.14. Unless the adaptive settings is used, the trajectory settles in the safe region of the impedance plane and the fault could not be detected.

6.5.3 Sequential Faults

The performance of the algorithm was evaluated for two sequential faults. Sequential faults could happen in the case the lightning hits the transmission line or one of the conductors breaks.

Fig. 6.15 illustrates the results obtained for the following conditions: two A-G and A-B-G sequential faults in front of the relay at 70 km, fault resistance 10 Ω, SCC ratio 1/2, relative angle -30 degrees. It is assumed that first an A-G fault happens at 0.2 s and then, after 5 ms, it changes to a A-B-G fault. For clarity in display, the phase A and B starter outputs are multiplied by 0.9 and 0.8, respectively. It shows

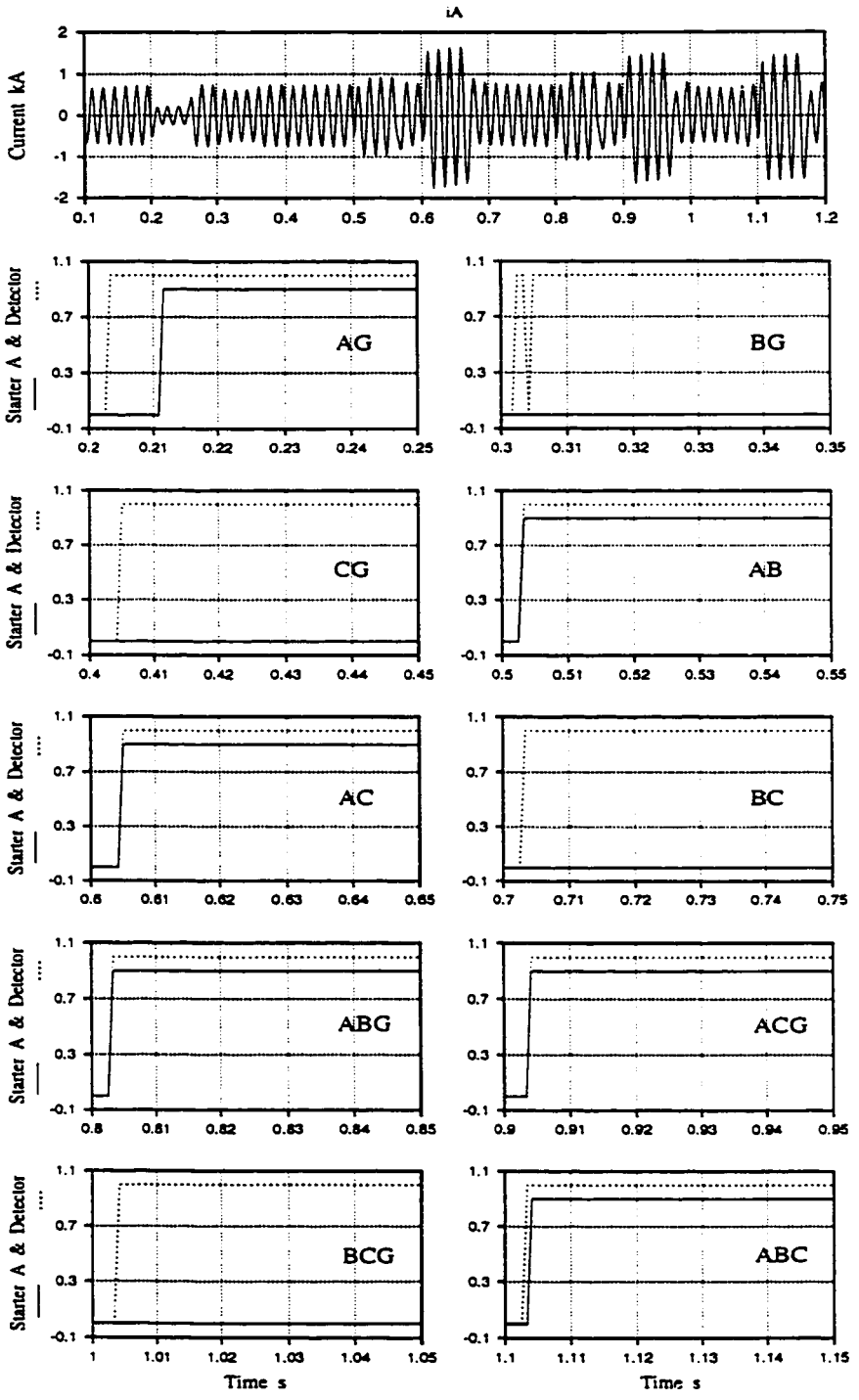

Figure 6.13: Phase A starter and detector outputs for faults at receiving-end, fault resistance 10 Ω for ground faults, SCC ratio 1/10, angle 30 degrees

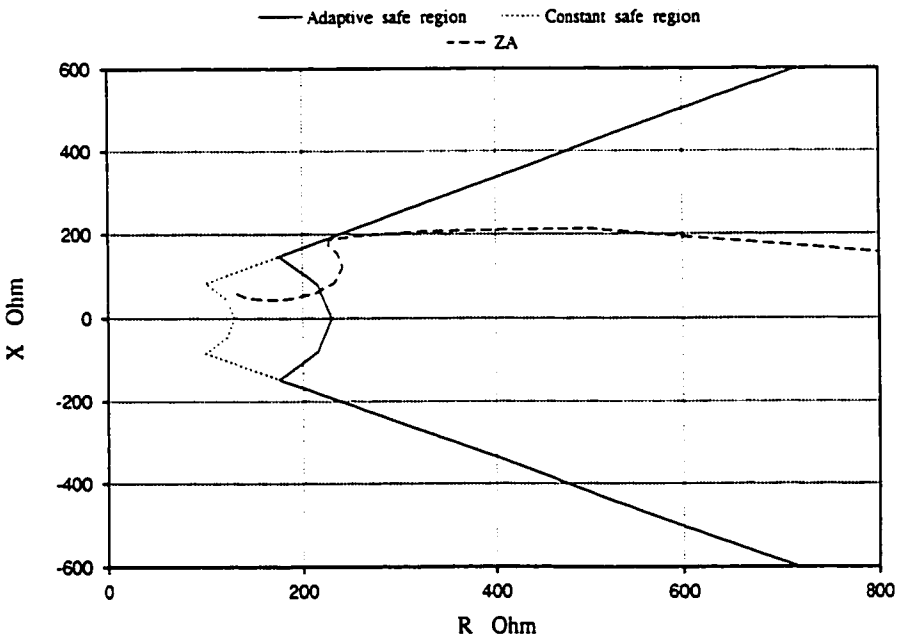

Figure 6.14: Phase A impedance trajectory for the A-G fault in comparison with two adaptive and constant safe regions

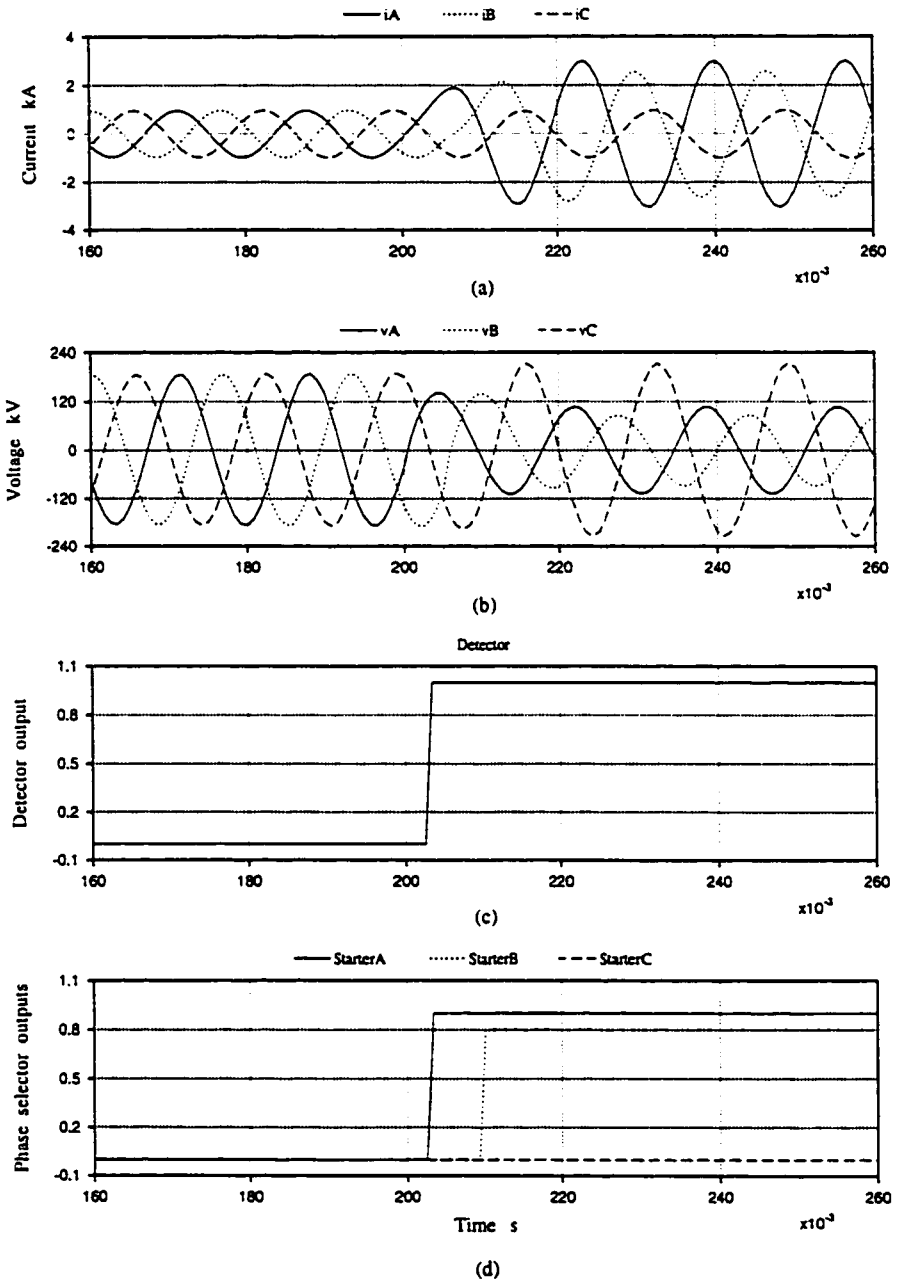

Figure 6.15: Phase starters and detector outputs for the *A-G* and *A-B-G* sequential faults

that the algorithm detects the fault rapidly and the starters classify the fault type accordingly.

6.5.4 Cross-Country Faults

The proposed algorithm was tested to check its performance during cross-country faults.

For this example the test conditions were: phase A to ground fault at 70 km, phase C to ground fault at 100 km, fault resistance 2 Ω for both faults, SCC ratio 2, relative angle 20 degrees. The measured voltage and current signals at the relay location and the outputs of the detector and three starters are shown in Fig. 6.16. As shown in this figure, the detector detects the faults very fast and the appropriate phase starters respond to the faults accordingly.

6.5.5 Line Charging

During line charging, breakers at one end of a transmission line are closed for some time before the breakers of the other end are closed. In the period in-between, a considerable inrush current is normally observed. It is desired that the relay installed at the energized end of the transmission line prevent tripping in such a case. The performance of the proposed scheme was checked for a line energization case. A three phase source with SCC of 5 GVA was closed on a 150 km transmission line. After some oscillation, the trajectories of the measured impedances settled inside the safe region of the impedance plane and none of the three starters detected this case as a faulty case.

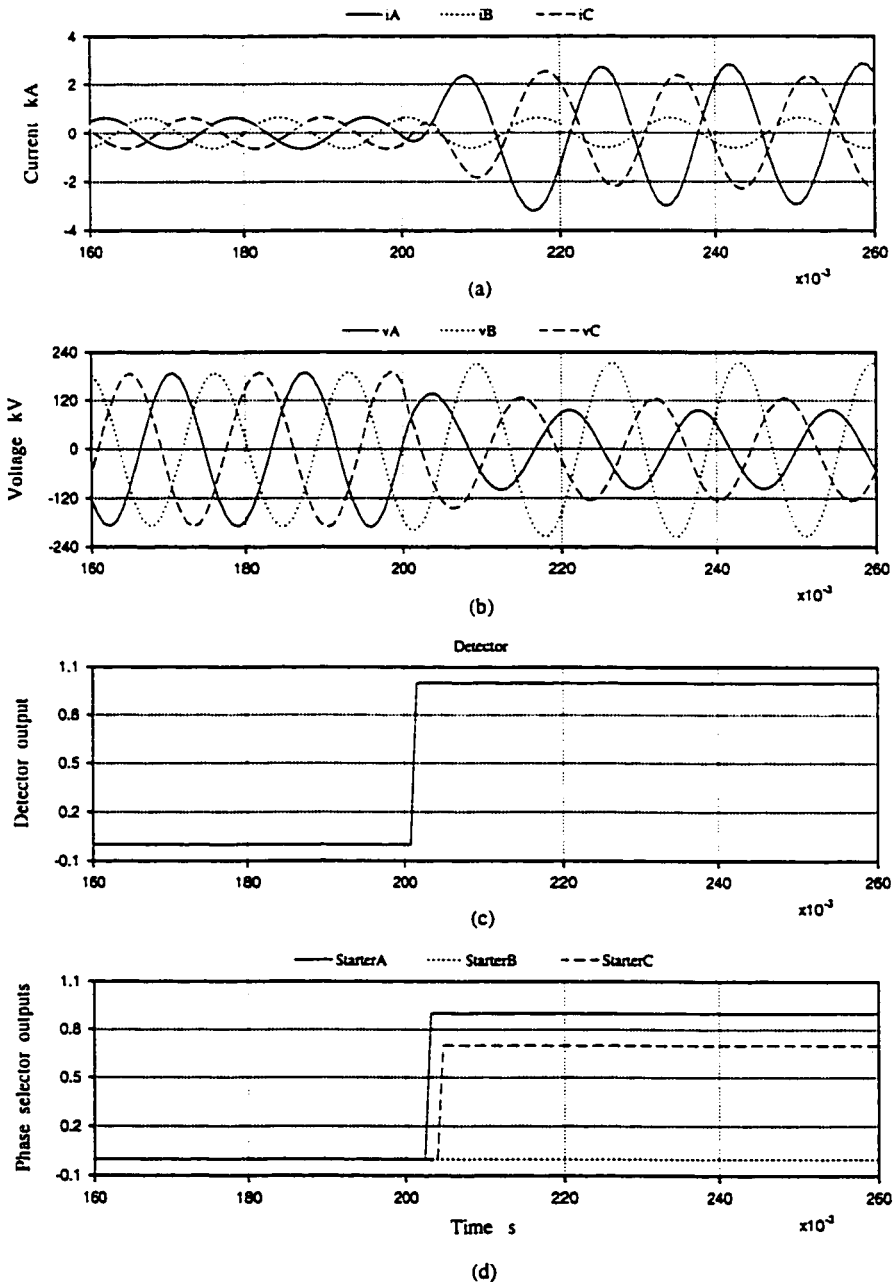

Figure 6.16: Phase starters and detector outputs for the A-G and C-G cross-country faults

For the first few cycles after energization, the measured currents and voltages at the relay location develop high amounts of nonfundamental power system frequency components. This is specially more severe for the current signals. The impedance measurement algorithm uses a short length window. Therefore, the measured impedance initially oscillates. The proposed algorithm covers a wide area of the impedance plane. The measured impedance might enter the nonhealthy area of the impedance plane during its initial oscillation. A few other line energization tests were performed and it was found that, in some cases during the first cycle after the energization, the measured impedance trajectory enters the nonhealthy area once or twice.

During line energization the coverage area of the impedance plane could be reduced by decreasing the radius of the outer circle. It prevents the starters to operate under line energization case. A power system similar to that used in Fig. 6.8 was used and a line energization study was performed. The sending-end source breakers were closed while the receiving-end source was disconnected from the end of the transmission line. The radius of the outer circle was decreased to 500 Ω. The measured voltage and current signals at the relay location and the outputs of the detector and three starters are shown in Fig. 6.17. The transient effect is considerable for current signals specially during the first 40 *ms* after line energization at 0.3 *s*. It shows that the detector and starters outputs remain stable during the line charging transients.

The simulation study results show that the proposed algorithm is able to detect and classify different faults correctly and very rapidly with wide changes in power system parameters and conditions like fault resistance changes, source impedance

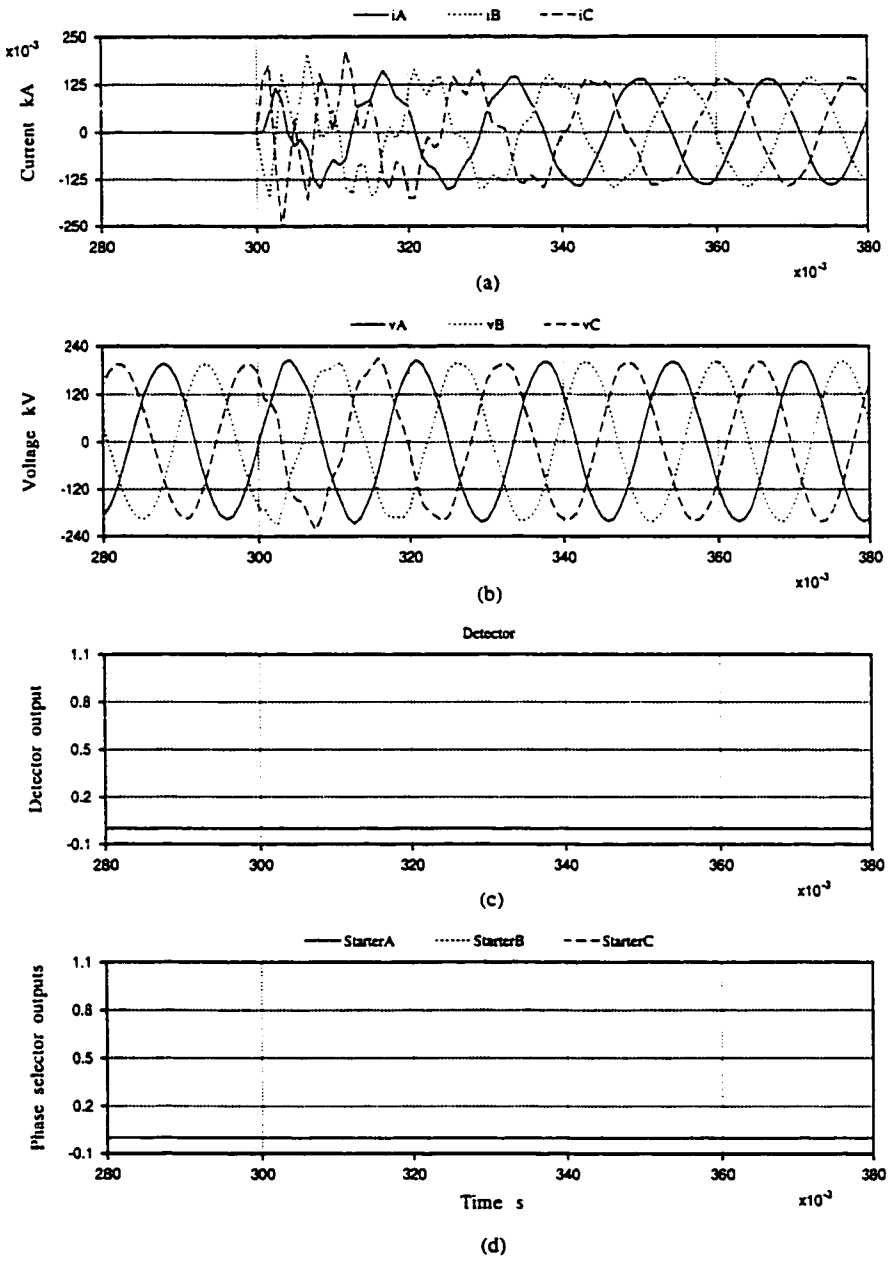

Figure 6.17: Phase starters and detector outputs for the line charging case

changes and different power flow directions. The results presented in this section mainly demonstrate the algorithm's performance for some extreme fault cases. In general, the proposed algorithm performs better and faster for more usual cases such as low resistance faults around the middle of the protected areas.

6.6 Summary

A new underimpedance starter which covers a wider area of impedance plane is proposed in this chapter. The measured impedance vector is compared with the safe region of the impedance plane to detect faults on a transmission line and to classify the fault type. Simulation studies are performed and the performance of the proposed scheme is investigated. Influence of changing system parameters such as fault location, fault resistance, source impedance and pre-fault power flow direction is studied. The performance of the proposed scheme is also checked for extreme cases like faults including high amount of resistance and also faults at the relay location. Adaptive features are also included to enable the starter to track the changing operating conditions of the system. Through extensive studies it is found that the proposed algorithm is able to detect and classify different fault types correctly and rapidly.

Part II

Real-Time Implementation

Chapter 7

Laboratory Experimental System

7.1 Introduction

Theoretical development and simulation studies of different modules of a transmission line protective relay are described in Chapters 2 to 6. Simulation studies show that the proposed modules are able to perform rapidly and correctly for a wide range of different changing system conditions.

Mathematical model of any real plant is always based on some assumptions and simplifications. Thus, although the computer simulation studies play an important role in the design of a new algorithm, on-line tests on a physical model are necessary before its practical use.

After the theoretical development and computer simulation studies, the performance of different modules of the proposed relay is investigated further on a physical model of a power system. Scaled physical model is able to emulate the behavior of the actual power plant in the laboratory environment. The relay modules have been implemented on a Digital Signal Processor (DSP) board mounted on a Personal Computer (PC). Details of implementation of the proposed modules are presented in this chapter. The laboratory set-up and experimental power system are also given. Results of experimental studies will be presented in Chapter 8.

7.2 Experimental System Set-up

A single-machine infinite bus power system was physically modeled in the power laboratory. This physical model represents a large system of approximately 600 MVA. An overall schematic diagram of the experimental system set-up is shown in Fig. 7.1.

The current and voltage signals from the power system are obtained through Current Transformers (CTs) and Potential Transformers (PTs). The low level output voltage signals from the CTs are amplified and then filtered. The PTs outputs are filtered as well. The Data Acquisition System (DAS) receives the analog signals through the Analog Input Card (AIC). The analog filtered signal is then transferred to the DSP board and is converted to digital by internal Analog to Digital (A/D) converters. Details of these blocks are presented in the following sections.

7.2.1 Power System Physical Model

A three-phase 3 kVA, 208 V synchronous micro-alternator driven by a 7.5 hp separately excited dc machine is employed to model the generating station. The station is connected to a constant voltage system (infinite bus) through a transmission line. In this model, the micro-alternator and the dc motor act as the generating unit and the turbine, respectively (Fig. 7.1).

The micro-alternator is designed to achieve, in most respects, an adequate model of a large generator. Because of size limitation, the field time constant is smaller than that of a corresponding large machine. To improve the performance during transient conditions, a Time Constant Regulator (TCR) designed to change the effective field

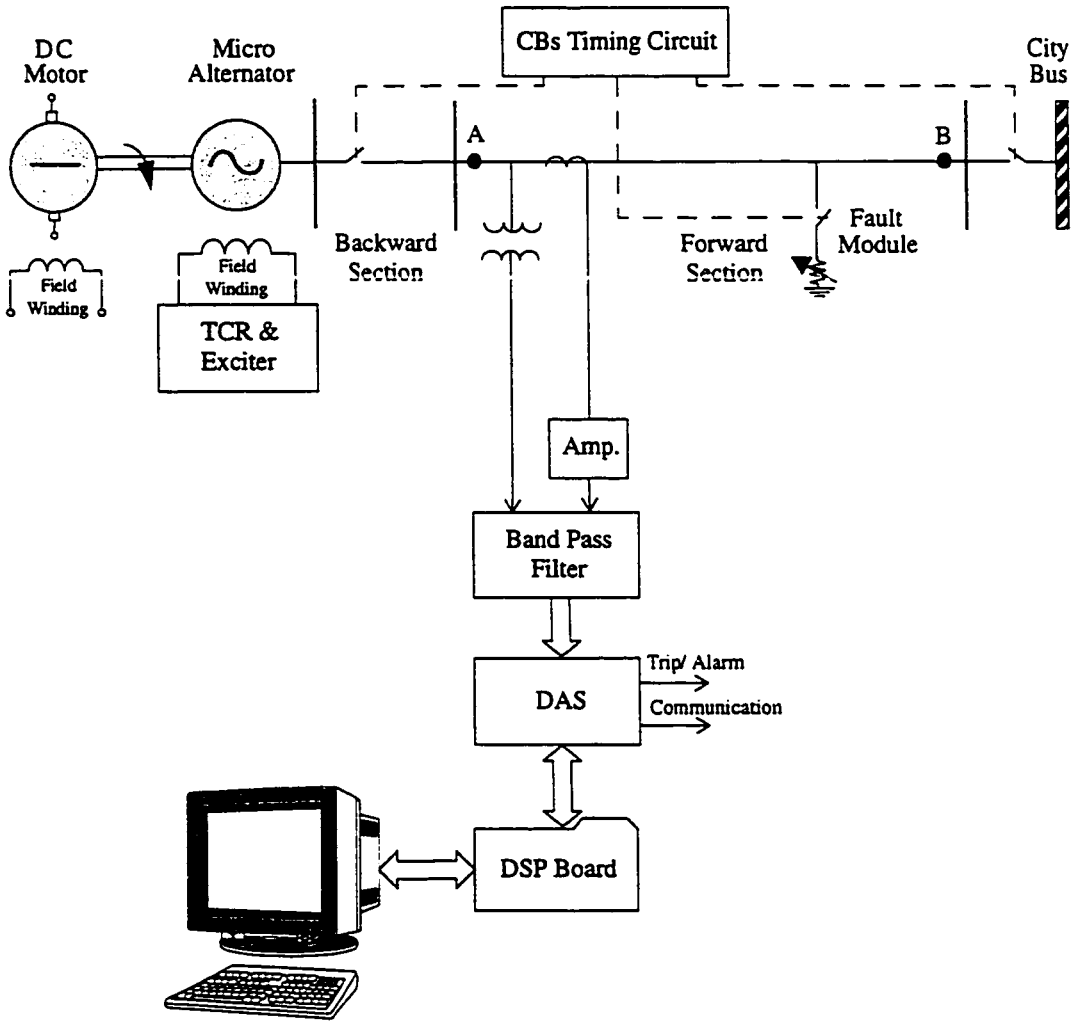

Figure 7.1: Schematic diagram of the experimental system set-up

time constant of the micro-alternator has been used.

The transmission line was modeled by a lumped element physical model. It was modeled by 6 identical π-sections, each section representing 50 km of a 500 kV transmission line, cascaded together to form a 300 km line length [71]. The parameters of the actual and the equivalent π-section model are given in Appendix D.

A system of 3 three-phase Circuit Breakers (CBs) controlled by a ROM based logic circuit is used. Of the three sets of breakers, two sets are used at the ends of the transmission line and the third is used to apply the fault at any distance. The contact open and close timings and their sequencing can be programmed.

Different types of faults including 1-phase to ground, 2-phase to ground, phase to phase and 3-phase can be applied to the power system model. Fault location and fault resistance could also be changed. By changing the armature and field current of the dc motor the active output power of the micro-alternator can be changed.

7.2.2 Current and Potential Transformers

The directional relay uses line to neutral voltage and line current input signals. The line to neutral voltages are obtained by the use of 115/6.3 V isolating potential transformers. The line currents are obtained through 15/5 A current transformers. The CT secondaries are connected to a shunt impedance to obtain an equivalent voltage signal. The output voltage signal is in the range of mili-volts. Therefore, it should be passed through an amplification stage before being converted to digital form.

Analysing the spectrum of the signals before and after the current transformer, it was found that the CTs used in the laboratory do not pass all frequencies in the signal. It was found that although the CTs change the shape of the signal to some extent, however, this effect is minor specially for the main frequency component [72].

7.2.3 Analog Filter

The sampling process is essential for microprocessor protection in that the analog signals must be converted into appropriate form so that the digital hardware can perform calculations and reach relaying decisions. A low-pass analog filter is required to limit the input signal frequency to avoid aliasing errors.

For the implementation of the scheme, a suitable sampling rate should be selected. The sampling frequency used in this work is 1200 Hz. According to the *Nyquist* theorem [73], signals with finite bandwidth can be completely described by sampling them at a rate at least as high as twice the highest frequency in the spectrum. In other words, the highest frequency allowed to pass by the analog filter must be less than half of the sampling frequency. In practice, the sampling rate must be chosen to be somewhat greater to ensure that the signal can be recovered considering practical hardware limitations.

When a fault occurs on a transmission line, voltage and current signals develop a decaying dc offset component whose magnitude depends on many factors that are random in nature. The dc components of the voltage and current signals are also required to be removed. This preprocessing enhances the training capabilities of the proposed neural networks and decreases the number of required patterns for training the networks.

An active 2nd-order Butterworth band-pass filter has been used to attenuate the dc component and high frequency components. The Butterworth filter has maximally flat response in the pass band. The filter is centered at the nominal system frequency and its passband is chosen to be 30 Hz. This value allows a considerable reduction

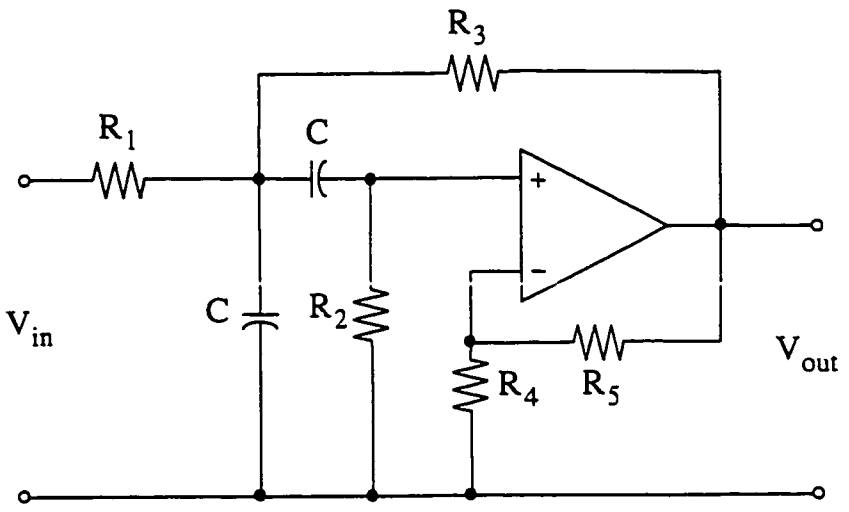

Figure 7.2: Analog filter circuit

of the high frequency and dc components with a small time delay. The filter circuit used is shown in Fig. 7.2.

An array of six circuits simultaneously filters the current and voltage signals before being fed to the data acquisition system. For current signals, the filter unit circuit is preceded by an amplifier circuit. The filter's parameters values have been calculated and are given in Appendix E [74].

7.2.4 Digital Signal Processor Board

Development of the real-time digital algorithm environment is based on a DSP board supplied by SPECTRUM Signal Processing Inc.. The board contains a TMS320C30 DSP chip which is a 32-bit floating-point device with 60 ns single cycle instruction execution time. Its performance is further enhanced through its large on-chip memory, concurrent Direct Memory Access (DMA) controller, two external interface ports and instruction cache. Furthermore, the two 200 kHz, 16-bit analog I/O channels on

board, coupled with direct access to all serial and parallel I/O channels of the DSP chip, provide the exterior input-output functions. The DSP board is installed on a PC with corresponding development software and debugging application program [75].

7.2.5 Data Acquisition System

The purpose of the DAS is to convert the analog data into a form usable by a digital processor. For the sampling rate of 1200 Hz, the time interval between the samples is about 0.83 ms which needs a fast DAS to acquire current and voltage signal inputs in less than 0.1 ms. Appropriate software and hardware setup for accomplishing fast data acquisition were designed and fabricated in the Power System Research Laboratory at the University of Calgary.

Using the two I/O channels of the DSP board, CHA and CHB, and an interrupt based routine, the data acquisition system was designed. The interrupt based program reads, scales and stores the data from DAS hardware. The DAS could handle up to 9 inputs and 2 outputs. The standard un-buffered DSP analog channel CHB acts as the first analog input. Using some external hardware, the DSP analog channel CHA was expanded to act as the inputs 2 to 9. The DSP standard analog outputs CHA and CHB could be directly used as two analog outputs.

The schematic diagram of the DAS hardware is shown in Fig. 7.3. Analog input 1 could be directly connected to the DSP analog channel CHB. Analog inputs 2 to 9 are first passed through a gain stage. The analog inputs to the DSP board should be limited to $\pm$ 3 V. Appropriate gains should be used for each input to limit the DSP

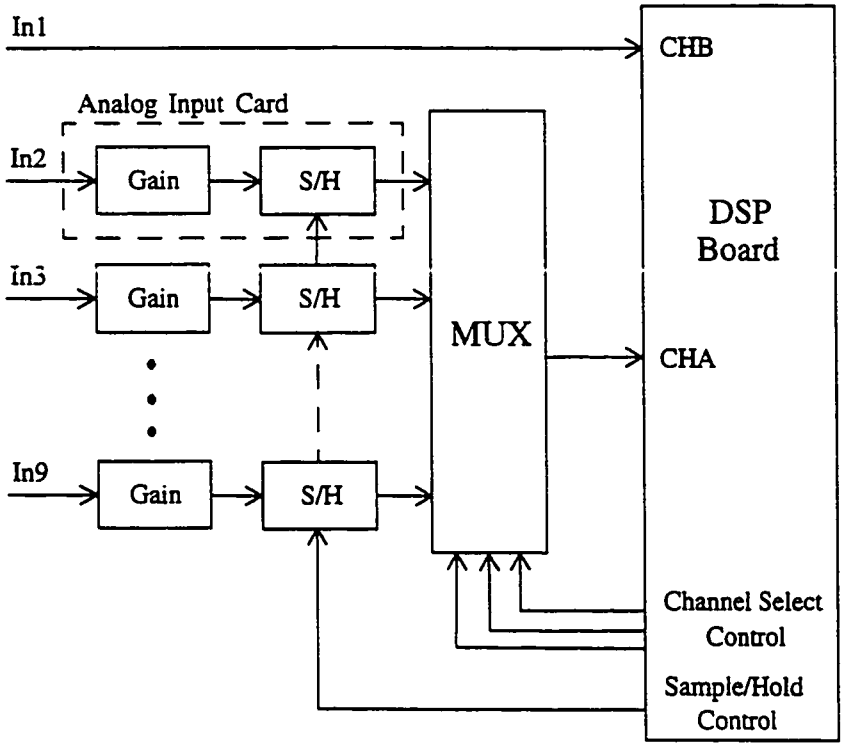

Figure 7.3: Schematic diagram of the data acquisition system

inputs to the desired specified range. Next, each analog input is passed through a high speed Sample & Hold (S/H) amplifier. The outputs of eight S/H amplifiers are routed to an 8 channel analog multiplexer. The DSP's input channel CHA receives the multiplexer's output signal. Using the built-in analog to digital converter, this signal is then converted to digital form internally.

A $\pm$ 3 V analog input range to the DSP provides full scale operation of the 16 bit A/D. In the area of power system digital protection, both 12 and 16 bit A/D converters are in use. The large difference between load and fault current is a driving force behind the need for more precision in the A/D conversion. It is difficult to measure load current accurately while not saturating for fault current with only 12 bits [9].

The DAS also features a possibility for 2 analog outputs. The analog outputs could be used to trip the circuit breakers or to trigger an alarm signal. They could also be used for sending trip/block signals between relays at each end of the transmission line.

The characteristic of the DSP board hardware is such that the same register is used for input and output. Therefore, any input is mapped to the respective output unless something is written to that register before the next A/D conversion. So, prior to reading anything to the DSP board, the outputs must be updated.

7.3 Embedded Software Structure

With the PC accommodating the DSP board, the digital relay program is developed in a modular form using the C programming language. The real time application program is primarily interrupt driven, with a basic structure as shown in Fig. 7.4.

Any project using the DSP board has two software modules, the DSP module and the PC module, that run in parallel. One primary function of the PC module is to download the running code for the DSP into its RAM, since there is no ROM storage on the DSP board. The control system is initiated by the execution of the PC module code on the personal computer. This in turn boots the DSP by loading the compiled DSP module code into the digital signal processor board memory through the personal computer's ISA bus.

After downloading the DSP program to the board, the PC program waits for the DSP signal to begin the main control loop. The DSP acknowledges by sending a message back confirming the application program is running on the DSP board.

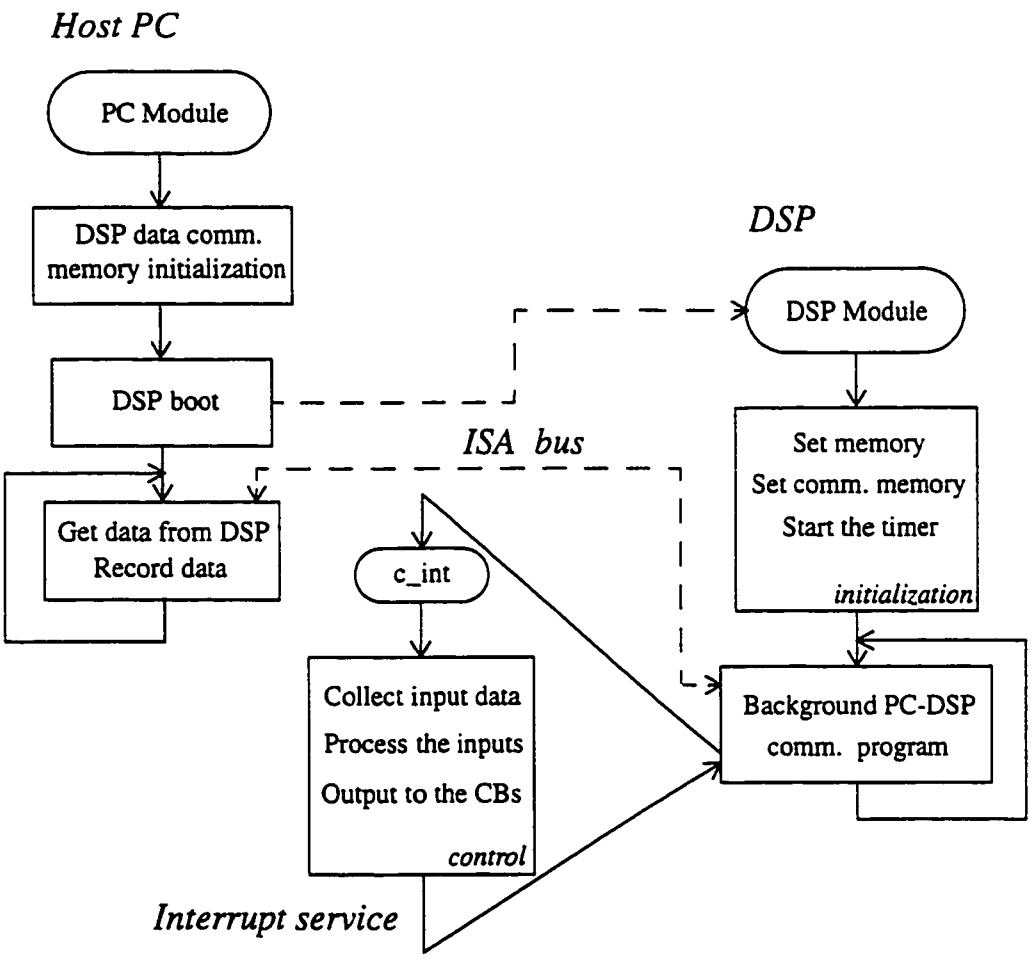

Figure 7.4: Application program structure for the digital relay

The personal computer then enters a loop communicating with the DSP board. It receives input-output signals of the application program running on the DSP board and records the data for further reference. A human-machine interface could be further added to display real-time graphs on screen.

The DSP boot procedure initializes the board and establishes the communication between PC and DSP processors. The required matrices and vectors for the application program are also allocated and initialized. After initialization, the DSP enables the interrupt service mechanism and the control executes as an interrupt service routine.

At each sampling time, the interrupt service routine is called which contains the protection application program. The interrupt routine first using the DAS hardware acquires, scales and stores all the input channel data. When the data collection is completed, DSP would return the DAS hardware to sampling mode and proceed with the protection scheme using saved inputs. When the processing is completed the input-output data would be communicated to the personal computer. The output signal computed by the application program could also be sent to the circuit breakers timing circuit using the DAS. Upon the arrival of the next sampling interval this process begins again.

7.4 Digital Relay Real-time Implementation

One of the most important tasks in designing a new protective relay for a power system is the performance of on-line tests. In this way, the performance of the newly designed digital relay can be further verified in a more realistic environment than

pure simulation.

A DSP board is used to implement the proposed digital relay modules. At each sampling point the input data window is moved forward by one point and the new set of the input data is presented to the DSP. The DSP board should complete processing of the new input information within one sampling period.

The implementation software for realizing the relay modules was programmed in the C language. After compilation and assembly it was down-loaded to the DSP board. The appropriate neural network's weights and biases were also loaded to the board. Floating-point arithmetic was used in the implementation.

Any one of the proposed neural networks could be chosen to act as the relay's directional module. Using different networks, it was found that it took only about 0.4 ms at most to execute the total directional module network. Given that the sampling interval is 0.8333 ms, this execution time is well within the available inter-sampling time. This leaves more than 0.4 ms for the acquisition of the current and voltage inputs through DAS and for the execution of the remaining modules of the relay which are in series with the directional module. For the conventional relaying programming, conditional statements tend to make the execution time variable. However, for the neural network based directional module execution time for all the input patterns is the same.

7.5 Summary

Real-time implementation of the proposed digital relay modules is presented in this chapter. A DSP board is used for realizing different modules of the relaying algo-

rithm. A physical model of a power system is used to test the relaying algorithm performance on-line. Various types of faults can be applied at different locations of the transmission line model and the relay performance could be investigated.

Experimental studies to test the relay modules performance have been performed on the micro-alternator power system model. Some of the results are presented in the next chapter.

Chapter 8

Experimental Studies

8.1 Introduction

The proposed relay modules have been implemented on a DSP board and their performance tested on a physical power system model. Results of experimental studies performed on the power system model with the different proposed modules are given in this chapter.

The laboratory power system set-up shown in Fig. 7.1 was used for the experimental studies and for simulating various types of faults. The micro-alternator was first synchronized with the system and then the desired operating condition was set up by adjusting the field and the armature currents of the drive motor and the field current of the micro-alternator. Faults were applied by means of the CBs' timing control circuit.

The measurement devices are located at 50 km (one π-section) from the generating station and look forward towards the infinite bus station (point A in Fig. 7.1). Thus, the transmission line between the relaying point and point B at one π-section from the infinite bus station is the forward protection zone and the transmission line between the relaying point and the generating station is the backward line section. Faults in the forward protection zone are called forward faults whereas faults

occurring on the opposite side of the relay are labeled as backward faults.

Different neural networks were proposed as the relay's directional module. These networks were originally trained for a different transmission line with different length and characteristics than that in the laboratory. They were not retrained for the laboratory implementation studies.

The trained networks were used to determine the direction of faults on the model transmission line. The ANN-based algorithms were tested to evaluate the performance of the proposed networks in terms of generalization, robustness and speed. The networks were tested with different independent test patterns which were not included in the training pattern set and promising results were obtained. The effect of fault resistance was also studied. The performance of the proposed starter module was also evaluated under different system conditions. Some of the test results are presented in the following sections.

8.2 Feedforward Network Directional Module

8.2.1 Thirty-Input Network

The thirty-input trained network of Ref. [61] was used and realized using the DSP board. This network was used to determine the direction of faults on the power system model in the laboratory. Although the voltages and currents of the power system model are different from voltage and current levels of the power system on which the directional module was originally trained, it was possible to use the same network because the voltage and current samples were normalized before being fed

to the neural network.

Various types of forward and backward faults were applied at different locations and at random instants in the *ac* cycle. Since the transmission line is made up of lumped π-sections faults may only be applied at discrete points on the line.

As an example, the network's output for two different types of forward faults is shown in Fig. 8.1. The faults were a double phase to ground *A-C-G* fault and a three phase *A-B-C* fault at 100 *km* and 50 *km* from the relay location, respectively. Four consecutive outputs of the network are considered and averaged. Averaged outputs of this post-processing unit which fall above 0.5 and below -0.5 are interpreted as forward and backward faults, respectively. The averaged output is shown for the first 20 samples after the fault detection (sample number 1). This figure shows that for both faults the network performs correctly and rapidly.

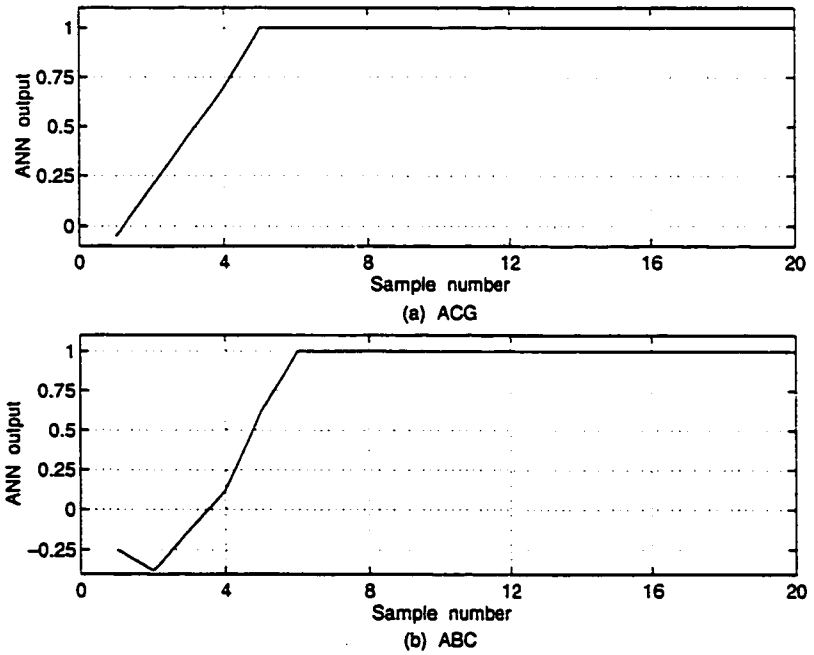

Figure 8.1: Thirty-input feedforward network averaged response to two different forward faults

8.2.2 Twenty-Input Network

The proposed twenty-input feedforward network of Ref. [61] is considered as the directional module of a transmission line protection system and its performance is investigated. Test results for four different forward and backward faults are presented.

The averaged network's output for a double phase to ground *A-C-G* forward fault at 100 *km* from the relay location is shown in Fig. 8.2a. A *B-G* forward fault was applied at 50 *km* from the relay location and the averaged output is shown in Fig. 8.2b.

Two different types of forward and backward faults were applied at 50 *km* from the relay location and the averaged output of the network is shown in Fig. 8.3. The first fault was a double phase to ground *A-C-G* forward fault including fault resistance, while the second fault was a phase to phase *A-B* backward fault without fault resistance. In the case of the *A-C-G* fault the amount of fault resistance was 0.3 Ω using the 208 V, 3 kVA model power system. In an equivalent 500 kV, 600 MVA system this amount translates to an equivalent resistance of about 9 Ω.

The directional network in all four cases classifies the fault direction correctly. The direction decision is made fast, as in the case of simulation studies.

8.3 Recurrent Network Directional Module

The proposed small size recurrent network has been implemented on a digital signal processor board and its behavior is investigated on the physical power system model [76]. Based on the structure of the proposed recurrent network, the implementation

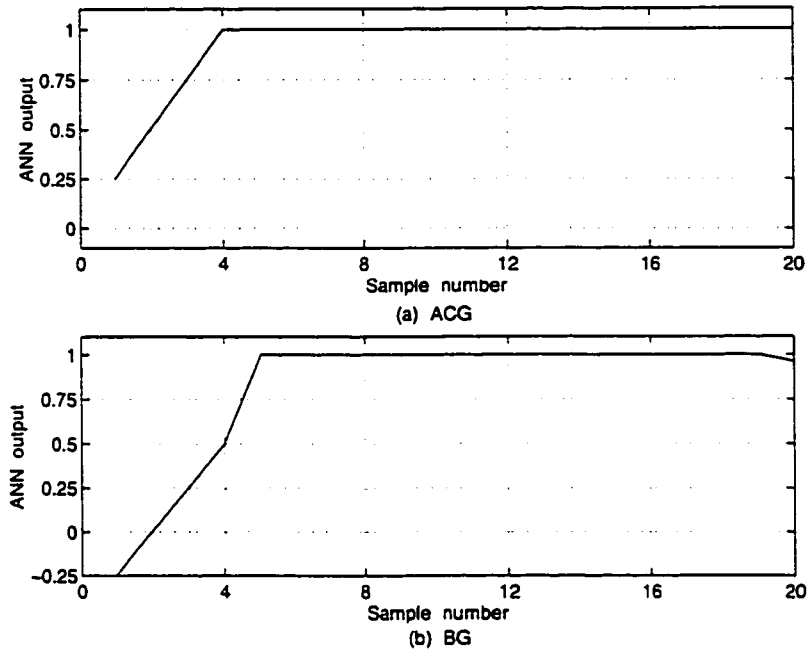

Figure 8.2: Twenty-input feedforward network averaged response to two different forward faults

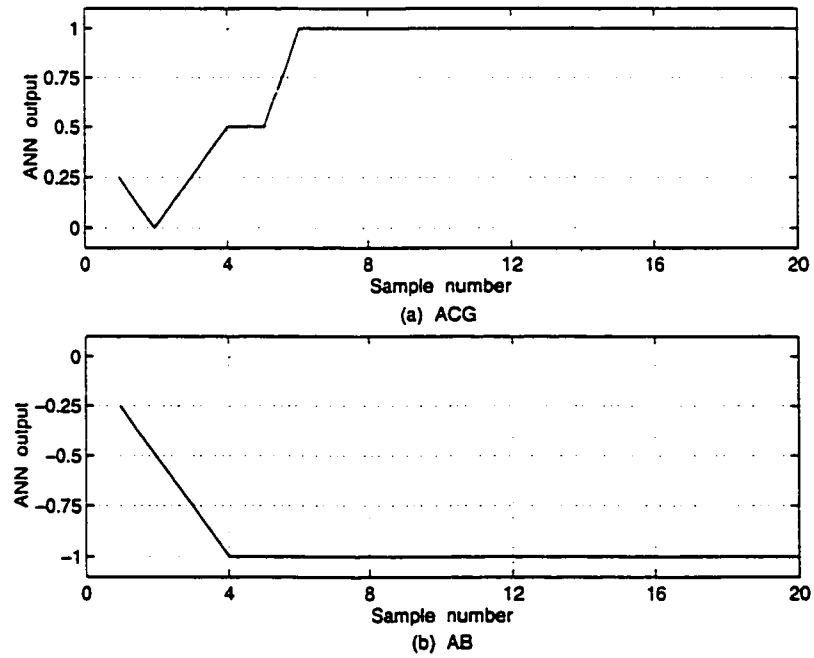

Figure 8.3: Twenty-input feedforward network averaged response to two different forward and backward faults

software was programmed in the C language. After compilation and assembly it was down-loaded to the DSP board. Network's weights and biases were also loaded to the board.

It was found that it took only about 0.25 ms to execute the total network. Given that the sampling interval is 0.8333 ms, this execution time is well within the available inter-sampling time. This leaves about 0.58 ms for the acquisition of the current and voltage inputs through DAS and for the execution of the remaining modules of a protection scheme which might be in series with the directional module. For the conventional relaying programming, conditional statements tend to make the execution time variable. However, for the neural network-based directional module execution time for all the input patterns is the same.

8.3.1 Forward Faults

The trained recurrent network was used to determine the direction of faults on the model transmission line. Various types of forward and backward faults were applied at different locations and at random instants in the ac cycle.

As an example, two different types of forward faults were applied at 100 km from the relay location and the network's output for the first three cycles after the detection of the fault (sample number 1) is shown in Fig. 8.4. The first fault was a three phase A-B-C fault, while the second fault was a single phase to ground C-G fault including fault resistance. In the case of C-G fault the amount of fault resistance was more than 0.3 Ω (equivalent to 9 Ω for the 500 kV system).

The network outputs which fall above 0.5 and below -0.5 are interpreted as forward and backward faults, respectively. For the faults presented in Fig. 8.4, it takes

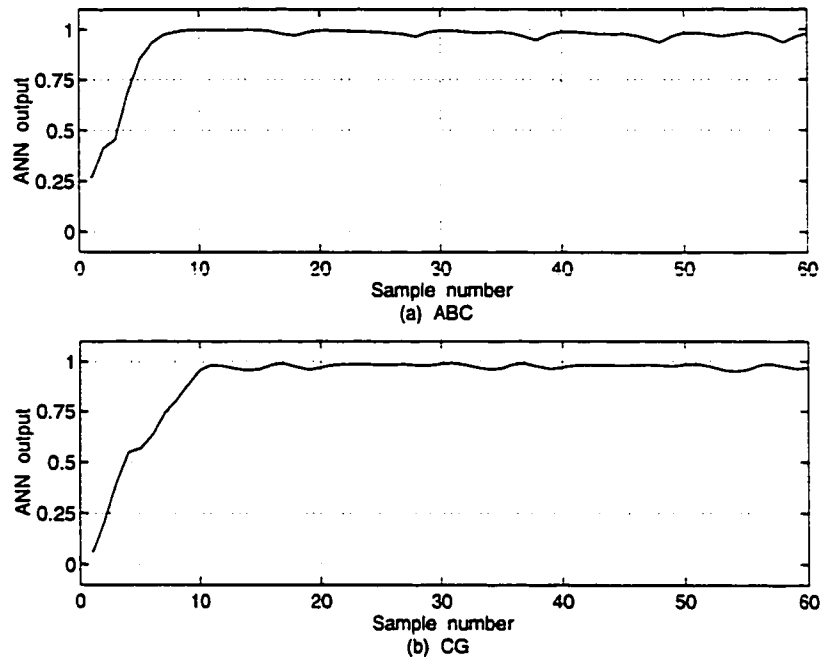

Figure 8.4: Recurrent network response to two different forward faults at 100 *km*

three samples after the fault detection for the output of the recurrent network to fall inside the forward fault area. The directional module needs just about 2.5 *ms* to classify the fault direction correctly after fault detection. As can be seen from Fig. 8.4, for both faults the fault direction identification is very fast and reliable.

Fig. 8.5 shows the output of the network for two different forward faults far from the relay location at 150 *km*. The first fault was a phase to phase *A*-*B* fault and the second fault was a double phase to ground *A*-*B*-*G* fault. It shows that the network performed correctly for the remote faults in a timely fashion.

Results of the tests for two different forward faults at the nearest possible location to the relay at 50 *km* are shown in the Fig. 8.6. Two different faults, a *A*-*B*-*C* fault and a *C*-*G* fault were applied and the network's output for these two faults is shown in Figs. 8.6a and 8.6b, respectively. The *C*-*G* fault involved 1.7 Ω (equivalent to

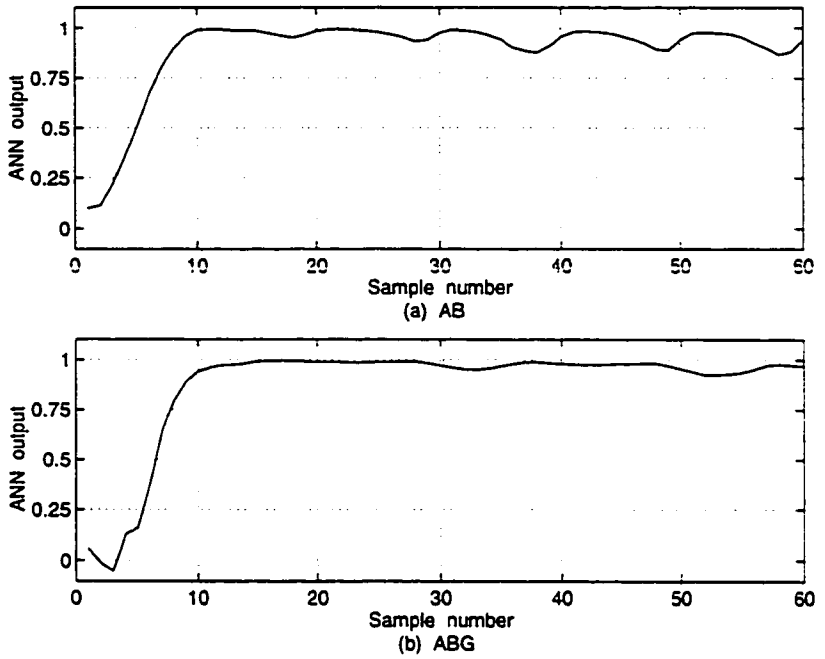

Figure 8.5: Recurrent network response to two different forward faults at 150 km

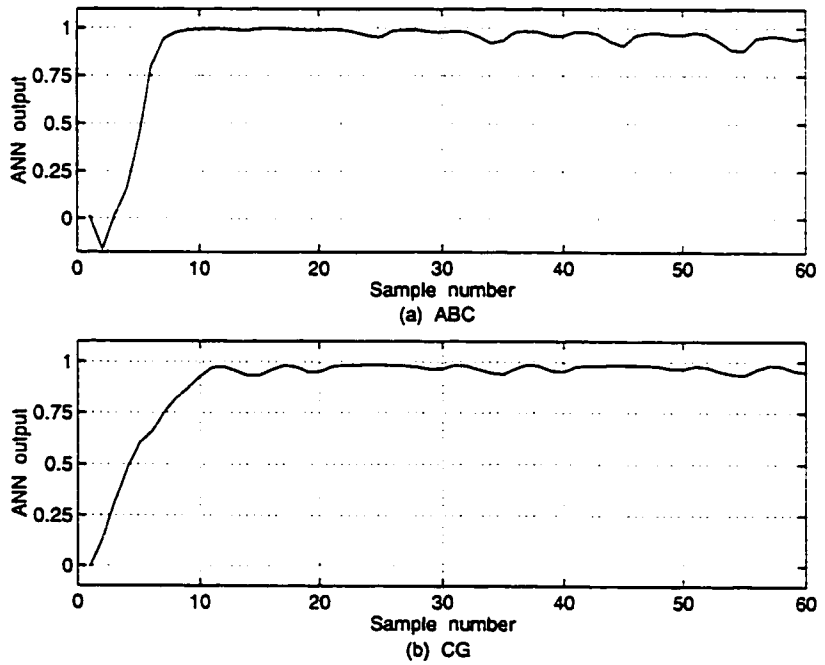

Figure 8.6: Recurrent network response to two different forward faults at 50 km

49 Ω) fault resistance. For both faults the fault direction identification is fast and reliable. The network performs correctly even for the case of the fault with very high amount of fault resistance. Although the network just uses the phase A voltage as its input, it correctly identifies the direction of the phase C to ground fault.

8.3.2 Backward Faults

Two different backward faults including 0.5 Ω (equivalent to 14 Ω) fault resistance were applied at 50 km from the relay location and the network's performance is presented in Fig. 8.7. The first fault was a single phase to ground A-G fault and the second fault was a double phase to ground A-C-G fault. The network identifies the fault direction very fast and its output remains stable for three cycles. It takes less than 3 ms to classify the fault direction.

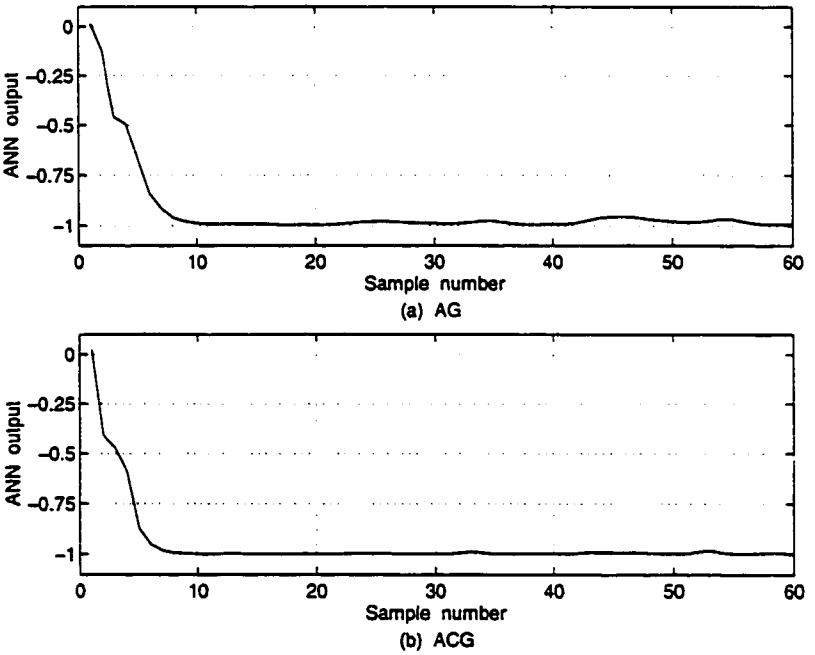

Figure 8.7: Recurrent network response to two different backward faults at 50 km

8.3.3 Faults at the Relay Location

Several faults were applied at the line side and bus side of the relay location and the capabilities of the new network were examined for faults at the relay location.

Results of the tests for two different forward faults at the relay location, a *A-B* fault and a *A-C-G* fault are presented in Fig. 8.8. The *A-C-G* fault involved 0.5 Ω (equivalent to 14 Ω) fault resistance.

The next example tests the network's performance for two different backward faults at the relay location. Two different faults, *A-G* fault and *A-B-G* fault were applied and the network's output for these two faults is shown in Figs. 8.9a and 8.9b, respectively.

These tests demonstrate that the network is able to classify forward and backward faults at the relay location correctly and rapidly. On average the directional module needs just about 3 *ms* to classify the fault direction correctly.

8.4 Elman Network Directional Module

The proposed Elman network has been used to determine the fault direction from the voltage and currents temporal input patterns. To evaluate the capabilities of the proposed network, it was tested by applying different faults on the laboratory model power system [77]. For different test faults, fault location, fault type, fault resistance, fault inception time, and pre-fault power flow condition were changed to investigate the effects of these factors on the performance of the network.

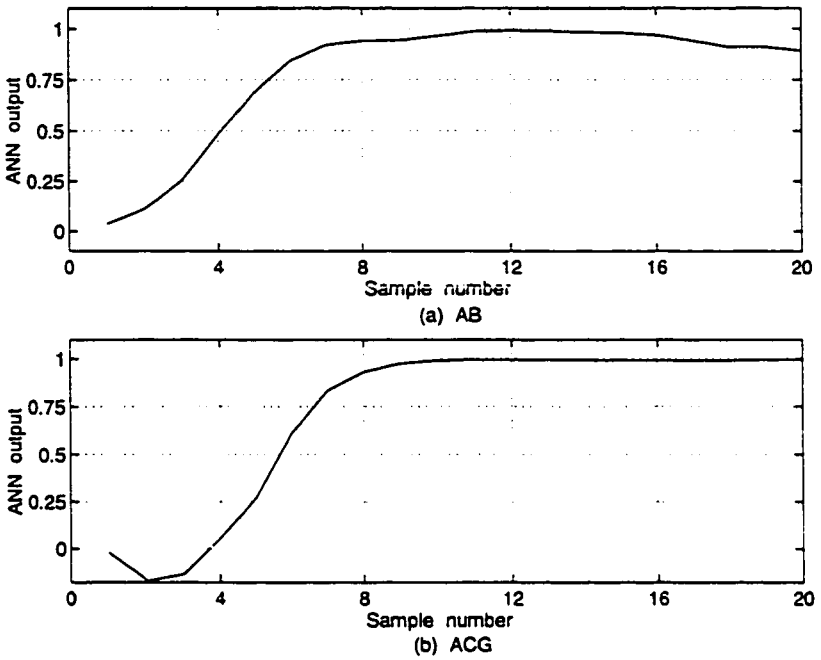

Figure 8.8: Recurrent network response to two different forward faults at the relay location

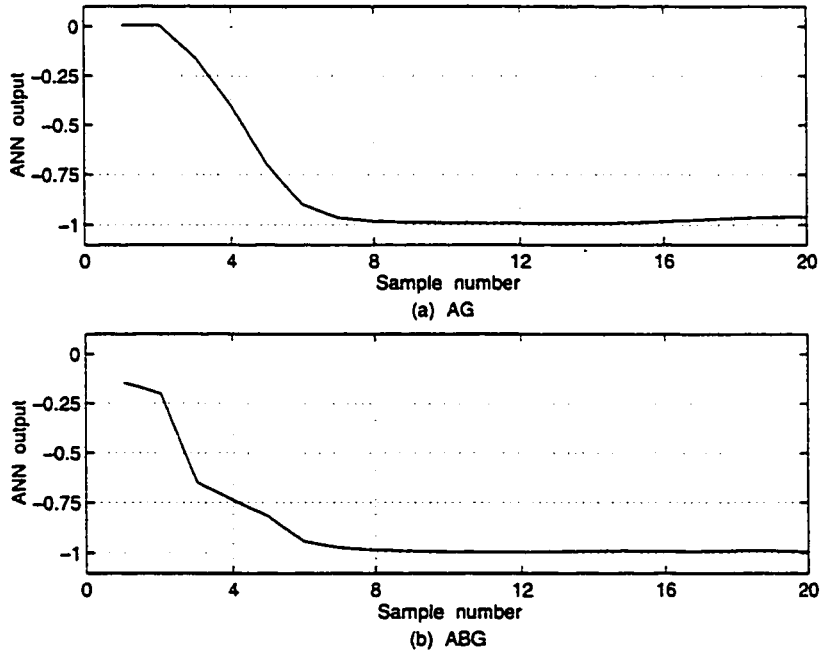

Figure 8.9: Recurrent network response to two different backward faults at the relay location

8.4.1 Forward Faults

As an example, the network's output for two different types of forward faults at 100 *km* from the relay location is shown in Fig. 8.10. The faults were a single phase to ground *A*-*G* fault and a double phase to ground *A*-*C*-*G* fault, respectively. The output is shown for the first three cycles after the fault detection (sample number 1). This figure shows that for both faults the fault direction identification is very fast and reliable.

The network outputs which fall above 0.5 and below -0.5 are interpreted as forward and backward faults, respectively. For the faults shown in Fig. 8.10, it takes two samples for the output of the Elman recurrent network to fall inside the forward fault area. The directional module needs just 1.7 *ms* to classify the fault direction correctly.

The next example tests the network's performance for faults at 150 *km* from the relay location. Two different faults, *A*-*G* fault and *A*-*B*-*G* fault were applied and the network's output for these two faults is shown in Figs. 8.11a and 8.11b, respectively. The network identifies the fault direction very fast and its output remains stable for three cycles.

Results of the tests for two different forward faults at the nearest possible location to the relay at 50 *km* are shown in the Fig. 8.12. Fig. 8.12a shows the network's output for a very high resistive phase to ground *C*-*G* fault, while the network's output for a phase to phase *A*-*C* fault involving no resistance is shown in Fig. 8.12b.

In the case of *C*-*G* fault the amount of fault resistance was about 1.7 Ω (equivalent to 49 Ω). The directional module needs just about 5 *ms* to classify the fault direction

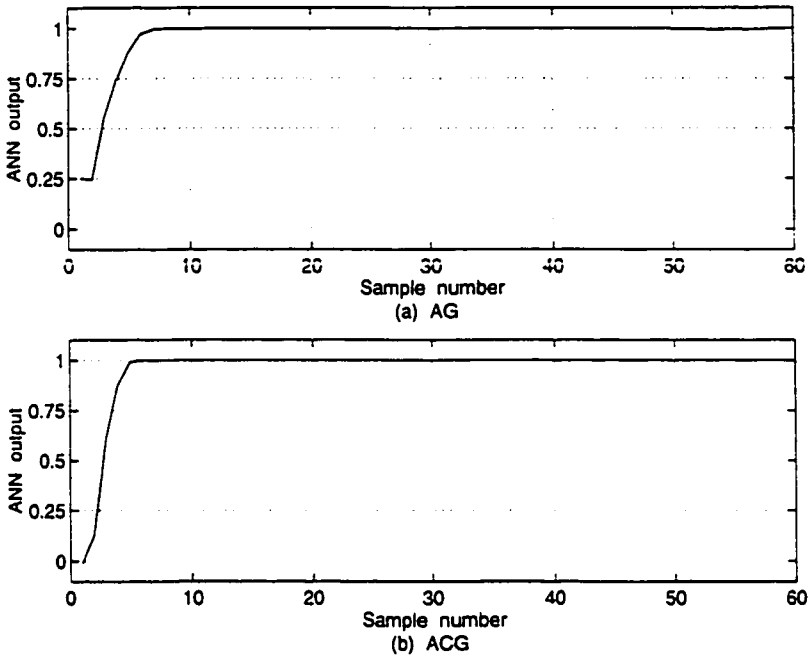

Figure 8.10: Elman network response to two different forward faults at 100 *km*

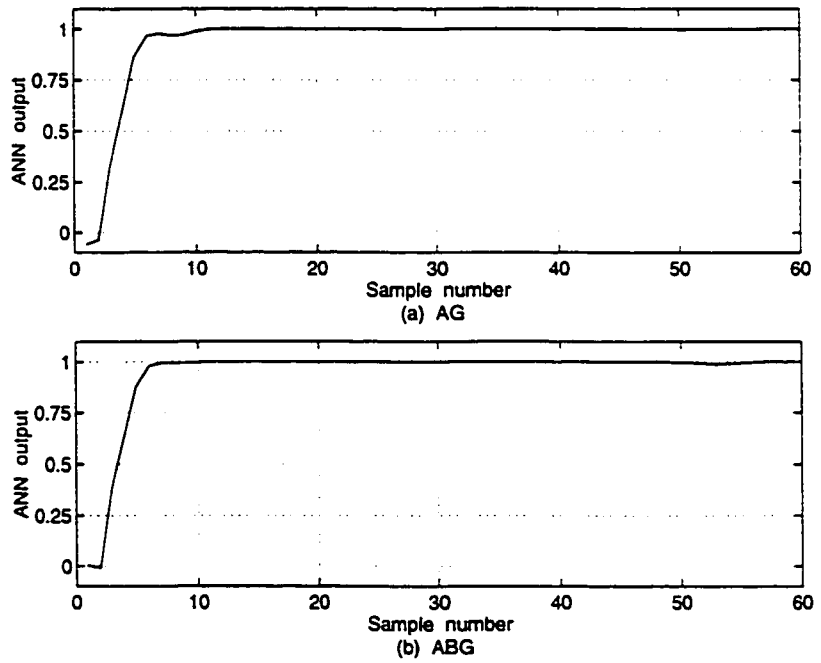

Figure 8.11: Elman network response to two different forward faults at 150 *km*

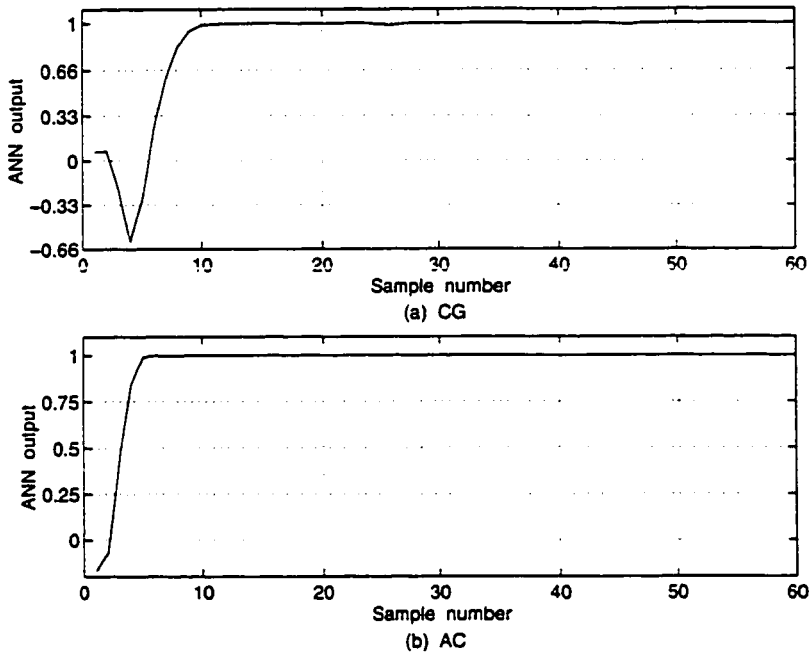

Figure 8.12: Elman network response to two different forward faults at 50 *km*

correctly, even for the case of the fault with such high resistance. For the case of *A*-*C* fault without fault resistance it is even faster; it takes 2.5 *ms* to determine the fault direction. Although the network just uses the phase *A* voltage as its input, it correctly identifies the direction of the phase *C* to ground fault.

8.4.2 Backward Faults

Two different backward faults with 0.5 Ω (equivalent to 14 Ω) fault resistance were applied at 50 *km* from the relay location and the network's performance is presented in Fig. 8.13. The first fault was a single phase to ground *B*-*G* fault and the second fault was a double phase to ground *A*-*C*-*G* fault. This study demonstrates that the network is able to classify the backward faults near the relay location correctly in a timely fashion.

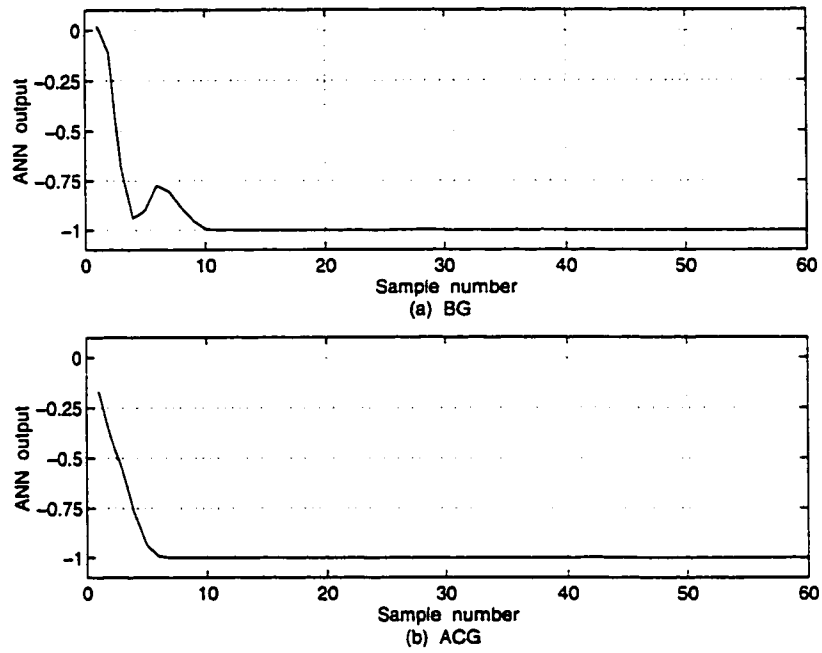

Figure 8.13: Elman network response to two different backward faults at 50 *km*

8.4.3 Faults at the Relay Location

Estimating the direction of a fault located at the relay location by using conventional methods is difficult. Memory action should be used in the design of a fault direction detection module in order to properly identify the fault direction with zero input voltages.

Commercially available directional relays use either voltage memory, cross-polarisation or a superimposed technique to prevent maloperation on close-up faults. In the proposed Elman recurrent network, the output depends both on the input and the previous outputs of the network. Therefore, using its built-in memory, provided by the feedback loops in its structure, the network should be able to correctly determine the direction of faults at the relay location and remain stable at least for some time after the fault inception.

The capabilities of the new network were also examined for faults at the relay location. Results of the tests for two different forward faults at the relay location, a *A-C-G* fault and a *A-G* fault are presented in Fig. 8.14. Both faults involved 0.5 Ω (equivalent to 14 Ω) fault resistance.

The network's output for two different backward faults at the relay location is shown in Fig. 8.15. The faults were a single phase to ground *A-G* fault and a double phase to ground *A-B-G* fault, respectively and involved no fault resistance.

These tests demonstrate that the network is able to classify forward and backward faults at the relay location correctly and rapidly. On average the directional module needs just about 2.3 *ms* to classify the fault direction correctly.

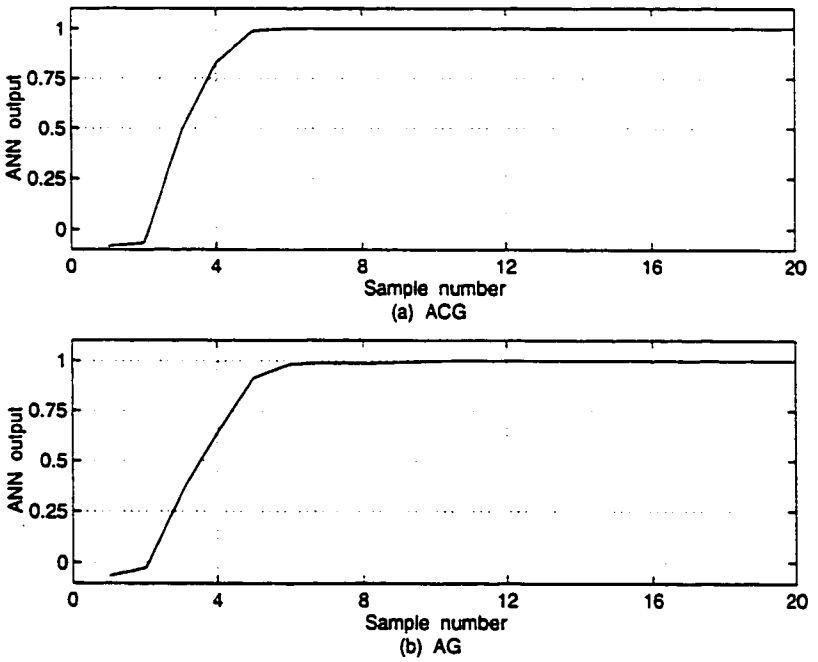

Figure 8.14: Elman network response to two different forward faults at the relay location

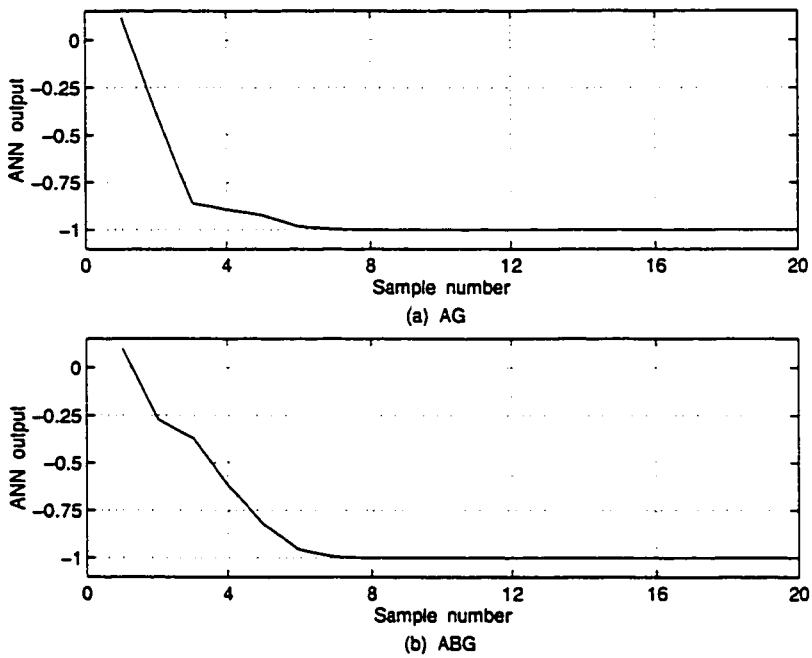

Figure 8.15: Elman network response to two different backward faults at the relay location

8.4.4 Directional Comparison Protection

A directional comparison protection scheme consists of directional relays at each terminal of the transmission line. Using the locally measured quantities, the direction to a fault is independently determined by the relay at each end of the transmission line. The relay hardware was installed at the other end of transmission line. The passband of the analog filter was chosen to be 20 Hz. Some more tests were performed and similar results were obtained confirming that for an internal fault, relays at both ends of the transmission line rapidly identify the fault direction as a forward fault. It shows that the proposed relay can be used for high speed directional comparison relaying.

As an example, two different forward faults were applied at 100 km from the relay

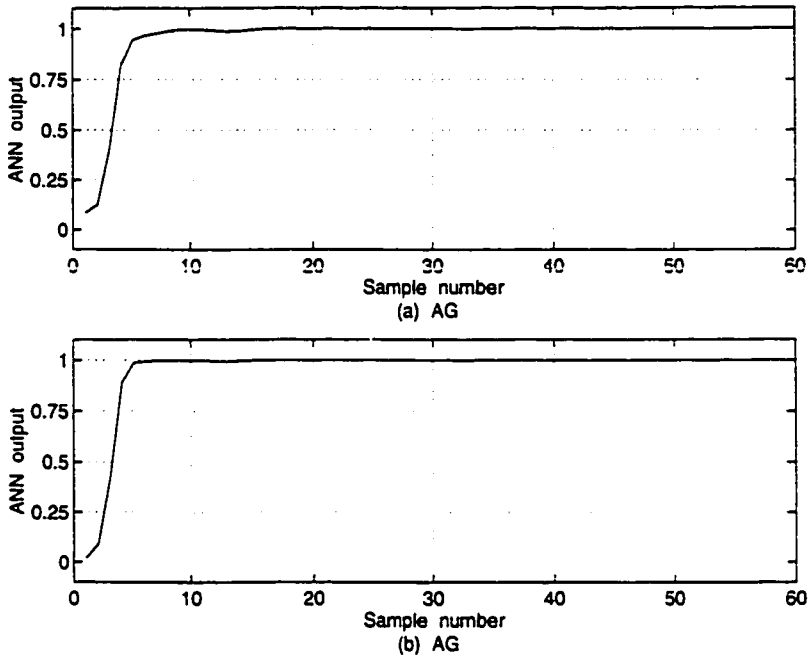

Figure 8.16: Elman network response to two different forward faults at 100 *km*, relay located at the other end

location and the network's output is shown in Fig. 8.16. Both of the faults were single phase to ground *A-G* fault without and with fault resistance, respectively. For the second fault, the amount of fault resistance was about 0.3 Ω (equivalent to 9 Ω). It shows that for both faults the fault direction identification is very fast and reliable as in the case of other studies in which the relay was located at the generator end.

8.5 Starter Module

The starter module was implemented on the DSP board. It was found that it took less than 0.3 *ms* for the acquisition of the current and voltage inputs through DAS and for the execution of the starter module. The necessary time to execute any one of the proposed directional module networks on the DSP board is about 0.4

ms at most, while the sampling interval time is 0.8333 *ms*. Therefore, any of the proposed neural network-based directional modules in conjunction with the starter module could be used as a directional relay. The combined directional relay is able to classify the fault type as well.

In order to assess the performance of the proposed starter module a wide range of faults on the laboratory power system model was applied. The performance of the algorithm has been evaluated for different system conditions. High amount of fault resistance was also considered. Some of the test results are presented in this section.

8.5.1 Relay at the Generator End

The measurement devices are located at 50 *km* (one π-section) from the generator and look forward towards the infinite bus station.

The first example evaluates the performance of the algorithm for a forward fault at the nearest possible location to the relay at 50 *km* from the relay point. A double phase to ground *A-C-G* fault with fault resistance of 0.3 Ω (equivalent to 9 Ω) was applied and the results are illustrated in Fig. 8.17. The filtered three phase currents and voltages are shown in Figs. 8.17a and 8.17b, respectively. The detector and phase starters outputs are also shown in Figs. 8.17c and 8.17d, respectively. As shown in this figure, the fault is detected rapidly and the appropriate starter outputs classify the fault type accordingly. The starter detects the fault momentarily and needs just about one quarter of a cycle to classify the fault type.

The performance of the algorithm was checked for faults with high amount of fault resistance. The next example tests the algorithm's performance for a single

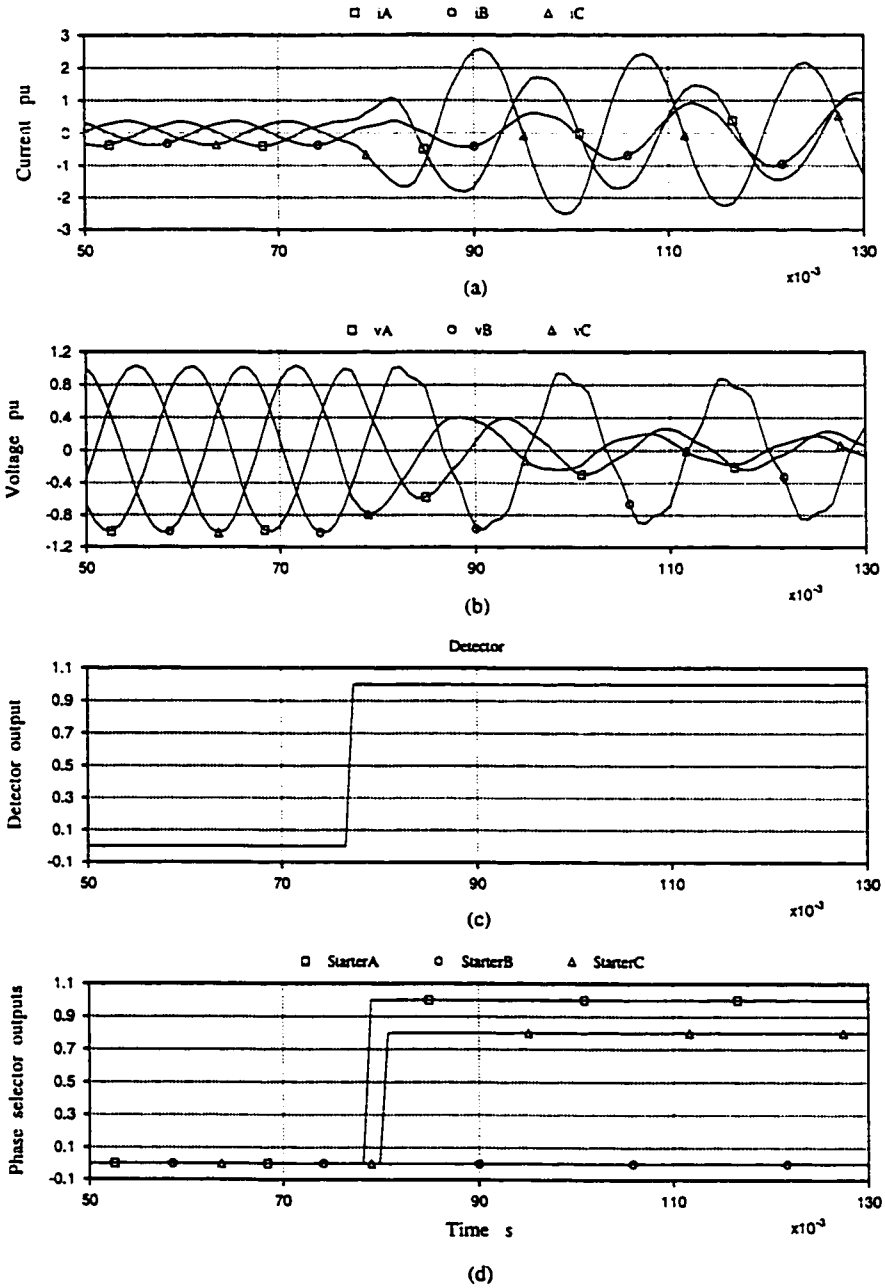

Figure 8.17: Phase starters and detector outputs for the *A-C-G* forward fault at 50 *km*

phase to ground *(C-G)* fault at 100 *km* from the relay location. Fig. 8.18 shows the results of this case study. For this case the amount of fault resistance was about 1 Ω (equivalent to 29 Ω). The fault is detected very rapidly. The starter module needs just about 7.5 *ms* to classify the fault type correctly, even for the case of the fault with such high resistance.

Two different *A-G* faults with and without fault resistance were applied at 100 *km* from the relay location. Measured impedance of phase *A* for two *A-G* faults with zero and 0.5 Ω fault resistance is compared with the safe region of the impedance plane in Fig. 8.19. For both cases, the impedance trajectory begins from the same point. However, for the fault including fault resistance, the trajectory settles at a point that indicates a fault resistance of about 2.6 Ω (0.18 pu). It shows that the fault resistance is magnified due to the effect of high fault current from the powerful end source.

Fig. 8.20 shows the results of another fault study at 100 *km* from the relay location. A single phase to ground *A-G* fault with fault resistance of 0.5 Ω (equivalent to 14 Ω) was applied and the voltage and current signals were presented to both of the starter and Elman network-based directional relay and their outputs are illustrated in Fig. 8.20. The fault is detected and classified very rapidly in 2.5 *ms* by the starter module. Moreover, the fault direction is determined by the directional relay in just about 2 *ms* after the fault detection.

The next example tests the algorithm for faults occurred far from the measurement point. A phase to phase *A-B* fault with no resistance was applied at 150 *km* from the relay location and the performance of the starter module was investigated. Moreover, the same fault data was processed by the recurrent network-based direc-

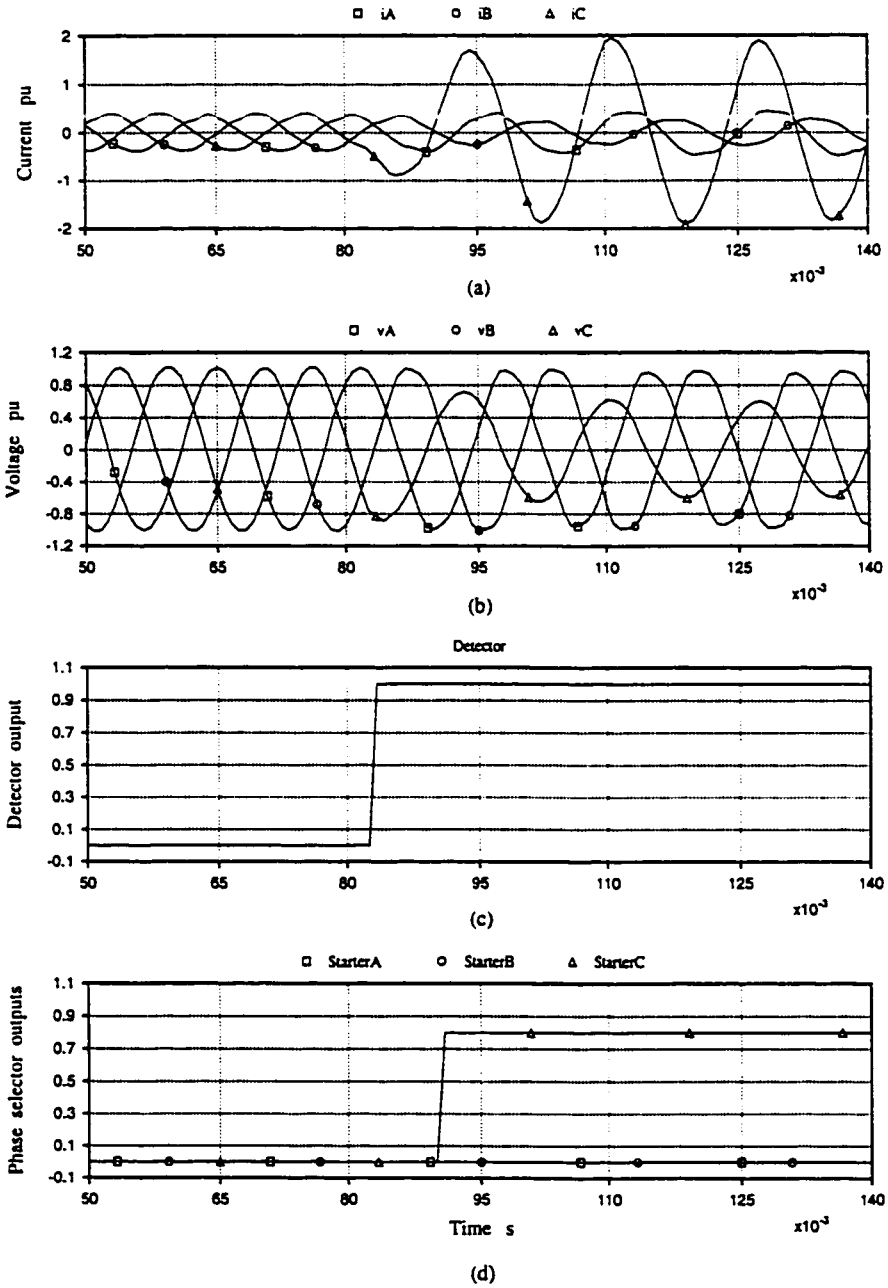

Figure 8.18: Phase starters and detector outputs for the *C-G* forward fault at 100 *km*

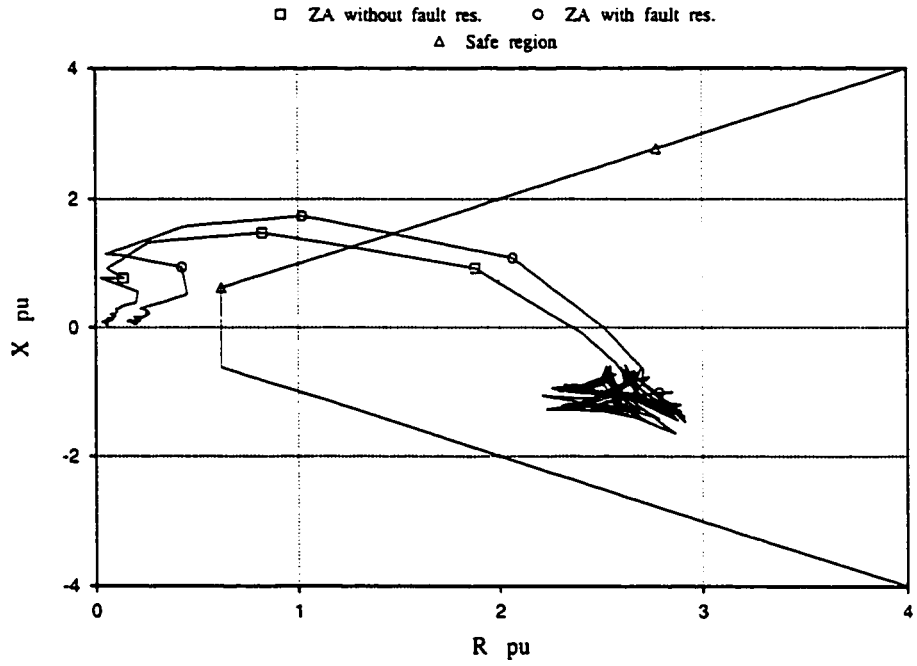

Figure 8.19: Phase A impedance trajectory for two A-G faults with and without fault resistance

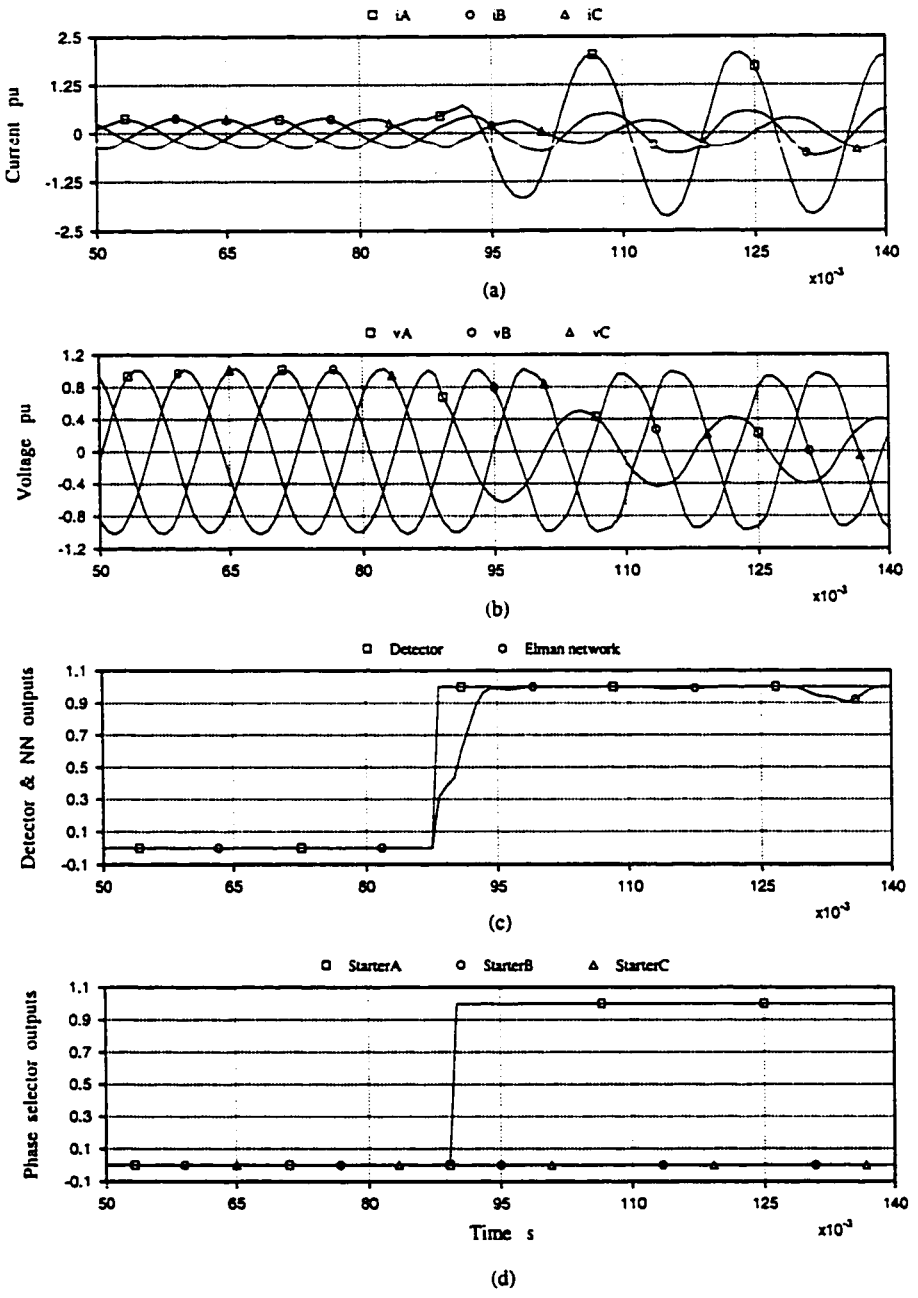

Figure 8.20: Phase starters, detector and Elman network-based directional relay outputs for the A-G forward fault at 100 km

tional relay. The results obtained from both units are shown in Fig. 8.21. It shows that it takes just three and five sampling periods to detect and classify the fault, respectively after the fault inception. Fault direction is correctly determined by the directional recurrent network as a forward fault.

The starter and Elman network-based directional relay outputs for a three pahse *A-B-C* fault at 50 *km* from the relay location are illustrated in Fig. 8.22. It shows that although the voltage input signals are noisy, the fault is detected and classified correctly and very rapidly. Fault direction is also determined very fast.

With the conditions similar to that of Fig. 8.22, another three pahse *A-B-C* fault at 100 *km* from the relay location was applied. Phase *A*, *B* and *C* measured impedances for this fault are compared with the safe region of the impedance plane in Fig. 8.23. All three measured impedances are located inside the safe region before the fault inception. However, after the inception of the fault, they all move outside the safe region quickly.

The capabilities of the algorithm were also examined for faults at the relay location. A single phase to ground *A-G* fault with fault resistance of 0.5 Ω (equivalent to 14 Ω) was applied in front of the relay location and the starter and Elman directional relay were evaluated. The outputs of these modules are shown in Fig. 8.24.

The same fault without fault resistance was applied at the relay location. However, this time the fault was applied behind the measurement point. Fig. 8.25 illustrates the outputs of the starter and Elman directional relay for this fault. For both forward and backward fault cases at the relay location the fault is detected and classified rapidly and correctly. The Elman network-based directional relay identifies the fault direction very fast and its output remains stable during the fault.

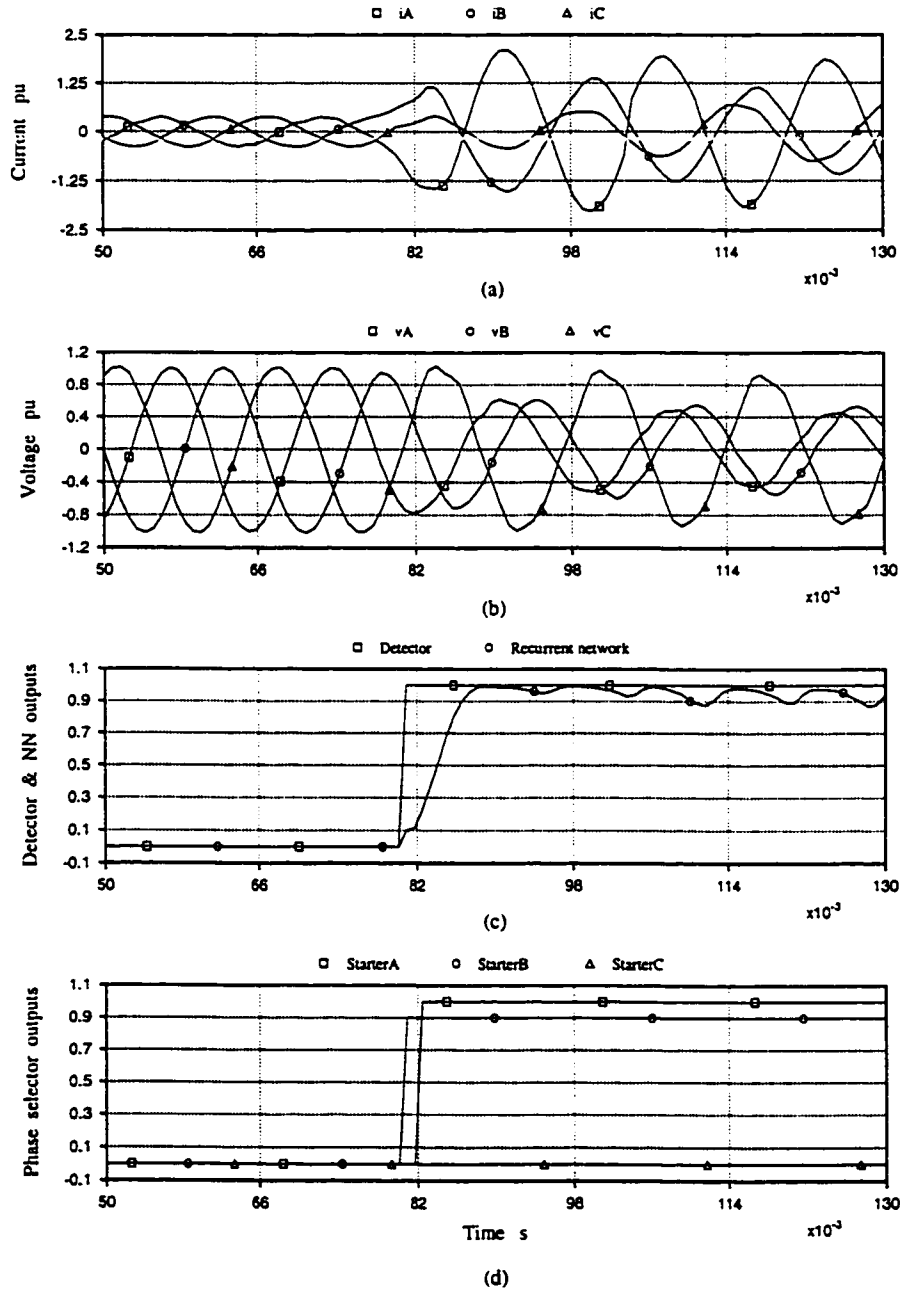

Figure 8.21: Phase starters, detector and recurrent network-based directional relay outputs for the A-B forward fault at 150 km

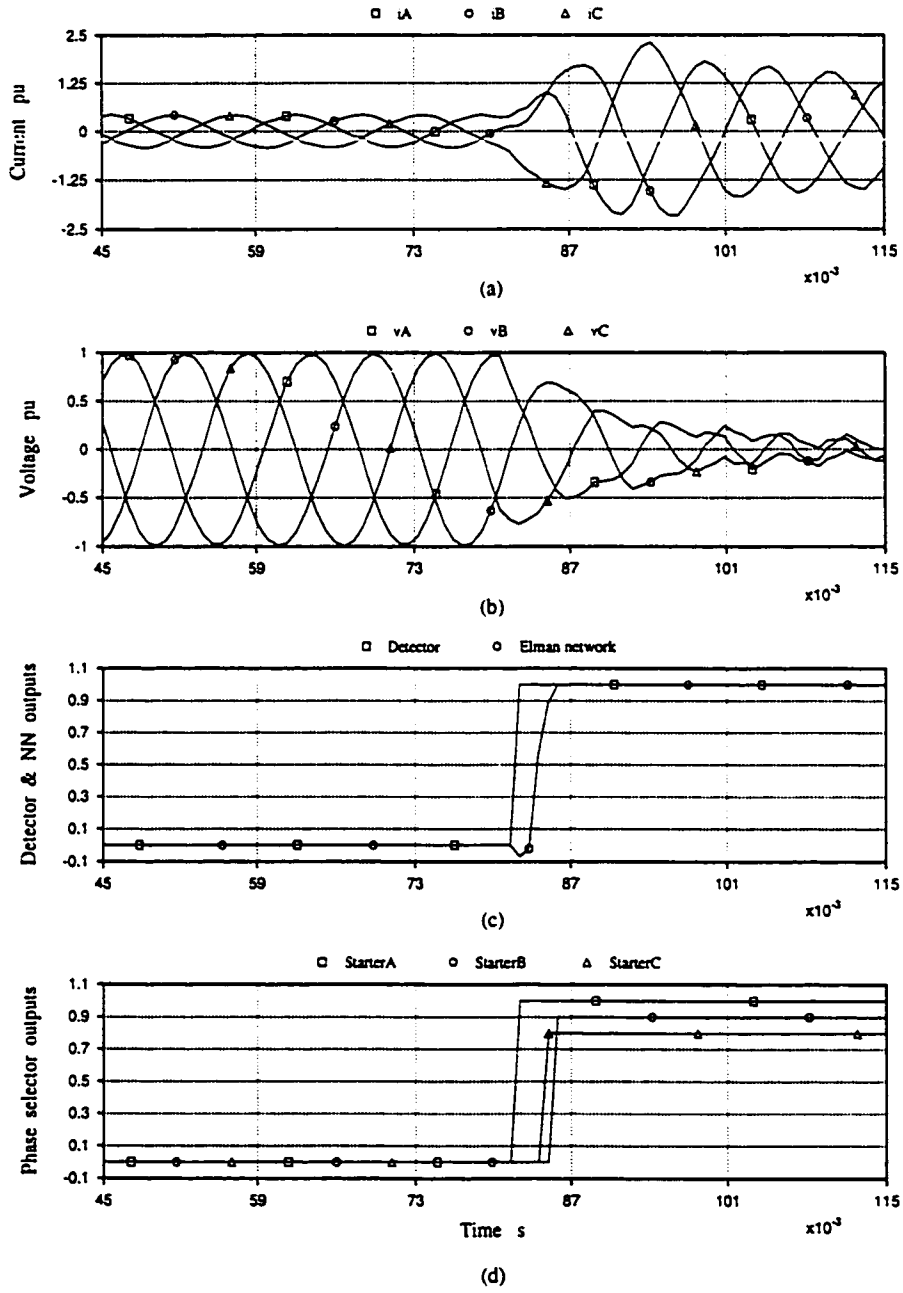

Figure 8.22: Phase starters, detector and Elman network-based directional relay outputs for the *A-B-C* forward fault at 50 *km*

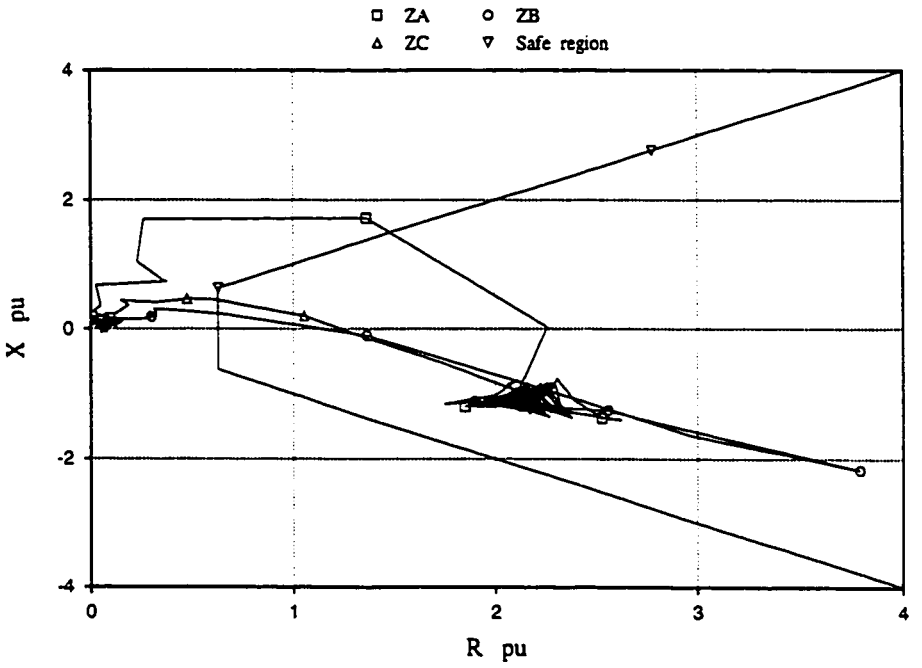

Figure 8.23: Phase A, B and C impedance trajectories for the A-B-C forward fault at 100 km

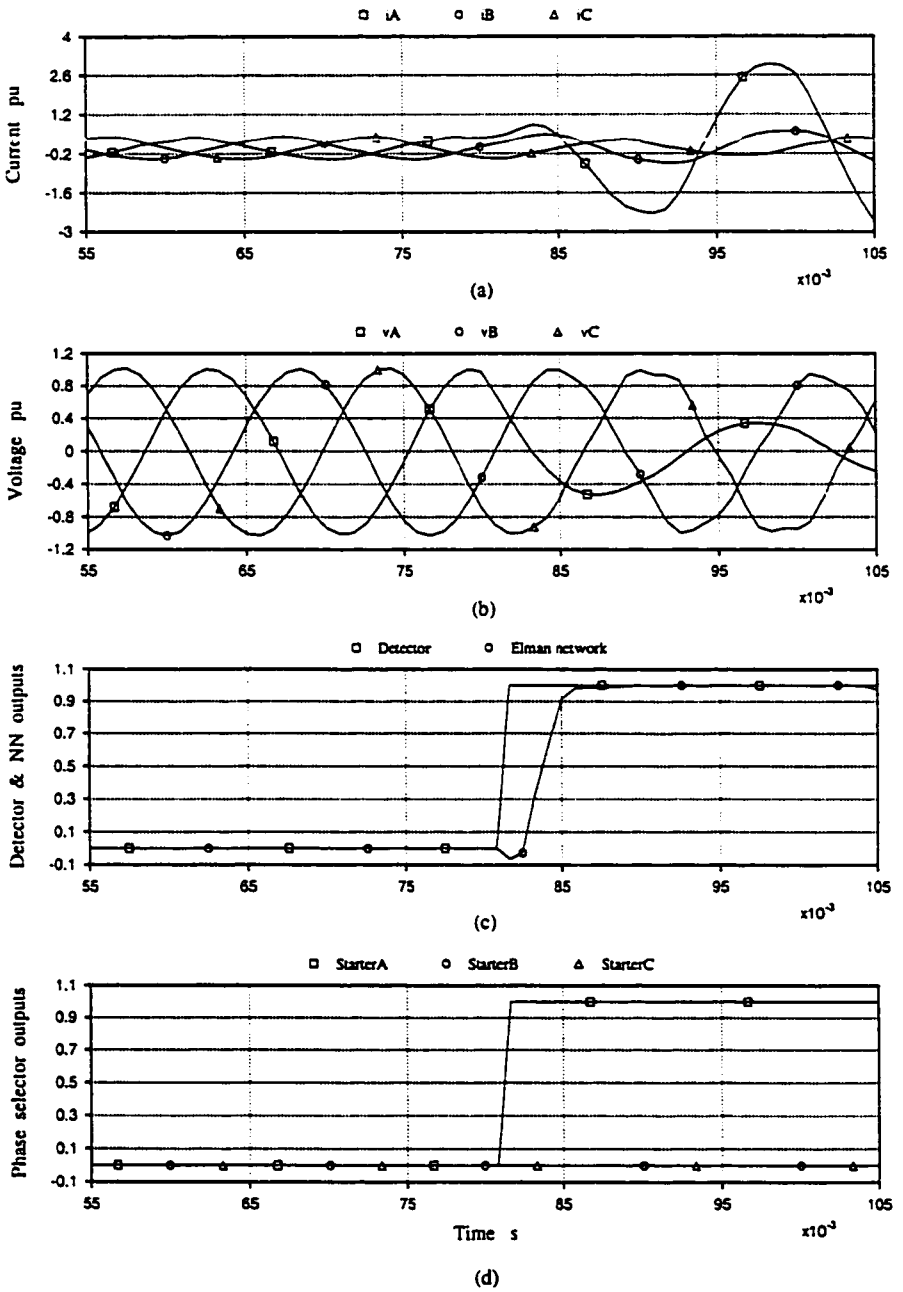

Figure 8.24: Phase starters, detector and Elman network-based directional relay outputs for the A-G forward fault at the relay location

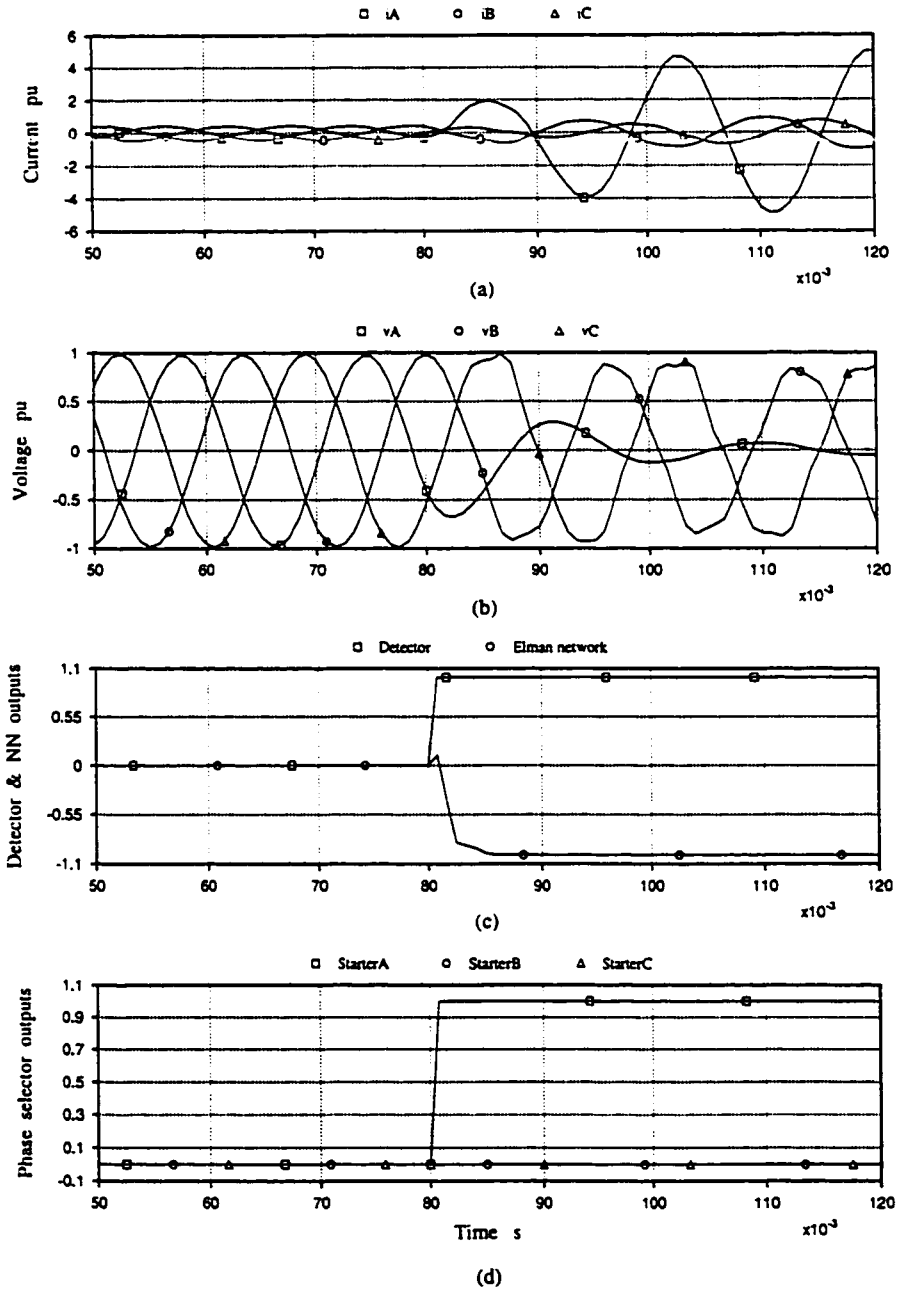

Figure 8.25: Phase starters, detector and Elman network-based directional relay outputs for the *A-G* backward fault at the relay location

A backward phase to phase A-B fault with no fault resistance was applied at 50 km from the relay location. The starter and recurrent network-based directional relay outputs are presented in Fig. 8.26. It shows that the fault is identified correctly in a timely fashion.

8.5.2 Relay at the Other End

The relay hardware was installed at the other end of transmission line. The measurement devices are located at 50 km (one π-section) from the infinite bus station and look forward towards the generator (point B in Fig. 7.1).

Some more tests were performed and similar results as of the results presented in the previous subsection were obtained. As an example the detector and phase starters outputs for a fault at 50 km from the relay location are shown in Fig. 8.27. The faults was a double phase to ground A-C-G fault without fault resistance. It shows that the starter module performs rapidly and correctly for this heavy fault. The A and C outputs of the phase selector classify the fault correctly while the B output remains stable during the the fault.

The next example tests the algorithm for faults occured far from the relay point including high fault resistance. A phase to ground A-G fault with fault resistance of 0.5 Ω (equivalent to 14 Ω) was applied at 150 km from the relay location and the performance of the starter module was investigated. The starter module results are presented in Fig. 8.28. Similar to the previous results, it shows that the fault is detected and classified correctly and very rapidly by the starter module.

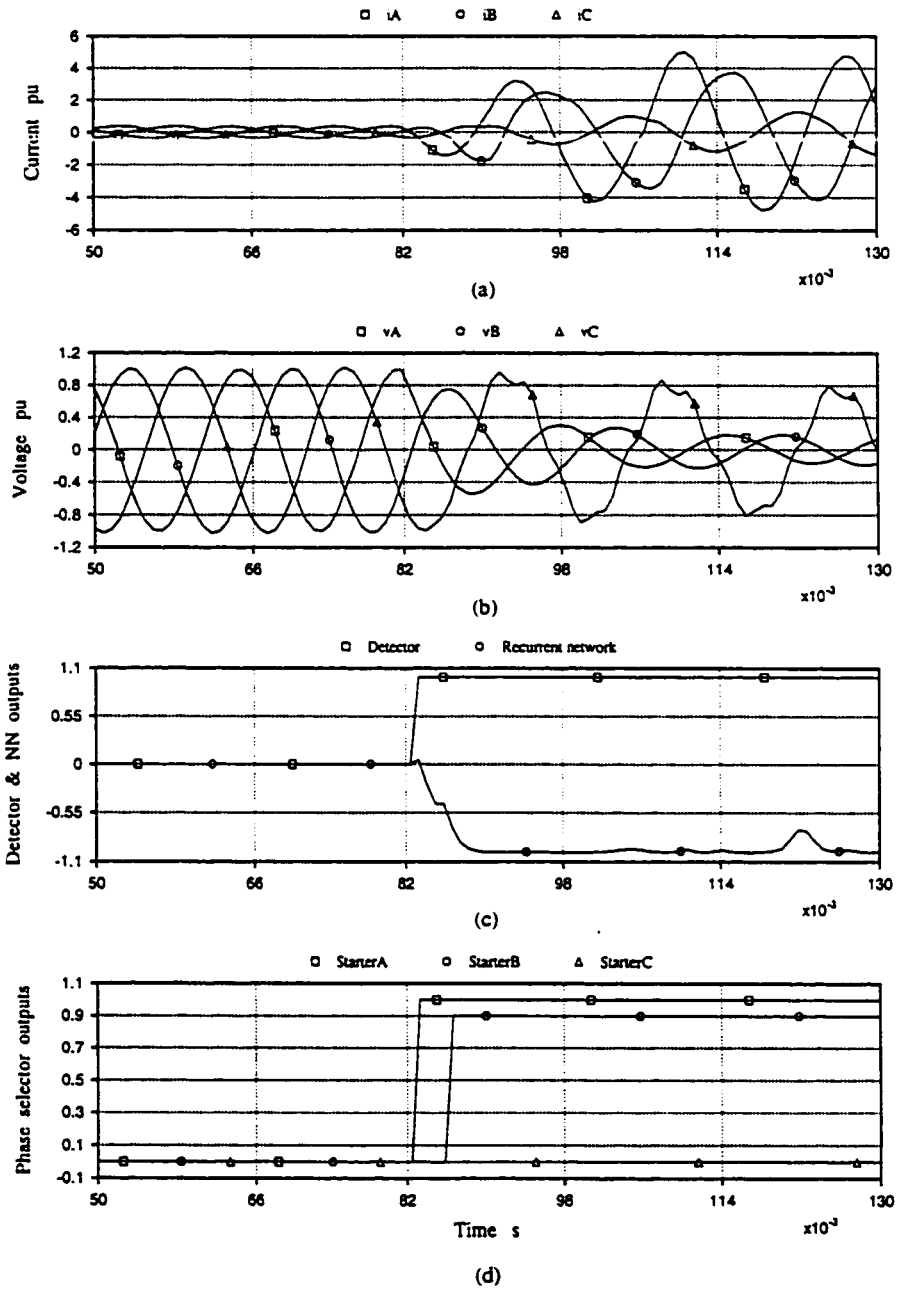

Figure 8.26: Phase starters, detector and recurrent network-based directional relay outputs for the A-B backward fault at 50 km

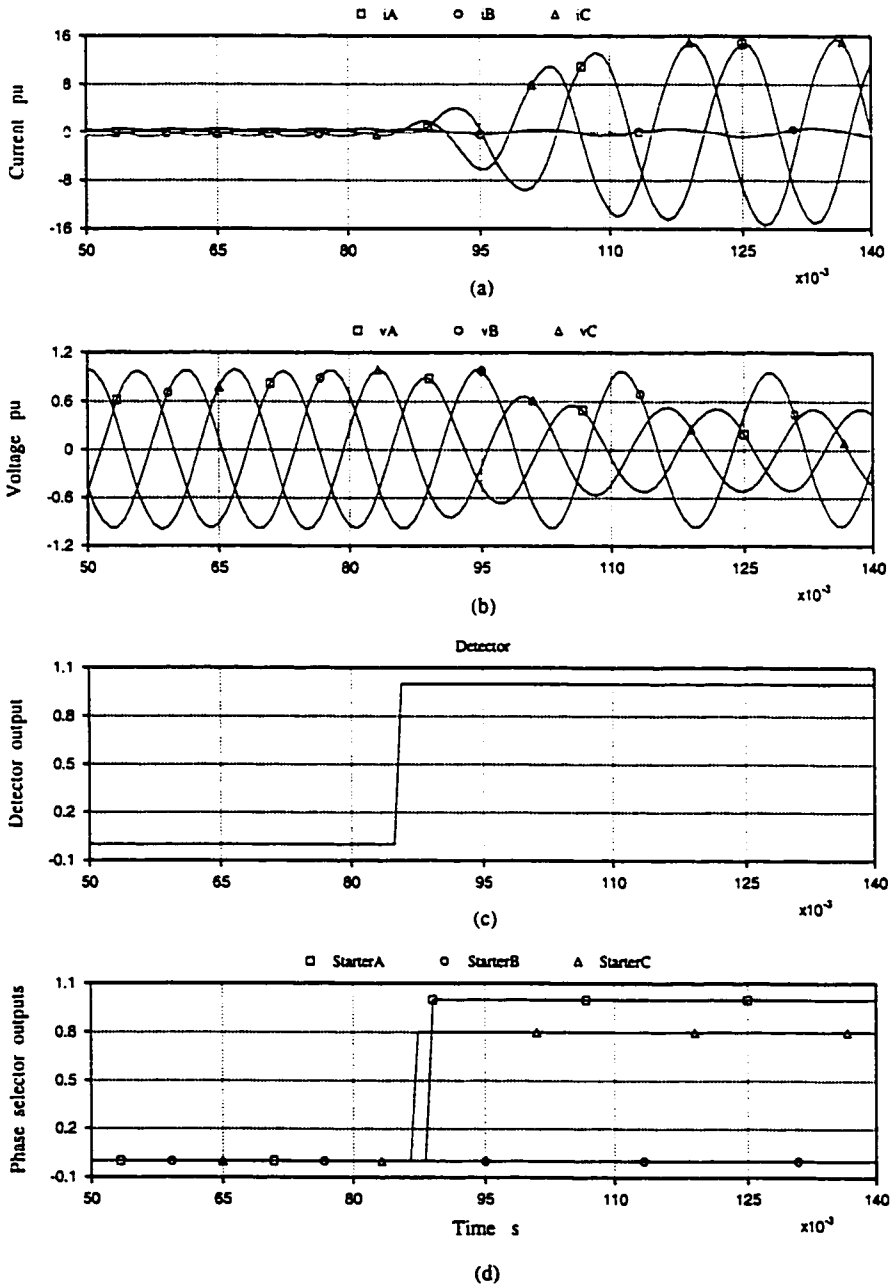

Figure 8.27: Phase starters and detector outputs for the *A-C-G* forward fault at 50 *km*, relay located at the other end

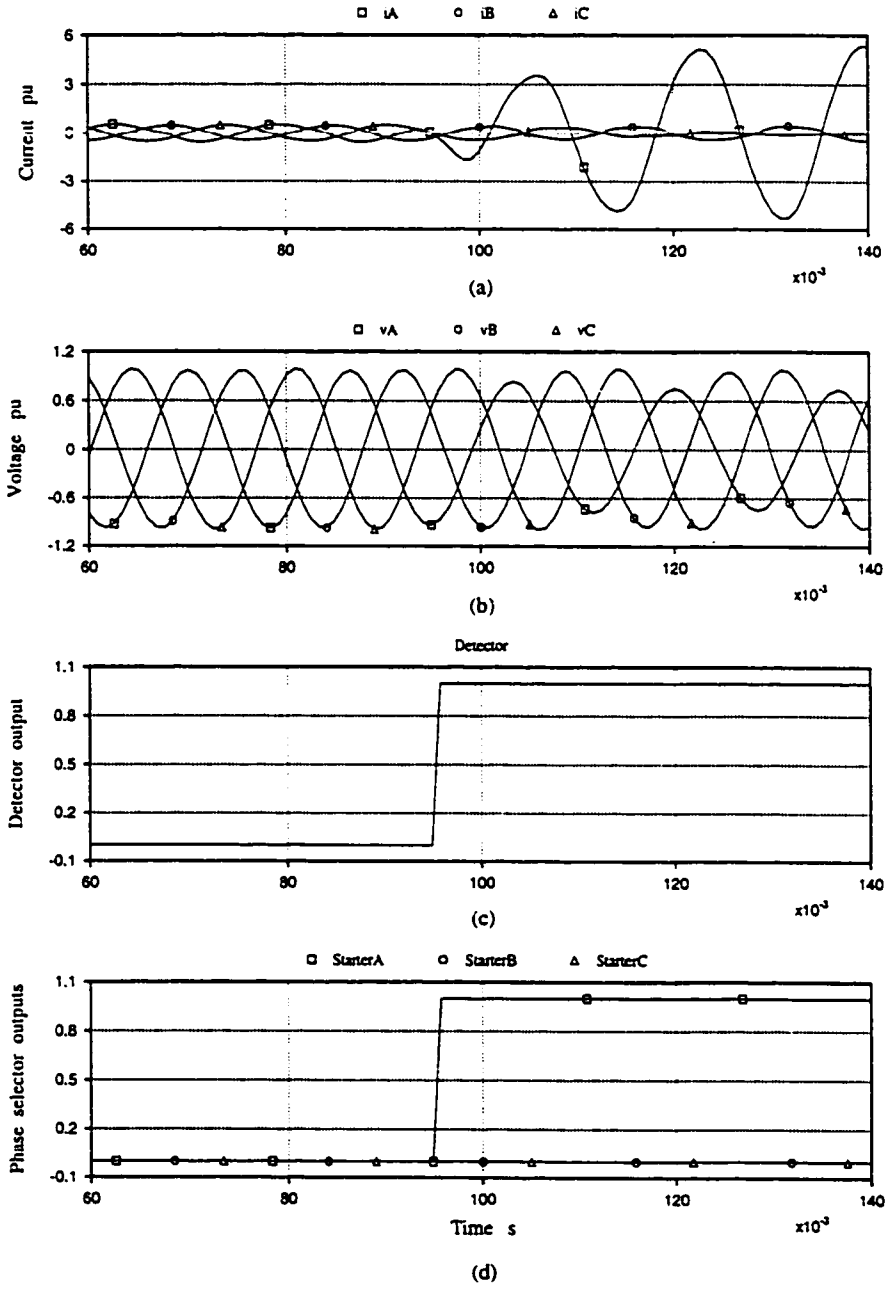

Figure 8.28: Phase starters and detector outputs for the A-G forward fault at 150 km, relay located at the other end

8.6 Summary

The performance of the different modules of the proposed relaying algorithm has been extensively evaluated in real-time using a laboratory model power system. A wide range of various types of forward and backward faults were applied at different locations on the modelled transmission line and the performance of different proposed modules was investigated. These results confirm the simulation studies results reported in the previous chapters, and show that the proposed modules performed correctly and reliably when tested in real-time. The proposed modules are able to perform very fast and reliably for different types of faults. Influence of changing system parameters such as fault location, fault resistance and fault inception time is studied. The performance of the proposed modules is also checked for faults including high amount of resistance and also faults at the relay location.

Results obtained show that the proposed directional neural networks are able to identify, without any further training, the direction of faults on a transmission line which has never been presented to them before. It indicates that the proposed neural network-based direction discrimination algorithms could be trusted as reliable algorithms for transmission line fault direction detection.

Comparing experimental studies performance of different proposed neural network-based directional modules, it was found that the recurrent and Elman networks performed better in comparison with the feedforward networks. Overall, it was found that the Elman network directional module performs as the most robust network when tested with the laboratory power system model.

Part III

Recorded Field Data Tests

Chapter 9

Digital Relay Evaluation using Field Data

9.1 Introduction

Simulation and experimental studies presented in previous chapters showed that the proposed digital relay modules were able to perform rapidly and correctly for a wide range of system conditions.

Testing of a newly designed digital relay using real field fault data is important in evaluating the relay performance. Performance of the proposed relay modules is investigated further using recorded fault data from a high voltage power system. The real world complex effects of the power system elements, which might have not been completely considered in the mathematical model of the power system, are already included in the recorded real fault data. In this way, the performance of the newly designed relaying modules can be further verified in a more realistic environment than pure simulation.

The recorded voltage and current fault signals are down-sampled and normalized and then presented to the relay modules. The performance of the proposed modules was checked in play back mode. Results obtained indicate that the proposed algorithms are robust, fast and accurate. Results of some of the test studies are reported in this chapter.

9.2 Recorded Field Faults

Alberta Power Ltd. records fault data on its 240 kV transmission system. A schematic diagram of the Province of Alberta 240 kV power transmission system is shown in Fig. 9.1. Performance of the proposed starter and ANN-based directional modules was investigated using the recorded fault data provided by Alberta Power Ltd.. Effects of the current transformers saturation, time-varying fault resistance and complex transients and nonlinearities of the power system elements are already included in the recorded real fault data. Therefore, the performance of the proposed modules can be further evaluated using more realistic field data.

Recorded current and voltage signals for two different faults on the Alberta transmission system are presented as two examples. The first fault was a single phase to ground A-G fault on the 135 km transmission line connecting Battle River and Sheerness substations. Recorded three phase current and voltage waveforms are shown in Fig. 9.2a and Fig. 9.2b, respectively. After the fault inception, the voltage and current signals contain considerable high frequency components.

The second fault was a double phase to ground A-B-G fault on the 135 km transmission line and the recorded current and voltage signals are shown in Fig. 9.3. For this fault, after about two cycles from the inception of the fault, the system encounters another transient and evolves to a different condition.

The recorded current and voltage fault signals are used to test the proposed relaying modules.

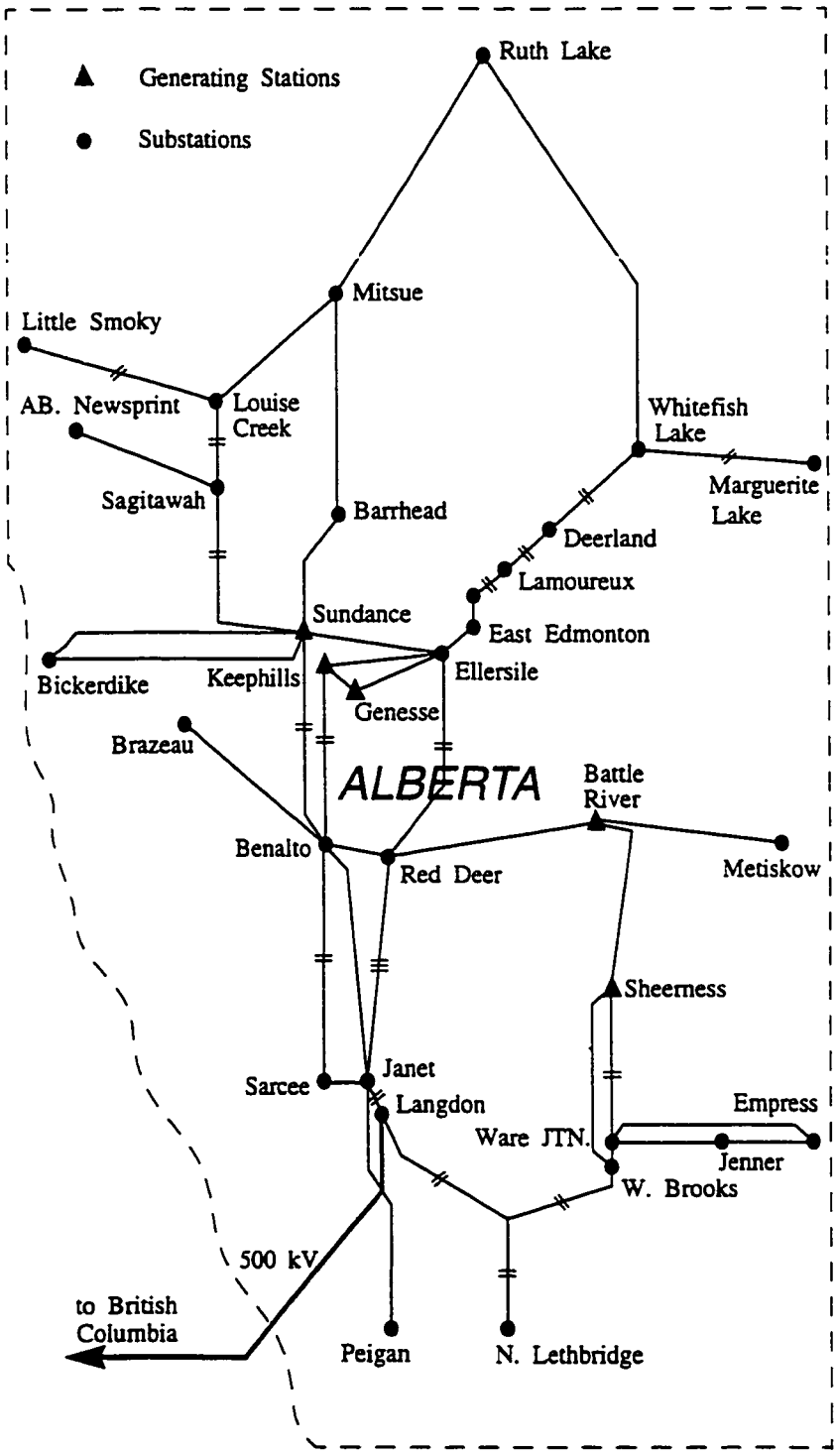

Figure 9.1: Schematic diagram of the Alberta 240 kV power transmission system

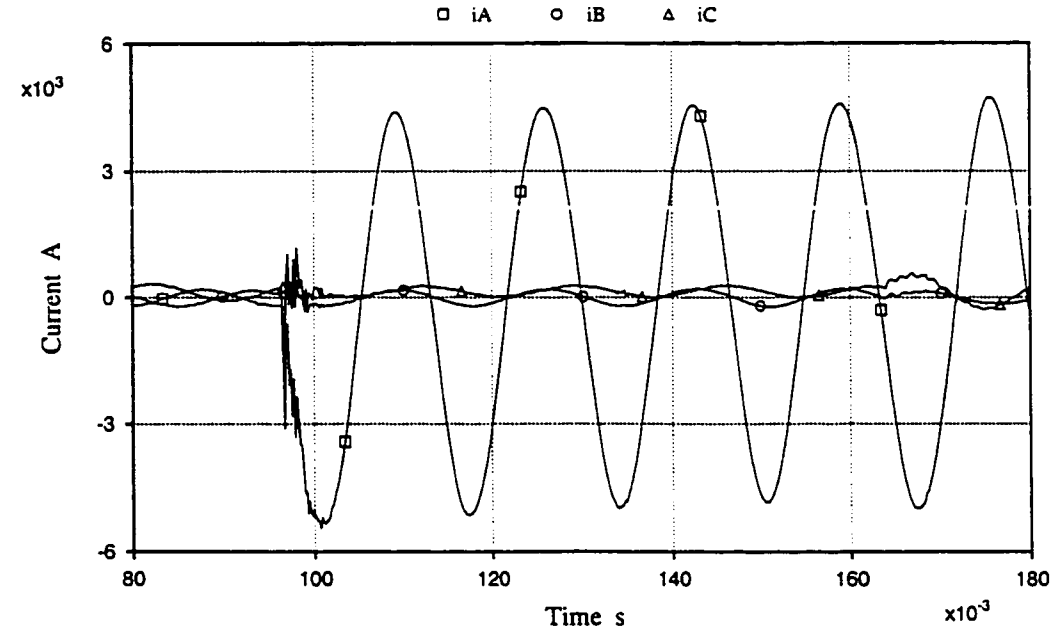

(a)

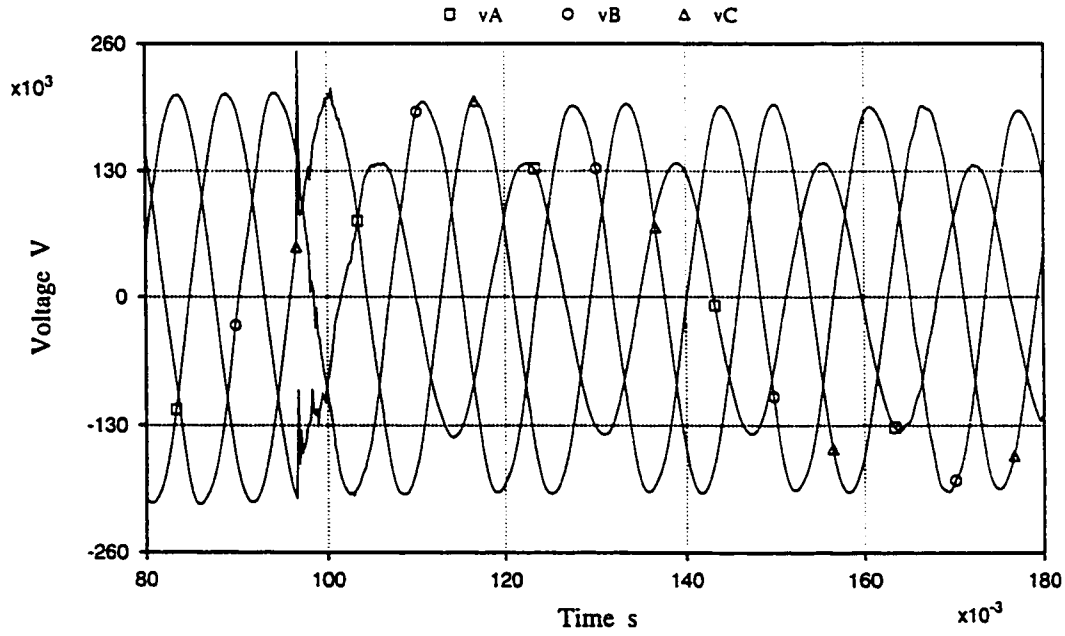

(b)

Figure 9.2: Three phase recorded currents and voltages for a A-G fault on the 135 km transmission line

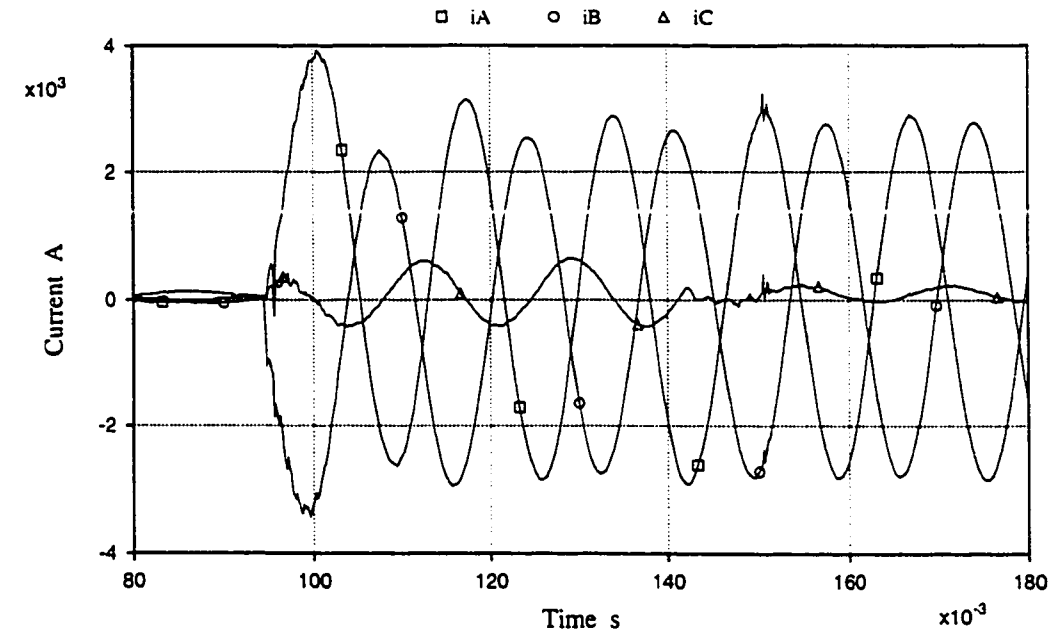

(a)

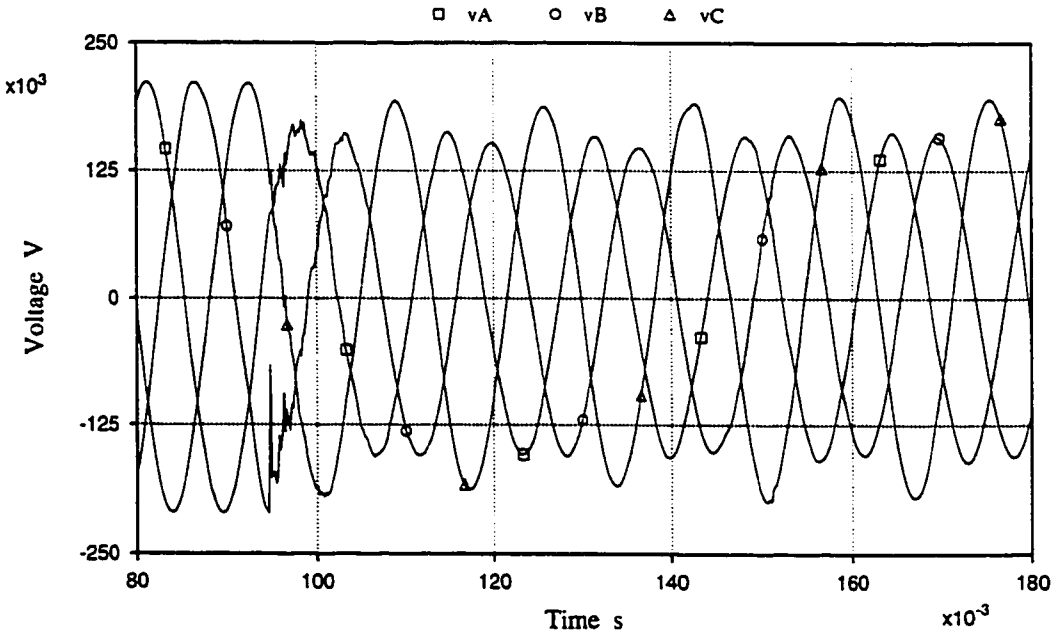

(b)

Figure 9.3: Three phase recorded currents and voltages for a *A-B-G* fault on the 135 *km* transmission line

9.2.1 Fault Data Exchange Sampling Rate

Digital Fault Recorders (DFR) are used to monitor power system voltages, currents and events. These devices record analog signals by periodically sampling them and converting the measured signals to digital values. Typical recorders monitor 16-64 analog channels and a comparable number of event (contact status) inputs [78].

Samples of voltage and current waveforms are usually captured at a high sampling rate. However, a lower sampling rate is usually required by the digital protective relays. The simple expedient of sampling rate reduction by an integer factor, called sampling rate compression, is not the correct way of making the conversion.

In general, the operation of reducing the sampling rate (including any prefiltering) is called down-sampling. Down-sampling can be done without aliasing if the bandwidth of the signal is reduced before sampling rate reduction. A general system for down-sampling includes a lowpass filter and a compressor. Such a system is called a decimator and down-sampling by lowpass filtering followed by compression has been termed decimation [73]. A decimator for down-sampling by a factor of M is shown in Fig. 9.4.

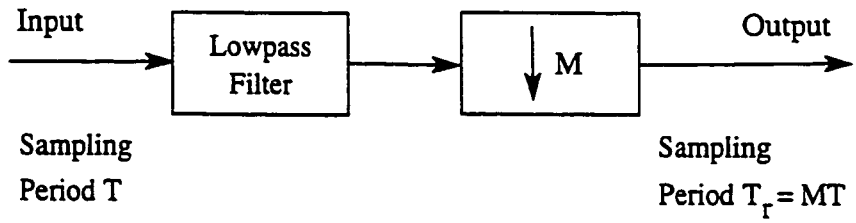

Figure 9.4: General system for sampling rate reduction by M

9.2.2 Decimation Filter

Decimation filters can be designed using finite-duration impulse response lowpass filters. The simplest method of FIR filter design is called the window method [73]. The basic principle of the window design method is to truncate the ideal impulse response with a finite-length window such as Kaiser window.

The original voltage and current waveforms are sampled with a rate of 6 kHz. A decimator is used to decrease the sampling rate to 1.2 kHz. In this study, the Kaiser window filter design method was used to calculate the coefficients of the decimation filter. An FIR filter with cutoff frequency of 360 Hz was selected. The frequency response of the decimation filter is shown in Fig. 9.5.

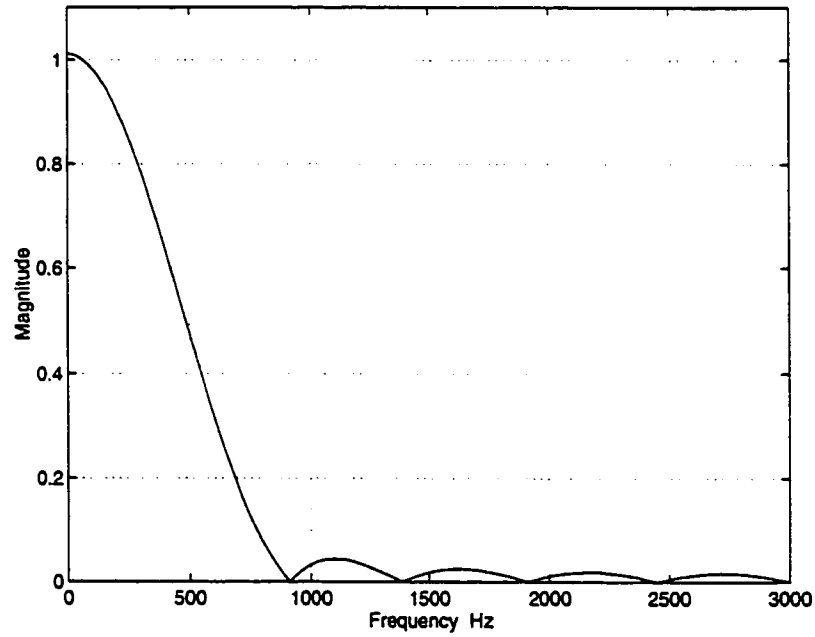

Figure 9.5: Frequency response of the Kaiser decimation filter

9.3 Performance Evaluation Studies

Different neural networks were proposed as the relay's directional module. The ANN-based algorithms were tested to evaluate the performance of the proposed networks in terms of generalization, robustness and speed.

The trained networks were used to determine the direction of faults on the transmission system shown in Fig. 9.1. These networks were originally trained for a different transmission line with different length and characteristics than those shown in Fig. 9.1. They were not retrained for the recorded field data studies. The performance of the proposed starter module was also evaluated using the same transmission system fault data.

The starter and directional modules have been implemented on a DSP board. The implementation software was programmed in the C language. After compilation and assembly it was down-loaded to the DSP board. Any of the proposed neural networks could be considered as the directional module and its performance could be investigated. Based on the structure of the selected network, appropriate network's weights and biases were also loaded to the board.

The performance of the starter and ANN-based directional modules was checked in play back mode using recorded field data. The field data is first preprocessed the same way as in the case of simulation studies. Then, it is down-sampled and read to the DSP board. The starter and directional module could be processed on the DSP board simultaneously or separately. The DSP board processes the input data and calculates the modules' outputs. The outputs are sent back to the PC to be saved on a file for further investigation (Fig. 9.6).

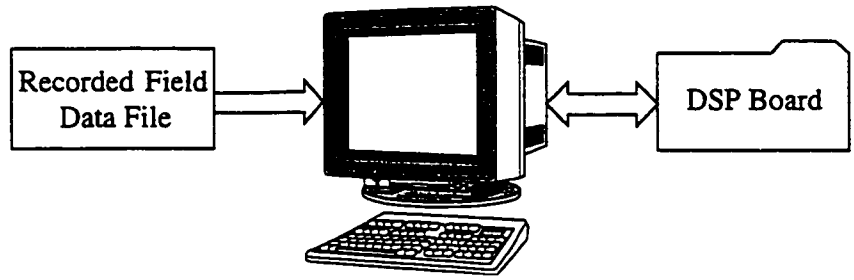

Figure 9.6: Processing of the fault data by the DSP board

The normalized voltage and current signals were presented to the relaying modules in a sequential manner. At each sampling point the input data window was moved forward by one point and the new set of the input data was presented to the modules, outputs were calculated and then saved.

The same data files were processed by a unix workstation off-line and the starter and neural network outputs were observed. The DSP board uses floating-point arithmetic to process the fault data. Therefore, it should be able to process the input data accurately. It was found that the results obtained from processing the input data using the DSP board and the unix workstation were very similar.

The proposed modules were tested with a set of 9 different faults. These faults occurred at different locations of different transmission lines of the Alberta power grid (Fig. 9.1), had different initial power flow conditions, occurred at different random instants in the *ac* cycle and involved different phases. Test results for a few faults are presented in the following sections.

9.4 Feedforward Network Directional Module

The proposed twenty-input feedforward network is considered as the directional module of a transmission line protection system and its performance is investigated [79]. For the examples presented in this section, the directional module is processed on the DSP board separately (not in conjunction with the detector module) and it is assumed that each fault is detected instantly after its inception.

The network's output for a forward fault on the 112 km transmission line between Metiskow and Battle River substations is shown in Fig. 9.7. The measurements were recorded at the Battle River substation. The Metiskow substation is connected to generation sources through the 138 kV transmission system. The fault was a single phase to ground C-G fault. The output is shown for the first cycle after the fault detection (sample number 1). This figure shows that the fault direction identification is very fast and reliable. Although the network just uses the phase A voltage as its input, it correctly identifies the direction of the phase C to ground fault.

Four consecutive outputs of the network are considered and averaged by a post-processing unit. Averaged outputs of this post-processing unit which fall above 0.5 and below -0.5 are interpreted as forward and backward faults, respectively.

To demonstrate the direction detection network's capabilities including a post-processing moving average filter, the network was tested with the fault presented in Fig. 9.2. The fault was a single phase to ground A-G forward fault on the 135 km transmission line connecting Battle River and Sheerness substations and the measurements were recorded at the Battle River substation. The averaged output of the network is shown in Fig. 9.8.

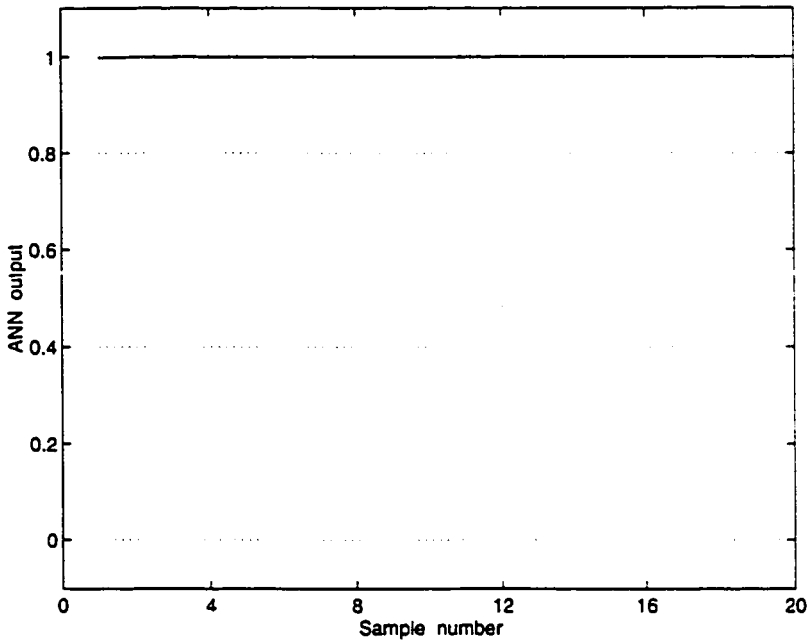

Figure 9.7: Twenty-input feedforward ANN response to the phase C to ground forward fault on the 112 km transmission line

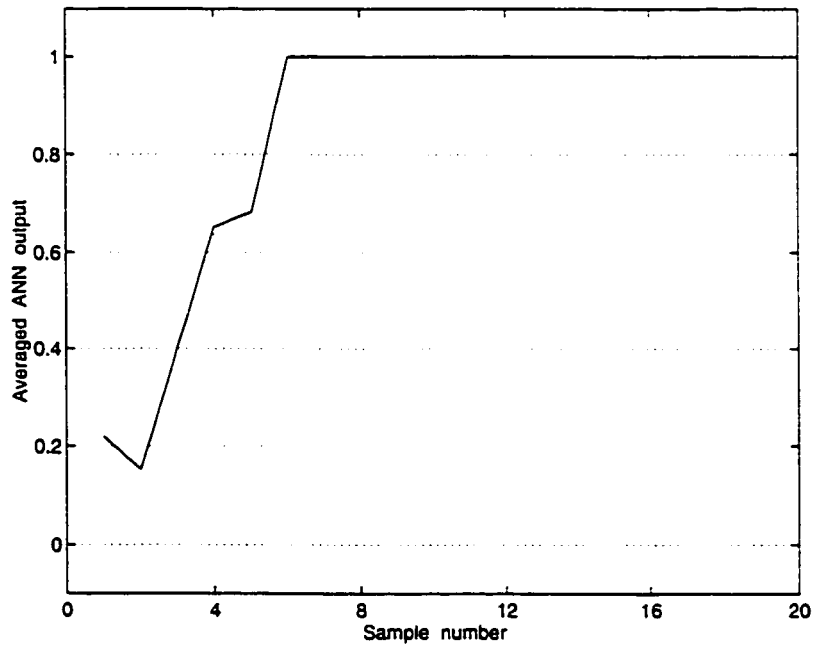

Figure 9.8: Twenty-input feedforward ANN averaged response to the phase A to ground forward fault on the 135 km transmission line

The directional module output is set equal to zero prior to the fault detection. For the first samples after fault detection, the post-processing unit averages network's output with zeros. Therefore, the speed of the direction decision initially decreases. For the faults shown in Fig. 9.8, it takes three samples for the output of the moving average filter to fall inside the forward fault area.

The performance of the feedforward directional module was evaluated using the same *A-G* fault with the measurements recorded at the other end of the transmission line, at the Sheerness substations. The averaged output of the network is shown in Fig. 9.9. The network correctly determines the fault direction two samples after the fault detection.

Fig. 9.10 shows the output of the network for the double phase to ground *A-B-G*

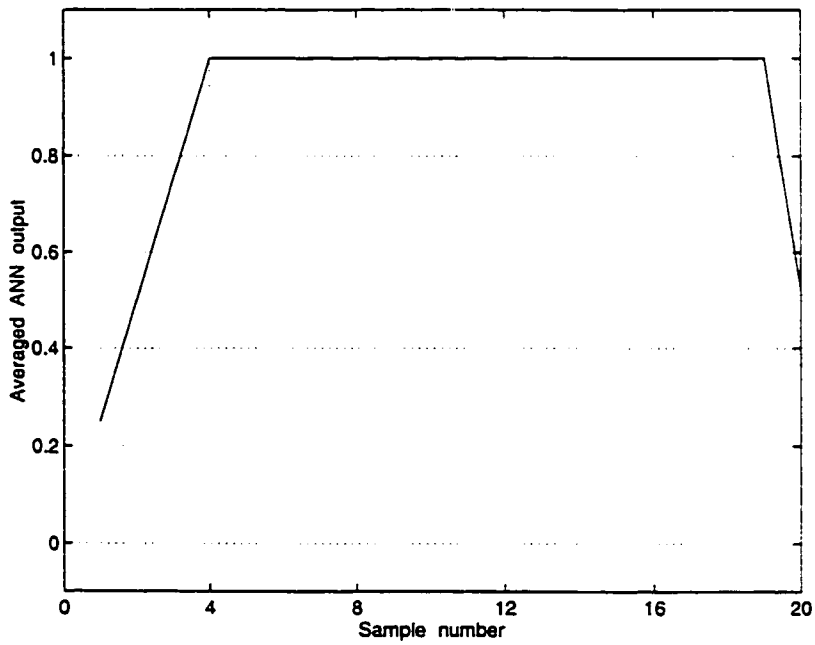

Figure 9.9: Twenty-input feedforward ANN averaged response to the phase *A* to ground forward fault on the 135 *km* transmission line, measurement at the other end

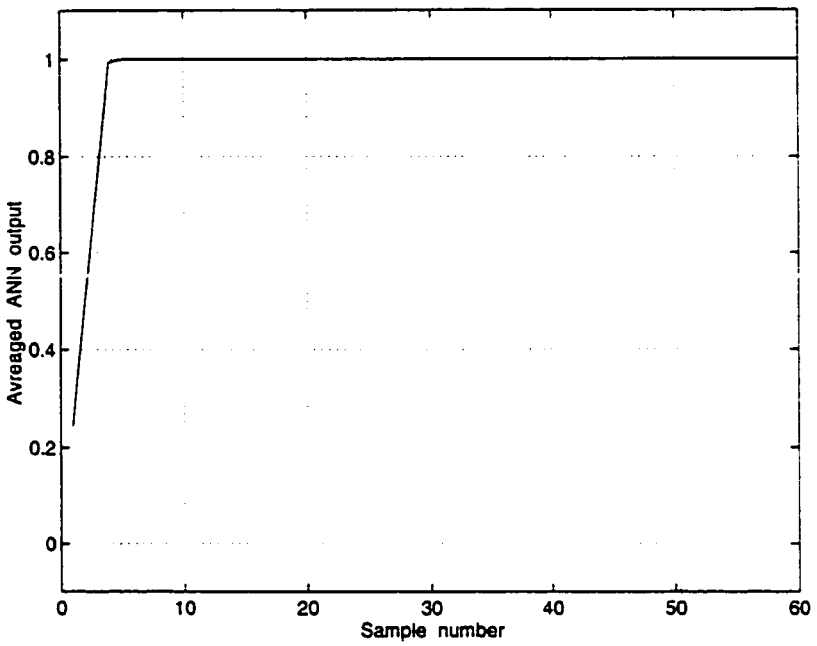

Figure 9.10: Twenty-input feedforward ANN averaged response to the phase A to phase B to ground forward fault on the 135 km transmission line

forward fault shown in Fig. 9.3. The output is shown during three cycles (60 samples) after the detection of the fault. It shows that the network detects the fault very fast and its output remains stable for three cycles.

9.5 Recurrent Network Directional Module

The proposed recurrent network-based fault direction discriminator module is tested with the recorded fault data [80]. For the examples presented in this section and the next section, the starter and directional module are processed simultaneously.

The recurrent network's output for a forward fault on the 135 km transmission line connecting Battle River and Sheerness substations is shown in Fig. 9.11. The measurements were recorded at the Sheerness substation. The fault was a double

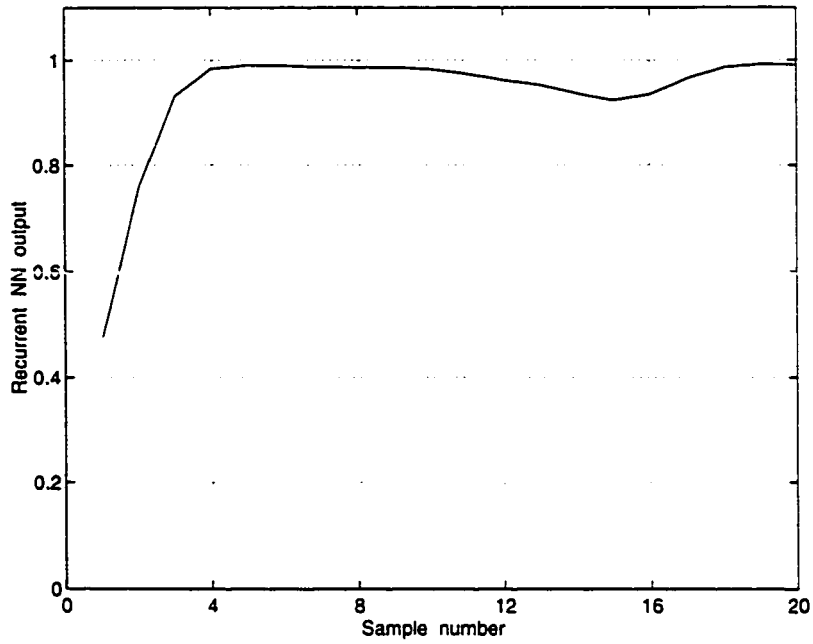

Figure 9.11: Recurrent ANN response to the phase A to phase B to ground forward fault on the 135 km transmission line

phase to ground A-B-G forward fault. The output is shown for the first cycle after the fault detection (sample number 1). The network outputs which fall above 0.5 and below -0.5 are interpreted as forward and backward faults, respectively. This figure shows that the fault direction identification is very fast and reliable. For this case, it takes just one sample after the fault detection for the output of the recurrent network to fall inside the forward fault area.

The proposed recurrent network-based directional module forms one component of a directional comparison relay. A fast fault detector module works in parallel with the ANN-based directional module. When the system is healthy, the fault detector output is zero and the directional module output is deactivated, i.e. set equal to zero. When a fault happens in the system, the fault detector module senses the fault quickly and activates the output of the directional module.

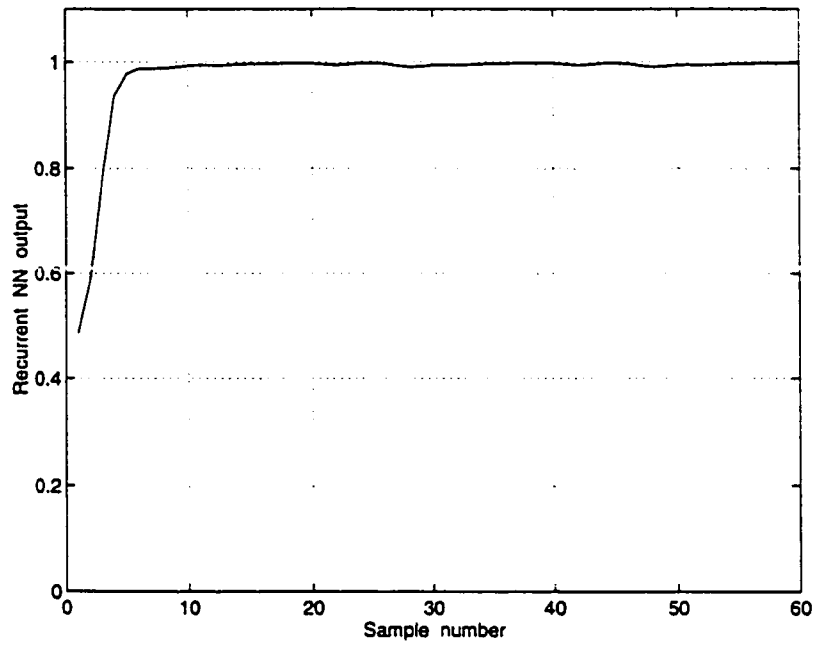

Figure 9.12: Recurrent ANN response to the phase C to ground forward fault on the 112 km transmission line

For this case, it was found that the fault detector needs two sampling periods (about 1.7 ms) to detect the fault. Therefore, in total the time needed to classify the fault direction is about 2.5 ms after the occurrance of the fault.

Fig. 9.12 shows the output of the network for a single phase to ground C-G forward fault on the 112 km transmission line between Metiskow and Battle River substations. The measurements were recorded at the Battle River substation. It shows that the network identifies the fault direction very fast and its output remains stable. The network correctly determines the fault direction just one sample after the fault detection. Although the network just uses the phase A voltage as its input, it correctly identifies the direction of the phase C to ground fault.

The next example tests the recurrent network's performance for a single phase to ground C-G forward fault on the 135 km transmission line. Network's output is

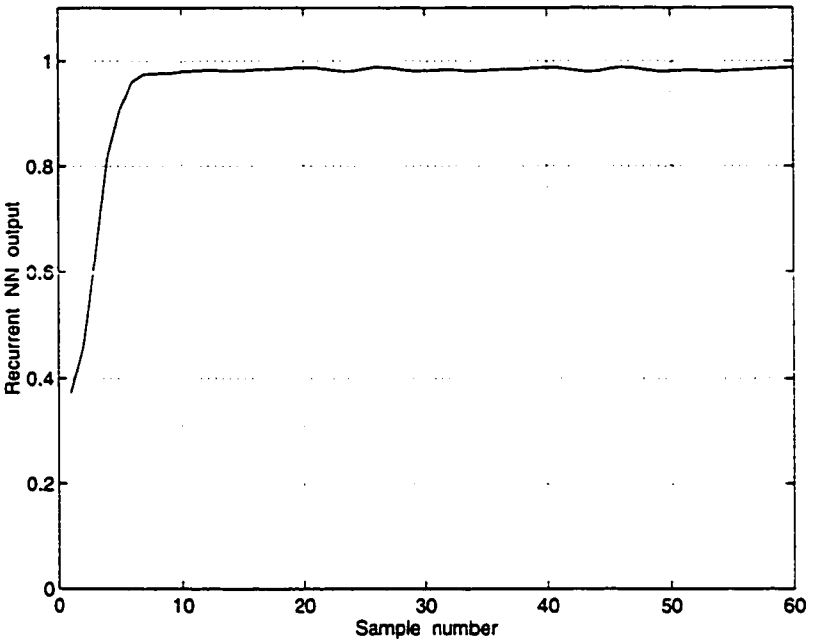

Figure 9.13: Recurrent ANN response to the phase C to ground forward fault on the 135 km transmission line

shown in Fig. 9.13 during three cycles after the detection of the fault. The directional module needs just about 1.7 ms after the fault detection to classify the fault direction correctly. The fault detector detects the fault in two sampling periods (about 1.7 ms). Therefore, in total the directional relay needs about 3.3 ms to detect the fault and discriminate its direction.

Fig. 9.14 shows the output of the network for the single phase to ground A-G forward fault illustrated in Fig. 9.2. It shows that the network classifies the fault direction very fast and its output remains stable for three cycles.

The output of the network for a phase to phase B-C backward fault behind the 135 km transmission line is shown in Fig. 9.15. It shows that the network performs correctly and rapidly.

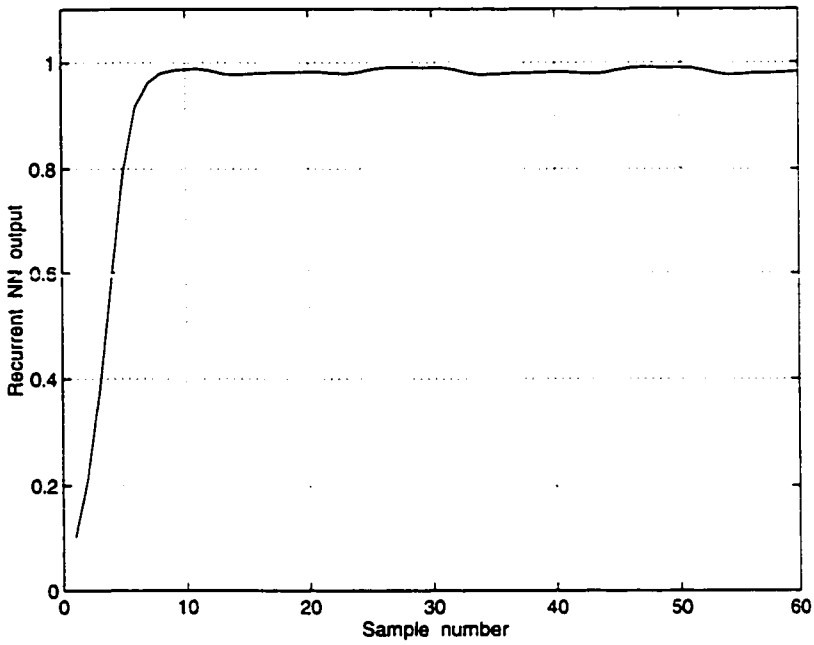

Figure 9.14: Recurrent ANN response to the phase A to ground forward fault on the 135 km transmission line

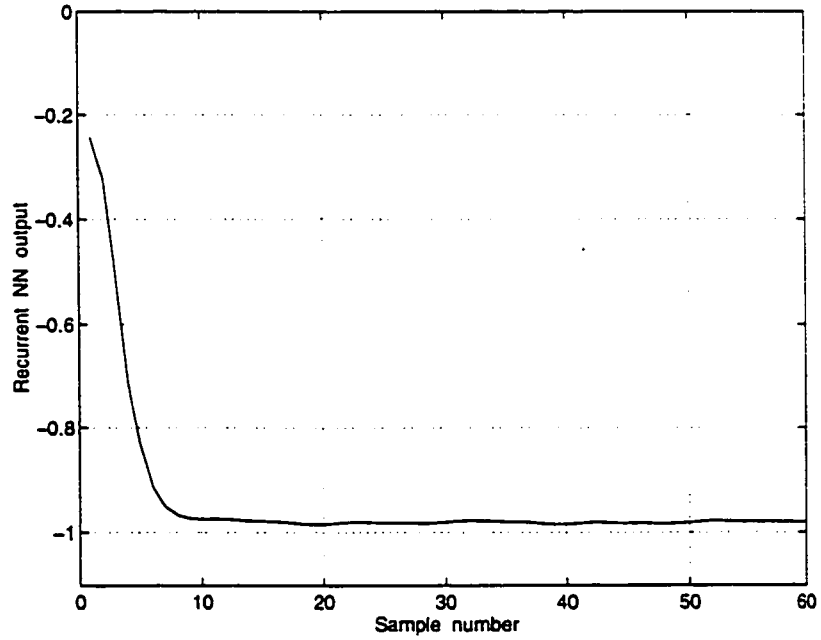

Figure 9.15: Recurrent ANN response response to the phase B to phase C backward fault behind the 135 km transmission line

9.6 Elman Network Directional Module

The performance of the proposed Elman network-based fault directional module is tested with the recorded fault data [81].

Output of the network for a forward fault on the 135 *km* transmission line connecting Battle River and Sheerness substations is shown in Fig. 9.16. The measurements were recorded at the Battle River substation. The fault was a single phase to ground *B-G* forward fault. The output is shown for the first three cycles after the fault detection (sample number 1). This figure shows that the fault direction identification is very fast and reliable. For this case, it takes two samples after the fault detection for the output of the recurrent network to fall inside the forward fault area.

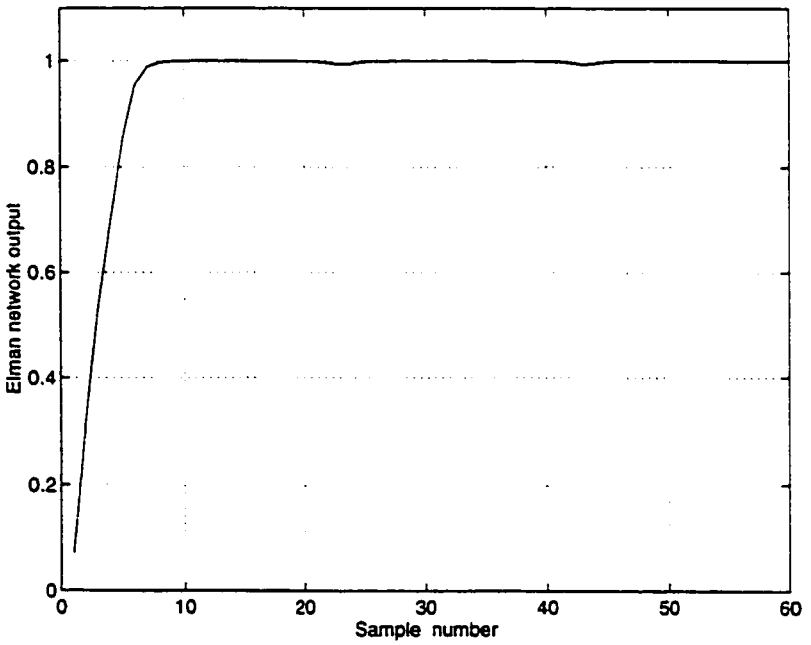

Figure 9.16: Elman network response to the phase *B* to ground forward fault on the 135 *km* transmission line

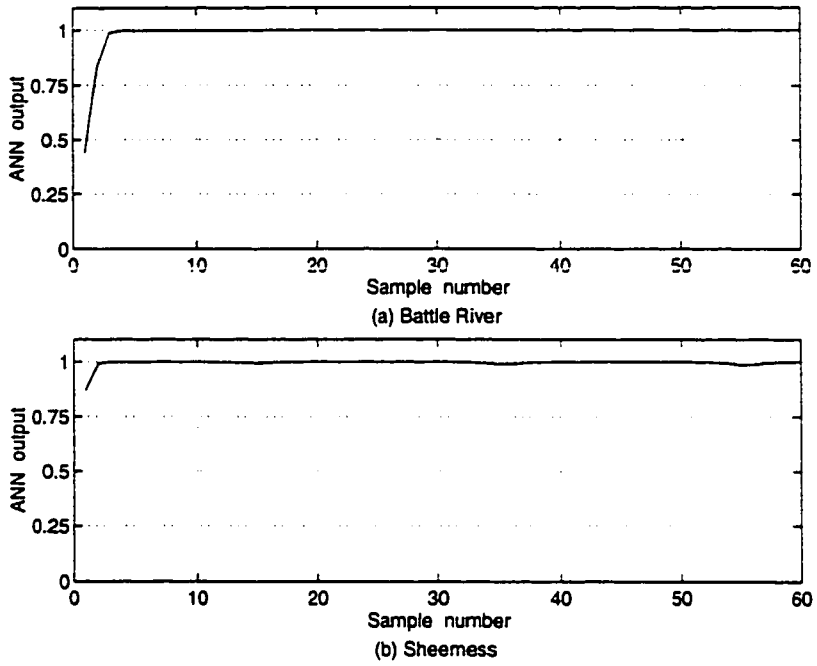

Figure 9.17: Elman network response to the phase A to phase B to ground forward fault on the 135 km transmission line, measurements at both ends

The output of the network for a double phase to ground A-B-G forward fault on the same 135 km transmission line is shown in Fig. 9.17a. The measurements were recorded at the Battle River substation. It shows that the network identifies the fault direction very fast and its output remains stable for three cycles. Similar results are observed for the same fault with the measurements recorded at the other end of the transmission line as evident from Fig. 9.17b. The network correctly determines the fault direction just one sample after the fault detection. Therefore, as shown in Fig. 9.17 the A-B-G fault is correctly identified as a forward (internal) fault at both ends of the transmission line.

In the next case, the Elman recurrent network's performance for a single phase to ground C-G fault on the 112 km transmission line between Metiskow and Battle

River substations is assessed. The measurements were recorded at the Battle River substation. Network's output is shown in Fig. 9.18 during three cycles after the detection of the fault. The directional module classifies the fault direction correctly just 2 samples after the fault detection. For this fault, the fault detector detects the fault just one sample after the fault inception. Therefore, in total it takes 3 samples to detect the fault and discriminate its direction.

Based on calculations from using the DFR currents on a fault location program it was found that the C-G fault distance from the measurement point was 16 km (about 14% of the transmission line's length). It shows that the directional module is able to correctly identify faults near to the relay location. Although the network just uses the phase A voltage as its input, it correctly identifies the direction of the phase C to ground fault.

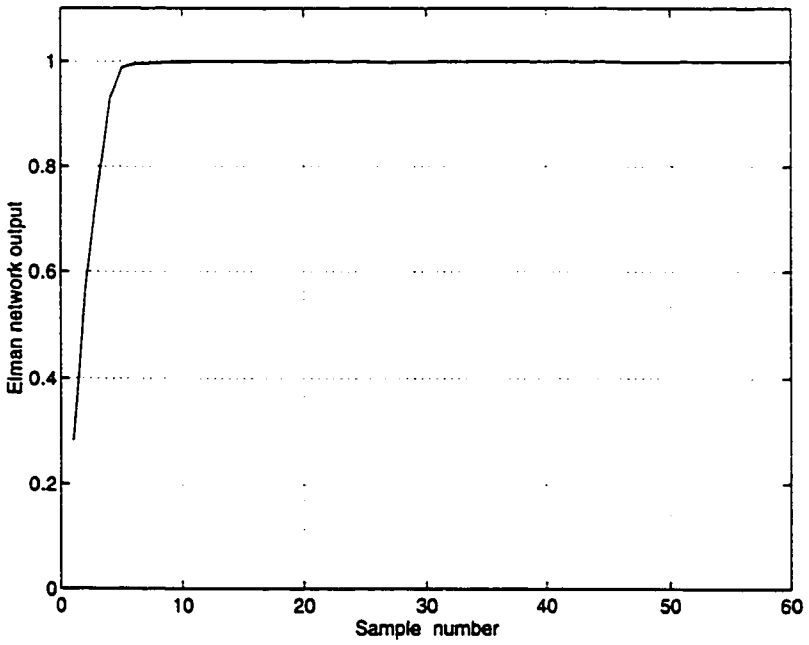

Figure 9.18: Elman network response to the phase C to ground forward fault on the 112 km transmission line

Elman network response to a double phase B-C backward fault behind the 135 km transmission line is shown in Fig. 9.19. The network output is shown after the detection of fault. It takes 3 sampling periods to identify the fault direction after detection of the fault. It shows that the network performs correctly and rapidly.

Fig. 9.20 shows the output of the network for a single phase to ground A-G forward fault on the 135 km transmission line during three cycles after the detection of the fault. Recorded fault data from both ends of the transmission line were presented to the Elman network. The network correctly identifies the forward fault in both cases. The directional relay could be used in a directional comparison relaying scheme.

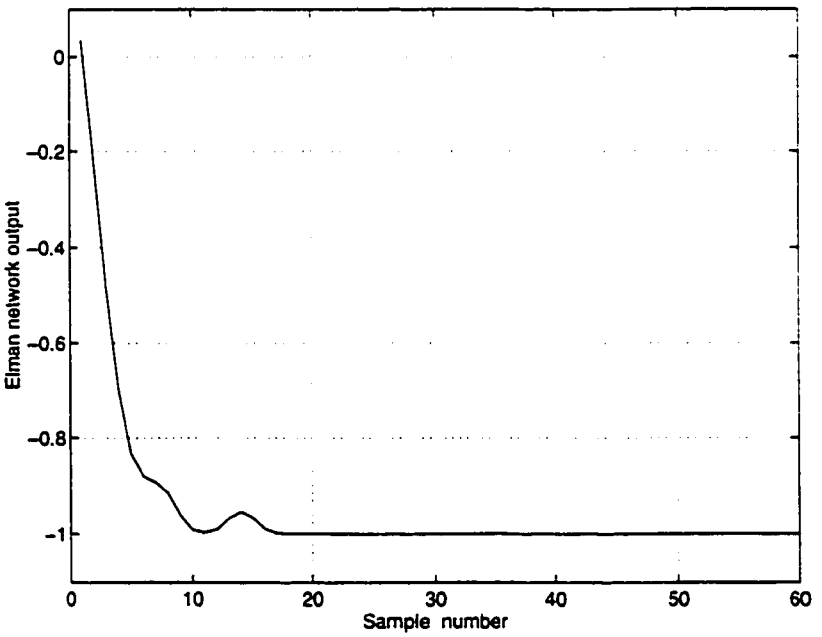

Figure 9.19: Elman network response to the phase B to phase C backward fault behind the 135 km transmission line

Using the other remaining recorded data files provided by Alberta Power Ltd. some more tests were performed and similar results were obtained. Output of the

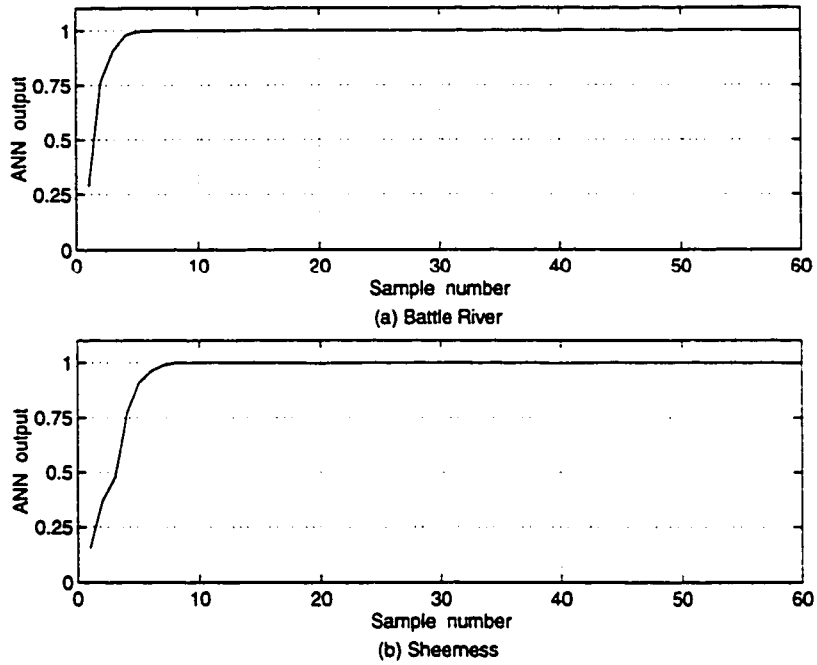

Figure 9.20: Elman network response to the phase A to ground forward fault on the 135 km transmission line, measurements at both ends

network in all cases classified the fault direction correctly. On average, it takes just about 3.2 ms to detect the fault and classify its direction.

These results confirm the simulation studies results and show that the proposed neural network-based directional module performed correctly and reliably when tested with field data. The decision is made very fast, as in the case of simulation studies. It indicates that the proposed neural network could be trusted as a robust scheme for transmission line fault direction estimation.

9.7 Starter Module

The performance of the proposed starter module was assessed using the recorded field fault data. Some of the results are presented in this section.

The first example evaluates the performance of the algorithm for a heavy *C-G* fault on the 112 *km* transmission line between Metiskow and Battle River substations near the measurement point. The measurements were recorded at the Battle River substation. The filtered three phase currents and voltages are shown in Figs. 9.21a and 9.21b, respectively.

The detector and phase starters outputs are also shown in Figs. 9.21c and 9.21d, respectively. The detector output could be used in conjunction with one of the proposed ANN-based directional modules to form a directional relay. The selector outputs could be used to classify the fault type. As shown in Fig. 9.21, the fault is detected rapidly and the appropriate starter output classifies the fault type accordingly. The fault is detected momentarily and it takes just two sampling times to classify the fault type.

The next example tests the algorithm's performance for the single phase to ground *A-G* forward fault illustrated in Fig. 9.2. Fig. 9.22 shows the results of this case study.

Similar results are observed for the same fault with the measurements recorded at the other end of the transmission line as evident from Fig. 9.23. In both cases, the starter detects and classifies the fault rapidly and correctly in two samples after the inception of the fault.

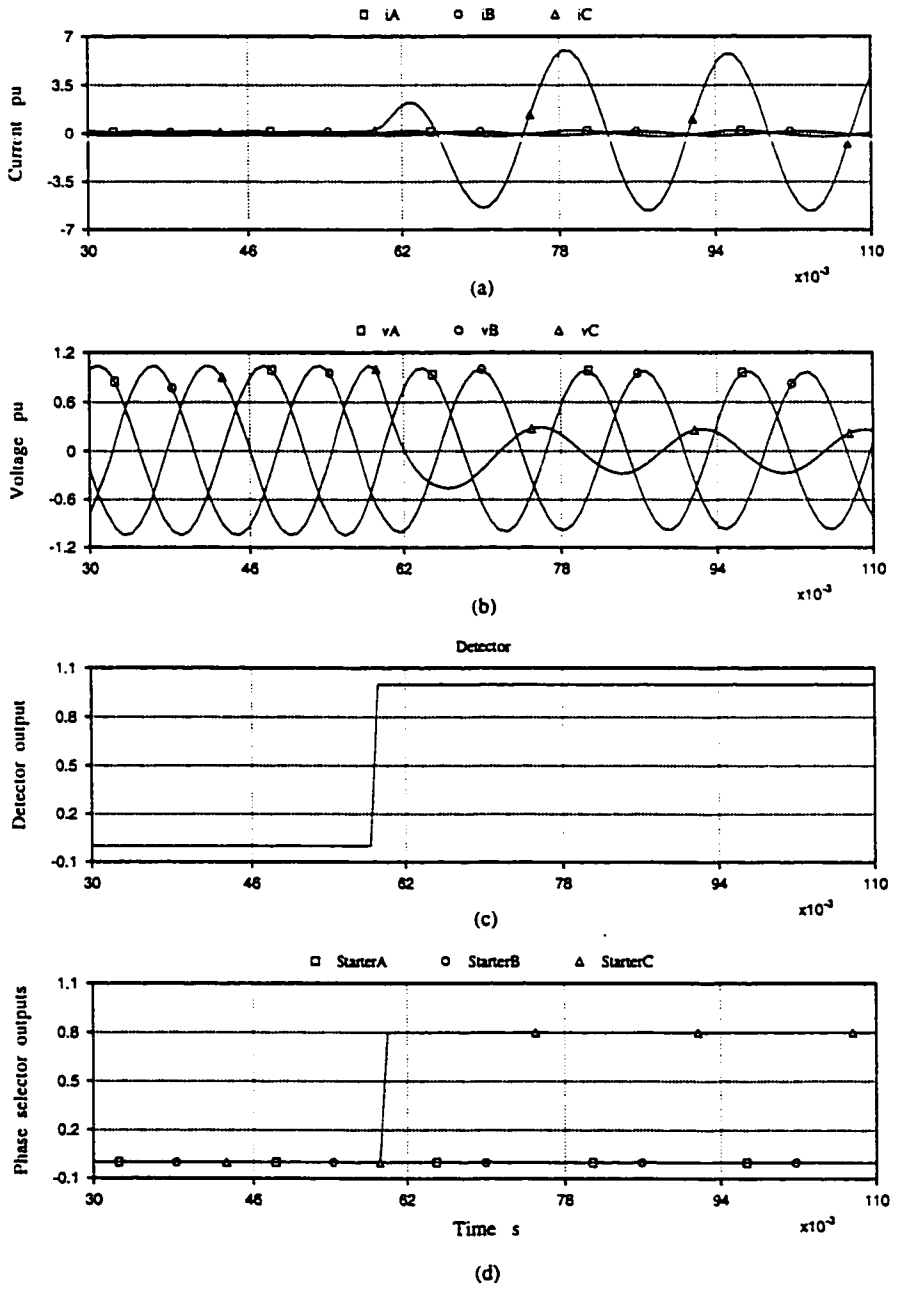

Figure 9.21: Phase starters and detector outputs for the C-G fault on the 112 km transmission line

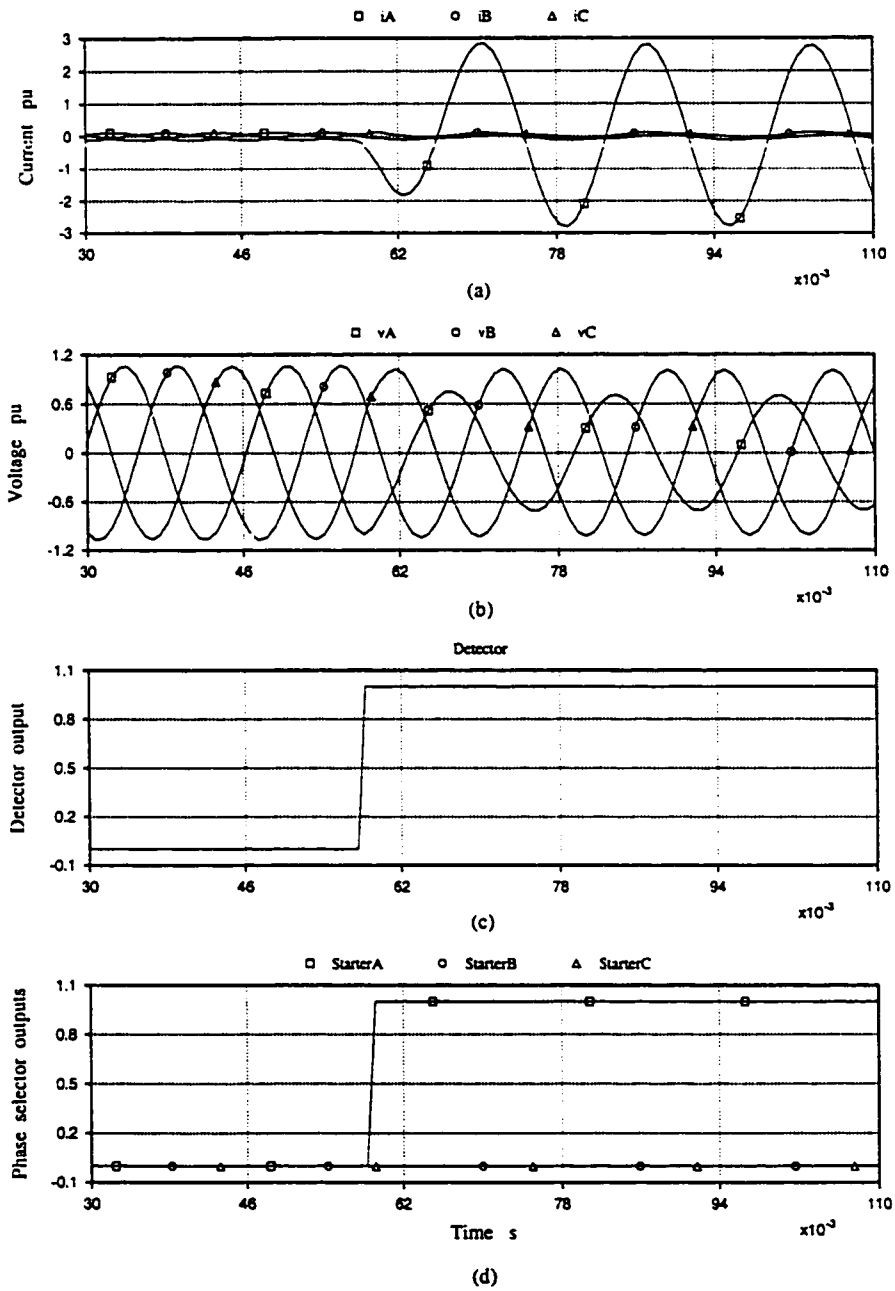

Figure 9.22: Phase starters and detector outputs for the A-G fault on the 135 km transmission line

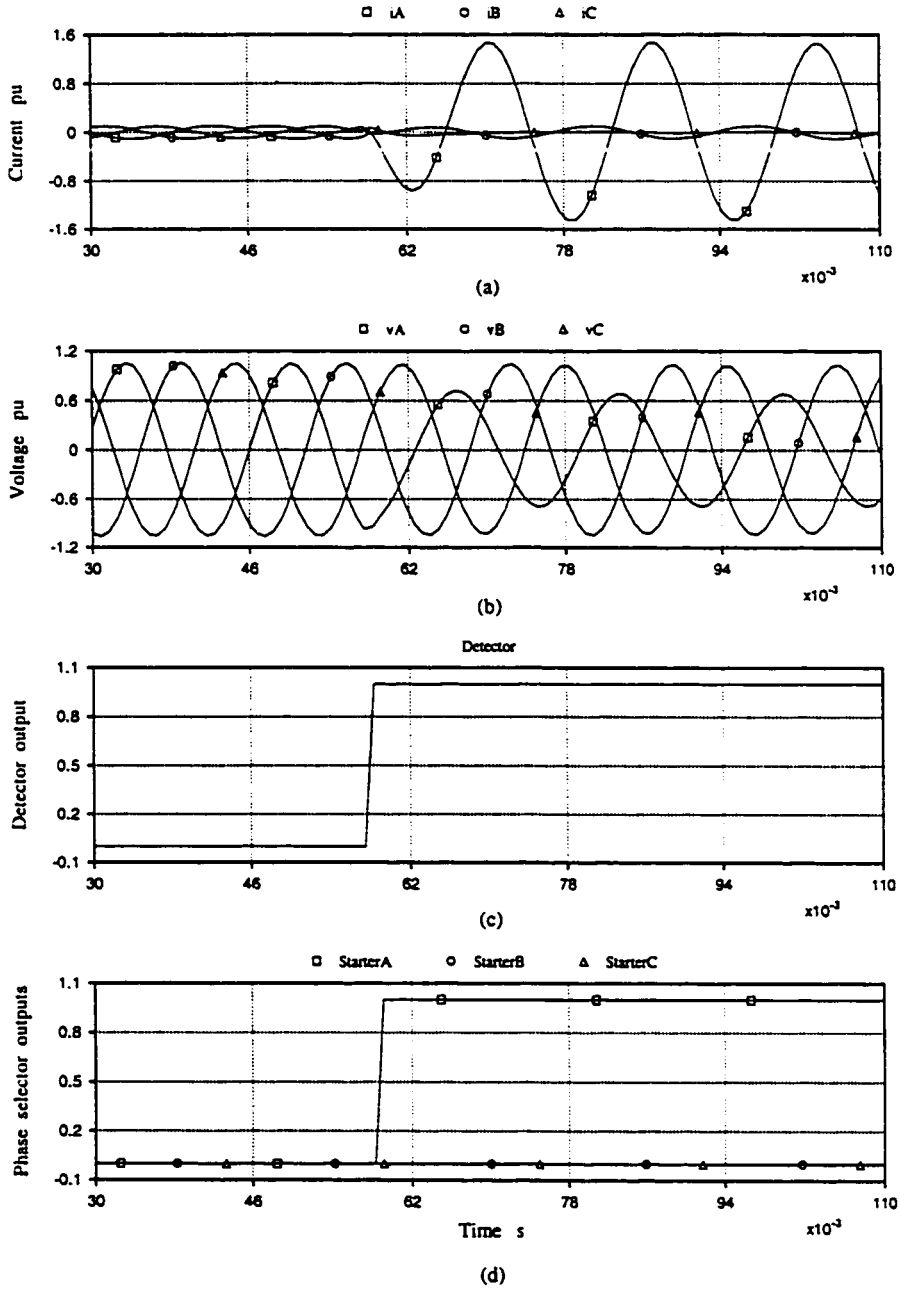

Figure 9.23: Phase starters and detector outputs for the A-G fault on the 135 km transmission line, relay located at the other end

The starter performance for the double phase to ground *A-B-G* forward fault shown in Fig. 9.3 is presented in Fig. 9.24. The measurements were recorded at the Battle River substation. Recorded fault data from other end of the transmission line at Sheerness substation were presented to the starter module and the results are shown in Fig. 9.25.

The fault was more towards the Sheerness substation. As shown in Figs. 9.24 and 9.25, fault is detected and classified very fast from both ends of the transmission line. For the case with measurements at the Battle River substation, the starter detects and classifies the fault in five samples after the inception of the fault. However, for the case with measurements at the Sheerness substation, the fault is detected and classified in three samples. The starter module outputs remain stable for three cycles after the fault inception.

9.8 Summary

Performance of the proposed relay modules was evaluated using recorded field data. Results obtained indicate that the proposed modules give promising results. It was found through different studies that the proposed starter module is able to detect and classify different faults correctly and very rapidly. The neural network-based algorithms have been tested to evaluate their performance in terms of generalization, robustness and speed. Investigations showed that the ANN-based directional modules are able to classify forward and backward recorded faults very rapidly. Results presented in this chapter confirm the simulation and experimental studies presented in previous chapters.

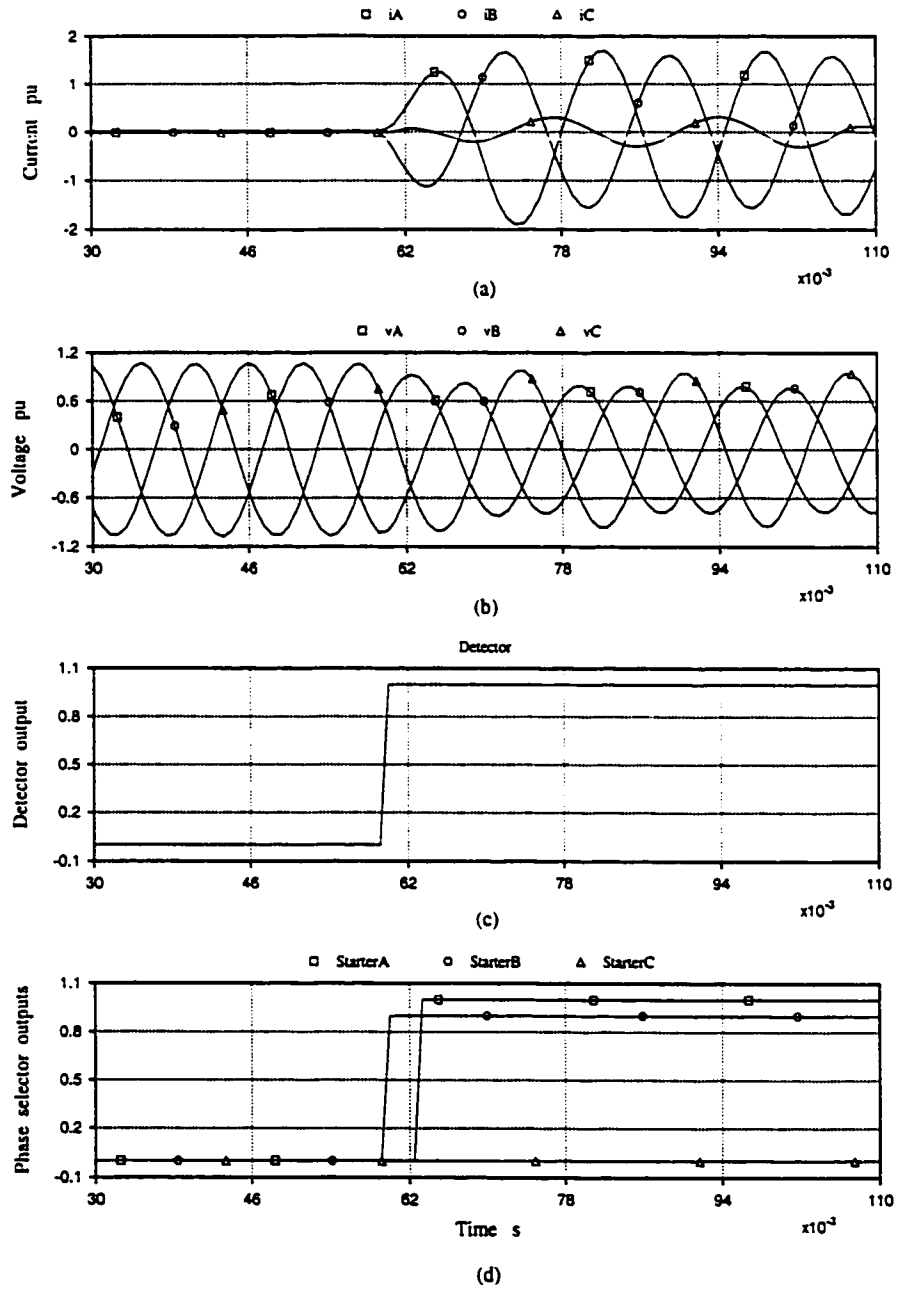

Figure 9.24: Phase starters and detector outputs for the A-B-G fault on the 135 km transmission line

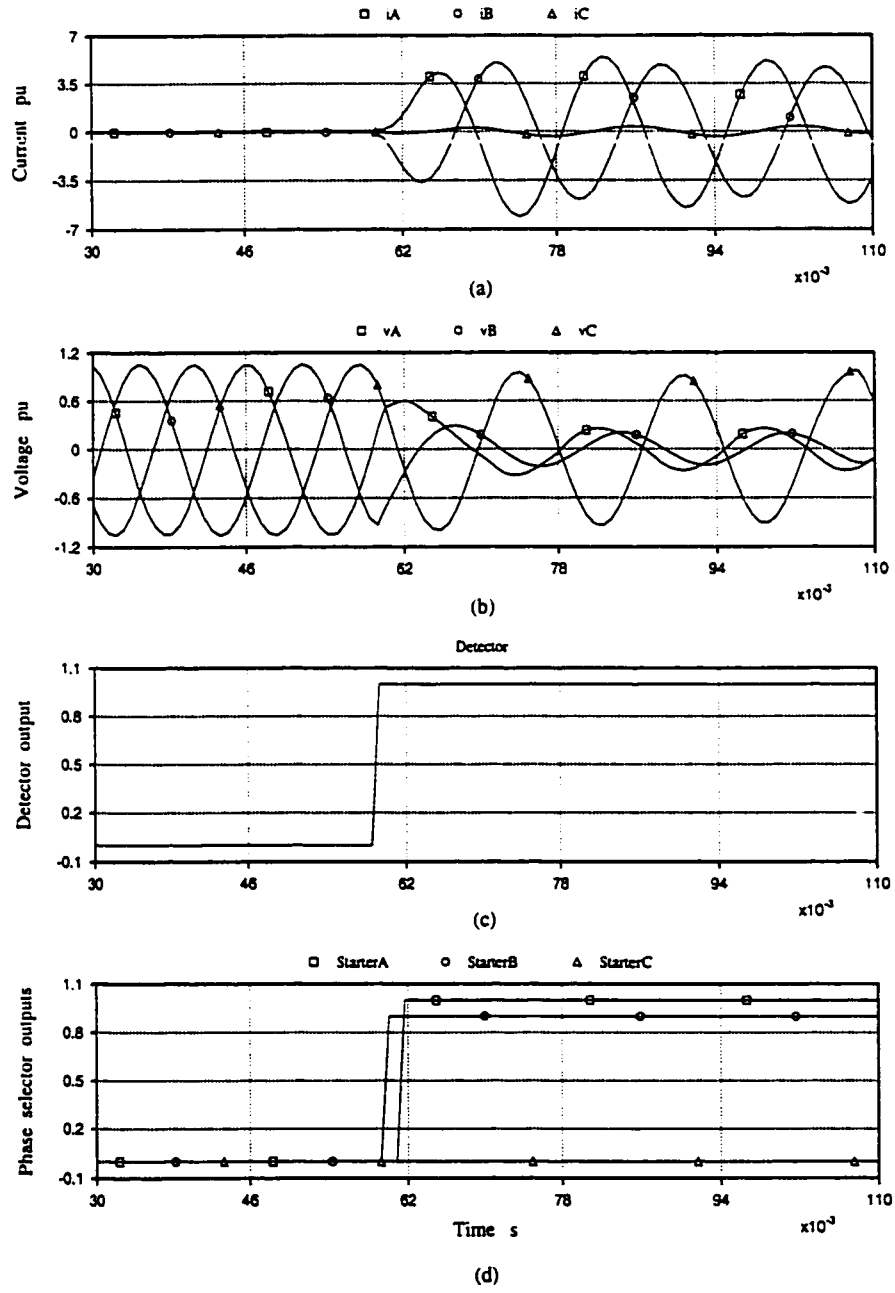

Figure 9.25: Phase starters and detector outputs for the *A-B-G* fault on the 135 *km* transmission line, relay located at the other end

It was found that the recurrent network-based directional modules performed better compared with the feedforward directional module. The recurrent networks are more robust schemes when tested with the field data which has never been presented to them before.

The proposed directional relay used alone can be employed as a transmission line directional module or in a directional comparison protection scheme by employing a relay at each end of the line.

Chapter 10

Conclusions and Future Work

10.1 Summary and Conclusions

Protective relays are used in power systems to protect equipment and to maintain stability by isolating the faulted equipment from the power system. The advent of large generating stations and highly interconnected power systems makes early fault identification and rapid equipment isolation imperative to maintain system integrity and stability.

Transmission line protection is a task of fundamental importance in a modern power system. It is also the most elaborate and challenging function in power system protection. Faults in the transmission system must be identified and the faulted line must be isolated from the network with minimal delay.

If faster clearance times are to be achieved, it is generally less expensive, on an existing system, to provide high speed relaying than to retain conventional relaying and use faster circuit breakers. One of major advantages of high speed relaying is increasing the system stability. Another main advantage is lesser arc ionization due to faster opening of the circuit breakers. This leads to the possibility of faster reclosure of the circuit breakers.

The concept of digital computer relaying has grown rapidly. Microcomputer-based relays are recommended for the protection task at the substation level. These

microcomputer relays can work in conjunction with the mainframe computers used for the overall power system control. A microprocessor relay offers the advantages such as reliability, flexibility, performance and economy.

It is desirable to develop fast and reliable transmission line relaying modules to identify faults on a given transmission line. The proposed modules should be fast and robust and their performance should not be affected by changes in power system conditions and parameters.

This dissertation is devoted to the development of different modules of a transmission line protection system. It has made contribution to different stages of developing such relaying modules namely theoretical development, simulation studies, experimental tests and performance evaluation using recorded real fault data.

Successful applications of neural networks in other areas of power engineering has demonstrated that they could be employed as alternative methods for solving certain long-standing problems where conventional techniques have experienced difficulties or have not achieved the desired performance such as speed, accuracy and efficiency. In this dissertation transmission line fault direction identification modules based on neural networks are developed. The proposed modules use the principles of neural networks to determine the direction of a fault on the basis of pattern classification. Neural network technique is employed and two feedforward directional modules are designed and trained.

An important class of neural networks has a recurrent structure. The recurrent connections of the neural network provide the network with memory. Two novel recurrent neural networks with temporal processing abilities are proposed to determine the direction of faults on transmission lines.

Simulation studies are performed and the performance of the proposed directional networks is investigated. Influence of changing system parameters such as fault location, fault resistance, fault inception time, source impedance and pre-fault power flow direction is studied. The performance of the proposed networks is also checked for faults including high amount of resistance and also faults at the relay location.

The directional modules are extensively tested by independent test fault patterns and promising results are obtained. It is found through extensive studies that the proposed networks are able to classify forward and backward faults correctly and very rapidly.

This research work and other published literature in the same area have established that different architectures of neural networks present a good potential for power system protection applications. The neural network-based approaches could be used as a part of a new generation of very high speed directional protection relays.

Despite all their advantages, ANNs have few acceptability issues associated with them. The major drawback of a neural network is its black-box characteristic. It is not easy to understand the knowledge stored in an ANN. Analytical methods to explain and modify the weights of a trained network are not readily available yet. Few definite rules exist for choosing optimal network training parameters and structure. The selection of number of hidden layers and number of neurons in each layer is not a trivial task.

The application of neural networks in power system protection is a new area. As protective relays must be highly reliable, the relay engineers are hesitant to embrace neural networks because their results are difficult to be explained using conventional analytical methods. In-spite of the above mentioned drawbacks, neural networks

have been successfully applied in different areas of power systems and the number of neural networks applications in power engineering is quite impressive. The research in the areas of neural networks and ANN-based protection techniques is continuing to overcome the above mentioned roadblocks.

It is desirable to develop a fast and reliable method to detect faults on a transmission line and to select faulty phases. A new high speed adaptive scheme is proposed for fault detection and phase selection. The proposed fault detector and phase selector modules are tested to evaluate their performance under different operating conditions. The performance of the proposed scheme is also checked for extreme cases like high resistance faults and faults at the relay location.

The proposed starter is able to rapidly and correctly detect and classify different fault types on the protected transmission line under different power system conditions. This starter in conjunction with a directional module could be used in a directional comparison transmission line protection scheme.

The ample results obtained from simulation studies show that the proposed relaying modules have many promising features. This makes them a strong candidate to complement the conventional relaying algorithms.

Next stage in the development process is the implementation of the device. Implementation is a critical step towards practical application of a newly proposed algorithm. By utilizing a DSP board mounted on a personal computer, a real-time digital environment has been established to implement the proposed relaying modules. Using a physical power system model various experiments have been conducted. Experimental studies have produced results consistent with the simulation studies, proving the capabilities of the proposed modules.

The operation time of the proposed modules implemented on the DSP board is well within the available inter-sampling time. This shows that the proposed modules are within the reach of the present technology and can be used for high speed protection relaying.

Testing of a newly designed digital relay using real field data is another important stage in evaluating the relay performance. Performance of the proposed relay modules is investigated further using recorded fault data from a high voltage power system. Results obtained confirm the simulation and experimental studies results. The proposed modules are able to perform correctly and rapidly when tested with real fault data.

The proposed directional neural networks were originally trained for a different transmission line with different length and characteristics. They were not retrained for the experimental and field data studies, and still are able to estimate the direction of faults on different transmission lines which have never been presented to them before. It indicates that the proposed neural networks could be trusted as robust schemes for transmission line fault direction estimation. It may be stated that neural network-based approaches could be used as a part of a new generation of high speed directional comparison relays.

10.2 Recommendations for Future Work

Research on neural networks has advanced rapidly in recent years and ANNs have found numerous applications in power engineering. Neural networks-based schemes have been employed in some parts of this dissertation. The results presented demon-

strate the feasibility of using neural networks for possible applications in power system protection. Since the application of neural networks in protection is a new area, some more investigations should be performed to further prove their industrial implementation.

Based on the work done in this dissertation, the followings are recommended as further research topics:

- Different neural network structures have been proposed and investigated in this research work. Other network structures could be considered and studied for performing different tasks in a protection system.

- The performance of the proposed relaying modules could be verified for a double transmission line configuration. Some preliminary studies and investigation have been already performed and encouraging results have been obtained. More investigations should be performed and necessary parts of the proposed modules should be modified.

- A complement module to identify the fault distance from the measurement point could be employed or developed. This distance module in conjunction with the other proposed modules could be employed in a transmission line distance protection scheme. This module could be based on neural networks or other available digital relaying techniques.

- Series-compensated transmission lines could be considered and studied. Different transmission line protective relay modules could be designed and investigated for this system model.

References

[1] P.M. Anderson and A.A. Fouad, *Power System Control and Stability*, Iowa State University Press, 1977.

[2] J.L. Blackburn, *Protective Relaying - Principles and Applications*, Marcel Dekker Inc., New York, 1987.

[3] A.R. van C. Warrington, *Protective Relays - Their Theory and Practice, Volumes 1 & 2*, Chapman and Hall, London, 1978.

[4] C.R. Mason, *The Art and Science of Protective Relaying*, John Wiley & Sons Inc., New York, 1956.

[5] M.S. Sachdev (Coordinator), *Computer Relaying - Tutorial Course Text*, IEEE, Publication no. 79EH0148-7-PWR, New York, 1979.

[6] G.D. Rockefeller, "Fault protection with a digital computer", *IEEE Trans. on Power Apparatus and Systems*, vol. PAS-88, no. 4, pp. 438–464, 1969.

[7] A.G. Phadke and J.S. Thorp, *Computer Relaying for Power Systems*, John Wiley & Sons Inc., New York, 1988.

[8] H. Ungrad, W. Winkler, and A. Wiszniewski, *Protection Techniques in Electrical Energy Systems*, Marcel Dekker Inc., New York, 1995.

[9] M.S. Sachdev (Coordinator), *Advancements in Microprocessor Based Protection and Communication - Tutorial Course Text*, IEEE, Publication no. 97TP120-0, New York, 1997.

[10] A.T. Johns and S.K. Salman, *Digital Protection for Power Systems*, Peter Peregrinus Ltd., United Kingdom, 1995.

[11] Electricity Training Association, *Power System Protection, Volume 4: Digital Protection and Signalling*, IEE, London, 1995.

[12] Walter A. Elmore (Editor), *Protective Relaying Theory and Application*, Marcel Dekker Inc., New York, 1994.

[13] A.G. Phadke, "Computer relaying: Its impact on improved control and operation of power systems", *IEEE Computer Applications in Power*, vol. 1, no. 4, pp. 5–10, 1988.

[14] M.S. Sachdev (Coordinator), *Microprocessor Relays and Protection Systems - Tutorial Course Text*, IEEE, Publication no. 88EH0269-1-PWR, New York, 1987.

[15] The Electricity Council, *Power System Protection, Volumes 1-3*, Peter Peregrinus Ltd., United Kingdom, 1981.

[16] Westinghouse Electric Corporation, *Applied Protective Relaying*, Westinghouse Electric Corporation, Relay-Instrument Division, Newark, 1976.

[17] G.S. Hope and O.P. Malik, "Sampling rates for computer transmission lines protection", *IEEE Catalog no. 75CH1034-8 PWR, IEEE PES Summer Meeting, San Francisco, Paper no. A 75 544-7*, July 1975.

[18] A.L. St-Jacques and G. Santerre, "A multiprocessor based distance relay : design features and test results", *IEEE Trans. on Power Apparatus and Systems*,

vol. PAS-102, no. 12, pp. 3842–3849, 1983.

[19] M.S. Sachdev and M.A. Baribeau, "A digital computer relay for impedance protection of transmission lines", *Trans. of the Engineering and Operating Division Canadian Electrical Association,*, vol. 18, Part 3, no. 79-SP-158, pp. 1–5, 1979.

[20] M.S. Sachdev and M.A. Baribeau, "A new algorithm for digital impedance relays", *IEEE Trans. on Power Apparatus and Systems*, vol. 98, no. 6, pp. 2232–2240, 1979.

[21] A.M. Ranjbar and B.J. Cory, "An improved method for the digital protection of high voltage transmission lines", *IEEE Trans. on Power Apparatus and Systems*, vol. PAS-94, no. 2, pp. 544–550, 1975.

[22] W.J. Smolinski, "An algorithm for digital impedance calculation using a single pi section transmission line model", *IEEE Trans. on Power Apparatus and Systems*, vol. PAS-98, no. 5, pp. 1546–1551, 1979.

[23] J.S. Thorp, A.G. Phadke, S.H. Horowitz, and J.E. Beehler, "Limits to impedance relaying", *IEEE Trans. on Power Apparatus and Systems*, vol. PAS-98, no. 1, pp. 246–260, 1979.

[24] B. Ling and W.S. Kwong, "LFCB current differential relay for use with digital communication systems", *Canadian Electrical Association Spring Meeting, Montreal*, pp. 1–19, 1988.

[25] M. Okamura, F. Andow, and S. Suzuki, "Improved phase comparison relaying

with higher performance", *IEEE Trans. on Power Apparatus and Systems*, vol. PAS-99, no. 2, pp. 522–527, 1980.

[26] K.S. Prakash, *Amplitude Comparator Based Directional Comparison Digital Protection Relay*, Ph.D. Dissertation, Dept. of Electrical Eng., The University of Calgary, Calgary, AB, Canada, 1989.

[27] M.A. El-Sharkawi and D. Niebur (Editors), *A Tutorial Course on Artificial Neural Networks with Applications to Power Systems*, IEEE Power Engineering Society, Publication no. 96TP 112-0, New York, 1996.

[28] *A special issue on AI Methods in Power System Protection*, International Journal of Engineering Intelligent Systems, vol. 5, no. 4, 1997.

[29] Q.Y. Yuan, Y.H. Song, A.T. Johns, R. Morgan, and D. Williams, "Performance of an adaptive protection scheme for series-compensated EHV transmission systems using neural networks", *Electric Power System Research*, vol. 36, no. 1, pp. 55–76, January 1996.

[30] J.J. Hopfield, "Neural networks and physical systems with emergent collective computational abilities", *Proceedings of the National Academy of Science*, vol. 79, pp. 2554–2558.

[31] B. Widrow and M.A. Lehr, "30 years of adaptive neural networks: perceptron, madaline and backpropagation", *Proceedings of IEEE*, vol. 78, pp. 1415–1442, 1990.

[32] G.A. Carpenter, "Neural network models for pattern recognition and associative memory", *Neural Networks*, vol. 2, pp. 243–247, 1989.

[33] R.P. Lippmann, "An introduction to computing with neural nets", *IEEE ASSP Magazine*, vol. 4, pp. 4–22, 1987.

[34] D.E. Rumelhart and J.L. McClelland, *Parallel Distributed Processing: Explorations in the Microstructure of Cognition, Volumes 1 & 2*, MIT Press, Cambridge, 1986.

[35] S. Haykin, *Neural Networks, A Comprehensive Foundation*, Macmillan College Publishing Company, New York, 1994.

[36] I. Aleksander and H. Morton, *An Introduction to Neural Computing*, Chapman & Hall, 1990.

[37] B. Kosko, *Neural Networks and Fuzzy Systems: A Dynamic Approach to Machine Intelligence*, Prentice-Hall, 1992.

[38] M. Brown and C. Harris, *Neurofuzzy Adaptive Modelling and Control*, Prentice-Hall, 1994.

[39] Y.H. Song, A.T. Johns, and R.K. Aggarwal, *Computational Intelligence Applications in Power Systems*, Science Press and Kluwer Academic, 1996.

[40] M. Kezunovic, "A survey of neural net applications to protective relaying and fault analysis", *International Journal of Engineering Intelligent Systems, a special issue on AI Methods in Power System Protection*, vol. 5, no. 4, pp. 185–192, 1997.

[41] G.S. Rahman, "Artificial intelligence in electric power systems - a survey of the Japanese industry", *IEEE PES Summer Meeting, Seattle, Paper no. 92SM 397-0 PWRS*, July 1992.

[42] T.S. Dillon and D. Niebur, *Artificial Neural Networks Applications in Power Systems*, CRN Press, 1996.

[43] V.S.S. Vankayala and N.D. Rao, "Artificial neural networks and their application to power system - a bibliographical survey", *Electric Power System Research*, vol. 28, pp. 67–79, 1993.

[44] H. Singh, *An Artificial Neural Network-Based Fault Direction Discriminator for Protecting Transmission Lines*, M.Sc. Thesis, Dept. of Electrical Eng., University of Saskatchewan, Saskatoon, SK, Canada, 1994.

[45] Y.Q. Xia, J.L. He, and K.K. Li, "A reliable digital directional relay based on compensated voltage comparison for EHV transmission lines", *IEEE Trans. on Power Delivery*, vol. 7, no. 4, pp. 1955–1962, October 1992.

[46] A.T. Johns, M.A. Martin, A. Barker, E.P. Walker, and P.A. Crossley, "A new approach to EHV direction comparison protection using digital signal processing techniques", *IEEE Trans. on Power Systems*, vol. 1, no. 2, pp. 24–34, April 1986.

[47] M. Vitins, "A fundamental concept for high speed relaying", *IEEE Trans. on Power Apparatus and Systems*, vol. PAS-100, no. 1, pp. 163–173, January 1981.

[48] F. Engler, O.E. Lanz, M. Hanggli, and G. Bacchini, "Transient signals and

their processing in an ultra high speed directional relay for EHV/UHV line protection", *IEEE Trans. on Power Apparatus and Systems*, vol. PAS-104, no. 6, pp. 1463–1474, June 1985.

[49] Manitoba HVDC Research Center, *EMTDC User's Manual*, Winnipeg, Manitoba, 1994.

[50] T. Dalstein, D.J. Sobajic, B. Kulicke, and Y.H. Pao, "Neural network approach to fault direction identification in electric power systems", *Proceedings of The North American Power Symposium, Cleveland, Ohio*, pp. 290–299, Oct. 11-12, 1993.

[51] T.S. Sidhu, H. Singh, and M.S. Sachdev, "Design, implementation and testing of an artificial neural network based fault direction discriminator for protecting transmission lines", *IEEE Transactions on Power Delivery*, vol. 10, no. 2, pp. 697–706, April 1995.

[52] Y.H. Song, A.T. Johns, and Q.Y. Yuan, "Artificial neural-network-based protection scheme for controllable series-compensated EHV transmission lines", *IEE Proc. on Generation, Transmission and Distribution*, vol. 143, no. 6, pp. 535–540, November 1996.

[53] Martin T. Hagan and Mohammad B. Menhaj, "Training feedforward networks with the marquardt algorithm", *IEEE Trans. on Neural Networks*, vol. 5, no. 6, pp. 989–993, 1994.

[54] I. Drezga and S. Rahman, "Input variable selection for ANN-based short-term

load forecasting", *IEEE PES Winter Meeting, Tampa, Florida, Preprint Paper no. PE-105-PWRS-0-12-1997*, February 1-5, 1998.

[55] M. Sanaye-Pasand and O.P. Malik, "Performance of a recurrent neural network-based power transmission line fault directional module", *International Journal of Engineering Intelligent Systems, a special issue on AI Methods in Power System Protection*, vol. 5, no. 4, pp. 221–228, 1997.

[56] J.L. Elman, "Finding structure in time", *Cognitive Science*, vol. 14, pp. 179–211, 1990.

[57] A. Waibel, T. Hanazawa, G. Hinton, K. Shikano, and K.J Lang, "Phoneme recognition using time-delay neural networks", *IEEE Transactions on Acoustics, Speech and Signal Processing*, vol. 37, no. 3, pp. 328–339, 1989.

[58] E.A. Wan, "Temporal backpropagation for fir neural networks", *IEEE International Joint Conference on Neural Networks, San Diego, CA*, pp. 575–580, 1990.

[59] Y.S. Abu-Mostafa, "Learning from hints in neural networks", *Journal of Complexity*, vol. 6, pp. 192–198, 1990.

[60] K.A. Al-Mashouq and I.S. Reed, "Including hints in training neural nets", *Neural Computation*, vol. 3, pp. 418–427, 1990.

[61] M. Sanaye-Pasand and O.P. Malik, "Power transmission lines fault direction estimation using artificial neural networks", *Proceedings of the Canadian Conference on Electrical and Computer Engineering, Calgary, AB*, vol. 2, pp. 758–761,

May 26-29, 1996.

[62] M. Sanaye-Pasand and O.P. Malik, "High speed transmission system directional protection using an Elman network", *IEEE PES Winter Meeting, Tampa, Florida, paper no. 98 WM 110*, Feb. 1-5, 1998, to be published in IEEE Trans. on Power Delivery.

[63] R.J. Williams and D. Zipser, "A learning algorithm for continually running fully recurrent neural networks", *Neural Computation*, vol. 1, pp. 270–280, 1989.

[64] A.J. Robinson and F. Fallside, "A recurrent error propagation speech recognition system", *Computer Speech and Language*, vol. 5, pp. 259–274, 1991.

[65] Chakravarty, Nayar, and N.R. Achutan, "Applying pattern recognition in distance relaying, part 1: concept", *IEE Proceedings-C*, vol. 139, no. 4, pp. 301–305, July 1992.

[66] Walter A. Elmore, "Zero sequence mutual effects on ground distance relays and fault locators", *Proceedings of the Western Protective Relay Conference, Spokane, WA*, October 20-22, 1992.

[67] G.E. Alexander and J.G. Andrichak, "Ground distance relaying: Problems and principles", *Proceedings of the Western Protective Relay Conference, Spokane, WA*, October, 1991.

[68] IEEE Committee, "Transient response of coupling voltage transformers", *IEEE Trans. on Power Apparatus and Systems*, vol. PAS-100, no. 12, pp. 4811–4814, 1981.

[69] A. Swift, "The spectra of fault induced transients", *IEEE Trans. on Power Apparatus and Systems*, vol. PAS-98, pp. 940–947, 1979.

[70] J.S. Thorp, S.H. Horowitz, and A.G. Phadke, "The application of an adaptive technology to power system protection and control", *CIGRE, Paris*, 1988.

[71] G.S. Hope, O.P. Malik, and M.E. Rasmy, "Digital transmission line protection in real time", *Proc. IEE*, vol. 123, no. 12, pp. 1349–1354, December 1976.

[72] M. Gilany, *A Microprocessor-Based Relay for Parallel Transmission Lines*, Ph.D. Dissertation, Dept. of Electrical Eng., The University of Calgary, Calgary, AB, Canada, 1992.

[73] A.V. Oppenheim and R.W. Schafer, *Discrete-Time Signal Processing*, Prentice-Hall Inc., New Jersey, 1989.

[74] D. Johnson and J. Hilburn, *Rapid Practical Design of Active Filters*, John Wiley & Sons Inc., New York, 1976.

[75] *TMS320C3x User's Guide*, Texas Instruments Inc., Texas, 1990.

[76] M. Sanaye-Pasand and O.P. Malik, "Laboratory investigation of a digital recurrent network for transmission line directional protection", *accepted for publication in the International Journal of Neurocomputing, a Special Isuue on Power Systems*, June 1998.

[77] M. Sanaye-Pasand and O.P. Malik, "Implementation & laboratory test results of an Elman network-based transmission line directional relay", *submitted to the IEEE PES Transactions on Power Delivery*, December 1997.

[78] IEEE Standards, "IEEE standard common format for transient data exchange (comtrade) for power systems", *Publication no. C37.111-1991, IEEE, New York*, 1991.

[79] M. Sanaye-Pasand and O.P. Malik, "Performance evaluation of a new transmission line directional module using field data", *Proceedings of the IEEE WESCANEX'97, Winnipeg, Manitoba*, pp. 197–201, June 26-27, 1997.

[80] M. Sanaye-Pasand, O.P. Malik, and R. Pecen, "A recurrent neural network architecture for transmission system fault direction discrimination: Test using field data", *Proceedings of the North American Power Symposium, Laramie, Wyoming*, pp. 312–318, October 13-14, 1997.

[81] M. Sanaye-Pasand and O.P. Malik, "High speed transmission line directional protection evaluation using field data", *submitted to the IEEE PES Transactions on Power Delivery*, December 1997.

[82] W.S. Mayer and T.H. Liu, *EMTP Rule Book*, Bonneville Power Administration, Portland, Oregon, 1982.

Appendix A

Electro-Magnetic Transient Programs

Simulation is but one method of analysis which can be used to examine a complicated or nonlinear model or process. The operation of that model can be tested by subjecting it to disturbances and parameter variations and the system response can be observed. Electromagnetic transient simulation is a fascinating field of study allowing exploration into uncharted areas of electric circuit and system analysis. Concepts, ideas and models of portions of planned or existing power systems can be evaluated quantitatively. The confidence one can place in such studies develops with understanding of the tool of analysis being used as well as familiarity with the operation and performance of the system under study. This section gives a brief description of two electromagnetic transient programs, EMTP and EMTDC.

A.1 EMTP Transient Program

The EMTP [82] was developed in the public domain at the Bonneville Power Administration (BPA), Portland, Oregon. The transient program can be used to solve the ordinary differential and/or algebraic equations associated with an arbitrary interconnection of elements such as lumped resistance, inductance and capacitance, multiphase pi-equivalents, multiple distributed parameter transmission lines, nonlinear resistors and inductors, voltage and current sources, switches and dynamic synchronous machines.

Trapezoidal rule (second order) implicit integration is used on the describing equations of the component elements so as to form an associated set of real simultaneous algebraic equations that must be solved at each time step. Program output consists of voltages and currents as function of time for those variables requested by the user.

A.2 EMTDC Transient Program

The EMTDC transient program [49] was used in this study to generate simulated fault data for training the neural network. The power of EMTDC lies in its ease of preparing user or already available functions or models and interfacing them with an electric circuit or control system. The program allows the user to graphically sketch the power system circuit to be simulated.

EMTDC is structured so that the electric circuit parameters such as circuit elements are easily addressed by the user during the course of a time-domain simulation. Voltages at nodes and currents in branches are easily accessible. Since the interface to the electric circuit is straightforward, the user can assemble or build models which detect voltages and currents, calculate power, reactive power and relative phase angles, process such inputs and control switches and sources using standard control functions or user written statements.

With the flexible modelling capability, complex power system networks can be modelled and studied. A graphical user interface called Power System Computer Aided Design (PSCAD) enables the user to select preprogrammed models of power system apparatus to graphically build the power system networks. PSCAD comes

complete with a built-in library of voltage and current sources, transmission line models, switches, transformers, machine models, etc. User defined components such as control blocks and protection relays can be added to the library. Examples of the type of problems which have been investigated using EMTDC program include control systems, subharmonic problems of ac systems, flexible ac transmission systems, dc transmission systems and power system protection studies.

Appendix B

Transmission Line Parameters for Simulation Studies

The parameters of the three-phase transmission line used for the simulation studies are given below:

Nominal voltage = 240 kV

Measured $Z_1 = 0.362\,(83°)\ \Omega/km$

Measured $Z_0 = 1.370\,(71°)\ \Omega/km$

The detailed parameters of transmission line are given in the next page.

PS-CAD - Transmission Line Analysis Program

Version 1.0
Wed Apr 15 21:14:59 1998

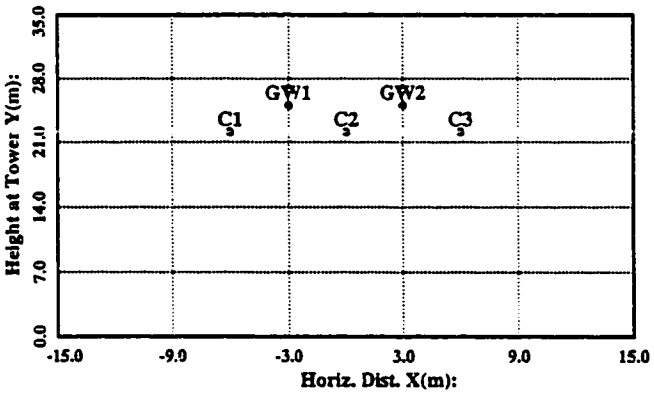

Summary of Main Data

Line Name:	Line100r
Line Length(km):	100.0
Gnd Resist.(ohm-m):	100.0
Low Freq(Hz):	5
High Freq(Hz):	1e+06
Ideally-Transposed Conductors	
Travel Times are Interpolated	
Transform Freq.(Hz):	2000

Summary of Conductor Data

Conductor # (1 - 3) ---->	1	2	3
Conductor Name:	Dove	Dove	Dove
Conductor Type (AC/DC):	AC	AC	AC
V(kV)(AC:L-L,rms/DC:L-G,pk):	240.0	240.0	240.0
V Phase(Deg.):	0.0	-120.0	120.0
Line I (kA)(AC:rms/DC:pk):	5.0	5.0	5.0
Line I Phase(Deg.):	20.0	-100.0	140.0
# of Sub-Conductors:	2	2	2
Sub-Cond Radius(cm):	1.17729	1.17729	1.17729
Sub-Cond Spacing(cm):	30.48	30.48	30.48
Horiz. Dist. X(m):	-6.0	0.0	6.0
Height at Tower Y(m):	22.0	22.0	22.0
Sag at Midspan(m):	7.0	7.0	7.0
DC Resistance(ohms/km):	0.10336	0.10336	0.10336

Summary of Ground Wire Data

Ground Wire # (1 - 2) ---->	1	2
Conductor Name:	7/16 Steel	7/16 Steel
Cond Radius(cm):	0.55245	0.55245
Horiz. Dist. X(m):	-3.0	3.0
Height at Tower Y(m):	25.0	25.0
Sag at Midspan(m):	7.0	7.0
DC Resistance(ohms/km):	2.8645	2.8645

Figure B.1: Transmission line detailed parameters

Appendix C

Training Algorithms

C.1 Back-Propagation Training Algorithm

Error back-propagation algorithm is a popular algorithm for training multilayer feed-forward neural networks. This algorithm is based on the error-correction learning rule. As such, it may be viewed as a generalization of the least-mean-square algorithm [35].

The squared-error cost function most frequently used in the ANN literature is defined as:

$$E(n) = \frac{1}{2}\sum_{j} e_j^2(n) \tag{C.1}$$

The symbol $e_j(n)$ refers to the error signal at the output of neuron j at iteration n (presentation of the nth training pattern to the network) and is defined by:

$$e_j(n) = d_j(n) - y_j(n), \quad \text{neuron j is an output node} \tag{C.2}$$

where $d_j(n)$ and $y_j(n)$ are the desired and actual responses respectively of neuron j for pattern n.

The back-propagation algorithm is a gradient descent method to minimize the squared-error cost function. The method of steepest descent for synaptic learning can be expressed as:

$$w_k(n+1) = w_k(n) + \eta(-\nabla_{w_k} E(n)) \tag{C.3}$$

where $w_k(n)$ and $w_k(n+1)$ are the weights at iterations n and $n+1$, respectively, η is the learning-rate parameter and $\nabla_{w_k} E(n)$ is the gradient of the error surface with respect to the w_k weight.

Weights w_{ji} (synaptic weight connecting the output of neuron i to the input of neuron j) of a neural network are adjusted to minimize $E(n)$ for a set of training patterns presented to the network. The weights are adjusted using a recursive algorithm starting at the output layer of the network and working back to the input layer, as per the following equation:

$$w_{ji}(n+1) = w_{ji}(n) + \Delta w_{ji}(n) \tag{C.4}$$

where Δw_{ji}, the correction applied to weight w_{ji} is:

$$\Delta w_{ji}(n) = \eta \delta_j(n) y_i(n) \tag{C.5}$$

where the local gradient $\delta_j(n)$ is itself defined by:

$$\delta_j(n) = \frac{\partial y_j(n)}{\partial v_j(n)} e_j(n), \quad \text{neuron j is an output node} \tag{C.6}$$

$$\delta_j(n) = \frac{\partial y_j(n)}{\partial v_j(n)} \sum_k \delta_k(n) w_{kj}(n), \quad \text{neuron j is a hidden node} \tag{C.7}$$

In the above equations, $v_j(n)$ refers to the net internal activity level of neuron j at iteration n, and $\delta_k(n)$ is for the neurons in the next hidden or output layer which are connected to neuron j.

A momentum term is usually included to speed up the training algorithm and to avoid local minima. In such a case the weight update is:

$$\Delta w_{ji}(n) = \alpha \Delta w_{ji}(n-1) + \eta \delta_j(n) y_i(n) \tag{C.8}$$

where α is the momentum factor. The incorporation of momentum factor could result in better convergence of the algorithm by preventing the learning process from terminating in a shallow local minimum of the error surface.

C.2 Marquardt-Levenberg Algorithm

While back-propagation is a steepest descent algorithm, the ML algorithm is an approximation to the Newton's method [53]. Suppose that a function $V(x)$ is to be minimized with respect to the parameter vector x. Then, the Newton's method would be:

$$\Delta(x) = -[\nabla^2 V(x)]^{-1} \nabla V(x) \tag{C.9}$$

where $\nabla^2 V(x)$ is the Hessian matrix and $\nabla V(x)$ is the gradient. If it is assumed that $V(x)$ is a sum of squares function in the form of:

$$V(x) = \sum_i e_i^2(x) \tag{C.10}$$

then it can be shown that

$$\nabla V(x) = J^T(x) e(x) \tag{C.11}$$

$$\nabla^2 V(x) = J^T(x)J(x) + S(x) \tag{C.12}$$

where $J(x)$ is the Jacobian matrix and

$$S(x) = \sum_i e_i(x)\nabla^2 e_i(x) \tag{C.13}$$

For the Gauss-Newton method it is assumed that $S(x) \approx 0$ and the update becomes:

$$\Delta x = [J^T(x)J(x)]^{-1}J^T(x)e(x) \tag{C.14}$$

The Marquardt-Levenberg modification to the Gauss-Newton method is:

$$\Delta x = [J^T(x)J(x) + \mu I]^{-1}J^T(x)e(x) \tag{C.15}$$

where μ is a scalar. This parameter is multiplied by some factor β whenever a step results in an increased $V(x)$. For a step which results in a reduction of $V(x)$, μ is divided by β. When μ is large, the algorithm becomes steepest descent, while for small μ the algorithm becomes Gauss-Newton.

Appendix D

Physical Model Power System

The parameters of the three-phase 500 kV transmission line and that of the equivalent π-section model [71] used for the experimental studies are:

500 kV line

$$\text{R}= 1.8 * 10^{-2}\ \Omega/km$$

$$\text{L}= 9.4 * 10^{-4}\ H/km$$

$$\text{C}= 1.13 * 10^{-8}\ F/km$$

π-section

$$\text{R}= 3.18 * 10^{-2}\ \Omega$$

$$\text{L}= 1.65 * 10^{-3}\ H$$

$$\text{C}= 8.03 * 10^{-6}\ F$$

The direct axis synchronous reactance of the micro-alternato is:

$$\text{X}_d = 34.9\ \Omega$$

Appendix E

Analog Bandpass Filter

The analog filter parameters are:

$R_1 = 106\ k\Omega$ $R_2 = 38\ k\Omega$ $R_3 = 22\ k\Omega$

$R_4 = 75\ k\Omega$ $R_5 = 75\ k\Omega$ $C = 0.1\ \mu F$

Op-Amp. : Dual 1458

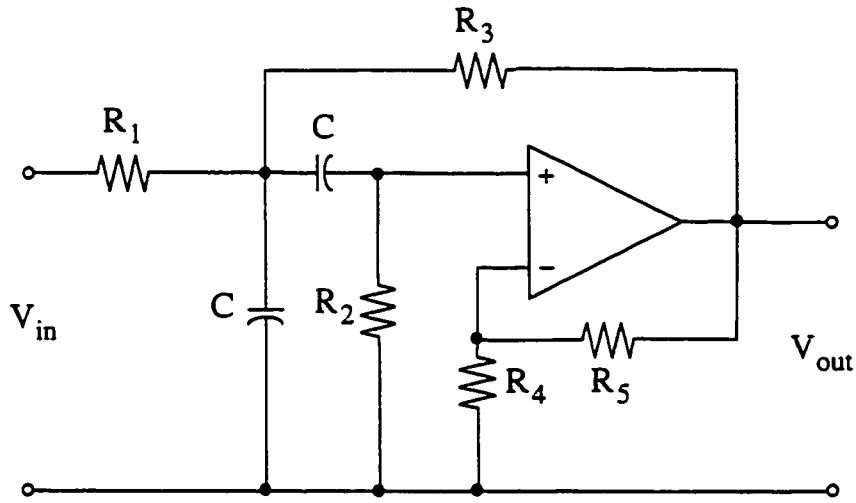

Figure E.1: Analog filter circuit